AD-A089 436 NAVAL OCEAN SYSTEMS CENTER SAN DIEGO CA F/G 9/5
ADVANCED MAIL SYSTEMS SCANNER TECHNOLOGY, EXECUTIVE SUMMARY AND--ETC(U)
OCT 79 F C MARTIN, T R LITTLE, L A WISE
UNCLASSIFIED NOSC/TR-520 NL

FIFTH ANNUAL REPORT
ADVANCED MAIL SYSTEMS SCANNER TECHNOLOGY

Executive Summary and Appendixes A-D

October 1979

Prepared by
NOSC Sensor Processing and Analysis Division (Code 732)
NAVAL OCEAN SYSTEMS CENTER
San Diego, California 92152

FOR
US POSTAL SERVICE
OFFICE OF ADVANCED MAIL SYSTEMS DEVELOPMENT

[illegible]

AN ACTIVITY OF THE NAVAL MATERIAL [illegible]

SL GUILLE, CAPT, USN [illegible]

[illegible]

ADMINISTRATIVE INFORMATION

This report contains a summary of work sponsored by the Office of Advanced Mail Systems Development, Research and Development Department of the US Postal Service, Rockville, Maryland 20852, under US Postal Service Agreement 104230-77-T-1604. The authorized USPS technical representative is J McGinn. The principal NOSC investigator is Frank C Martin of the Signal Analysis and Image Processing Branch, NOSC Code 7323. Associate investigators are Thomas R Little, Lee A Wise, and Robert W Basinger, also of Code 7323. Contributions were also made by Waldo R Robinson of Code 8236. This report is a compilation of data presented by all team members and was approved for publication in October 1979.

Released by
RL Petty, Head
Sensor Processing and
Analysis Division

Under authority of
RE Shutters, Head
Surface/Aerospace
Surveillance Department

METRICATION

Refer to American Society for Testing and Materials Standard for Metric Practice, ASTM designation E380-76, IEEE Std 268-1976, for metric equivalents and conversion factors for units used in this report.

DISCLAIMERS

The findings in this report are not to be construed as an official [illegible] Department of the [illegible]

[illegible] commercial [illegible] service [illegible]

UNCLASSIFIED

SECURITY CLASSIFICATION OF THIS PAGE (When Data Entered)

(14) NOSC/TR-520

REPORT DOCUMENTATION PAGE

READ INSTRUCTIONS BEFORE COMPLETING FORM

1. REPORT NUMBER	2. GOVT ACCESSION NO.	3. RECIPIENT'S CATALOG NUMBER
NOSC Technical Report 520 (TR 520)	AD-A089436	(9) Annual rept. no. 5

(6)

4. TITLE (and Subtitle)

ADVANCED MAIL SYSTEMS SCANNER TECHNOLOGY,

Executive Summary and Appendixes A-D.

5. TYPE OF REPORT & PERIOD COVERED

1 Oct 1978 – 9 Oct 1979

6. PERFORMING ORG. REPORT NUMBER

7. AUTHOR(s)

NOSC Sensor Processing and Analysis Division (Code 732)

8. CONTRACT OR GRANT NUMBER(s)

Agreement 104230-77-T-1604

9. PERFORMING ORGANIZATION NAME AND ADDRESS

Naval Ocean Systems Center
San Diego, California 92152

10. PROGRAM ELEMENT, PROJECT, TASK AREA & WORK UNIT NUMBERS

O, USPS, O (NOSC EE25)

11. CONTROLLING OFFICE NAME AND ADDRESS

Office of Advanced Mail Systems Development
US Postal Service, 11711 Parklawn Ave, Rockville, MD 20852
Attn: Mr J McGinn, Program Manager

(11)

12. REPORT DATE

Oct 1979

13. NUMBER OF PAGES

235

14. MONITORING AGENCY NAME & ADDRESS (if different from Controlling Office)

(12) 237

15. SECURITY CLASS. (of this report)

Unclassified

15a. DECLASSIFICATION/DOWNGRADING SCHEDULE

16. DISTRIBUTION STATEMENT (of this Report)

Approved for public release; distribution unlimited

17. DISTRIBUTION STATEMENT (of the abstract entered in Block 20, if different from Report)

18. SUPPLEMENTARY NOTES

See reverse

19. KEY WORDS (Continue on reverse side if necessary and identify by block number)

Charge coupled devices	Image storage	Self-scanned arrays
Data compression	Optical scanning	Solid-state scanners
Image acquisition	Photodiodes	Video processing
Image processing	Run length coding	

20. ABSTRACT (Continue on reverse side if necessary and identify by block number)

The objective of the effort described herein is to provide technical consultation, equipment, and support services to the US Postal Service which will contribute to the development of the system definition of a new-concept processing system, the Electronic Message Service (EMS). Included in the scope of effort are investigations of high-speed image scanning technology, image frame memory storage, image enhancement, and the fabrication of a scanner/frame-store memory test assembly. The fifth annual report briefly describes the individual efforts of the reporting period in an executive summary and provides in-depth data in four appendixes: Appendix A, Data Capture; Appendix B, Color Imaging; Appendix C, Data Display Systems Performance Analyses; and Appendix D, EDM Hardware Evaluation.

DD FORM 1 JAN 73 1473 EDITION OF 1 NOV 65 IS OBSOLETE
S/N 0102-LF-014-6601

UNCLASSIFIED

SECURITY CLASSIFICATION OF THIS PAGE (When Data Entered)

393159

18. Previous annual reports:

First Annual Report, Advanced Mail Systems Scanner Technology, Naval Electronics Laboratory Center (NELC) TR 1965, 22 October 1975, DTIC AD A020175

Second Annual Report, Advanced Mail Systems Scanner Technology, NELC TR 2020, October 1976, volume 1 (Executive Summary and Appendixes A-F), DTIC AD A039962; volume 2 (Appendix G: Proprietary Supplement, High Speed Imaging Device), DTIC AD B018468L (now released for unlimited distribution)

Third Annual Report, Advanced Mail Systems Scanner Technology, NOSC TR 170, October 1977, DTIC AD A051508

Fourth Annual Report, Advanced Mail Systems Scanner Technology, NOSC TR 358, October 1978, DTIC AD A070546

Also see:

CCD Page Reader for Mail-Scanning Applications, Final Report for period 15 March 1976 to 15 May 1977, RCA Princeton Laboratories Report PRRL-77-CR-42, DTIC A062399

Available from:
Defense Technical Information Center
Cameron Station
Alexandria, VA 22314

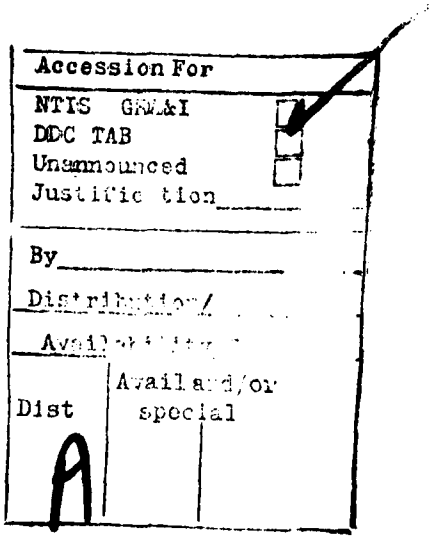

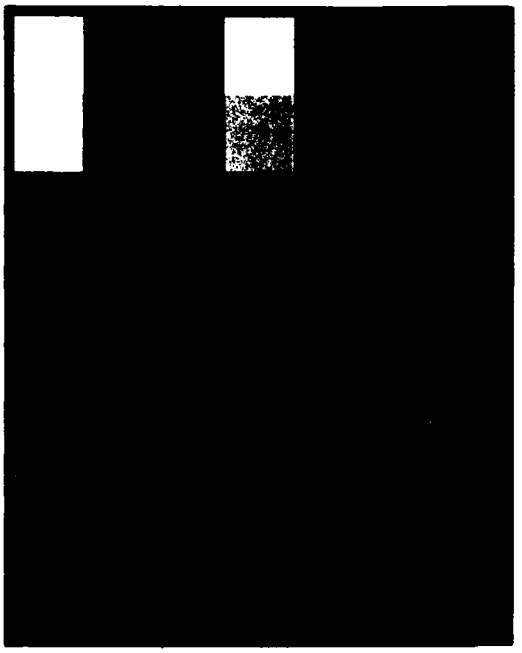

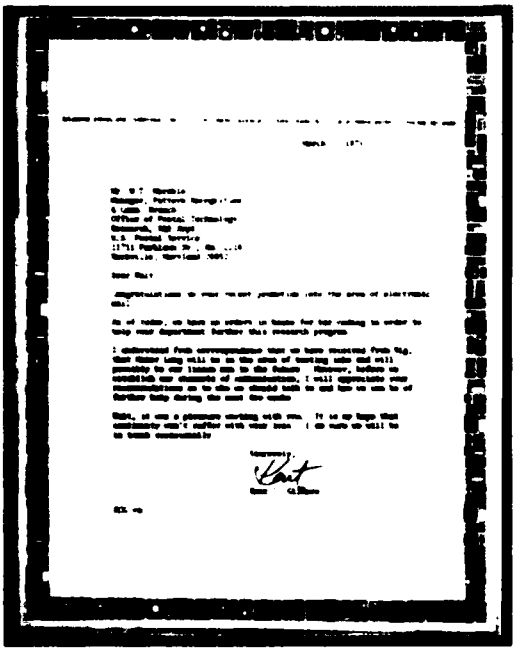

Frontispiece

OBJECTIVES

1. Provide the US Postal Service the technical consultation, equipment, and support services which will contribute to the development of the system definition of a new-concept processing system, the Electronic Message Service System (EMSS). Include in this scope of effort (1) investigations in scanner technology, image frame memory storage, and image enhancement, and (2) the design and fabrication of a scanner/frame-store memory test assembly.

2. Contribute to the selection of the most optimum imaging devices and techniques for high-speed image acquisition. Provide reliable designs of high-speed image processing logic which will preserve the quality of the image while reducing the image storage and transmission requirements and minimizing vulnerability of the image information to noise during processing, transmission, and reproduction.

3. Act as technical consultants to the USPS Office of Advanced Mail Systems Development in preparing technical requirements and statements of work and evaluating technical proposals and contractor performance; and perform technical evaluation of contractor-produced developmental equipment.

RESULTS

1. The upgrade of the ICAS was completed. The entire 25-megabit memory is now operable and capable of accepting image data at the 20-page-per-second data rate of over 500 million bits per second.

2. All planned interfaces including the Dicomed recorder, the Comtal image processor, the Tektronix disk operating system, the Wavetek waveform generator, and the HP digital multimeter are now operational.

3. Important software routines were added to the program library. These provide capability for digital filtering, minifying, and array processing of image data.

4. A characterization of a high-performance scanner, the Fairchild 2048-pel, 10-page-per-second unit, was completed, and a major report was written.

5. A laser data display subsystem for high-resolution, continuous-tone printing was evaluated and compared to a CRT – wet display subsystem.

FUTURE NOSC PLANS

1. Study and report on methods of performing high-speed document classification, particularly typed page documents.

2. Design and install a high-performance driver facility for charge-coupled device (CCD) imagers and install the Fairchild CCD 143 imager.

3. Interface, operate, and characterize the TRW 8-bit A/D converter performance.

4. Investigate methods of performing hardware illumination correction in real time.

5. Monitor the USPS contract for time-delay-and-integration (TDI) imaging device development.

CONTENTS

CONTENTS

GLOSSARY

GLOSSARY

ac	Alternating current
A/D	Analog to digital
address	Peripheral device selection or memory location specification
ALU	Arithmetic/logic unit
AMSD	Office of Advanced Mail Systems Development
ASCII	American Standard Code for Information Interchange
baud	Effective bit rate in bits per second
bit	The smallest piece of digital information – either 0 or 1
bit serial	The bits of a character are transmitted serially
bootstrap	A built-in function which eases system start-up
byte	A logical group of bits (8 is standard)
CCD	Charge-coupled device
CCPD	Charge-coupled photodiode
CPE	Central processing element
CPU	Central processing unit
CTF	Contrast transfer function
D/A	Digital to analog
dc	Direct current
DIA	Digital Image Analyzer
DIP	Dual In-line Package
DMA	Direct memory access
DPCM	Differential pulse code modulation
EAROM	Electrically alterable read-only memory
ECL	Emitter-coupled logic
EDM	Engineering development model
EMSS	Electronic Message Service System
FCU	Format Control Unit
FDS	First-difference statistics
FET	Field effect transistor
Fetch	Microroutine which retrieves MCU instructions from program memory
file	On magnetic tape, a grouping of logical records
filemark	A logical gap between tape files
firmware	System control by use of ROMs and a microprogram sequencer
fpf bit	Front-panel fetch bit; indicates that MCU instruction is from front panel
FSM	Frame-Store Memory
GFE	Government furnished equipment
GOMAC	Government Microcircuits Applications Conference

GPIB	IEEE STD 488-1975 General-Purpose Interface Bus for asynchronous data communications
Gray code	A binary code in which only one bit changes at each increment
HCU	Hard-copy unit
HIC	Hardware Illumination Corrector
Hz	Hertz; cycles per second
ICAS	Image Capture and Analysis System
IEEE	Institute of Electrical and Electronics Engineers
interrecord gap	Physical space between magnetic tape logical records
I/O	Input/output
k	1024
kW	Kilowatts
LDTB	Large Drum Test Bed
LED	Light-emitting diode
LFPM	Linear feet per minute
LIES	Laboratory Image Exploitation System
listener	A device which may receive data on the GPIB
logical record	A logical grouping of data on magnetic tape. In an image, a video line is treated as a logical record
LSI	Large-scale integration
M	Mega-; million
machine language	Operation instructions interpretable by the machine being operated
macroinstruction	A machine language instruction which initiates a sequence of basic machine operations
macrolevel	A level at which an operator may directly communicate with a machine; ie, machine language level
macroprogram	A logical sequence of macroinstructions
MARB	Memory Address Register Bus
MCU	Memory Control Unit
message	On the GPIB, a sequence of data and/or control operations transmitted
MIC	Memory Interface Card
MICC	Memory Interface Control Card
microaddress	Micromemory address
microcode	Bit-by-bit implementation of microinstructions
microcontrol	Control of individual hardware resources by use of a micro-program structure
microinstruction	A basic machine operation instruction containing control for all hardware resources (eg, data paths, registers, ALUs)
microlevel	Hardware direct-control level
micromemory	Memory (usually ROM) which contains microinstructions
micromemory address	Specification of location within a micromemory

microprogram	A logical sequence of microinstructions
microroutine	A microprogram or part thereof
MIU	Memory Interface Unit
MOS	Metal oxide semiconductor
MSB	Most significant bit
MTBF	Mean time between failures
MTF	Modulation transfer function
n	Multiplex ratio
NELC	Naval Electronics Laboratory Center
nm	Nanometre
NOSC	Naval Ocean Systems Center
ns	Nanosecond
NTC	National Telecommunications Conference
OCR	Optical Character Recognition
page	An 8½-by-11-inch acquired image or original copy
PBS	Pel brightness statistics
PC	Personality chassis
PCR	Print contrast ratio = $(r_{max} - r_{min})/r_{max}$
pel	Picture element
pixel	Picture element
PPHE	Printer and paper-handling equipment
PPHE/IU	Printer and paper-handling equipment/input unit
PPE	Printer/plotter equipment
program	Sequence of machine instructions
PROM	Programmable read-only memory
r	Reflectivity
RAC	Relative address coding
RALU	Register arithmetic logic unit
RAM	Random-access (read/write) memory
record	Logical record
RLC	Run length coding
RLS	Run length statistics
ROM	Read-only memory
s	Second
SDC	System Development Corporation
SDTB	Small Drum Test Bed
SFI	Spatial Frequency Identification
SID	Silicon imaging device
SPADE	Storage, Processing, and Display Equipment
SPIE	Society of Photo-Optical Instrumentation Engineers
t_{mac}	Memory access time
t_{mcy}	Memory cycle time
talker	A device which may transmit asynchronous data on the GPIB

TDI	Time delay and integration
TDMA	Time-division multiple access
three-wire handshake	The Hewlett-Packard patented method of guaranteeing asynchronous communication capability on the GPIB
TTL	Transistor-transistor logic
UDK	User Definable Key
USPS	United States Postal Service
UV	Ultraviolet
VTS	Video transmission system (Navy)
word	A grouping of 1 or more bytes (in the MCU, a word contains 6 bytes, or 48 bits)

RELEVANCE TO DOD MISSION

RELEVANCE TO DoD MISSION

Approval for the US Postal Service (USPS) Electronic Message Service System (EMSS) has been signed by the President for the high-speed distribution of letter mail. The concept of EMSS includes the very high-speed transmission of digital information throughout the United States on a vast network of available transmission systems. When instrumented, it will become the second largest communication and information exchange system in the US. The requirements for speed, privacy, security, reliability, and area of coverage closely parallel the requirements for several military information dissemination networks. Participation on interface aspects of the system such as imagery and facsimile transmission, buffer storage, and compressibility provides the Navy intimate familiarity. Because of this familiarity, the Navy may assist in utilization of the network for military purposes in a time of national need.

Both DoD and USPS have a requirement for high-speed dissemination of imagery-like data, and there is a multifold increase in DoD use of high-speed digital imagery transmission and soft-copy display. The expected size of digital images is increasing to include areas up to 4000 by 4000 picture elements (pels) and larger. Military requirements for continuous-tone images (photographs) and color images are placing ever-increasing demands on acquisition, storage, and display technology to provide the user with the efficient analytic tools necessary to make rapid and accurate decisions and conclusions. Hard-copy documentary records of a desirable subset of the displayed data are often required. The EMSS encompasses the same technical requirements: the need for digitization of hard-copy imagery as inputs, the buffer storage of imagery data, the transmission of compressed or uncompressed imagery data, the soft-copy display of images, and the decompression and final hard-copy printing of the received image.

The USPS Image Capture and Analysis System (ICAS) has been designed to acquire and interchange data with the NOSC video testbed in the Display Equipment Development Branch, Code 8247. Digital image tapes can be generated by scanning or converting tapes from other sources to a format compatible with the Laser Recording System located in the Marine Corps and Special Systems Branch, Code 8125. An image has been scanned, digitized, and analyzed for Code 823. Radar tapes in various configurations from Codes 8215 and Code 8247 have been accepted by ICAS and displayed. Other digital nonliteral imagery such as lofargrams, side-look sonar (SLS), and synthetic aperture radar (SAR) can be digitized, stored, analyzed, and displayed by ICAS.

A large high-speed charge-coupled device (CCD) which can operate in the time-delay-and-integration (TDI) mode is being developed for the program. This single device is capable of acquiring full-page data at a rate of 20 pages per second. The high performance of the device makes it applicable for telereconnaissance, teleguidance, battlefield surveillance, and intrusion detection as well as document imaging. Successful operation of the first-phase device was witnessed at the contractor's facility and a second contract is underway for refinement and advancement of this important work.

The very high-speed requirements resulting from the data rate standards established by the USPS have resulted in the need for high-performance special microprocessor architecture for the acquisition, correction, enhancement, storage, and display of the imagery. Very little of the work within the DoD and academic communities involves high-speed, real-time hardware and algorithm developments which support current military applications such as those listed below:

- ocean surveillance
- telereconnaissance

- teleguidance
- battlefield surveillance
- intrusion detection
- image transmission systems
- image interpretation
- pattern/character recognition
- word processing

EXECUTIVE SUMMARY

INTRODUCTION

The major goal of the total Scanner Technology Program is to identify and resolve the problems associated with producing digital equivalent images from a wide variety of hard-copy documents at very high speed. Major goals for the project at NOSC can be divided into the following three categories:

(1) High-quality image acquisition
- 20 pages per second of 8-1/2-by-11-inch sheets
- Typed, handwritten, or continuous-tone images
- Resolution of 200 by 200 (or perhaps 300 by 300) pels per inch; equal to 84×10^6 pels per second (504 megabits per second) or higher rate

(2) Image enhancement
- Edge enhancement
- Nonlinear video techniques
- Thresholding
- Color filtering

(2) Picture bandwidth compressibility techniques
- Run length encoding
- Walsh, slant, Fourier encoding
- Block void encoding

This report is the fifth in a series of annual summary reports* and covers work during the period October 1978 through September 1979. During this period the accomplishments were reasonably well balanced among the four categories of hardware, software, support, and documentation deliverables. For the most part the hardware and software accomplishments were not part of the program deliverables but were required improvements to the ICAS so that the scheduled tasks could be performed efficiently.

1979 TASKS

The accomplishments for the year ending October 1979 have been divided into four categories. The categories and the tasks within each are described in the following paragraphs.

---

*First Annual Report, Advanced Mail Systems Scanner Technology, Naval Electronics Laboratory Center (NELC) TR 1965, 22 October 1975, DTIC AD A020175

*Second Annual Report, Advanced Mail Systems Scanner Technology, NELC TR 2020, October 1976, volume 1 (Executive Summary and Appendixes A-F), DTIC AD A039962; volume 2 (Appendix G: Proprietary Supplement, High Speed Imaging Device), DTIC AD B018468L (now released for unlimited distribution)

*Third Annual Report, Advanced Mail Systems Scanner Technology, NOSC TR 170, October 1977, DTIC AD A051508

*Fourth Annual Report, Advanced Mail Systems Scanner Technology, NOSC TR 358, October 1978, DTIC AD A070546

HARDWARE ACCOMPLISHMENTS

MARK II MEMORY INTERFACE UNIT

Although some success was reported in last year's annual report regarding operation of the full 25-megabit memory, occasional problems in the consistency of data obtained from memory were experienced throughout the first quarter of this reporting period. The source was localized as a cross-talk problem in the Memory Interface Unit (MIU). Efforts to shield the 48-bit data lines and the cross-talk on address lines were unsuccessful. Therefore, a second version of the MIU was designed with special attention given to assignment of card locations and minimization of long parallel runs of signal pairs of high-speed data. The unit was completed and most of the problems associated with high-speed operation on the large image memory were resolved. Although the twisted-pair differential signal paths between the Memory Control Unit (MCU) and the MIU prevented a problem with ground loops, considerable time was spent in establishing a reliable timing and protocol interface between the MIU and the MCU. The full 25-megabit memory has now been on-line approximately 9 months with almost no failures. In the past 9 months only five of the 6144 4k X 1 MOS/RAM circuits have failed.

DISK OPERATING SYSTEM

To accommodate storage of program routines for the 4051 Graphic Computer System and the nonvolatile storage of large quantities of software or data, a Tektronix type 4907 file manager was procured and has been interfaced to the ICAS. This unit has a capacity of 630k bytes per disk and contains three disk drives total.

DICOMED INTERFACE

A digital image recorder, a Dicomed D-47, was procured and is interfaced to ICAS. The unit accommodates 4-by-5-inch film, either monochrome or color, and has adapters for Polaroid print film and 35-mm rolls. The usable film recording area is 86 mm square (3.38 by 3.38 inches). In this area an array of 4096 by 4096 spots of light exposes the film. Resolutions of 2048 and 1024 can be accommodated by writing each spot in a 2-by-2 or 4-by-4-pixel area, respectively. The unit will accept 8 bits per pel, providing a range of 256 brightness levels which may be exposed either in the normal method or in the complement (reversal) mode and will either produce a logarithmic transfer function or provide a linear exposure proportional to the input.

COMTAL INTERFACE

A Comtal Vision One digital image processor was procured by the USPS and provided for use with the NOSC ICAS. The major revision of the MCU including the upgrade of the secondary data bus provided the necessary capability to exchange data between the digital image processor and the MCU. The Vision One processor was provided with an SRL 1024-by-1024-pel color monitor. The image processor contains refresh memory for three-color, 8-bit 512-by-512-pel images to be displayed and contains two 512-by-512-by-1-bit overlay planes as well. The unit is provided with a track ball and keyboard which allow a number

of image processing functions and pseudocolor representations of images to be generated and analyzed.

EIGHT-BIT A/D CONVERTER

Although they operate at conversion rates of 60 megapixels per second and up, the four Phoenix Data A/D converters now in ICAS can only provide 6-bit data. For experiments in advanced illumination correction, it was felt desirable to test the applicability of an 8-bit A/D converter and its possible alleviation of the imaging device odd-even problem. The principal component of this converter is the TRW 8-bit A/D device model TDC 1007J. This 8-bit converter will provide nominally 30 megasamples per second. An accompanying demonstration board was procured. This unit is now being interfaced to ICAS. The relative value of utilizing 8-bit pel data for acquisition and illumination correction will be discussed in an ICAS upgrade report in April 1980.

OTHER INSTRUMENTATION INTERFACES

Two other instrumentation interfaces were incorporated into ICAS for the purpose of characterizing such components as A/D converters and imaging device responses. The first of these is the model 175 waveform generator. This unit provides arbitrary waveforms of precisely controlled amplitudes and rise times, since these are generated digitally. With this equipment it was possible to generate some precision slowly varying voltage ramps which were quite useful in characterizing the Phoenix Data A/D converters. The second instrument used in conjunction with the characterization was the HP 3455A digital multimeter. This equipment has a microprocessor-controlled 5-1/2-digit integrating digital voltmeter that measures dc volts, ac volts, and resistance and can make readings at rates up to 24 per second. Both of these instruments are tied to IEEE 488 (HP GPIB) interface.

HARDWARE ACCOMPLISHMENTS SUMMARY

The configuration of the control circuits for ICAS in the time period about mid-1978 is shown in figure ES1(a). The corresponding upgraded control circuits at the end of this reporting period are all shown in ES1(b). This represents a vast improvement in ICAS capability and versatility. Figure ES2 shows the present data flow for ICAS.

The principal components of ICAS are contained in a four-bay rack mount. Previous equipment assignments within the racks were reported in appendix D of the Fourth Annual Report, 1978. Figure ES3 shows the present rack equipment assignments within ICAS. The major ICAS peripheral equipments are shown on figure ES4. The Comtal Vision One image processing equipment can operate in a stand-alone mode. Once loaded with an image, its memory can refresh the color monitor. The keyset and track ball can then be used to perform manipulation of the stored image data.

Because of current software limitations, the Tektronix 4051 cannot presently be used to perform independent functions while the display system is being used to support ICAS operation. With some program software modifications, stand-alone operations could be accommodated. When ICAS is not running, of course, the 4051 is capable of operating in a stand-alone mode in conjunction with the auxiliary cartridge tape recorder, the file manager, and the joystick.

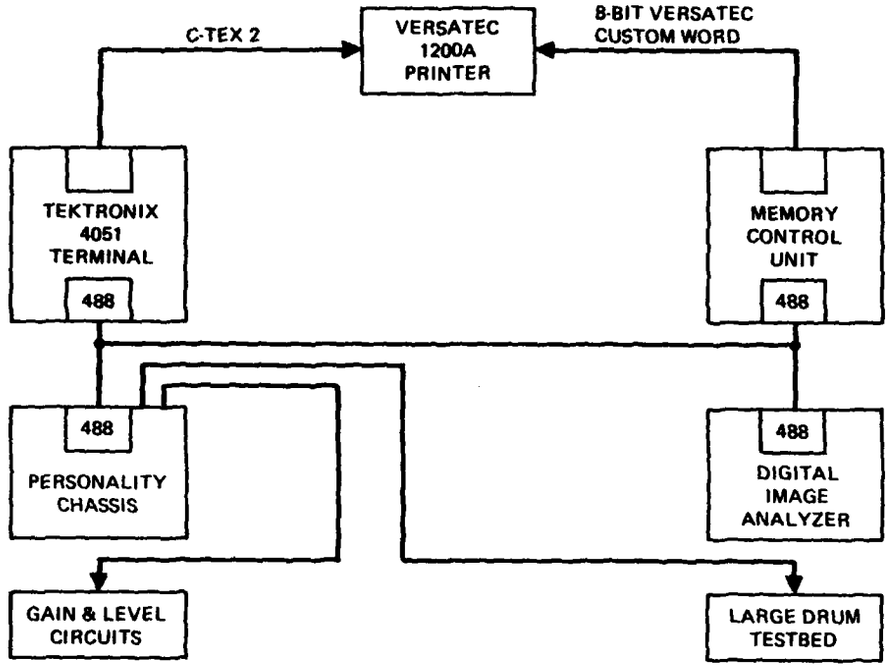

Figure ES1(a). ICAS control circuits (1978).

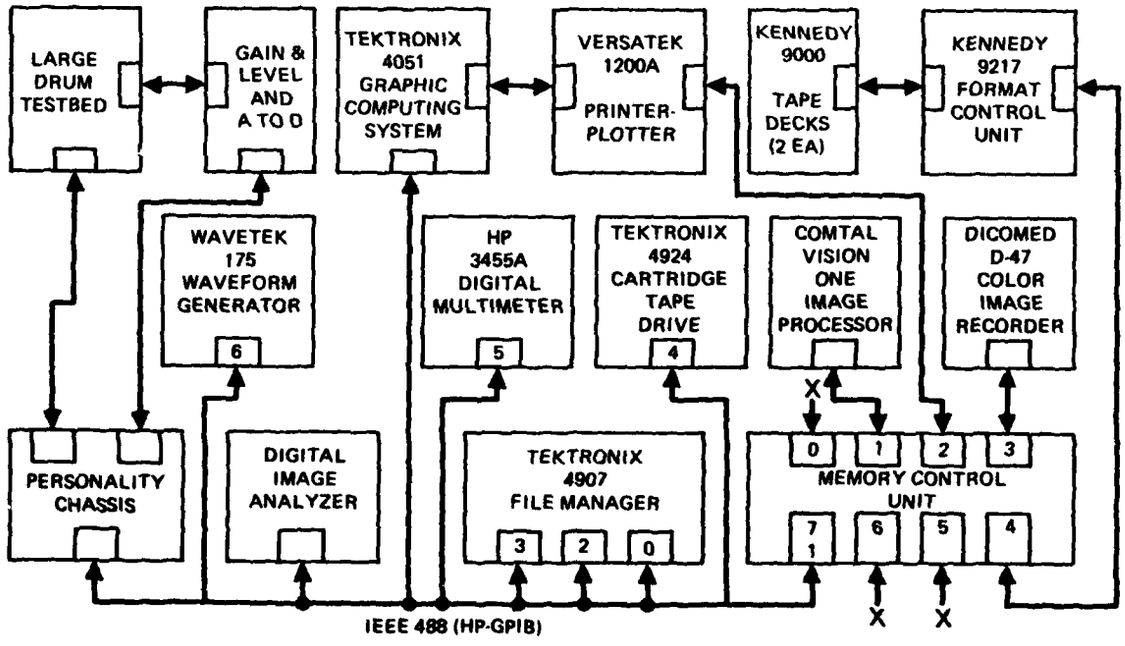

Figure ES1(b). ICAS control circuits (1979).

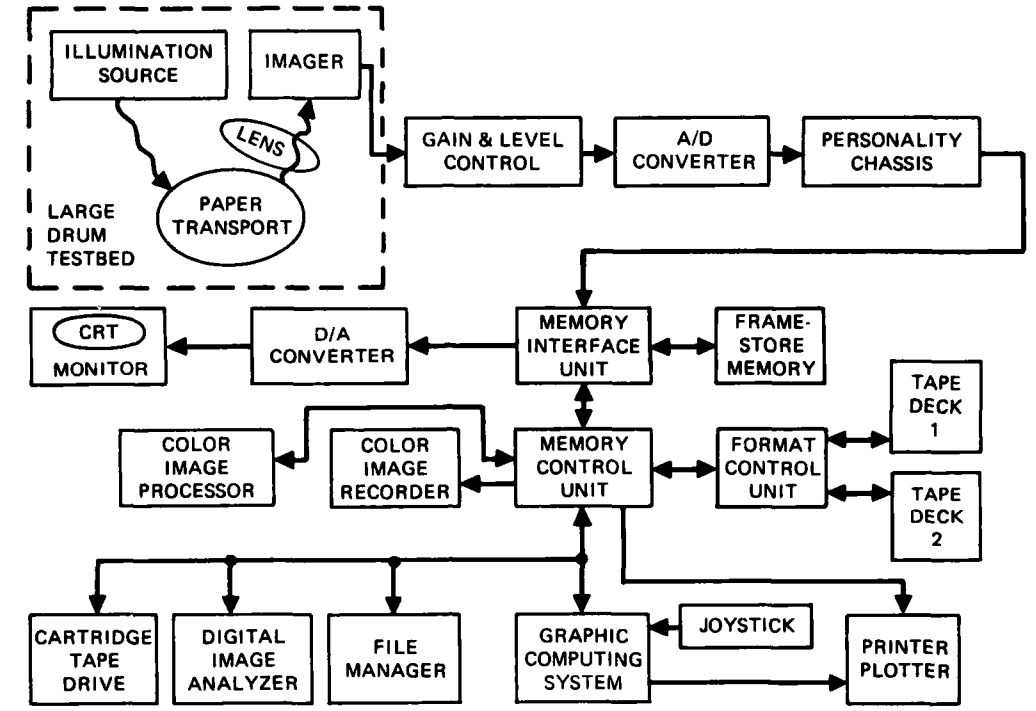

Figure ES2. ICAS data flow.

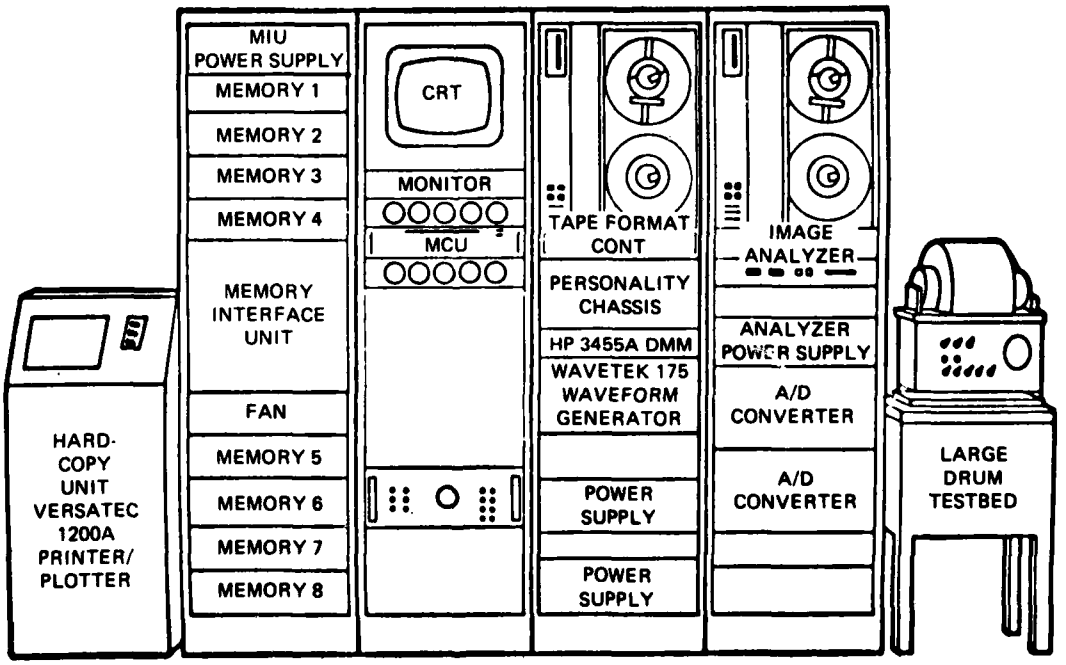

Figure ES3. ICAS equipment configuration.

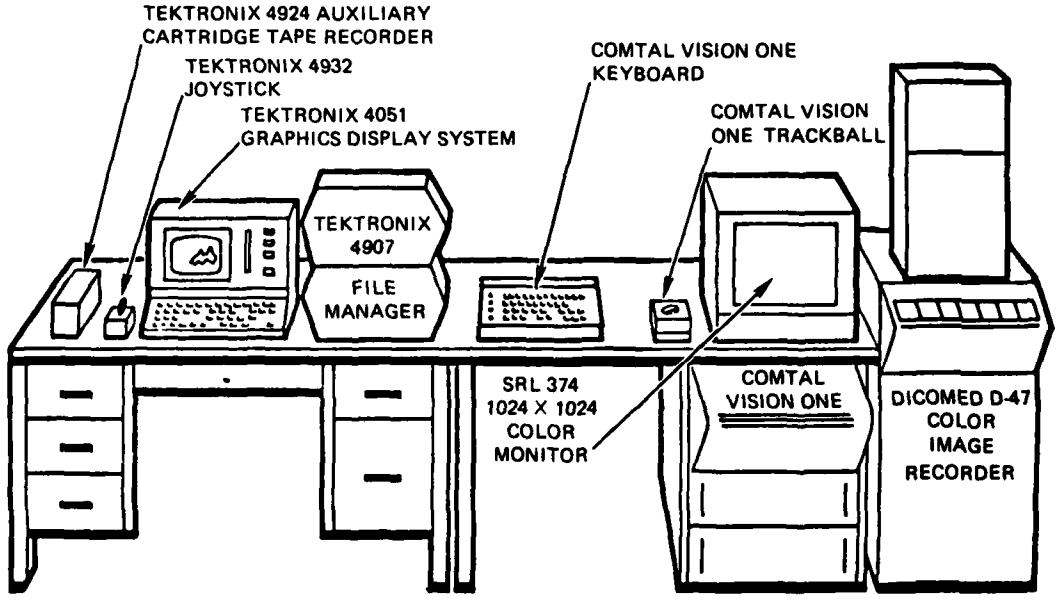

Figure ES4. Major ICAS peripheral equipments.

SOFTWARE ACCOMPLISHMENTS

MICROPROGRAMMED MEMORY TEST ROUTINE

Immediately following the beginning of operations with the 25-megabit image memory, it became obvious that there was a need for a comprehensive automatic test of the operability of all memory components. For this reason a microprogrammed memory test routine was developed which could produce patterns of ones, zeros, walking ones, etc, for evaluating and isolating the location of defective memory components. As mentioned in the hardware section, the infant mortality problems have been overcome, and only five devices have been replaced in the last 9 months.

ARRAY PROCESSING SOFTWARE

Appendix A of this report describes data capture interim studies which included an analysis of system noise associated with the imaging device, A/D converters, and analog circuits in ICAS. Part of this study included an examination of the noise of white standard material and the repeatability of the ICAS output to produce duplicate image acquisitions with a fixed nonmoving white standard target. The array processing software includes the spatial frequency identification (SFI) capability which was discussed in the 1978 Annual Report. The new array processing solutions which can be accommodated are as follows: arithmetic mean, mean deviation, quadratic mean, difference (the difference between two SFI vectors), normalization (conversion of one data set mean value to another mean value), and mean squared difference.

IMAGE MINIFY ALGORITHM

The purpose in generating the image minify algorithm was to allow full-page USPS images to be visible on medium-performance cathode ray tube (CRT) monitor displays. The size of a full-page image at 200 by 200 pixels per inch is 1700 by 2200 pixels. There does not exist a CRT monitor system which will provide a flicker-free display of digital images having these dimensions. It was felt useful then to provide a program for ICAS which, by combining a number of adjacent pixels, would provide a minified image having dimensions of approximately 480 pixels on a side which is visible in its entirety for inspection on a conventional CRT monitor.

SELECTIVE FILTER ALGORITHM

A careful analysis of ICAS image data revealed that a considerable amount of low-amplitude, high-spatial-frequency activity was present in the image data. The amplitude of this signal was found to be one or two of the 64 possible brightness levels. The spatial frequency was found to be very nearly at the Nyquist limit. Probably the greatest contributor to this was the odd-even problem (in the imaging device and driver characteristics), which was not completely nullified by the illumination correction process. For this reason a selective filter algorithm was written which allows an operator to optionally remove certain small excursions having higher frequency components and examine the remainder of the data for cosmetic degradation or improvement as a result. Tests have shown that using the selective filter at the Nyquist limit and filtering out only amplitudes having one brightness level of excursion improved the compressibility of the data by approximately 35%.

SUPPORT DELIVERABLES

FAIRCHILD SCANNER CHARACTERIZATION

A major accomplishment for FY79 was the characterization of the Fairchild CCD scanner. Acceptance tests by USPS for the scanner were successfully completed in the spring of 1979. The unit was then shipped to NOSC to operate in conjunction with ICAS. The purpose of this characterization was to determine the expanded applicability of the analog portions of the circuitry and the optically abutted CCDs to acquire continuous-tone imagery as well as the bilevel facsimile acquisitions for which the unit was designed. Appendix D of this report contains a detailed discussion and the results of this test.

SUPPORT TO INTELPOST

One team member, Mr Bob Basinger, was tasked to interface with the USPS in Washington, DC, to provide assistance on the INTELPOST project. The purpose of the visit was to become familiar with the software requirements for INTELPOST and to assist in writing the technical portions of a tentative software specification for an RFP to be forwarded to the INTELPOST office.

MMMIT PROPOSAL REVIEW

Two team members, Mr Frank Martin and Mr Lee Wise, participated in a proposal review in response to an RFP for a multimedia message input terminal to be designed and fabricated for the US Postal Service R&D Center.

LARGE DRUM TEST BED

A new upgraded large drum testbed (LDTB) has been designed. Fabrication is underway. This drum was built specifically for the use of RCA Princeton, New Jersey, for characterization of the time-delay-and-integration (TDI) charge-coupled device (CCD) arrays. This testbed provides the accurate document velocity control required for exacting characterization measurements of the time-delay-and-integration process.

DOCUMENTATION DELIVERABLES

DATA BASE CATALOG

A document data base catalog was generated in 1978 to provide archival records pertaining to the image documents used in the USPS studies. This record existed in the form of magnetic tape. During 1979, the data base was completely revised, updated, and placed on a disk file in the Tektronix file manager. This file is updated continually to provide a reference source for up-to-date information on each image processed.

GOMAC PRESENTATION AND PAPER

In 1979 a team member, Mr Tom Little, gave a presentation to the Government Microcircuits Applications Conference (GOMAC). The architecture and processing capabilities of ICAS were described. The goals of the USPS and the EMSS program were also explained.

DATA CAPTURE INTERIM REPORT

The Data Capture Interim Report is included herein as appendix A. The purpose of this report was to characterize the performance of A/D converters and also to study white standard acquisition improvements. The noise of the ICAS system was characterized and the data are presented in detail in this appendix.

COLOR IMAGING REPORT

The Color Imaging Report is included herein as appendix B. The purpose of this report was to determine the basic differences in the acquisition of monochrome and color imagery. The report describes initial attempts to acquire color imagery. The report identifies two major problem areas in ICAS. One of these is the stability of the analog gain and level circuits. The other is the stability and uniformity of the illumination source. Details of this work and a few captured color images are included in this appendix.

LASER PRINTER EVALUATION

During 1979 an opportunity existed to participate in an evaluation of the comparison of a laser printer to a cathode ray tube printer. This work was done for the Naval Oceanography Command Facility (NOCF). The primary data base for the report consisted of a standardized test pattern. Secondary standards included weather data printouts made over approximately a 5-month period. The results of this study are contained in appendix C of this report. The major conclusion of the report is that the laser printer system tested at NOCF is superior to the existing CRT printer system at that facility.

FAIRCHILD SCANNER REPORT

During the summer, the scanhead and card cage (but not the page store memory) was shipped from Fairchild Syosset to NOSC for evaluation of the Fairchild scanner with ICAS. The purpose of this evaluation was to investigate the possibility of utilizing a CCD type scanner for high-speed acquisition of monochrome photographic imagery. Both the Fairchild scanner and ICAS performed very well and much useful data were obtained. The results of this evaluation are discussed in appendix D of this report. The major conclusion of this study was that a very uniform illumination source was required unless an illumination algorithm will be used to compensate for the resulting input data anomalies.

APPENDIX A:

DATA CAPTURE

by
RW Basinger
Code 7323
Naval Ocean Systems Center

CONTENTS

ILLUSTRATIONS

TABLES

INTRODUCTION

In previous reports, image acquisition problems have been noted, the most obvious effects of which have been illumination roll-off at the edges of the page and the racing stripes resulting from subsequent illumination correction. The term "racing stripes" is used to describe vertical striations in image intensity, sometimes extending the full height of an acquired image. This report is the result of an investigation conducted in an attempt to characterize the present weaknesses in, and subsequently improve upon, the image acquisition performance.

OBJECTIVE

The objective of the task was to localize the source of input acquisition error in ICAS. The factors considered to be the most likely causes of acquisition problems are nonuniformity of the white standard used for illumination correction; temporal variation in illumination intensity; and differential nonlinearity of A/D converter response characteristics, ie, nonuniform step sizes. The first two of these factors do not affect an image until the illumination correction, and the third has no obvious cosmetic effect (disregarding, for the moment, any effect on compressibility). A procedure was therefore devised to attempt to isolate the magnitudes of the errors introduced by the specific error sources. Cursory examination of the initial results of the tests indicated that the intensity time instability and white standard nonuniformity probably contributed only negligibly to the "racing stripe" problem, compared to A/D differential nonlinearity. It was therefore decided to first characterize the A/D converters.

A/D CONVERTER CHARACTERIZATION

Goals

The initial A/D converter analysis objective was a static threshold characterization. It was hoped that these results would lead to an explanation and possible solutions to the apparent differential nonlinearity problem.

Test Setup

For the purpose of the A/D analysis, the analog input to the A/D was moved from the imaging electronics output to the output of a Wavetek 175 Arbitrary Waveform Generator. The 175 is programmable via the IEEE-488 interface bus, allowing automatic control of the test procedure. An analog resolution of 1 mV from the signal source was desired; however, the 175 is capable of only three-digit resolution (eg, $\pm$5 mV at 1 volt). Therefore, a slow ramp from -2 V to +2 V (digital levels 0 to 63) was programmed into the 175, yielding a resolution of $\sim$1 mV. In order to verify the analog output, an HP-3455A digital voltmeter (DVM) was connected to the interface bus, allowing continuous monitoring of both analog and digital levels. A simplified diagram of the ICAS test configuration is shown in figure A1.

Programmable Instrumentation Software

A software procedure was written to support the A/D converter analysis test. The program was written to standardize the initialization and sequential steps through the test procedure with a minimum of operator interaction.

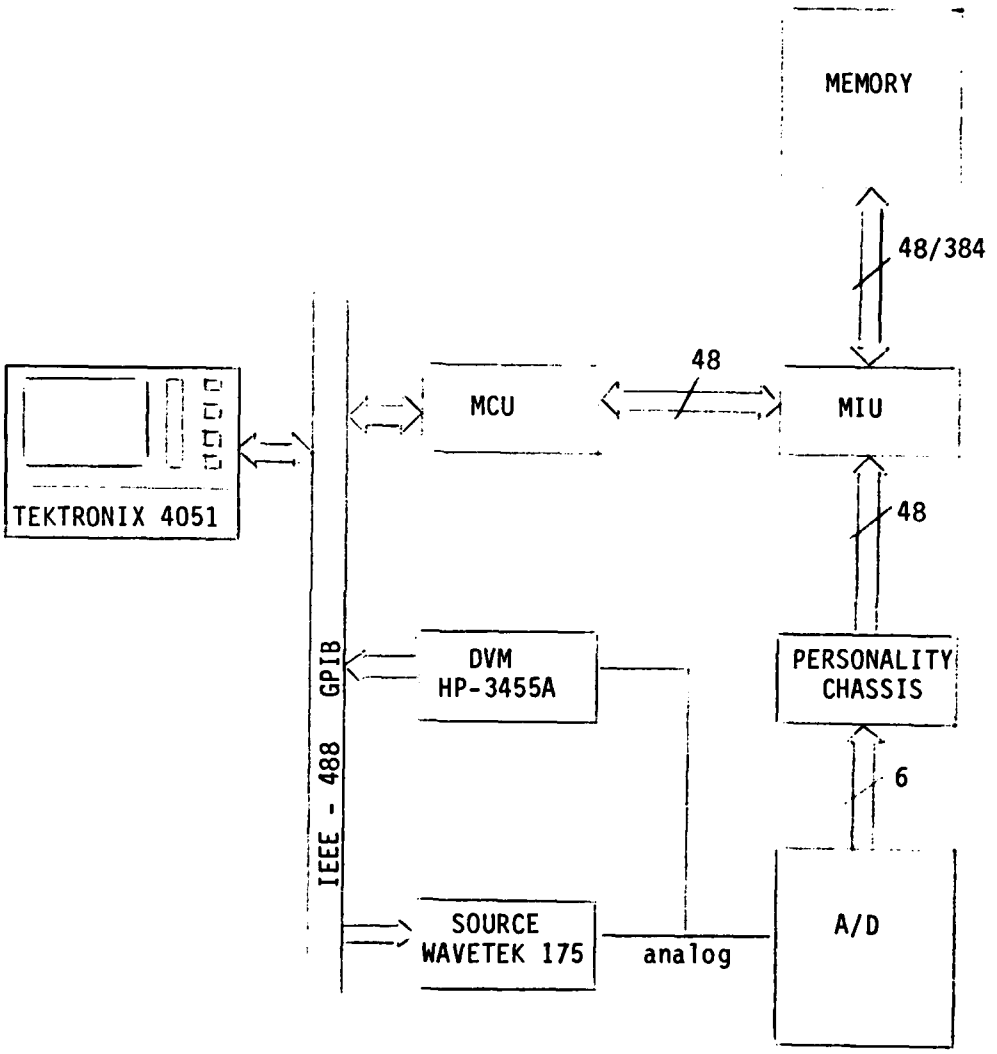

Figure A1. Image Capture and Analysis System (ICAS) test configuration.

Test Procedure

The test procedure was as follows:

1. Initialize the Wavetek 175 source by issuing a command to start the ramp. The ramp is started somewhat below -2 V to allow time to settle into a steady ramp. The voltage is then read from the HP-3455A DVM until -2 V is reached.

2. Issue a command to capture one line which will enable verification that the initial digital level is, in fact, zero.

3. Sample the 3455A output until it is at least 1 mV higher than the reading at which the last capture line command was output.

4. Output another capture one line command, then input the digital value from the Memory Control Unit (MCU). If this value is the same as the previous digital value, then return to step 3. If it is exactly one level higher than the previous value, then note the voltage from the previous step 3 as being the transition point for the new digital value. If the new digital level is less than 63, then return to step 3; otherwise this portion of the test is complete.

5. Repeat steps 1 to 4 using a ramp downward from +2 V to -2 V.

Results

The result of this procedure was a pair of tables of transition points which were used to generate tables of step sizes. The procedure was performed twice for each of the four A/D channels in the ICAS. Annex A contains complete data for both runs on one A/D in both graphic and tabular form.

Figure A2 shows a breakdown of the results of this testing method. Figure A2a shows the low end of the converter characteristic. The T points are the transition points; eg, T_{1-0} is the voltage at which the output code changes from 1 to 0. Figure A2b shows the method of interpreting step sizes. "Monotonic" step sizes are the differences in transition voltages between two successive output codes; eg, S_{U33} is the difference between T_{32-33} and T_{33-34} and S_{D31} is the difference between T_{32-31} and T_{31-30}. Hysteresis step sizes are a measure of the input voltage variation allowed without altering the output code. For example, once an output code of 32 is achieved, the input voltage may vary between T_{32-31} and T_{32-33} without altering the output code; hence, $S_{H32} = T_{32-33} - T_{32-31}$.

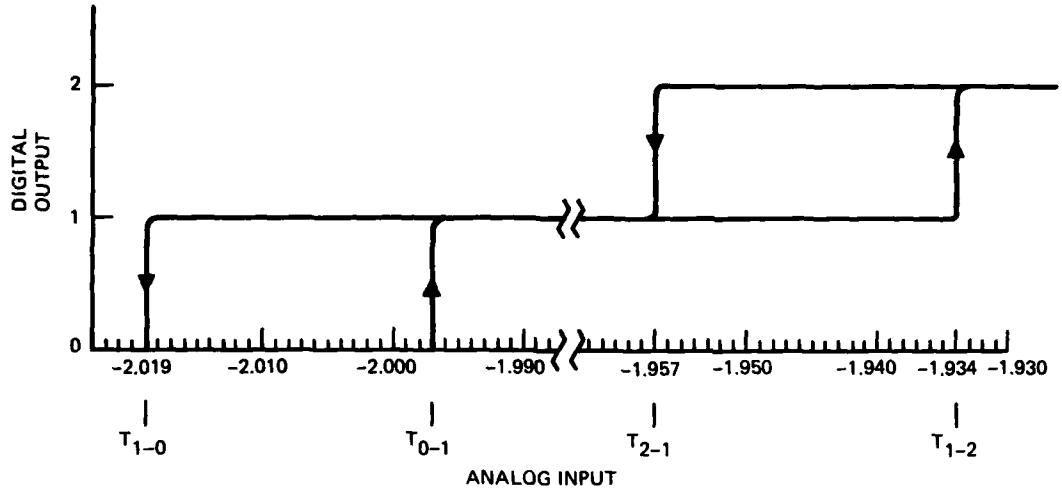

Figure A2a. Low end of A/D converter response characteristic.

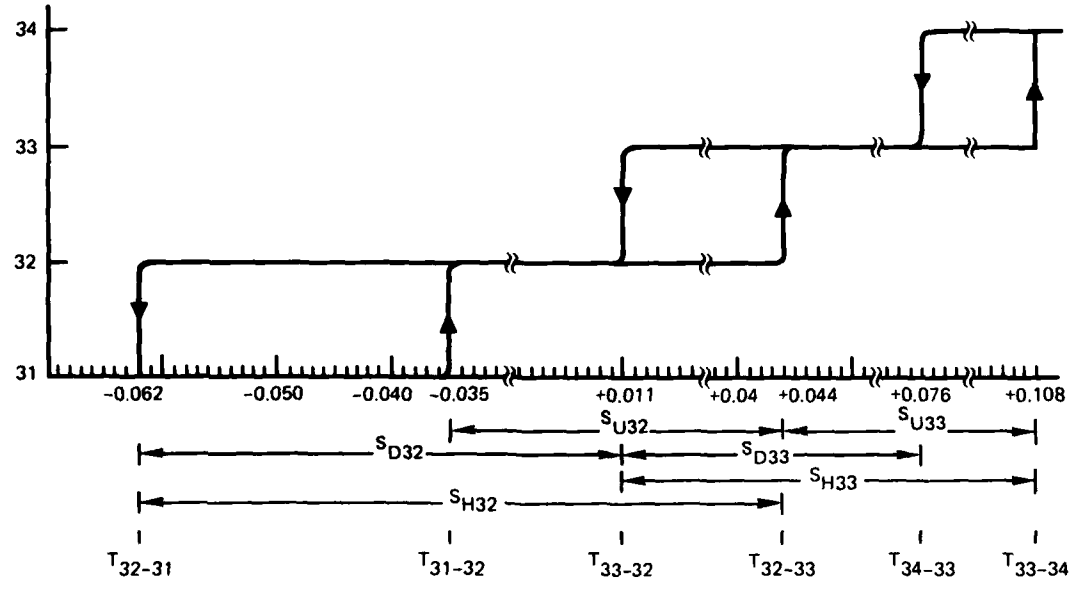

Figure A2b. Step size determination.

A/D differential nonlinearity

Of significant interest is the differential linearity, or lack of it, of the A/D converters, as nonlinearity can greatly contribute to acquisition errors. The plots of step sizes in annex A readily demonstrate a great lack of differential linearity, with a range of half to twice the specified step size. The most obvious manifestation of this problem can be seen in a plot of a standard illumination curve (fig A3). Those levels with smaller than normal step sizes result in sharper rises in the level of the curve, while the larger step sizes cause flat spots in the curve, as shown in figure A3 (levels 49 and 60, respectively). This effect can, in illumination correction, cause undesirable results when applied to image data at digital levels having different analog step sizes, due to a corresponding increase in sensitivity to small input voltage fluctuations. These quantization errors are better observed in the error characteristics of the converters. Figure A4 is a plot of the error characteristic for one A/D channel, output levels 24 to 31. The theoretical solid codes are represented by tick marks on the centerline. The A/D converters in ICAS have a specified accuracy of $\pm 1/2$ least significant bit (lsb) $\pm 0.75\%$ of full scale. One lsb is 62.5 mV and full scale is 4 volts, yielding an error specification of ± 61.25 mV, which is almost one full step size (nominal). In figure A4, this value is at midpoint on both the positive and negative error scales. As readily seen, the error is almost exclusively positive in this input voltage range and, in fact, exceeds the specified error for several output codes. Another interesting effect can be seen in the hysteresis effects on the error characteristic. For example, the downward transition from output level 27 to level 26 occurs at a lower input voltage than the upward transition from level 25 to 26, giving a hysteresis characteristic as such:

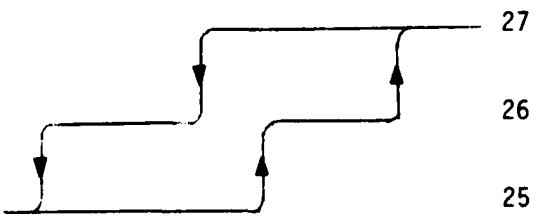

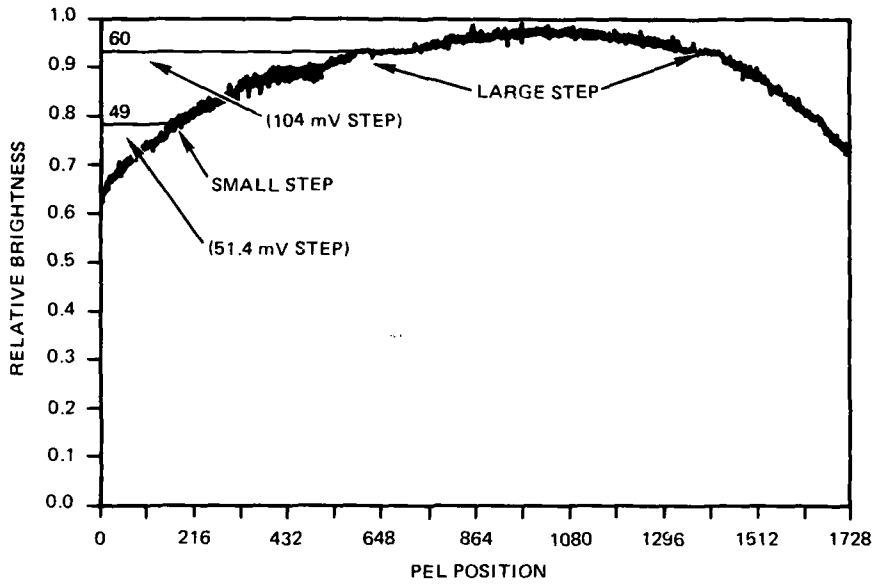

Figure A3. Illumination profile sample.

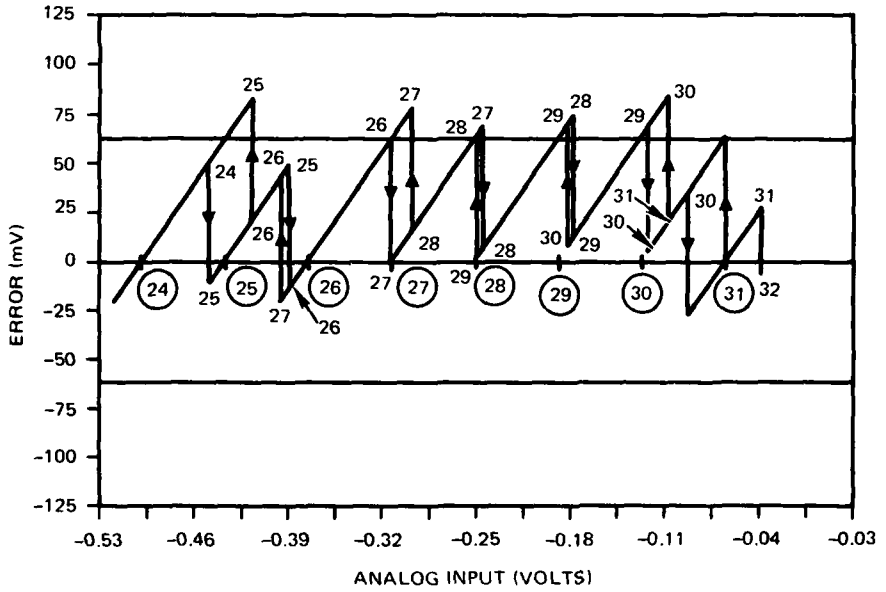

Figure A4. Error characteristic – A/D 0, run 1. Plot of output levels 24 to 31.

Annex B contains error characteristic plots for each of the four A/D converters.

Measurement error

Sources of error in the measurement process must be accounted for. These error sources are an interdependent combination of measurement accuracy and procedural errors. The measurement error in the DVM is about 65 μV (worst case). Amplitude errors in the waveform generator output voltage are ±40.5 mV (worst case). This, however, is compensated for in the procedure design. The procedure cannot compensate for amplitude errors due to generator timing inaccuracy, but this amplitude error is only about 0.16 mV (worst case).

The only significant error source is in the measurement procedure. The maximum sample rate is about three samples per second ($\approx$ 350 ms/sample). The analog voltage is increased by 0.156 mV every 50 ms, or about 1.1 mV for each sample taken. In addition, the digital value acquisition requires about 150 ms, allowing another increase of about 0.5 mV. This indicates that as much as a 2-mV error is possible in determination of transition voltages. This error is not cumulative but can account for up to 2 mV of inconsistency between runs of the procedure. As can be seen in the first two tables in annex A, the average magnitude of the discrepancy between runs is 1.575 mV for the up ramp and 0.925 mV for the down ramp. This includes an inexplicable discrepancy of 19 mV at the level 57 to level 58 transition, which if eliminated from the results lowers the average by about 0.3 mV. On the average, therefore, the discrepancies are within the 2 mV possible due to procedural errors.

WHITE STANDARD ACQUISITION IMPROVEMENTS

Goals

Following the A/D converter test, an attempt was made to upgrade the illumination correction process by improving white standard acquisition. From the knowledge gained about the A/D nonlinearities and consistency of response (flat spots and repeatability), meaningful tests characterizing the white standard target material, the illumination source, and amplified sensor output signal could be devised.

Test Plan

The test plan was devised to provide control of the parameters affecting the form and amplitude of the white standard calibration curve. These parameters were the illumination source Variac current, the spatial coordinates of the white standard area used, and a logical strategy for partitioning each of two passes at each of eight intensity level settings into subsets for more detailed analysis of short-term stability. Figure A5 indicates the white standard segmentation scheme. The eight rectangles on the left represent the same repeated area, used in all the 16 scans of the 256 lines, each of which was 1700 pels long. One of the 256-by-1700 areas is shown exploded into four equal segments on the right of the figure. Nomenclature of the subsets is given.

Spatial frequency identification (SFI) is a process used in document analysis to detect row and/or column statistics. Only SFI_h or horizontal spatial frequency data have been acquired for this test. The term SFI(I2P2 [0-63]) indicates a horizontal vector containing vertical sums of the respective pel brightnesses in each of the 1700 pel positions in the first 64 lines taken during pass two at intensity level two. In this manner four average brightness profile curves are generated and stored which are in turn added together to provide an aggregate brightness profile curve for the entire 256-by-1700 white standard area (SFI(I2P2)).

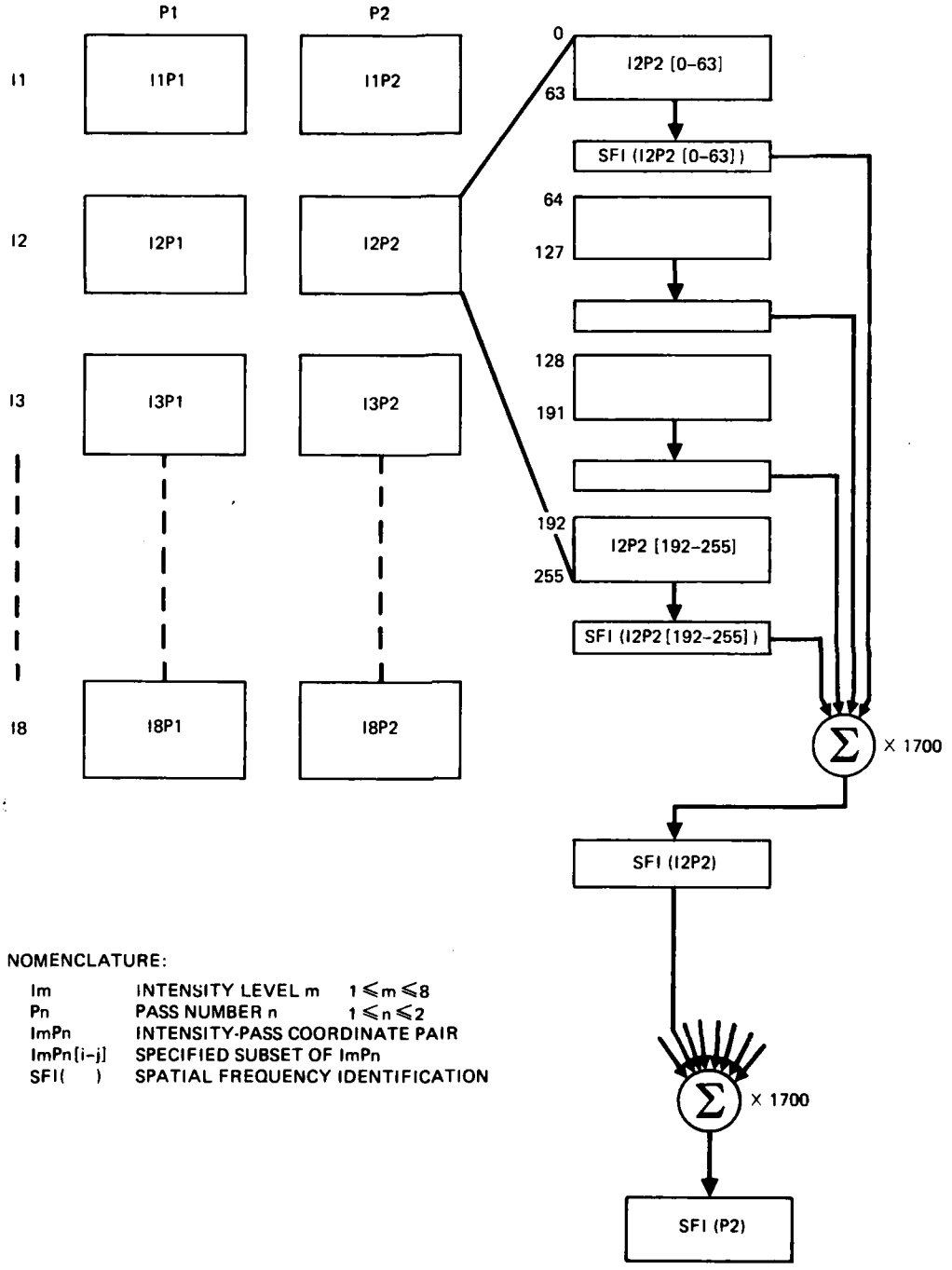

Figure A5. White standard image segmentation scheme.

Array Processing Software

Some meaningful mathematical relationships are needed to measure the statistical results of the white standard acquisition test. Since a large number of measurements and comparisons were involved, array processing software was written for the Tektronix 4051 Terminal. This software controls the Memory Control Unit (MCU) and the memory in ICAS and provides reasonable processing rates for simple one-dimensional arrays of data.

The array processing software package was written to allow the manipulation of the spatial frequency characteristics on an element-by-element basis with a single operator command. It also allows the calculation of basic statistical values based on these sets of data (henceforth referred to as vectors).

For the results required in these tests, comparison of one such vector with respect to others was required. The software was written so that the arithmetic operations of addition, subtraction, multiplication, or division of each pair of terms in two vectors can be executed by utilizing a simple operator command. A series of such commands provides the statistical values shown in table A1.

Room is provided in memory for nine vectors, or variables, each referred to by one of the alphabetic labels A to I. Each vector may consist of up to 2048 elements of up to 48 bits each. (For the purposes of this task only 1700 elements were required.) The following operations may be performed on the data of concern.

Table A1. Array processing definitions.

1. SFI statistics

For a given image X, each pel being labelled $X_{i,j}$ (i = line, j = pel position) where:
$0 \leq i < m$ and $0 \leq j < n$

$$SFI_j(X) = \sum_{i=0}^{m-1} X_{i,j} \quad (0 \leq j < n)$$

For the purposes of this report, m=256 (in most cases) and n=1700. Also, $SFI_j(X)$ may be abbreviated as S_j.

For a given SFI vector S:

2. Arithmetic Mean

$$\bar{S} = \frac{1}{n} \sum_{j=0}^{n-1} S_j$$

3. Mean deviation

$$\bar{D}_s = \frac{1}{n} \sum_{j=0}^{n-1} |S_j - \bar{S}|$$

4. Quadratic mean

$$\bar{Q}_s = \left(\frac{1}{n} \sum_{j=0}^{n-1} S_j^2\right)^{1/2}$$

For two given SFI vectors, S and T:

5. Difference C=S-T

$$C_j = S_j - T_j \qquad (0 \leq j < n)$$

6. Normalization T to S

$$\hat{T}_j = (\bar{S}/\bar{T}) \times T_j \qquad (0 \leq j < n)$$

7. Mean-square difference

$$MSD = \left(\frac{1}{n} \sum_{j=0}^{n-1} (S_j - T_j)^2\right)^{1/2}$$

or, for C = S-T

$$MSD = \left(\frac{1}{n} \sum_{j=0}^{n-1} C_j^2\right)^{1/2} = \bar{Q}_c$$

1. Place SFI data in a vector.
2. Generate a vector from a line of image.
3. Perform vector-vector arithmetic operations.
4. Perform vector-scalar arithmetic operations.
5. Generate statistical values (table A1).

With this complement of operations, it was possible to compare any SFI characteristic to any other. For example, to find the difference in characteristic between a 256-line characteristic and a 64-line characteristic, the following operations are required (and diagrammed in fig A6):

1. Place 256-line SFI characteristic in Vector A.
2. Place 64-line SFI characteristic in Vector B.
3. Normalize Vector B to Vector A and place in Vector C.
4. Subtract Vector C from Vector A and place in Vector C.
5. Calculate statistics for Vector C.

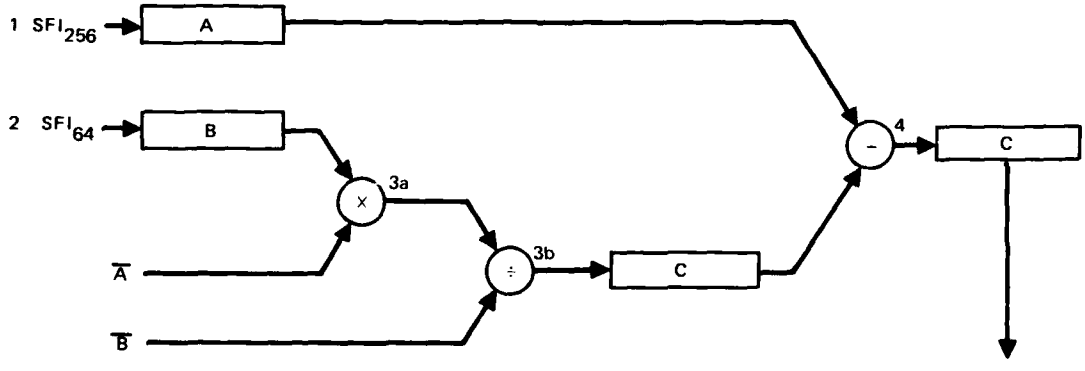

Figure A6. Method of comparing SFI characteristics.

Test Procedure

The first step was to acquire 16 segments of white standard image (256 lines each), two segments at each of eight different illumination intensity levels. These segments will be referred to as IrPs, r representing the intensity and s the pass number. The white standard was mounted on the drum, which was then positioned to the page sync mark to provide a known starting point for acquisition of successive segments. The illumination was then set to I1 and segment I1P1 was acquired and stored on magnetic tape. The drum was then repositioned to the drum sync mark and, without adjusting illumination intensity, I1P2 was acquired and saved on tape. The illumination intensity was then set to I2, following which I2P1 and I2P2 were acquired and saved on tape, repositioning to the drum sync mark before each acquisition. This procedure was repeated for intensity levels I3 to I8.

The next step was to calculate the spatial frequency identification (SFI) statistics for the acquired white standard images. First, the SFI statistics were calculated for the first 64 lines of I1P1 (ie, I1P1 [0-63]) and saved on tape. This was repeated for successive blocks of 64 lines of I1P1, yielding four files of SFI data. These four data sets were then added together, giving the overall SFI characteristic for I1P1, which was also saved on tape. This procedure was repeated for each of the 16 segments, in the order in which they were acquired (ie, I1P2, I2P1, ..., I8P2), yielding a total of 80 data files. The summation of all-intensity levels for each pass was then performed, giving two more data files, ie, $\sum$ SFI (IiP1) and $\sum$ SFI (IiP2), for the overall characteristic of each of the two passes at the various illumination levels. With this complete set of SFI statistics it became possible to analyze variation in white standard acquisition spatially, temporally, and, with appropriate scale factors, across intentional and unintentional changes in intensity.

Results

This section includes an explanation of the tabulated data followed by an attempt to relate the data to the white standard acquisition process.

Table A2 contains data based upon spatial position, time, and intensity of illumination. Vertically (in the table), the white standard images of 256 lines each are divided into four groups of 64 lines each. This is done for each of the eight illumination intensities. Horizontally, the first and third columns contain the average digital output value for the specified groupings, for passes one and two, respectively. All statistics shown in table A2 are normalized as defined in table A1 to a single average brightness level.

The second column contains the difference in average output level between the two passes. The fourth and fifth columns contain $\overline{D}$ and $\overline{Q}$ for the difference between pass one and pass two of the entire 256-line segment. For example, for I1, $\overline{D}$ = 0.15, meaning that, on the average, a single pel in pass one differed from the corresponding pel in pass 2 by 0.15 brightness level, after normalizing pass two to the same average level as pass one. This is done in an attempt to determine variation over time and intensity.

Table A3 contains a summarization of the spatial dependence data. Columns 1, 2, and 3 contain the differences in average intensity level between the first group of 64 lines and each other group of 64 lines in each of the 256-line segments, as well as the differences for corresponding comparisons in pass one and pass two. Column 6 contains the average level of the intensity-pass combination and, again, the difference between the two passes. Columns 4 and 5 contain $\overline{D}$ and $\overline{Q}$ for the tabulated difference data.

Table A2. Spatial position and illumination intensity comparisons.

		Pass I $\bar{X}$	$\Delta_{1,2}$	Pass 2 $\bar{X}$	$\hat{P1-P2}$ $\bar{D}$	$\bar{Q}$
I1	(00-63)	56.61	.28	56.89		
	(64-127)	56.70	.25	56.95		
	(128-191)	56.58	.37	56.95		
	(192-255)	56.39	.34	56.73		
I1		56.57	.32	56.89	0.15	0.18
I2	(00-63)	55.96	.18	56.14		
	(64-127)	56.05	.15	56.20		
	(128-191)	55.98	.12	56.10		
	(192-255)	55.79	.15	55.94		
I2		55.95	.14	56.09	0.08	0.09
I3	(00-63)	55.51	.70	56.21		
	(64-127)	55.34	.86	56.20		
	(128-191)	55.68	.54	56.22		
	(192-255)	55.47	.46	55.93		
I3		55.59	.55	56.14	0.22	0.26
I4	(00-63)	54.92	.41	55.33		
	(64-127)	54.90	.46	55.44		
	(128-191)	54.71	.62	55.33		
	(192-255)	54.53	.68	55.21		
I4		54.77	.56	55.33	0.28	0.22
I5	(00-63)	55.25	-.20	55.05		
	(64-127)	55.37	-.26	55.11		
	(128-191)	55.30	-.27	55.03		
	(192-255)	55.21	-.38	54.83		
I5		55.28	-.27	55.01	0.19	0.22
I6	(00-63)	54.78	.22	55.00		
	(64-127)	54.79	.31	55.10		
	(128-191)	54.73	.23	54.96		
	(192-255)	54.53	.42	54.95		
I6		54.71	.29	55.00	0.20	0.22

Table A2 (cont)

		Pass 1 $\bar{X}$		Pass 2 $\bar{X}$	$P1 - \hat{P2}$ $\bar{D}$	$\bar{Q}$
I7	(00-63)	54.71	-.67	54.04		
	(64-127)	54.77	-.53	54.24		
	(128-191)	54.69	-.57	54.12		
	(192-255)	54.45	-.49	53.96		
I7		54.66	-.57	54.09	0.22	0.27
I8	(00-63)	53.81	.06	53.87		
	(64-127)	53.86	.09	53.87		
	(128-191)	53.67	.05	53.72		
	(192-255)	53.76	.22	53.54		
I8		53.77	.00	53.77	0.03	0.03
Average all I						
	(00-63)	55.19	.13	55.32		
	(64-127)	55.22	.15	55.37		
	(128-191)	55.17	.11	55.28		
	(192-255)	55.02	.12	55.14		
Overall Average		55.16	.13	55.29	0.06	0.07

	[00-63]-[64-127]	[00-63]-[128-191]	[00-63]-[192-255]	$\bar{D}$	$\bar{Q}$	$\bar{I}$
I1P1	0.09	-0.03	-0.22	0.11	0.14	56.57
I1P2	0.06	0.06	-0.16	0.10	0.10	56.89
2-1	-0.03	0.09	0.06	0.05	0.06	0.32
I2P1	0.09	0.02	-0.17	0.10	0.11	55.95
I2P2	0.06	-0.04	-0.20	0.09	0.12	56.09
2-1	-0.03	-0.06	-0.03	0.01	0.04	0.14
I3P1	-0.17	0.17	-0.04	0.12	0.14	55.59
I3P2	-0.01	0.01	-0.28	0.12	0.16	56.14
2-1	0.16	-0.16	-0.24	0.16	0.19	0.55
I4P1	-0.02	-0.21	-0.39	0.12	0.26	54.77
I4P2	0.11	0.00	-0.12	0.09	0.09	55.33
2-1	0.13	0.21	0.27	0.05	0.21	0.56
I5P1	0.12	0.05	-0.04	0.06	0.08	55.28
I5P2	0.06	-0.08	-0.22	0.09	0.14	55.01
2-1	-0.06	-0.13	-0.18	0.04	0.13	-0.27
I6P1	0.01	-0.05	-0.25	0.10	0.15	54.71
I6P2	0.10	-0.04	-0.05	0.06	0.07	55.00
2-1	0.09	0.01	0.20	0.07	0.13	0.29
I7P1	0.06	-0.02	-0.26	0.12	0.15	54.66
I7P2	0.20	0.08	-0.08	0.10	0.13	54.09
2-1	0.14	0.10	0.18	0.03	0.14	-0.57
I8P1	0.05	-0.14	-0.05	0.06	0.09	53.77
I8P2	0.08	-0.15	-0.33	0.14	0.21	53.77
2-1	0.03	-0.01	-0.28	0.13	0.16	0.00
P1	0.03	-0.02	-0.17	0.08	0.10	55.16
P2	0.03	-0.04	-0.18	0.08	0.11	55.29

Table A3. Spatial position and illumination intensity comparisons.

Table A4 contains more detailed data on the differences in the characteristics at different intensities. This includes $\overline{D}$ and $\overline{Q}$ for the differences of the different intensities normalized to the same average level. When one set of data is normalized to another and the difference taken, the result is the difference in the fine variation between the original two sets.

Referring to table A2, it is first seen that there is actually a drift in the intensity level between the two passes at the same nominal intensity. This drift ranges from -0.57 level to +0.56 level. The results in table A2 also indicate that fine structure in the curve is dependent upon absolute magnitude of the curve. Two curves, when normalized to the same average level, yield a $\overline{D}$ roughly proportional to the difference between the averages of the original curves. For example, at I1 the average levels for passes one and two were 56.57 and 56.89, respectively, or 0.32 difference. $\overline{D}$ in this case is 0.15. At I2, where the difference between the average levels is only 0.14, $\overline{D}$ is only 0.08, or about half that at I1. Similarly, the overall average for pass one and pass two is only 0.13 and $\overline{D}$ is only 0.06. A preliminary interpretation, from table A2 alone, is that an illumination standard acquired and averaged over several intensity levels would have the greatest reliable consistency in fine structure.

In table A3, the primary entries are measurements of spatial differences. Sixty-four lines represents approximately 1/3 inch of copy. The results in table A3 indicate that the first three each 1/3-inch segments are of roughly equal reflectivity ($\pm$0.03 level in average brightness). The fourth segment, however, is of noticeably higher average brightness. The average increase is less than one-fifth of a brightness level, but it must be considered as a possible source of error. While $\overline{D}$ and $\overline{Q}$ cannot in this case be interpreted directly in terms of brightness levels, they do provide

a measure of the consistency of results. $\overline{D}$ is a relative measure of consistency of the differences between 1/3-inch segments, while $\overline{Q}$ is a relative measure of the magnitude of the differences. These values provide the following indications:

1. Good consistency in the results of the spatial comparison ($\overline{D}$ for IXP1, IXP2) indicates reliability of the brightness dependence upon spatial position.

2. Good consistency in $\overline{D}$ for IXP2 - IXP1 indicates that the spatial dependence is fairly consistent between passes despite a drift in average brightness.

3. $\overline{Q}$ for IXP2-1XP1 indicates a wide variation (0.04 to 0.21) in the magnitude of the spatial dependence between passes.

4. Once again the greatest consistency is realized from an average over all intensity levels against drift over time and against spatial position.

Table A4 provides an indication of the dependence of fine structure upon absolute intensity. Referring to the $\overline{I}$ column in table A2, it can be seen that the greatest consistency in fine structure of the illumination curve occurs in cases with the most similar original intensity averages. For example, I5P2 and I6P2 acquisitions were separated by several minutes and a deliberate alteration of the nominal intensity (as the difference between I5P1 and I6P1). Intensity drift (presumably) brought the actual level back to 0.01 level average difference, yielding a $\overline{D}$ of 0.02. I5P1 and I6P1 were taken at approximately the same interval, yet have an average brightness difference of 0.57 and a (normalize-subtract) $\overline{D}$ of 0.32. This is a definite indication that fine structure in an illumination curve is directly dependent upon the magnitude of the intensity. Here, also, the greatest consistency is seen in the comparison of a full pass with each of its subsets (normalized).

Table A4. Difference in characteristics at various intensities.

	$\bar{D}$	$\bar{Q}$		$\bar{D}$	$\bar{Q}$
I1P1 - $\hat{I}$2P1	.22	.27	I1P2 - $\hat{I}$2P2	.21	.28
$\hat{I}$4P1	.30	.37	$\hat{I}$3P2	.22	.27
$\hat{I}$4P1	.30	.37	$\hat{I}$4P2	.29	.35
$\hat{I}$5P1	.30	.37	$\hat{I}$5P2	.27	.34
$\hat{I}$6P1	.30	.37	$\hat{I}$6P2	.28	.35
$\hat{I}$7P1	.31	.38	$\hat{I}$7P2	.30	.37
$\hat{I}$8P1	.26	.33	$\hat{I}$8P2	.25	.32
I2P1 - $\hat{I}$3P1	.19	.22	I2P2 - $\hat{I}$3P2	.05	.06
$\hat{I}$4P1	.32	.39	$\hat{I}$4P2	.26	.32
$\hat{I}$5P1	.27	.32	$\hat{I}$5P2	.28	.36
$\hat{I}$6P1	.33	.39	$\hat{I}$6P2	.29	.37
$\hat{I}$7P1	.34	.40	$\hat{I}$7P2	.28	.35
$\hat{I}$8P1	.27	.33	$\hat{I}$8P2	.26	.32
I3P1 - $\hat{I}$4P1	.31	.37	I3P2 - $\hat{I}$4P2	.24	.31
$\hat{I}$5P1	.19	.21	$\hat{I}$5P2	.29	.35
$\hat{I}$6P1	.32	.39	$\hat{I}$6P2	.29	.36
$\hat{I}$7P1	.33	.40	$\hat{I}$7P2	.28	.34
$\hat{I}$8P1	.26	.32	$\hat{I}$8P2	.25	.31

Table A4 (cont)

	$\overline{D}$	$\overline{Q}$		$\overline{D}$	$\overline{Q}$
I4P1 - $\hat{I}$5P1	.28	.32	I4P2 - $\hat{I}$5P2	.20	.23
$\hat{I}$6P1	.07	.09	$\hat{I}$6P2	.22	.25
$\hat{I}$7P1	.10	.12	$\hat{I}$7P2	.33	.40
$\hat{I}$8P1	.22	.30	$\hat{I}$8P2	.29	.40
I5P1 - $\hat{I}$6P1	.32	.36	I5P2 - $\hat{I}$6P2	.02	.03
$\hat{I}$7P1	.33	.38	$\hat{I}$7P2	.28	.36
$\hat{I}$8P1	.30	.35	$\hat{I}$8P2	.26	.33
I6P1 - $\hat{I}$7P1	.05	.06	I6P2 - $\hat{I}$7P2	.28	.36
$\hat{I}$8P1	.22	.30	$\hat{I}$8P2	.27	.33
I7P1 - $\hat{I}$8P1	.22	.30	I7P2 - $\hat{I}$8P2	.14	.17
P1 - $\hat{I}$1P1	.18	.23	P2 - $\hat{I}$1P2	.17	.21
$\hat{I}$2P1	.19	.23	$\hat{I}$2P2	.15	.20
$\hat{I}$3P1	.17	.21	$\hat{I}$3P2	.15	.19
$\hat{I}$4P1	.19	.18	$\hat{I}$4P2	.17	.21
$\hat{I}$5P1	.19	.23	$\hat{I}$5P2	.16	.20
$\hat{I}$6P1	.19	.14	$\hat{I}$6P2	.16	.20
$\hat{I}$7P1	.15	.11	$\hat{I}$7P2	.20	.24
$\hat{I}$8P1	.17	.11	$\hat{I}$8P2	.17	.20

CONCLUSIONS

Because of the nature of the problem, ie, several (possibly interdependent) potential sources of error, no conclusions can be drawn from these data. It is only possible to recognize correlation between the data and cosmetic characteristics symptomatic of underlying sources of error. The most obvious correlation is drawn between the nonuniformity in the white standard image and the nonuniformity of A/D converter step sizes. Temporal drift, causing alteration of characteristics in the illumination intensity, is also indicated. Although relatively insignificant, there also appears to be a slight spatial variation in the standard image.

Recommendations for improvement of white standard acquisition, and therefore image acquisition and correction, are as follows:

1. Attempt to decrease the differential nonlinearity of the A/D converters. This would smooth the basic illumination curve, decreasing the sensitivity to small fluctuations at levels with noticeably smaller than normal step sizes.

2. Acquire and average white standard data in such a way as to mitigate any characteristics peculiar to one intensity or one spatial position. The probable procedure would be to repeat the experiment, acquiring 256 lines at each of eight intensity levels (preferably over a wider range than used here), then normalizing this result so that the peak value of the curve is at the saturation level.

ANNEX A TO APPENDIX A

This annex contains the complete data for one converter channel (one run). Each of the other three converters displays similar characteristics (eg, differential nonlinearity). Complete data for all converters are on file and available at NOSC, Code 7323.

The first two pages of this annex show the differences in transition points between the two runs. These are included to demonstrate repeatability of the procedure.

LEVEL	VALUE	LEVEL	VALUE	LEVEL	VALUE	LEVEL	VALUE
0	-0.0007	16	0.0016	32	-0.0014	48	0.0007
1	0.0006	17	-0.0007	33	-0.0044	49	0.0006
2	-0.0010	18	-0.0014	34	0.0015	50	-0.0027
3	-0.0010	19	-0.0004	35	-0.0009	51	0.0004
4	-0.0020	20	0.0021	36	-0.0005	52	-0.0009
5	-0.0030	21	-0.0002	37	-0.0030	53	-0.0049
6	-0.0025	22	-0.0002	38	0.0001	54	-0.0009
7	-0.0012	23	-0.0010	39	-0.0032	55	0.0011
8	0.0007	24	0.0006	40	-0.0010	56	0.0003
9	-0.0045	25	0.0021	41	-0.0016	57	0.0002
10	-0.0023	26	-0.0023	42	-0.0006	58	0.0190
11	-0.0010	27	-0.0001	43	-0.0024	59	-0.0019
12	-0.0009	28	-0.0003	44	-0.0015	60	0.0021
13	-0.0017	29	-0.0005	45	0.0007	61	-0.0006
14	0.0003	30	-0.0003	46	0.0005	62	-0.0008
15	-0.0014	31	-0.0007	47	-0.0004	63	0.0007

TRANSITION POINTS – A/D 0 – RUN 2 – UP RAMP
DIFFERENCES BETWEEN RUN 1 AND RUN 2
SERIAL NUMBER B1051 (60 MHz)

LEVEL	VALUE	LEVEL	VALUE	LEVEL	VALUE	LEVEL	VALUE
0	0.0004	16	0.0012	32	-0.0007	48	0.0022
1	0.0013	17	0.0005	33	0.0010	49	0.0001
2	0.0004	18	0.0016	34	0.0010	50	0.0004
3	0.0002	19	-0.0004	35	0.0004	51	0.0019
4	-0.0008	20	0.0015	36	0.0006	52	0.0011
5	0.0004	21	-0.0005	37	-0.0016	53	0.0000
6	0.0005	22	-0.0005	38	0.0015	54	-0.0008
7	0.0002	23	-0.0004	39	0.0003	55	-0.0001
8	0.0005	24	-0.0013	40	0.0022	56	-0.0001
9	-0.0011	25	-0.0006	41	0.0001	57	0.0015
10	-0.0001	26	0.0018	42	0.0011	58	-0.0001
11	-0.0001	27	0.0004	43	0.0013	59	0.0010
12	-0.0001	28	0.0006	44	0.0004	60	0.0010
13	-0.0003	29	-0.0004	45	0.0012	61	-0.0006
14	0.0020	30	-0.0014	46	-0.0016	62	0.0001
15	-0.0012	31	-0.0002	47	0.0001	63	0.0002

TRANSITION POINTS – A/D 0 – RUN 2 – DOWN RAMP
DIFFERENCES BETWEEN RUN 1 AND RUN 2
SERIAL NUMBER B1051 (60 MHz)

LEVEL	VALUE	LEVEL	VALUE	LEVEL	VALUE	LEVEL	VALUE
0	-2.0000	16	-1.0295	32	-0.0355	48	1.0055
1	-1.9978	17	-0.9727	33	0.0439	49	1.0569
2	-1.9349	18	-0.9166	34	0.1081	50	1.1109
3	-1.8780	19	-0.8525	35	0.1543	51	1.1668
4	-1.8048	20	-0.7663	36	0.2284	52	1.2531
5	-1.7436	21	-0.6865	37	0.2958	53	1.3102
6	-1.6905	22	-0.6503	38	0.3742	54	1.3755
7	-1.6406	23	-0.6078	39	0.4039	55	1.4428
8	-1.5505	24	-0.5206	40	0.4908	56	1.5168
9	-1.4816	25	-0.4489	41	0.5378	57	1.5561
10	-1.4236	26	-0.3881	42	0.6095	58	1.6329
11	-1.3679	27	-0.3130	43	0.6483	59	1.6950
12	-1.2939	28	-0.2434	44	0.7291	60	1.7986
13	-1.2359	29	-0.1754	45	0.7816	61	1.8361
14	-1.1729	30	-0.1202	46	0.8534	62	1.8991
15	-1.1093	31	-0.0910	47	0.9166	63	1.9514

TRANSITION POINTS – A/D 0 – RUN 1 – UP RAMP
SERIAL NUMBER B1051 (60 MHz)

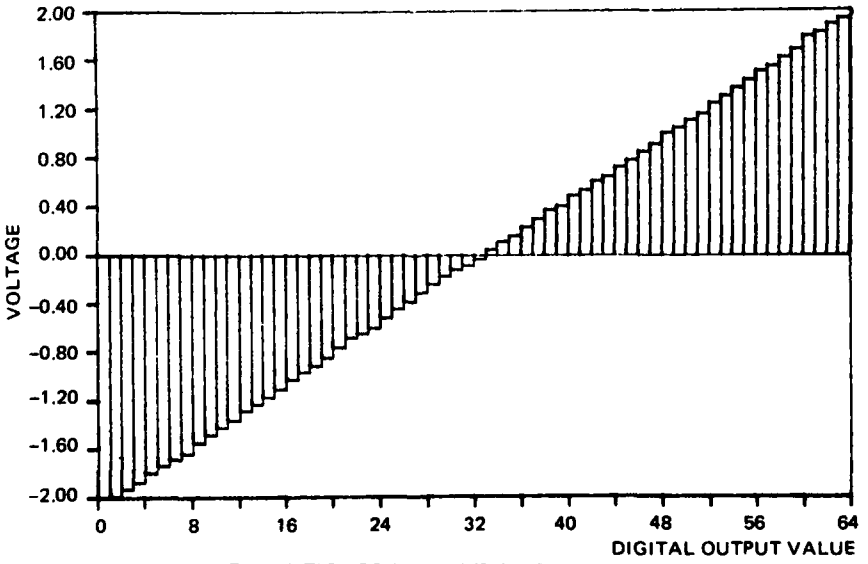

TRANSITION POINTS – A/D 0 – RUN 1 – UP RAMP
SERIAL NUMBER B1051 (60 MHz)

LEVEL	VALUE	LEVEL	VALUE	LEVEL	VALUE	LEVEL	VALUE
0	0.0022	16	0.0568	32	0.0794	48	0.0514
1	0.0629	17	0.0561	33	0.0642	49	0.0540
2	0.0570	18	0.0642	34	0.0462	50	0.0560
3	0.0732	19	0.0862	35	0.0741	51	0.0862
4	0.0612	20	0.0798	36	0.0674	52	0.0571
5	0.0531	21	0.0362	37	0.0784	53	0.0654
6	0.0499	22	0.0425	38	0.0297	54	0.0672
7	0.0901	23	0.0872	39	0.0868	55	0.0741
8	0.0688	24	0.0717	40	0.0470	56	0.0393
9	0.0581	25	0.0609	41	0.0718	57	0.0768
10	0.0557	26	0.0751	42	0.0388	58	0.0621
11	0.0839	27	0.0696	43	0.0808	59	0.1036
12	0.0481	28	0.0680	44	0.0525	60	0.0375
13	0.0630	29	0.0552	45	0.0718	61	0.0630
14	0.0636	30	0.0293	46	0.0632	62	0.0524
15	0.0799	31	0.0555	47	0.0889	63	0.0486

MONOTONIC STEP SIZES – A/D 0 – RUN 1 – UP RAMP
SERIAL NUMBER B1051 (60 MHz)

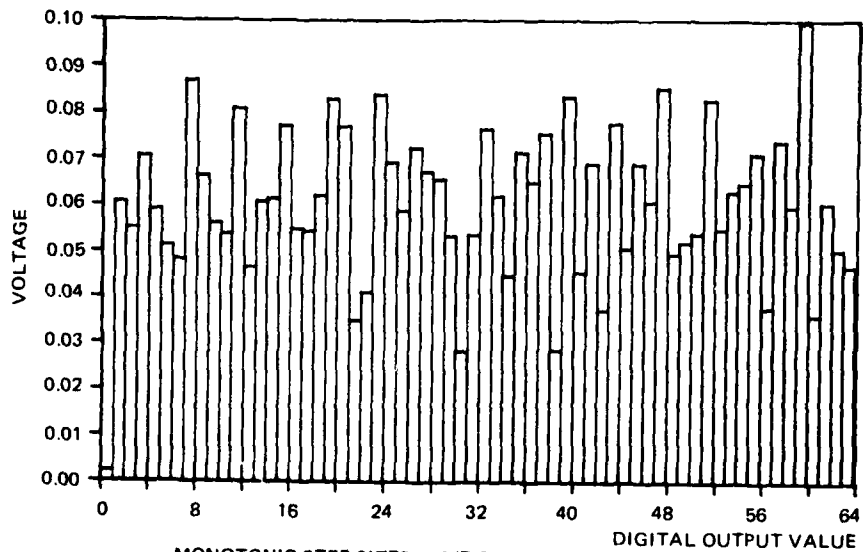

MONOTONIC STEP SIZES – A/D 0 – RUN 1 – UP RAMP
SERIAL NUMBER B1051 (60 MHz)

LEVEL	VALUE	LEVEL	VALUE	LEVEL	VALUE	LEVEL	VALUE
0	-2.0198	16	-0.9835	32	0.0113	48	1.0422
1	-1.9576	17	-0.9200	33	0.0760	49	1.1071
2	-1.9003	18	-0.8821	34	0.1252	50	1.1589
3	-1.8281	19	-0.7960	35	0.2120	51	1.2454
4	-1.7627	20	-0.7355	36	0.2672	52	1.3019
5	-1.7095	21	-0.6788	37	0.3383	53	1.3664
6	-1.6442	22	-0.6344	38	0.3865	54	1.4055
7	-1.5666	23	-0.5504	39	0.4810	55	1.4963
8	-1.5151	24	-0.4780	40	0.5384	56	1.5489
9	-1.4574	25	-0.4162	41	0.5948	57	1.6182
10	-1.4135	26	-0.3946	42	0.6402	58	1.6377
11	-1.3186	27	-0.2965	43	0.7215	59	1.7413
12	-1.2486	28	-0.2466	44	0.7804	60	1.8104
13	-1.1891	29	-0.1791	45	0.8526	61	1.8625
14	-1.1424	30	-0.1042	46	0.8980	62	1.9201
15	-1.0519	31	-0.0619	47	0.9918	63	2.0009

TRANSITION POINTS – A/D 0 – RUN 1 – DOWN RAMP
SERIAL NUMBER B1051 (60MHz)

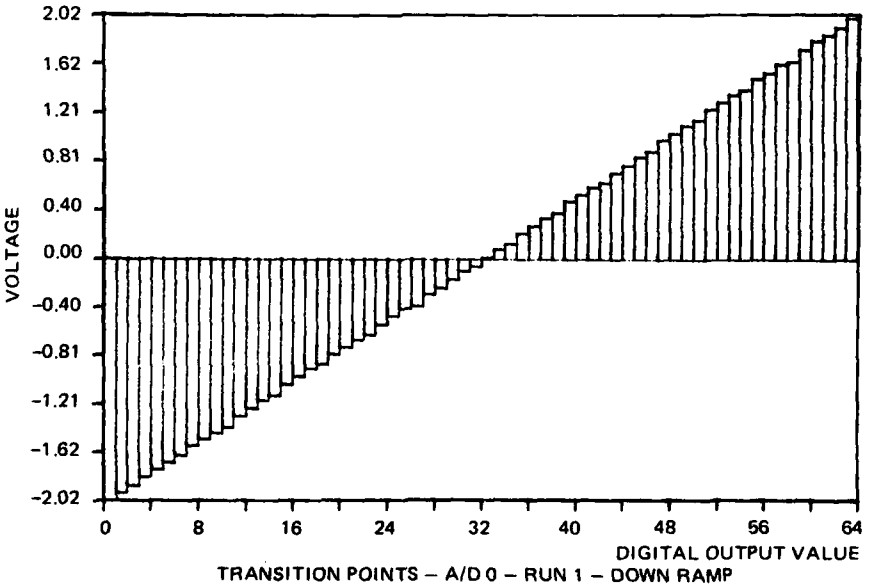

TRANSITION POINTS – A/D 0 – RUN 1 – DOWN RAMP
SERIAL NUMBER B1051 (60 MHz)

LEVEL	VALUE	LEVEL	VALUE	LEVEL	VALUE	LEVEL	VALUE
0	0.0000	16	0.0685	32	0.0732	48	0.0505
1	0.0623	17	0.0635	33	0.0647	49	0.0649
2	0.0573	18	0.0379	34	0.0492	50	0.0518
3	0.0722	19	0.0861	35	0.0868	51	0.0865
4	0.0655	20	0.0605	36	0.0552	52	0.0565
5	0.0532	21	0.0567	37	0.0712	53	0.0645
6	0.0653	22	0.0444	38	0.0482	54	0.0392
7	0.0776	23	0.0840	39	0.0945	55	0.0908
8	0.0515	24	0.0724	40	0.0574	56	0.0526
9	0.0576	25	0.0619	41	0.0564	57	0.0693
10	0.0439	26	0.0215	42	0.0454	58	0.0195
11	0.0950	27	0.0981	43	0.0813	59	0.1036
12	0.0700	28	0.0499	44	0.0589	60	0.0691
13	0.0595	29	0.0675	45	0.0721	61	0.0521
14	0.0467	30	0.0749	46	0.0455	62	0.0576
15	0.0905	31	0.0423	47	0.0938	63	0.0809

MONOTONIC STEP SIZES – A/D 0 – RUN 1 – DOWN RAMP
SERIAL NUMBER B1051 (60 MHz)

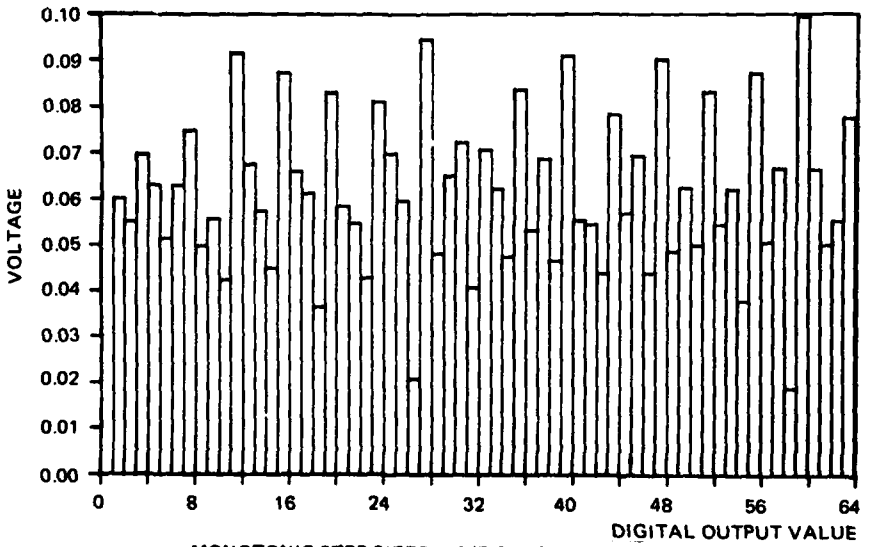

MONOTONIC STEP SIZES – A/D 0 – RUN 1 – DOWN RAMP
SERIAL NUMBER B1051 (60 MHz)

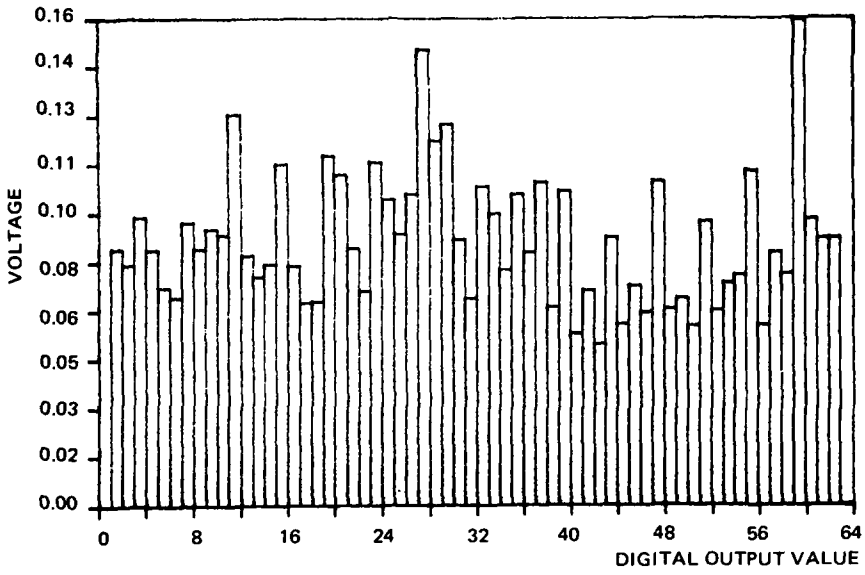

HYSTERESIS STEP SIZES – A/D 0 – RUN 1
SERIAL NUMBER B1051 (60 MHz)

LEVEL	VALUE	LEVEL	VALUE	LEVEL	VALUE	LEVEL	VALUE
0	0.0000	16	0.0792	32	0.1058	48	0.0651
1	0.0849	17	0.0669	33	0.0967	49	0.0686
2	0.0796	18	0.0675	34	0.0783	50	0.0597
3	0.0955	19	0.1158	35	0.1032	51	0.0941
4	0.0845	20	0.1095	36	0.0838	52	0.0647
5	0.0721	21	0.0852	37	0.1071	53	0.0736
6	0.0689	22	0.0710	38	0.0656	54	0.0764
7	0.0937	23	0.1138	39	0.1043	55	0.1113
8	0.0849	24	0.1015	40	0.0568	56	0.0598
9	0.0915	25	0.0900	41	0.0711	57	0.0840
10	0.0896	26	0.1032	42	0.0535	58	0.0768
11	0.1296	27	0.1512	43	0.0889	59	0.1609
12	0.0827	28	0.1211	44	0.0601	60	0.0948
13	0.0757	29	0.1264	45	0.0729	61	0.0887
14	0.0797	30	0.0881	46	0.0640	62	0.0898
15	0.1130	31	0.0687	47	0.1075	63	0.0000

HYSTERESIS STEP SIZES – A/D 0 – RUN 1
SERIAL NUMBER B1051 (60 MHz)

ANNEX B TO APPENDIX A

This annex contains the error characteristics for each of the four converters.

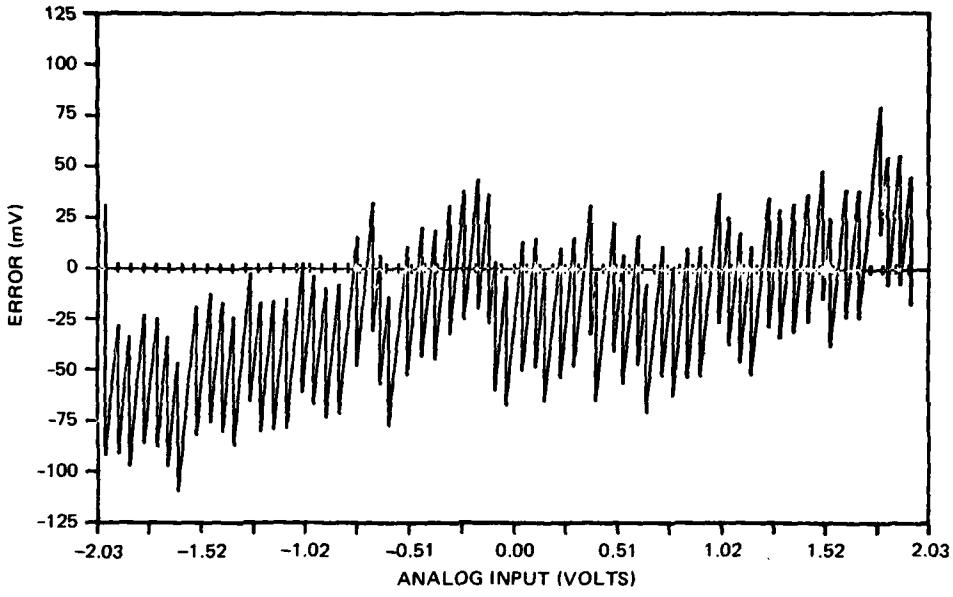

ERROR CHARACTERISTIC – A/D 0 – RUN 1 – UP RAMP
PLOT FOR DIGITAL OUTPUT LEVELS 00 – 63

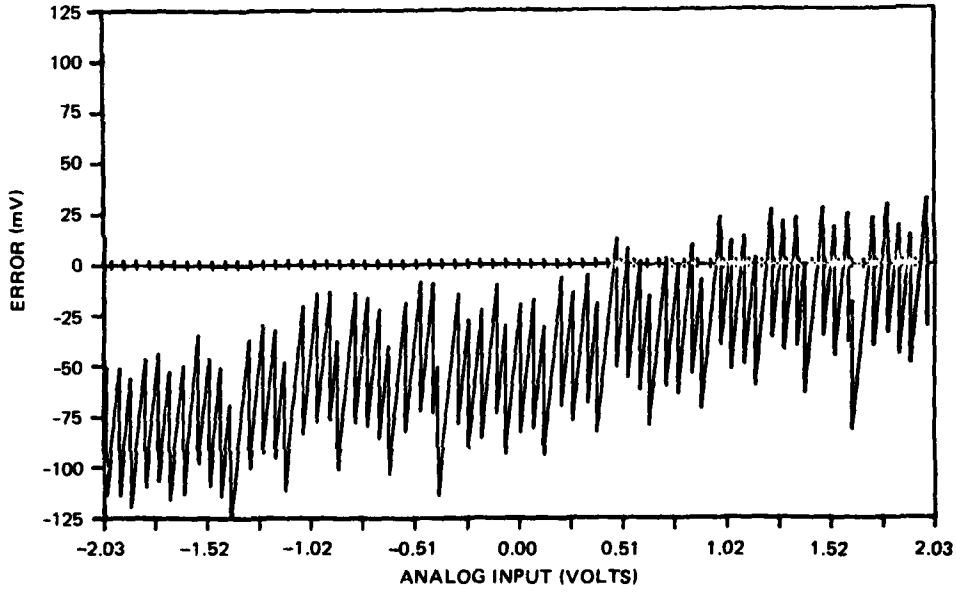

ERROR CHARACTERISTIC – A/D 0 – RUN 1 – DOWN RAMP
PLOT FOR DIGITAL OUTPUT LEVELS 00 – 63

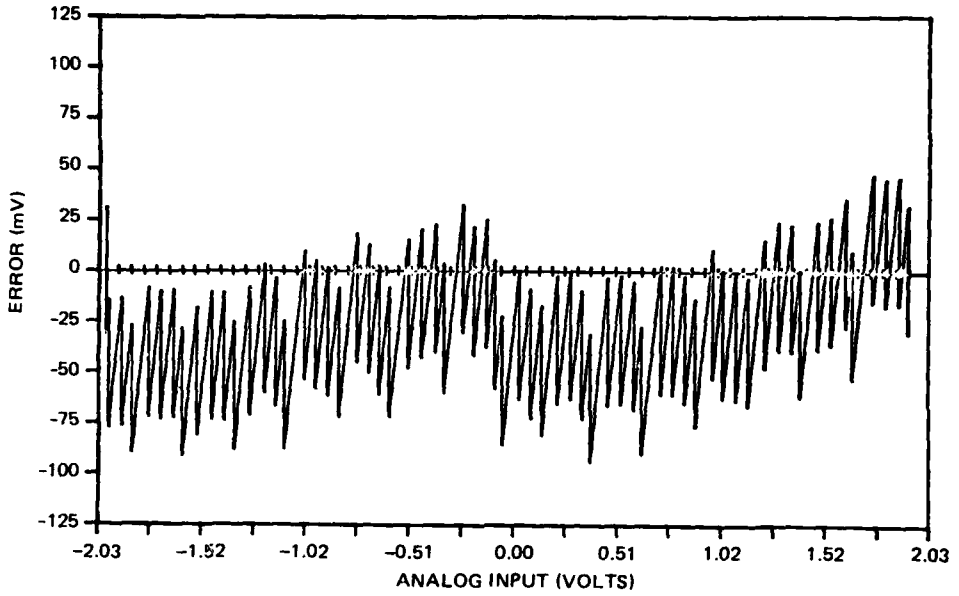

ERROR CHARACTERISTIC – A/D 1 – RUN 1 – UP RAMP
PLOT FOR DIGITAL OUTPUT LEVELS 00 – 63

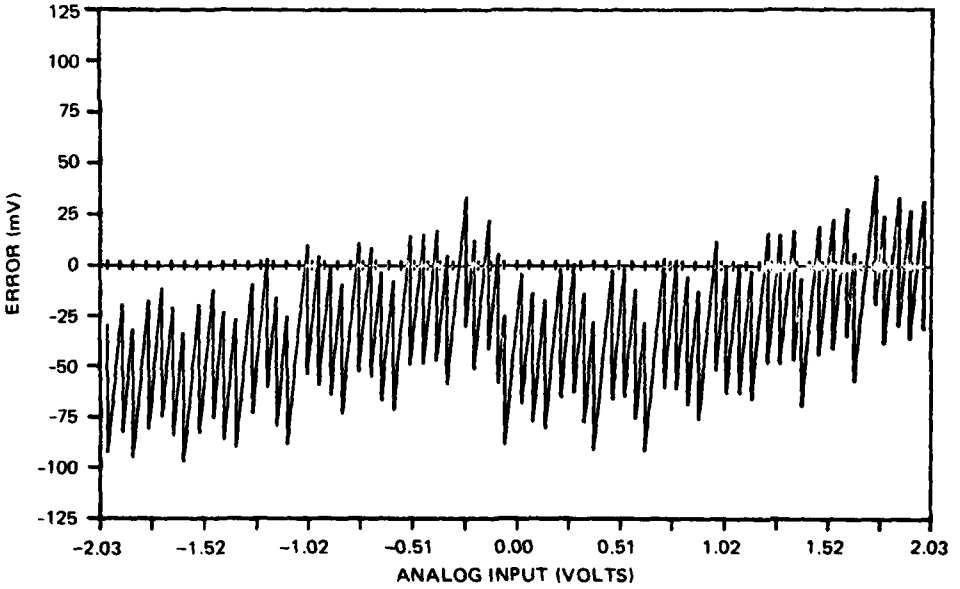

ERROR CHARACTERISTIC – A/D 1 – RUN 1 – DOWN RAMP
PLOT FOR DIGITAL OUTPUT LEVELS 00 – 63

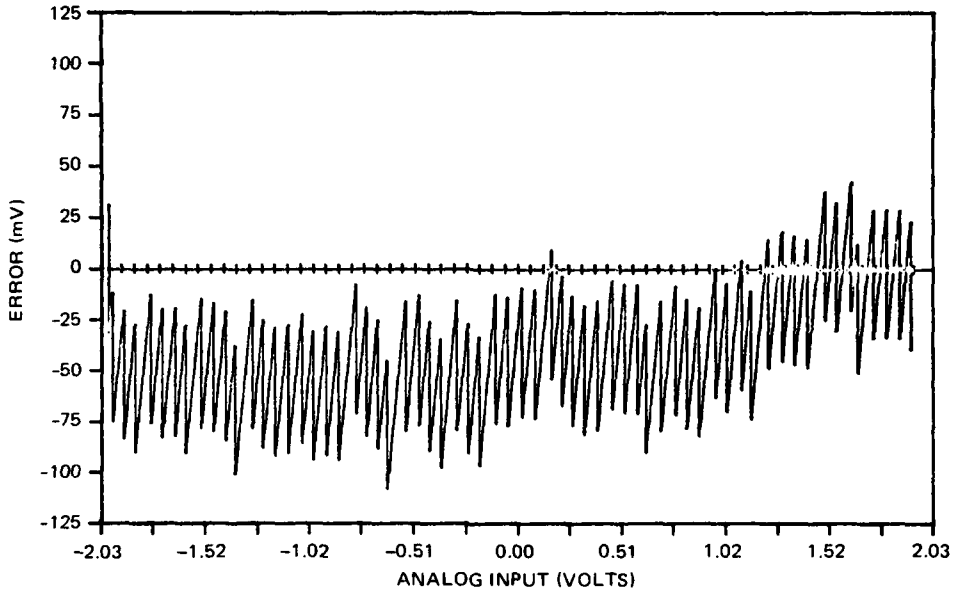

ERROR CHARACTERISTIC – A/D 2 – RUN 1 – UP RAMP
PLOT FOR DIGITAL OUTPUT LEVELS 00 – 63

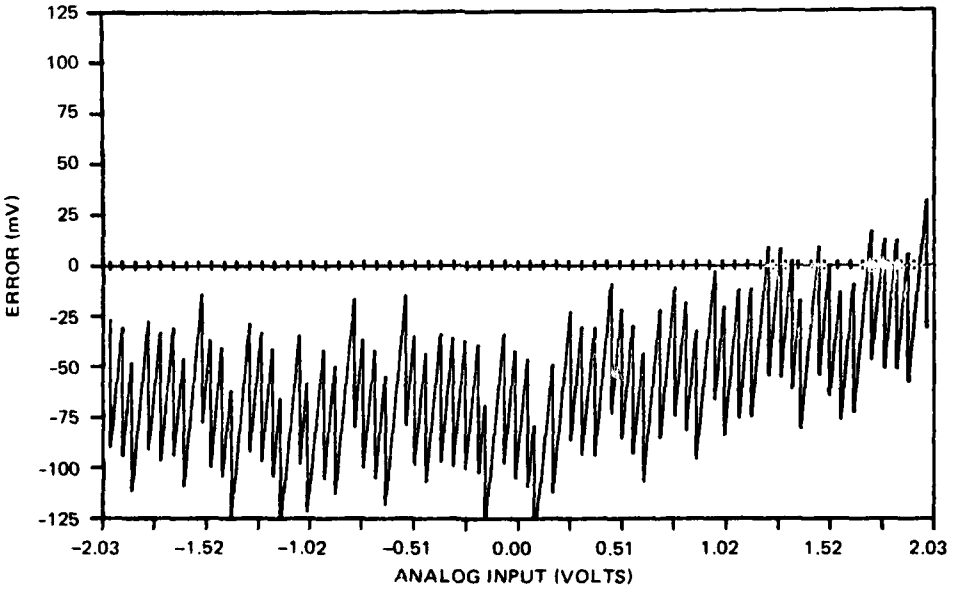

ERROR CHARACTERISTIC – A/D 2 – RUN 1 – DOWN RAMP
PLOT FOR DIGITAL OUTPUT LEVELS 00 – 63

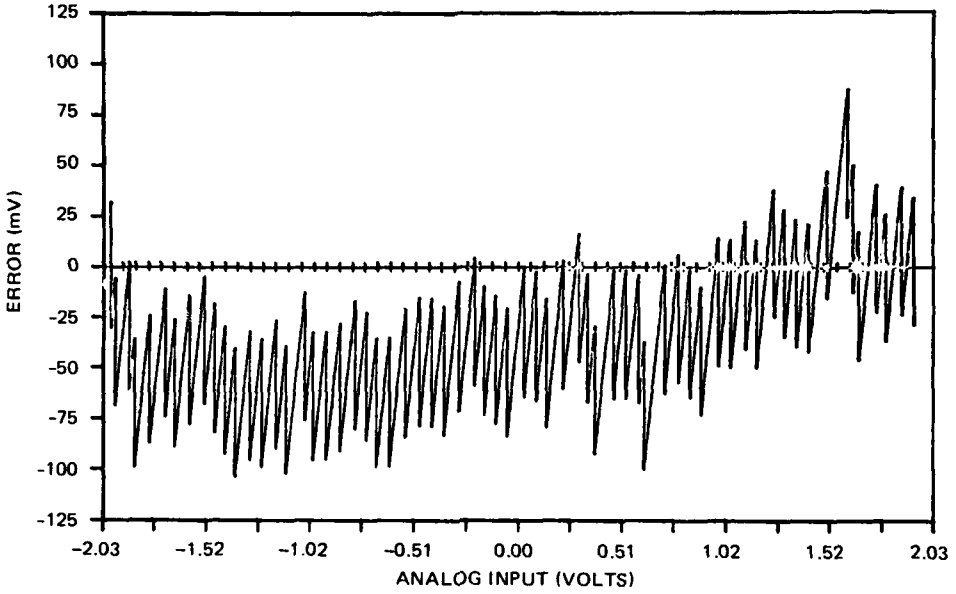

ERROR CHARACTERISTIC – A/D 3 – RUN 1 – UP RAMP
PLOT FOR DIGITAL OUTPUT LEVELS 00 – 63

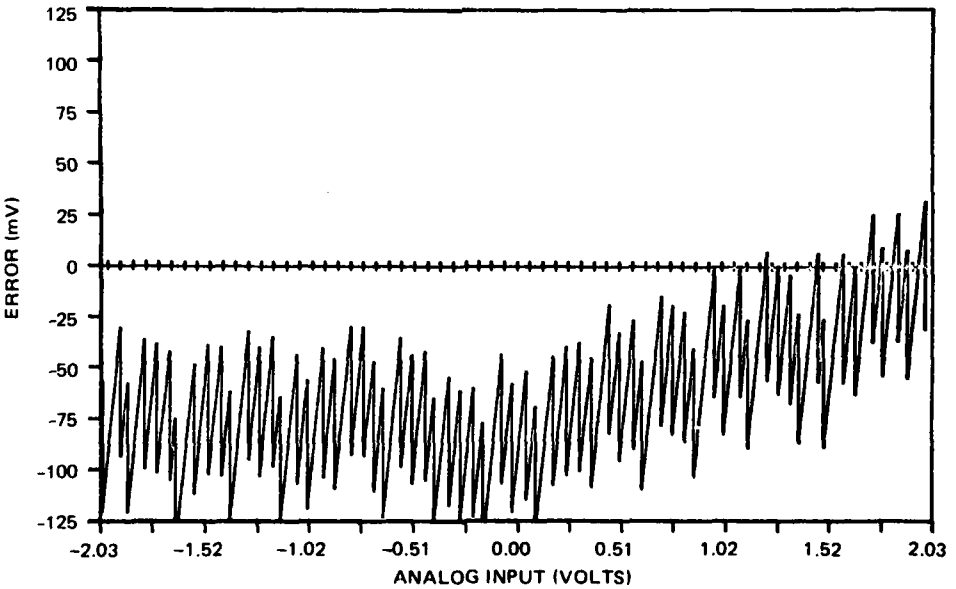

ERROR CHARACTERISTIC – A/D 3 – RUN 1 – DOWN RAMP
PLOT FOR DIGITAL OUTPUT LEVELS 00 – 63

APPENDIX B:
COLOR IMAGING

This is an abridged version of the original color imaging report. Color samples acquired as described in section 3 and color-corrected as described in section 4 are available for study at NOSC, Code 7323.

by

TR Little
Code 7323
Naval Ocean Systems Center

CONTENTS

1.0 INTRODUCTION

The acquisition, storage, enhancement, and compression of color digital imagery is an extension of the monochrome studies which have been ongoing at NOSC for the past few years. Although color continuous-tone image acquisition/transmission is not being considered a high priority for the initial goals of the US Postal Service Electronic Message Service System (EMSS), the additional requirements for acquisition, storage, and processing equipment, bandwidth, and printing techniques should be well understood at the time specifications for a monochrome EMSS are finalized. Perhaps the majority of the additional requirements for processing color imagery can be imbedded into the monochrome system at little or no cost so that in the desired time frame the EMSS can be upgraded to accommodate color with little impact on the existing system.

2.0 HARDWARE CONSIDERATIONS

Using a new scan head developed by Fairchild Imaging Systems, Syosset, NY, the ICAS recently performed some high-speed monochrome image acquisitions at approximately nine pages per second. These tests not only confirmed the excellent performance of the Fairchild scanner but also verified for the first time the full extent of the ICAS capabilities to acquire, store, and process full-page images at up to one-half its maximum rate.

Tricolor separation images have been acquired in the past to demonstrate changes in monochrome image contrast, but no method was available to display or print the results in color for interpretation. Two important additions to ICAS have now been interfaced into the system which provide these needed capabilities (see fig B1.1 shaded areas). Figure B1.2 details the variety of image data paths.

With the addition of high-quality color display and printing equipment, the ICAS has become an extremely versatile and highly capable processing system. The new equipment was selected primarily for the purpose of adding color capability to the ICAS; however, the hard- and soft-copy output devices are also capable of producing black and white images.

2.1 COMTAL IMAGE PROCESSING EQUIPMENT

2.1.1 EQUIPMENT DESCRIPTION

A Comtal Vision One image processing system was acquired by USPS for use by NOSC with the ICAS. This equipment contains random-access memory (RAM) modules capable of providing three 512-by-512-pel images having 2^8 (256) brightness levels each. Access times for image display refresh from the RAM are designed to provide 30-frame-per-second color images with overlays. In addition, four 512-by-512 one-bit overlay planes are provided.

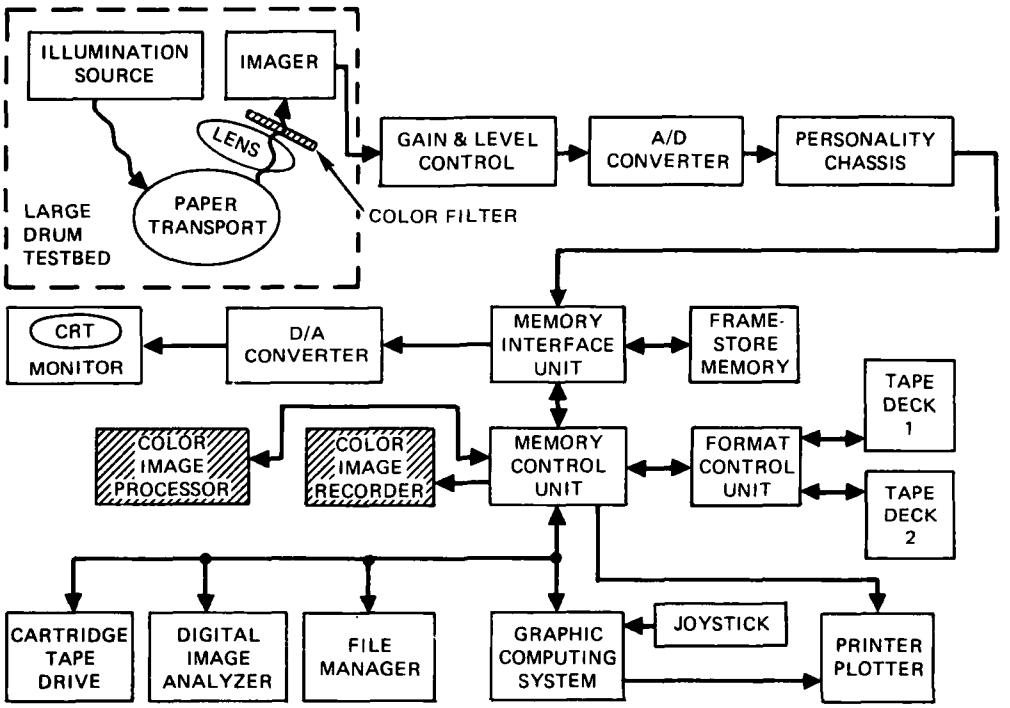

Figure B1.1. Image Capture and Analysis System.

2.1.2 KEY FEATURES

The equipment can be operated in a stand-alone mode using an integrated LSI 11 processor. Digital image data must be entered into the system from an external source such as a magnetic tape controller or a computer interface.

The unit contains a full alphanumeric keyboard plus 20 special function keys. A trackball is included to position a cursor or designate locations on the display. Location of the cursor can also be controlled by the processor software. The internal processor software contains over 100 commands to control display, setup, presentation, enhancement, graphics, and utility programs.

The display ordered by USPS for soft-copy presentation is the Systems Research Laboratories (SRL) model 374 color television display. This display contains a high-resolution (approximately 80 color dot triads per inch) cathode ray tube (CRT) and can support 1024-by-1024-pel displays at 30 frames per second via its 43-MHz video amplifier. The CRT is a new 20-inch version and has a usable diagonal dimension of approximately 18 inches.

2.2 DICOMED MODEL D-47 IMAGE RECORDER

The second equipment acquired for the purpose of generating color image hard copy is a Dicomed model D-47 digital image recorder. This recorder equipment gives the ICAS for the first time the capability of printing full-resolution, high-quality color images as well as black and white images. Although relatively slow, it has the capability of generating images

ICAS
IMAGE DATA PATHS

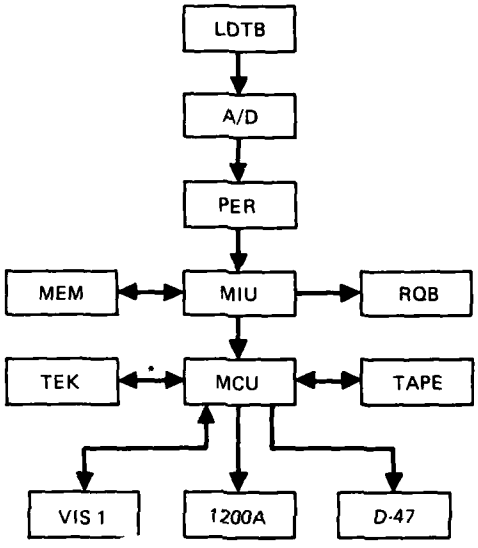

DEFINITIONS

LDTB – LARGE DRUM TEST BED – SCANNER

A/D – ANALOG TO DIGITAL CONVERTER – VIDEO RATES – ONE TO FOUR CHANNELS

PER – PERSONALITY MODULE – DIGITAL VIDEO FORMATTING – 6 TO 48 BIT DEMULTIPLEX

MIU – MEMORY INTERFACE UNIT

MCU – MEMORY CONTROL UNIT

MEM – MEMORY – VIDEO REFRESH – PROGRAM AND DATA STORAGE

RQB – CONRAC RQB MONOCHROME MONITOR

TAPE – KENNEDY MAGNETIC TAPE SYSTEM

D47 – DICOMED D-47 COLOR IMAGE RECORDER

1200A – VERSATEC 1200A BLACK AND WHITE, BILEVEL PRINTER/PLOTTER

VIS 1 – COMTAL VISION ONE COLOR IMAGE PROCESSING AND DISPLAY SYSTEM

TEK – TEKTRONIX 4051 GRAPHIC DISPLAY SYSTEM WITH PERIPHERALS

* CONTROL AND STATISTICAL INFORMATION ONLY – NOT IMAGES

Figure B1.2.

of the quality and resolution desired by the Postal Service. Previous to the acquisition of the Dicomed, the only image hard-copy capability in the ICAS was the Versatec electrostatic printer. Although this equipment has the necessary 200-by-200-point-per-inch resolution, it records bilevel, black and white images only. The Dicomed has the capability of generating full-color, full-resolution images with either 64 or 256 grey levels per color.

2.2.1 EQUIPMENT DESCRIPTION

As shown in figure B2.1, the Dicomed D-47 is a CRT based digitally controlled image recorder. Horizontal and vertical deflection counter/registers control beam position through a 4096-point range. Spot intensity is controlled from incoming digital video by time modulation of the beam current.

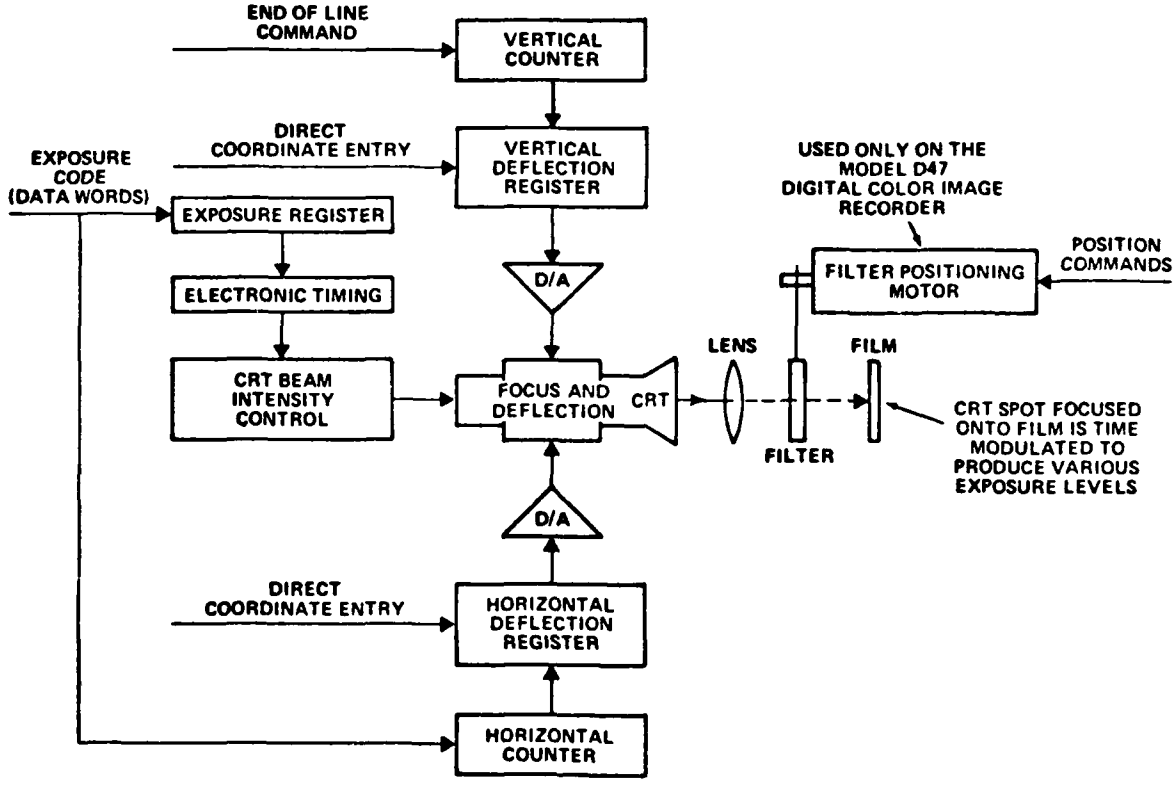

Figure B2.1. Simplified block diagram of the DICOMED digital image recorder.

2.2.2 KEY FEATURES

The record time for a monochrome image of full resolution, a function of the average brightness of the image, is on the order of 5 minutes. In order to record color imagery, the CRT image is focused on the film through one of three tricolor (RGB) filters similar to the ICAS large drum testbed acquisition filters. It therefore requires upwards of 15 minutes to record a full-size, full-color, full-resolution image. Film options for the D-47 include 35-mm roll film and Polaroid or Kodak 4-by-5 sheet film. The highest quality image reproduction is achieved by using the Kodak 4-by-5 film, since photographic blow-up to the original 8-½-by-11-inch image size requires less magnification.

3.0 COLOR IMAGE ACQUISITION

Acquisition and processing of color imagery requires that the image data be separated into three primary color components. As previously reported, a dual-scanner tricolor image acquisition system has been proposed as a solution to the image acquisition problem for the USPS (see fig B3.1). This configuration attempts to solve two potential difficulties peculiar to the acquisition of color imagery. In general terms, these problems are related to the registration of the tricolor images during the acquisition and reproduction processes, and the color balance between the tricolor separated components. In laboratory tests using the ICAS and large drum testbed, the registration problem does not exist, since tricolor images are acquired in serial fashion without moving the paper on the drum. In actual USPS production equipment, the images would be acquired in parallel, which requires the three scanners as shown in either the prescan or main-scan station.

3.1 TRICOLOR IMAGE REGISTRATION

Since it is required that a color image be separated into three primary components, there are two choices available to implement the acquisition hardware. In the simplest case (which was selected for the ICAS equipment) the tricolor images are captured in series and then processed and stored separately. Using this configuration, the image source is attached to the drum and not moved until after all three images are acquired. Since a highly accurate "once per revolution" synchronization signal is available from a shaft encoder, no mis-registration of the color images is possible. The alternative approach, which has been described, is shown in figure B3.1. Either the prescanner or the main scanner is an example of a fully parallel tricolor image acquisition scheme. By using a beamsplitter prism, the image is focused simultaneously through three optical paths and three color filters onto three separate imaging devices. The mechanical alignment necessary to assure tricolor image registration must be performed with dimensional tolerances which are more exacting than the tolerances involved with the image array itself. Alternatively, the image devices can be directly attached to the beamsplitter with optical cement, and the alignment can be performed on an optical bench and permanently fixed. In this case, however, the beamsplitter, filters, and imager chips would probably become a nonrepairable assembly. Also, the tricolor separation filters must be an integral part of the assembly.

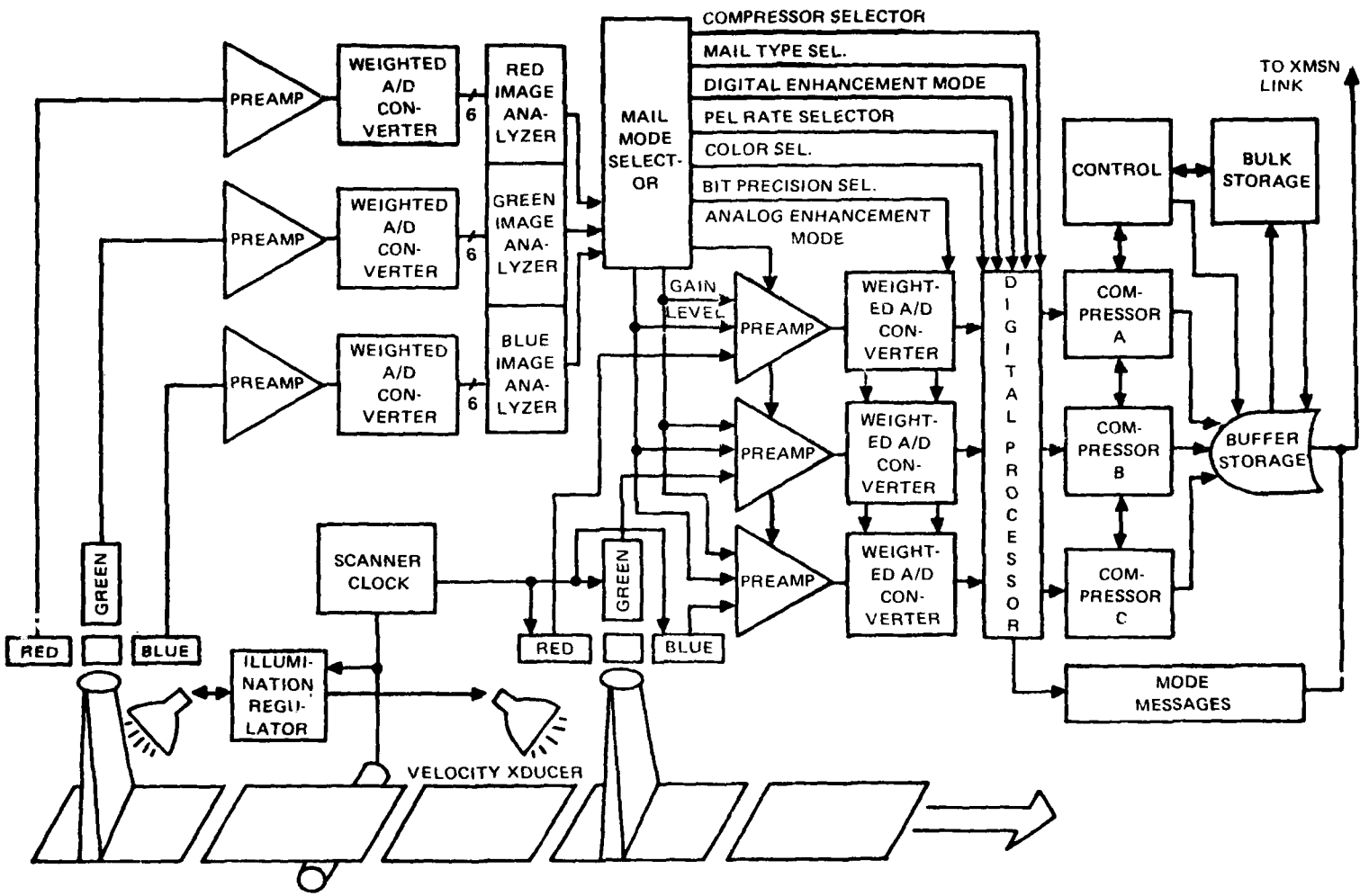

Figure B3.1. Image acquisition system.

3.1.1 SUMMARY OF ADVANTAGES AND DISADVANTAGES

3.1.1.1 TRICOLOR PARALLEL CAPTURE (SEE FIG B3.1). The principal advantage of the parallel capture scheme is that all three color image components are available simultaneously for processing, display, and/or printing (if an appropriate printer is available). Some problem areas include the dimensional tolerances for mechanical alignment necessary to register the tricolor images. In addition, the light source required must be tricolor balanced and the lens must be color corrected.

3.1.1.2 TRICOLOR SERIAL CAPTURE (SEE FIG B1.1, B1.2, and B3.1). This configuration, as in the ICAS, has no registration problem since the image is fixed with respect to the acquisition hardware through all three captures. The serial image acquisition may turn out to be an advantage rather than a disadvantage in view of the potential requirement to transmit the images in serial and the potential availability of a three-pass printing device. Fundamental difficulties arise, as in the previous case, such as requirements for a balanced light source and a color-corrected lens, and, unique to the serial tricolor scan, the filters must be changed between scans.

3.1.1.3 VERY LARGE DRUM SERIAL CAPTURE. An alternative approach which may overcome the disadvantages of the previously described methods is shown in figure B3.2. In this case, a very large drum would be utilized to move the document past three independent acquisition stations without the necessity of removing the document from the drum. The lens and imager assembly would be optically aligned and focused on an optical bench and mounted as a unit. The problem of tricolor image registration still exists. The serial capture would be a significant advantage for serial image transmission and the more probable availability of three-pass color printers. Other potential advantages include three independent monochrome light sources. In this case a color-balanced light and a filter are not required. Light intensity can be easily adjusted for color balance in the system through electrical means. Also, the lens designs may be optimized for a narrower bandwidth than the normal visible spectrum, thereby achieving increased resolution.

Assuming that the magnification ratio from image source to imaging device is approximately 10 to 1, the adjustments necessary to assure adequate color registration must be precise down to the 10–100-microinch range. This level of precision is probably out of the range of practical mechanical adjusting devices. However, a combination of mechanical adjustments and electrically counting lines and pels should be able to achieve image registration to plus or minus one pel. A dynamic closed-loop control system could possibly achieve the necessary subpel dimensional accuracy. Registration marks located on the edge of the drum could provide the input to a relatively simple pattern recognition algorithm and generate a registration error signal. This signal would be nulled to a minimum with a hybrid feedback control system. Differential hydraulic pressure or mechanical force applied to a deformable beam and controlled by a dedicated microprocessor might be a candidate for further investigation.

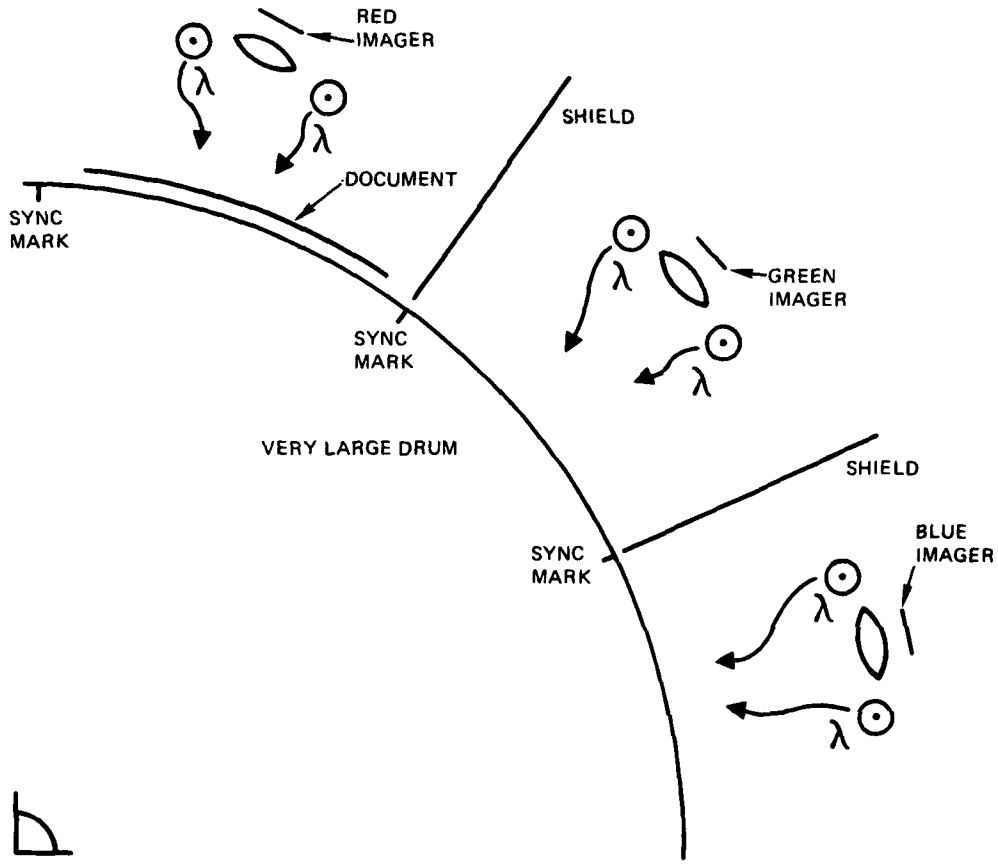

Figure B3.2. Very large drum serial capture.

3.1.2 LIGHT SOURCE CONSIDERATIONS

The amplitude response characteristics of a silicon imaging device heavily favor the red end of the spectrum. In order to achieve accurate color acquisition and reconstruction, it is necessary to flatten the overall system response as a function of wavelength by the introduction of a compensating transfer function. In the ICAS this has been attempted by the acquisition of a special fluorescent slit-aperture lamp producing a predominantly blue response.

The phosphor mixture is approximately eight parts blue to two parts green to one part red. It is intended that when light from these fluorescent tubes is reflected from a white object through tricolor separation filters onto the silicon imager, the resulting signals will recombine (in a properly color-balanced hard- or soft-copy device) to form a white image. This ideal situation has not yet been achieved, although current results indicate that it is definitely feasible. A summary of the relative response curves of the optical components is shown in figure B3.3.

3.2 SCANNER SETUP AND OPERATION

The acquisition of color images is essentially the same as the acquisition of three monochrome images plus the addition of one more complication. In order to acquire and

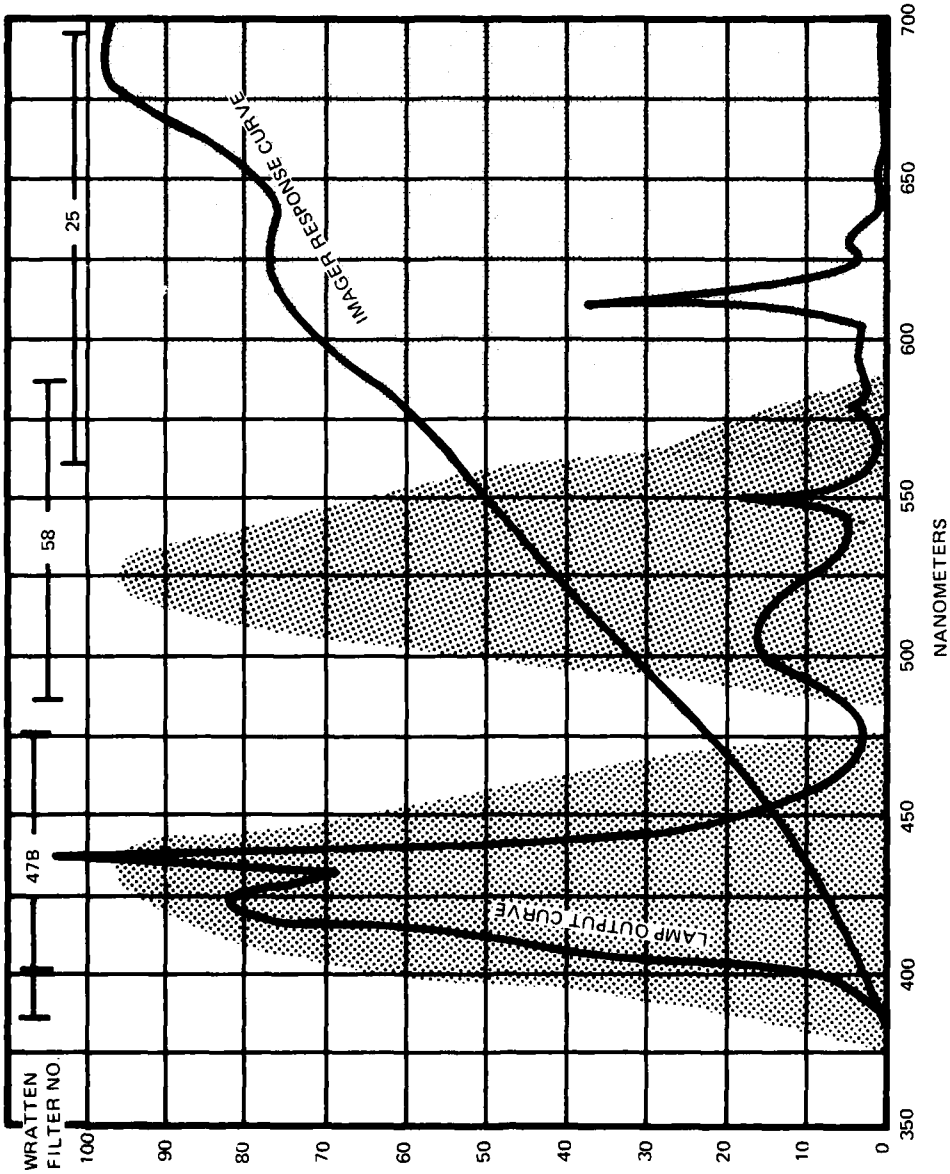

Figure B3.3 Lamp and imager spectral response.

reproduce a faithful representation of the original color image, the intensities of the three tricolor components must be properly balanced. Failure to achieve correct color balance in the tricolor acquisition process results in undesirable color distortion. This distortion is most easily noticed in white areas of the color image which contain tints instead of appearing to be truly white.

3.2.1 COLOR FILTERS

Color separation is achieved by placing a Kodak Wratten filter in the optical path in front of the imaging lens. The filters are number 47B for the blue primary, number 58 for green, and number 25 for red. These filters perform the tricolor separation quite well. However, the total system intensity response still favors the red end of the spectrum.

3.2.2 NEUTRAL DENSITY FILTERS

In spite of the predominance of the blue light, the addition of neutral density filters in the optical path for the red and green image attenuates these colors to be nearly equal to the blue. The addition of neutral density filters of 0.6 for the red and 0.2 for the green comes close to balancing the blue response. Unfortunately, the neutral density filters are not available in density increments small enough to achieve an adequate color balance. It is therefore necessary to fine tune the balance by using amplifier gain adjustments or by slightly varying the light intensity for the three color images.

4.0 COLOR IMAGE CORRECTION

A process of illumination intensity correction has been applied to black and white images in an effort to reduce nonuniformities in intensity caused by the acquisition hardware. In this illumination correction process, a calibration curve of system response across a scan line is used to correct the nonuniformities on a pel-by-pel basis. This procedure has proved highly successful in correcting nonuniformities in monochrome images. Unfortunately, the first attempt to apply the same correction procedure to the tricolor components of a color image was not successful.

The problem was that the color image components after being corrected in the normal manner were excessively saturated. A detailed examination into the characteristics and cause of the problem was undertaken using image 04-01 as a sample. The saturation of the color image components after correction was quite surprising since extreme care had been taken in the preparation of the white standard calibration curve used in the correction process.

After a thorough analysis, it was discovered that the cause of the saturation in the corrected images was the use of a *white* standard correction curve on a *color* component image. The solution was simply to generate separate tricolor correction curves to be applied to the corresponding color image components.

4.1 APPLICATION OF CORRECTION CURVES

The following data demonstrate the results of applying the correction process to color components of test image 04-01. The pel brightness statistics for the image color components are shown in figures B4.1 through B4.3 before the correction process. There are two

notable features in the statistics. First, all images contain an artifact at pel value zero. The 2200 zero-level pels are the result of a timing error in the ICAS acquisition hardware and should not be considered as part of the actual image. Also interesting is the number of 63-level pels in the blue image. This indicates that the image was captured with a slightly excessive light level; however, since the number of pels represents only about 0.2% of the total image, reprocessing to eliminate the error was not considered essential.

Figures B4.4 through B4.6 are the pel brightness statistics for the RGB components when corrected with a white correction curve. It can be seen from these data that the green image is now saturated to approximately the 0.4% level and the blue image contains about 4.25% saturated pels.

Figures B4.7 through B4.9 reflect the improvement achieved by using tricolor correction curves on the color image components. In the blue image the level of saturation was reduced from the previous 4.25% to about 1%.

4.2 CORRECTION CURVE GENERATION

Previous monochrome image acquisition and correction utilized a calibration curve which was an average of 16 lines of a white standard image. New software has been generated to allow processing of calibration images containing any number of lines. For this report, the calibration standard curves were generated by using averages over a full 1024 lines of standard image data in order to reduce the level of time-varying noise contained in the calibration curve. The acquisition process by which the color correction curves were generated involves the acquisition of color standard images containing 1024 lines. The image source was the same white photographic paper used previously for monochrome corrections. For this study, the images were acquired by use of tricolor separation filters.

Figures B4.10 through B4.12 relate to the tricolor calibration images and correction curves. For the red image, figures B4.10A and B are the pel brightness statistics for the 1024-line standard image. Figure B4-10C shows the results of a statistical analysis on pel brightness data. Of notable interest is the relative location of the maximum value (pel location 858). Figures B4.10D and E are graphical representations of the image brightness across the page and the normalization of those data, respectively. Figure B4.10E is the actual illumination profile used as the calibration standard for the red image. Similarly, figures B4.11 and B4.12 show statistical information applicable to the green and blue standard image components.

Of particular interest is the relative location of the maximum brightness value for the three color component images. Specifically, the location of the maximum for the red image was pel 858; for the green image, pel 606; and for the blue image, pel 1034. Since the illumination profiles computed for the tricolor separated standard images are clearly different, it is apparent that a single white correction profile would not provide the appropriate correcion for the color separated images. Indeed, significant distortions result when the wrong calibration curve is applied in the correction process.

In order to visualize the effect of the correction process on a typical line of image data, figures B4.13 and B4.14 are presented. In figure B4.13, line 1800 was plotted from each of the three color component images after correction with the white standard profile. Line 1800 was specifically selected since there was no typing or other information content on the line and the adverse saturation effects could most easily be seen. In figure B4.13B and C, the excessive saturation in the green and blue images is clearly apparent. In figure B4.14, the respective color component images were corrected with the proper color correction curve, and little saturation is seen.

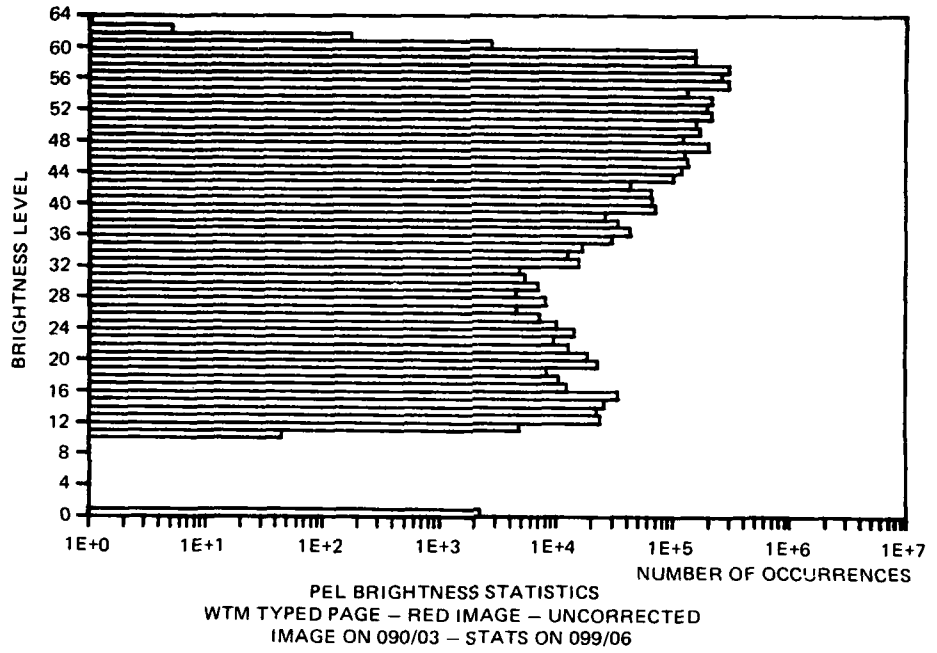

Figure B4.1.

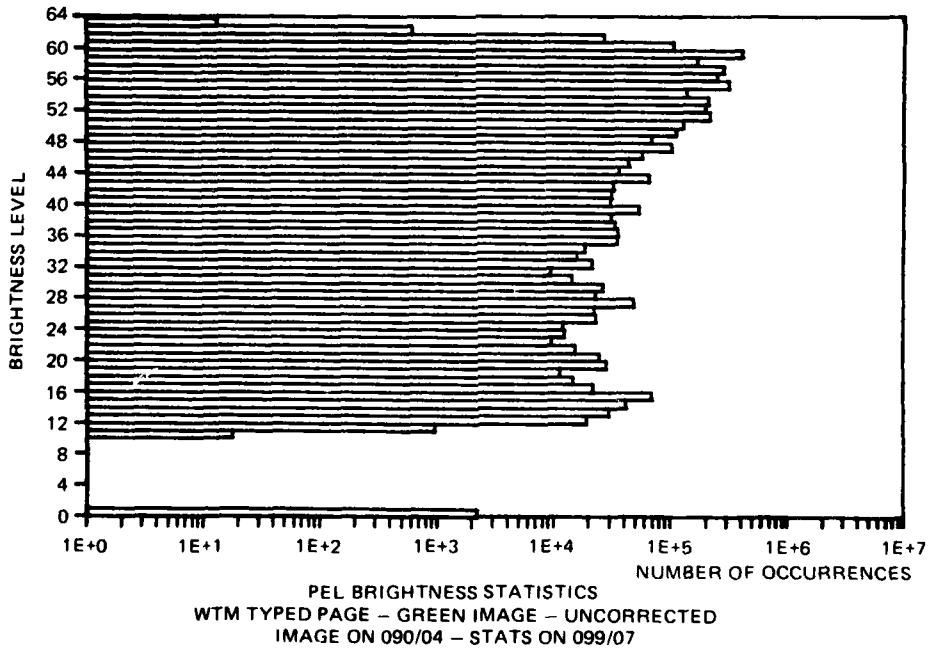

Figure B4.2.

LEVEL	VALUE	LEVEL	VALUE	LEVEL	VALUE	LEVEL	VALUE
0	2200	16	42555	32	26310	48	56531
1	0	17	45517	33	20305	49	71033
2	0	18	35803	34	25667	50	82657
3	0	19	64118	35	40005	51	151336
4	0	20	41843	36	31619	52	146894
5	0	21	23896	37	21333	53	154114
6	0	22	16173	38	15653	54	93613
7	0	23	19525	39	31025	55	237054
8	0	24	10081	40	30312	56	208899
9	0	25	11632	41	32941	57	254806
10	0	26	13800	42	24951	58	160407
11	0	27	28568	43	58383	59	457042
12	60	28	14824	44	47731	60	240359
13	630	29	23764	45	39818	61	279092
14	5917	30	14125	46	40079	62	119786
15	40180	31	10058	47	91212	63	44564

PEL BRIGHTNESS STATISTICS
WTM TYPED PAGE – BLUE IMAGE – UNCORRECTED
IMAGE ON 090/05 – STATS ON 099/08

Figure B4.3A.

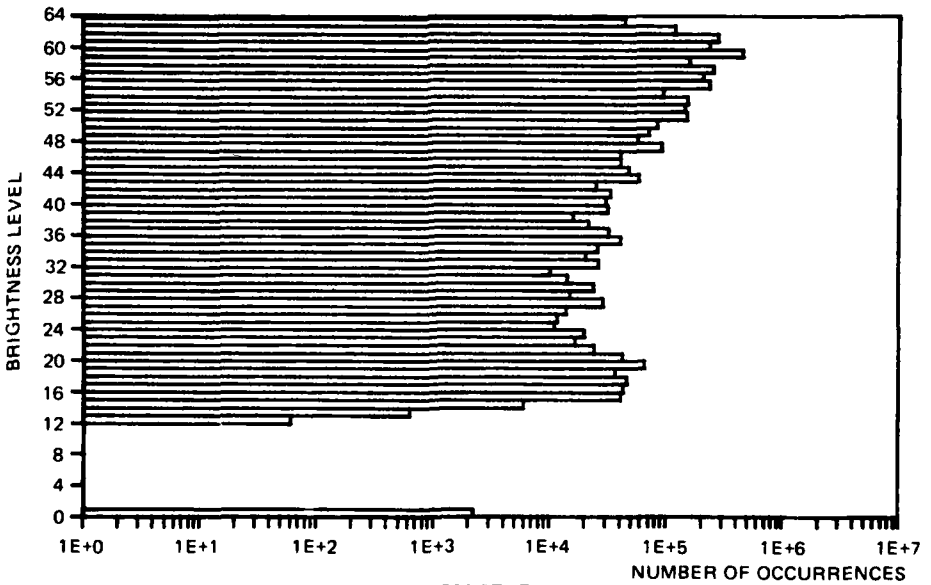

PEL BRIGHTNESS STATISTICS
WTM TYPED PAGE – BLUE IMAGE – UNCORRECTED
IMAGE ON 090/05 – STATS ON 099/08

Figure B4.3B

LEVEL	VALUE	LEVEL	VALUE	LEVEL	VALUE	LEVEL	VALUE
0	2200	16	26324	32	4175	48	44154
1	0	17	16146	33	4693	49	39579
2	0	18	15025	34	4700	50	42723
3	0	19	13487	35	4628	51	63012
4	0	20	10271	36	5146	52	85366
5	0	21	6318	37	5967	53	148142
6	0	22	5667	38	5743	54	236014
7	0	23	10156	39	6698	55	344987
8	0	24	17748	40	9412	56	495678
9	0	25	15703	41	8941	57	611726
10	13	26	13561	42	8683	58	593216
11	520	27	10711	43	9722	59	428005
12	6172	28	7694	44	17122	60	192458
13	10964	29	6765	45	22015	61	25296
14	16300	30	5615	46	32528	62	4235
15	29328	31	4684	47	44330	63	1134

PEL BRIGHTNESS STATISTICS
WTM TYPED PAGE – RED IMAGE CORRECTED WITH WHITE CURVE
IMAGE ON 097/00 – STATS ON 099/00 – CORRECTION CURVE ON 094/3

Figure B4.4A.

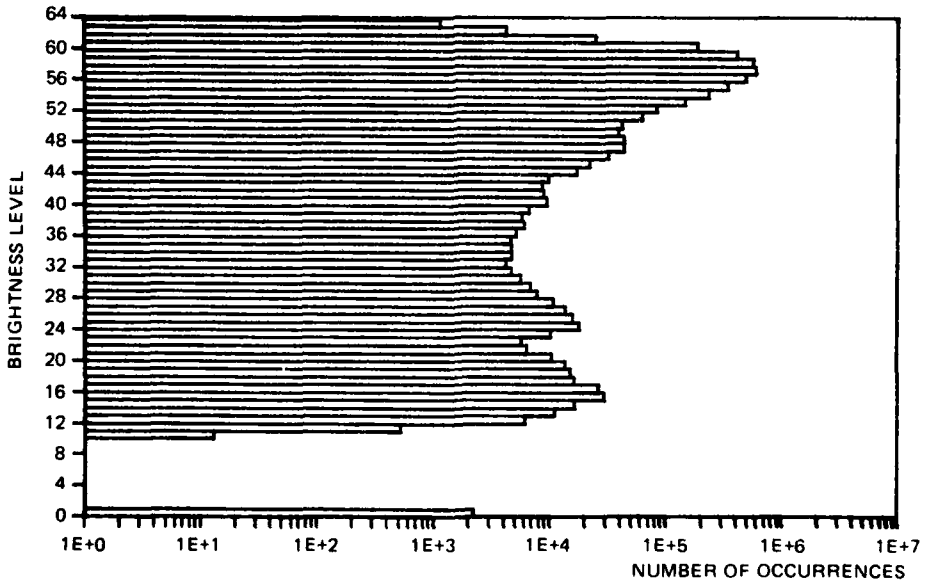

PEL BRIGHTNESS STATISTICS
WTM TYPED PAGE – RED IMAGE CORRECTED WITH WHITE CURVE
IMAGE ON 097/00 – STATS ON 099/00 – CORRECTION CURVE ON 094/3

Figure B4.4B.

LEVEL	VALUE	LEVEL	VALUE	LEVEL	VALUE	LEVEL	VALUE
0	2200	16	30513	32	12872	48	22831
1	0	17	17297	33	16949	49	27287
2	0	18	18937	34	23405	50	28625
3	0	19	31869	35	20019	51	35586
4	0	20	28266	36	22140	52	45715
5	0	21	19972	37	22214	53	63438
6	0	22	16196	38	17422	54	77091
7	0	23	11419	39	14767	55	94831
8	0	24	14705	40	15515	56	151523
9	0	25	10793	41	13466	57	225291
10	12	26	11459	42	12571	58	354728
11	526	27	15387	43	14315	59	583929
12	6543	28	16751	44	21705	60	685748
13	14471	29	21177	45	24516	61	428137
14	23214	30	18957	46	20442	62	226496
15	30524	31	15288	47	17768	63	83782

PEL BRIGHTNESS STATISTICS
WTM TYPED PAGE – GREEN IMAGE CORRECTED WITH WHITE CURVE
IMAGE ON 097/01 – STATS ON 099/01 – CORRECTION CURVE ON 094/3

Figure B4.5A.

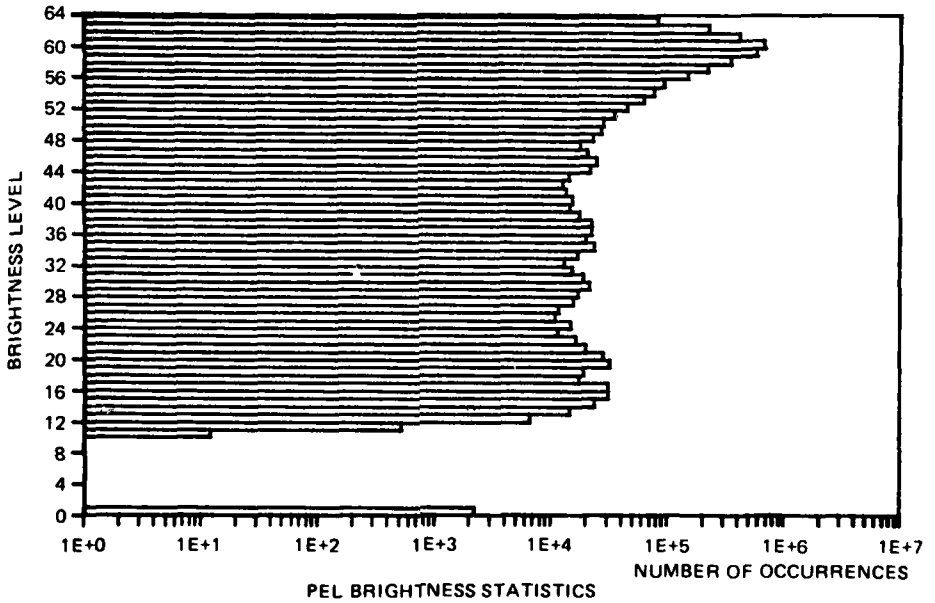

PEL BRIGHTNESS STATISTICS
WTM TYPED PAGE – GREEN IMAGE CORRECTED WITH WHITE CURVE
IMAGE ON 097/01 – STATS ON 099/01 – CORRECTION CURVE ON 094/3

Figure B4.5B.

LEVEL	VALUE	LEVEL	VALUE	LEVEL	VALUE	LEVEL	VALUE
0	2200	16	23991	32	13281	48	31243
1	0	17	30825	33	15613	49	31534
2	0	18	26205	34	17740	50	24473
3	0	19	28069	35	9888	51	23243
4	0	20	31303	36	11828	52	26318
5	0	21	26007	37	15696	53	30717
6	0	22	19953	38	16286	54	41611
7	0	23	19642	39	17808	55	60130
8	0	24	28255	40	19795	56	91151
9	0	25	28454	41	18465	57	143135
10	0	26	27136	42	16058	58	186872
11	0	27	16535	43	16592	59	253216
12	41	28	12316	44	18644	60	373001
13	233	29	16739	45	16559	61	444346
14	1441	30	21037	46	19019	62	416069
15	14564	31	18336	47	25619	63	962368

PEL BRIGHTNESS STATISTICS
WTM TYPED PAGE – BLUE IMAGE CORRECTED WITH WHITE CURVE
IMAGE ON 097/02 – STATS ON 099/02 – CORRECTION CURVE ON 094/3

Figure B4.6A.

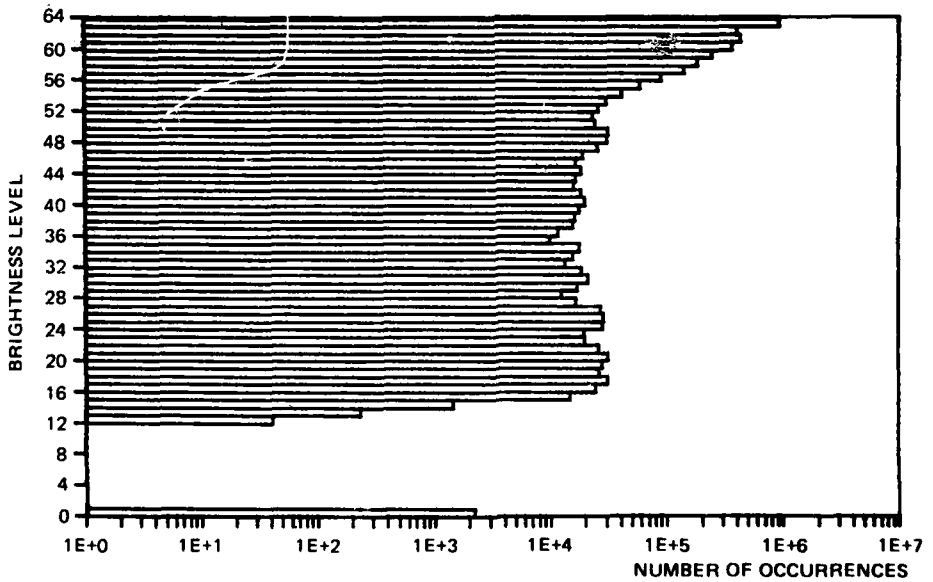

PEL BRIGHTNESS STATISTICS
WTM TYPED PAGE – BLUE IMAGE CORRECTED WITH WHITE CURVE
IMAGE ON 097/02 – STATS ON 099/02 – CORRECTION CURVE ON 094/3

Figure B4.6B.

LEVEL	VALUE	LEVEL	VALUE	LEVEL	VALUE	LEVEL	VALUE
0	2200	16	26180	32	4161	48	49751
1	0	17	17654	33	4956	49	45203
2	0	18	13821	34	4218	50	54829
3	0	19	12674	35	4998	51	74828
4	0	20	7750	36	5557	52	120001
5	0	21	6602	37	5689	53	188334
6	0	22	7067	38	6151	54	322751
7	0	23	13811	39	6928	55	460123
8	0	24	16881	40	10034	56	559445
9	0	25	17653	41	9462	57	510414
10	11	26	12539	42	9184	58	460760
11	533	27	8055	43	13897	59	296551
12	6197	28	7171	44	21212	60	172344
13	13151	29	5823	45	31041	61	17188
14	16887	30	5588	46	34827	62	404
15	29736	31	4139	47	44222	63	14

PEL BRIGHTNESS STATISTICS
WTM TYPED PAGE – RED IMAGE CORRECTED WITH RED CURVE
IMAGE ON 097/03 – STATS ON 099/03 – CORRECTION CURVE ON 094/6

Figure B4.7A.

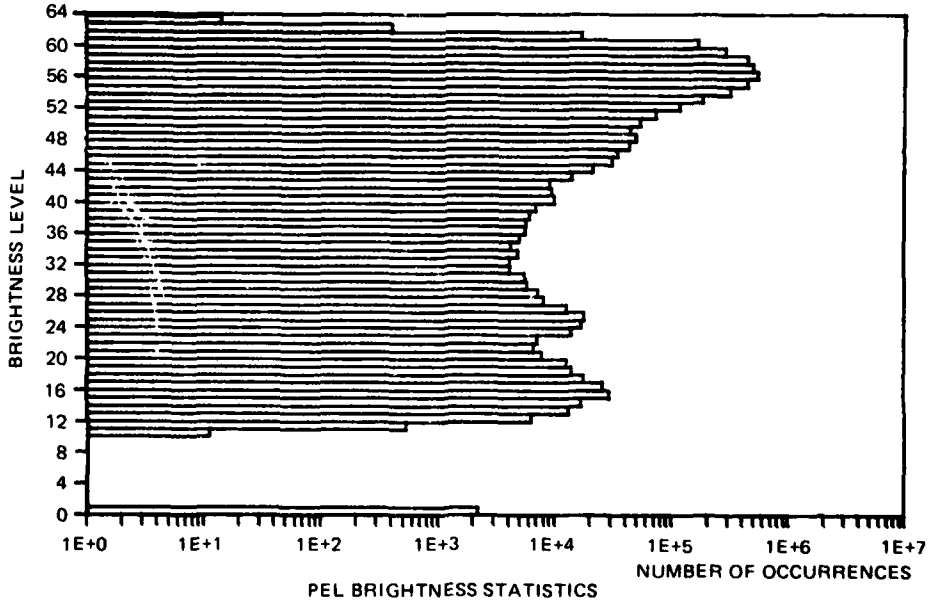

PEL BRIGHTNESS STATISTICS
WTM TYPED PAGE – RED IMAGE CORRECTED WITH RED CURVE
IMAGE ON 097/03 – STATS ON 099/03 – CORRECTION CURVE ON 094/6

Figure B4.7B.

LEVEL	VALUE	LEVEL	VALUE	LEVEL	VALUE	LEVEL	VALUE
0	2200	16	35649	32	19976	48	28784
1	0	17	32821	33	18415	49	30570
2	0	18	12499	34	15485	50	31994
3	0	19	15564	35	15408	51	42499
4	0	20	22594	36	20824	52	61289
5	0	21	29757	37	18797	53	75087
6	0	22	19938	38	16489	54	92113
7	0	23	11511	39	21669	55	161875
8	0	24	8951	40	23004	56	251090
9	0	25	7318	41	16355	57	279456
10	14	26	11302	42	15732	58	300824
11	568	27	14949	43	17708	59	369272
12	8313	28	22006	44	20910	60	563150
13	18809	29	19971	45	23056	61	599002
14	21929	30	26474	46	27193	62	173355
15	32503	31	19617	47	28288	63	26674

PEL BRIGHTNESS STATISTICS
WTM TYPED PAGE – GREEN IMAGE CORRECTED WITH GREEN CURVE
IMAGE ON 097/04 – STATS ON 099/04 – CORRECTION CURVE ON 094/9

Figure B4.8A.

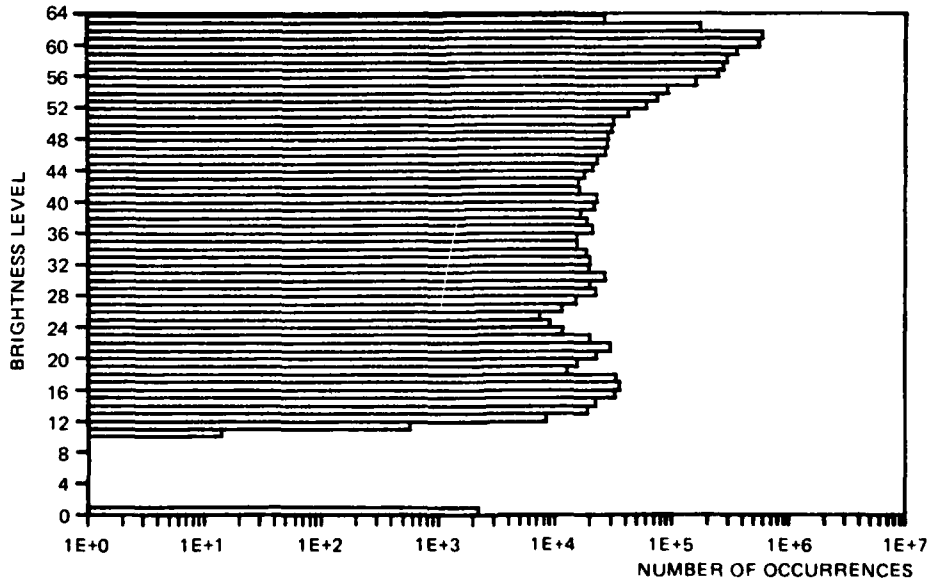

PEL BRIGHTNESS STATISTICS
WTM TYPED PAGE – GREEN IMAGE CORRECTED WITH GREEN CURVE
IMAGE ON 097/04 – STATS ON 099/04 – CORRECTION CURVE ON 094/9

Figure B4.8B.

LEVEL	VALUE	LEVEL	VALUE	LEVEL	VALUE	LEVEL	VALUE
0	2200	16	31897	32	9731	48	26395
1	0	17	37379	33	10731	49	40622
2	0	18	36697	34	11266	50	52081
3	0	19	30989	35	13082	51	37658
4	0	20	30488	36	24205	52	50553
5	0	21	29666	37	22128	53	75425
6	0	22	23550	38	22696	54	103223
7	0	23	30627	39	22299	55	163586
8	0	24	30048	40	19757	56	179220
9	0	25	16749	41	19398	57	176313
10	0	26	13515	42	24738	58	222973
11	0	27	12518	43	22210	59	291606
12	44	28	19811	44	25135	60	427839
13	270	29	18980	45	22708	61	523669
14	1654	30	24696	46	20683	62	449801
15	17421	31	17551	47	20779	63	242340

PEL BRIGHTNESS STATISTICS
WTM TYPED PAGE – BLUE IMAGE CORRECTED WITH BLUE CURVE
IMAGE ON 097/05 – STATS ON 099/05 – CORRECTION CURVE ON 094/12

Figure B4.9A.

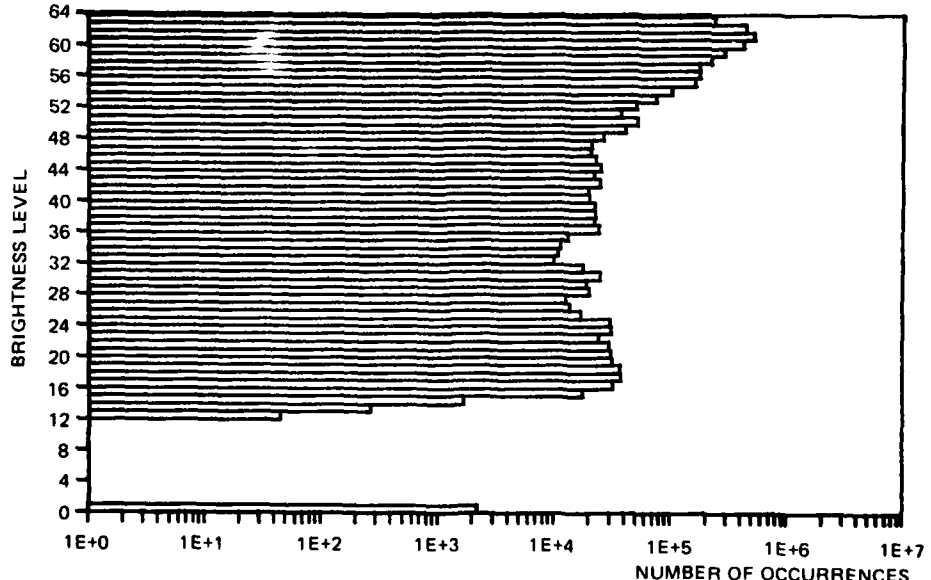

PEL BRIGHTNESS STATISTICS
WTM TYPED PAGE – BLUE IMAGE CORRECTED WITH BLUE CURVE
IMAGE ON 097/05 – STATS ON 099/05 – CORRECTION CURVE ON 094/12

Figure B4.9B.

LEVEL	VALUE	LEVEL	VALUE	LEVEL	VALUE	LEVEL	VALUE
0	1024	16	0	32	0	48	41192
1	0	17	0	33	0	49	77578
2	0	18	0	34	0	50	70893
3	0	19	0	35	0	51	90416
4	0	20	0	36	2	52	83960
5	0	21	0	37	2	53	77910
6	0	22	0	38	1	54	54036
7	0	23	0	39	5	55	172093
8	0	24	0	40	6	56	121918
9	0	25	0	41	14	57	119012
10	0	26	0	42	19	58	97082
11	0	27	0	43	6967	59	450856
12	0	28	0	44	33658	60	147830
13	0	29	0	45	38202	61	12353
14	0	30	0	46	30276	62	22
15	0	31	0	47	42153	63	0

PEL BRIGHTNESS STATISTICS
RED STANDARD IMAGE – 1024 LINES – TAPE NO. 094 – FILE 13
CAPTURED 12/5/79 – STATS ON 094/4

Figure B4.10A.

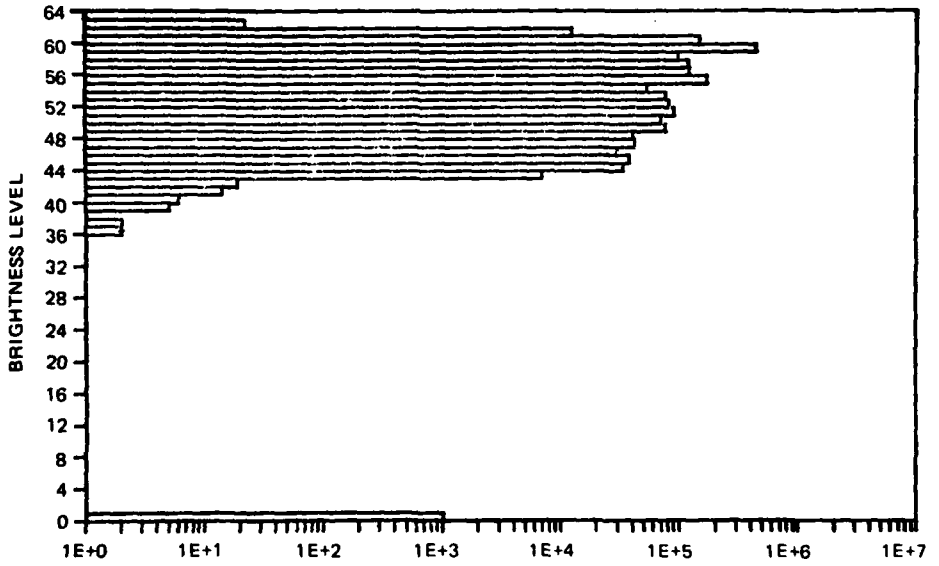

PEL BRIGHTNESS STATISTICS
RED STANDARD IMAGE – 1024 LINES – TAPE NO. 094 – FILE 13
CAPTURED 12/5/79 – STATS ON 094/4

Figure B4.10B.

STATISTICAL VALUES

FIRST ELEMENT	=	1
NUMBER OF ELEMENTS	=	1727
MAXIMUM VALUE	=	61925
RELATIVE LOCATION OF MAXIMUM	=	858
MINIMUM VALUE	=	44188
RELATIVE LOCATION OF MINIMUM	=	1715
SUM OF ELEMENTS	=	97154715
ARITHMETIC MEAN	=	56256.4
MEAN DEVIATION	=	3857.5
STANDARD DEVIATION	=	4593.0
VARIANCE	=	21095987.4
QUADRATIC MEAN	=	56443.5

RED STANDARD IMAGE – 1024 LINES – TAPE NO. 094 – FILE 13
CAPTURED 12/5/79 – STATS ON 094/5

Figure B4.10C.

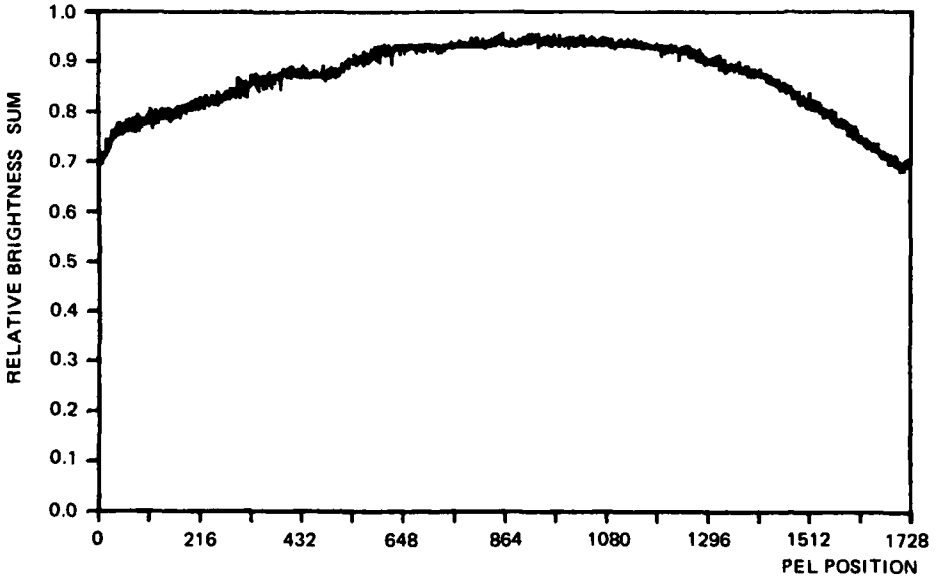

SPATIAL FREQUENCY IDENTIFICATION – HORIZONTAL
RED STANDARD IMAGE – 1024 LINES – TAPE NO. 094 – FILE 13
CAPTURED 12/5/79 – STATS ON 094/5

Figure B4.10D.

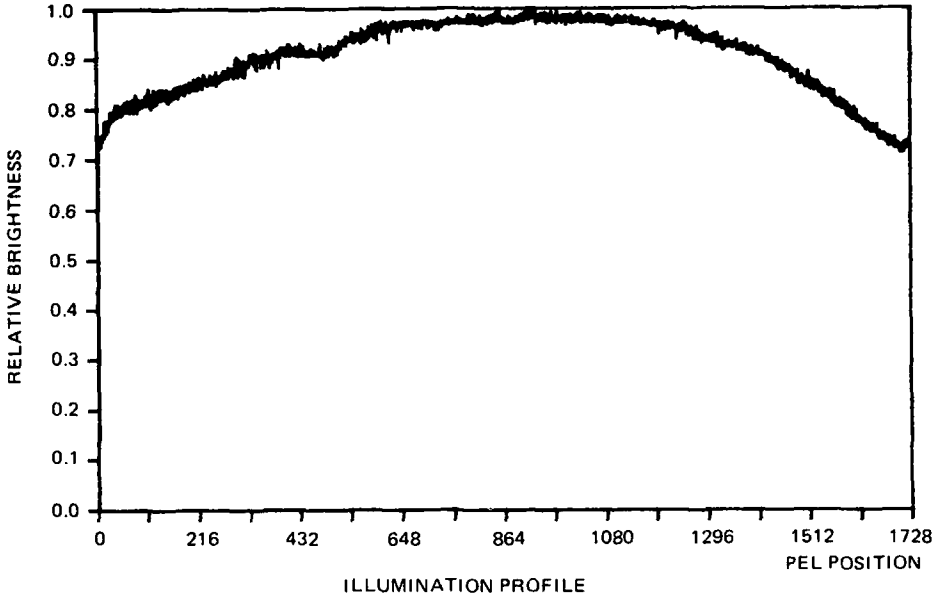

ILLUMINATION PROFILE
RED STANDARD IMAGE – 1024 LINES – TAPE NO. 094 – FILE 13
CAPTURED 12/5/79 – STATS ON 094/6

Figure B4.10E.

LEVEL	VALUE	LEVEL	VALUE	LEVEL	VALUE	LEVEL	VALUE
0	1024	16	0	32	0	48	22677
1	0	17	0	33	0	49	35491
2	0	18	0	34	0	50	31764
3	0	19	0	35	0	51	45350
4	0	20	0	36	3	52	47906
5	0	21	0	37	1	53	76568
6	0	22	0	38	0	54	64020
7	0	23	0	39	9	55	146014
8	0	24	0	40	36	56	113411
9	0	25	0	41	2687	57	177673
10	0	26	0	42	13598	58	105670
11	0	27	0	43	33419	59	398310
12	0	28	0	44	29440	60	229774
13	0	29	0	45	24822	61	115705
14	0	30	0	46	19307	62	1970
15	0	31	0	47	32811	63	12

PEL BRIGHTNESS STATISTICS
GREEN STANDARD IMAGE – 1024 LINES – TAPE NO. 094 – FILE 14
CAPTURED 12/5/79 – STATS ON 094/7

Figure B4.11A.

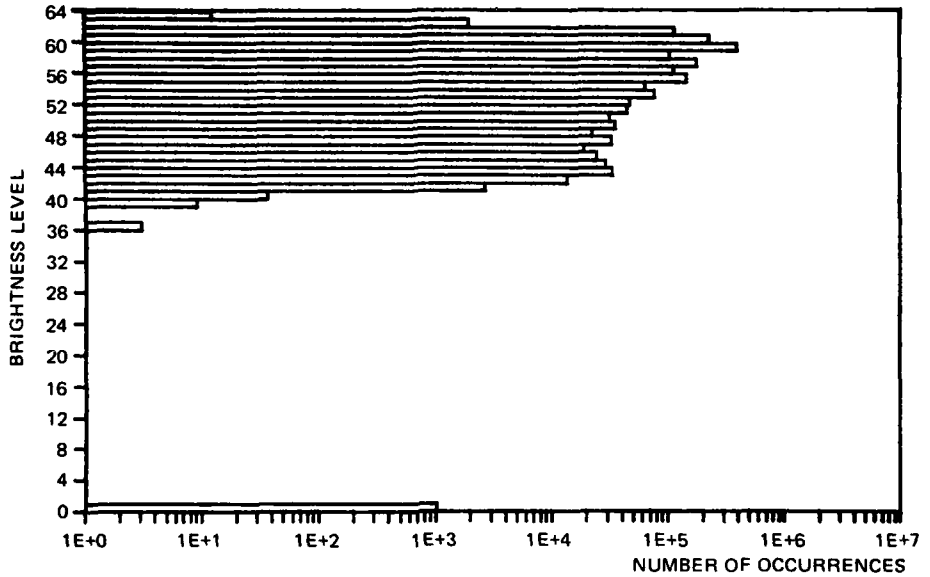

PEL BRIGHTNESS STATISTICS
GREEN STANDARD IMAGE – 1024 LINES – TAPE NO. 094 – FILE 14
CAPTURED 12/5/79 – STATS ON 094/7

Figure B4.11B.

STATISTICAL VALUES

FIRST ELEMENT	=	1
NUMBER OF ELEMENTS	=	1727
MAXIMUM VALUE	=	62746
RELATIVE LOCATION OF MAXIMUM	=	606
MINIMUM VALUE	=	42455
RELATIVE LOCATION OF MINIMUM	=	1715
SUM OF ELEMENTS	=	98803364
ARITHMETIC MEAN	=	57211.0
MEAN DEVIATION	=	3744.3
STANDARD DEVIATION	=	4775.3
VARIANCE	=	22803694.8
QUADRATIC MEAN	=	57409.9

GREEN STANDARD IMAGE – 1024 LINES – TAPE NO. 094 – FILE 14
CAPTURED 12/5/79 – STATS ON 094/8

Figure B4.11C.

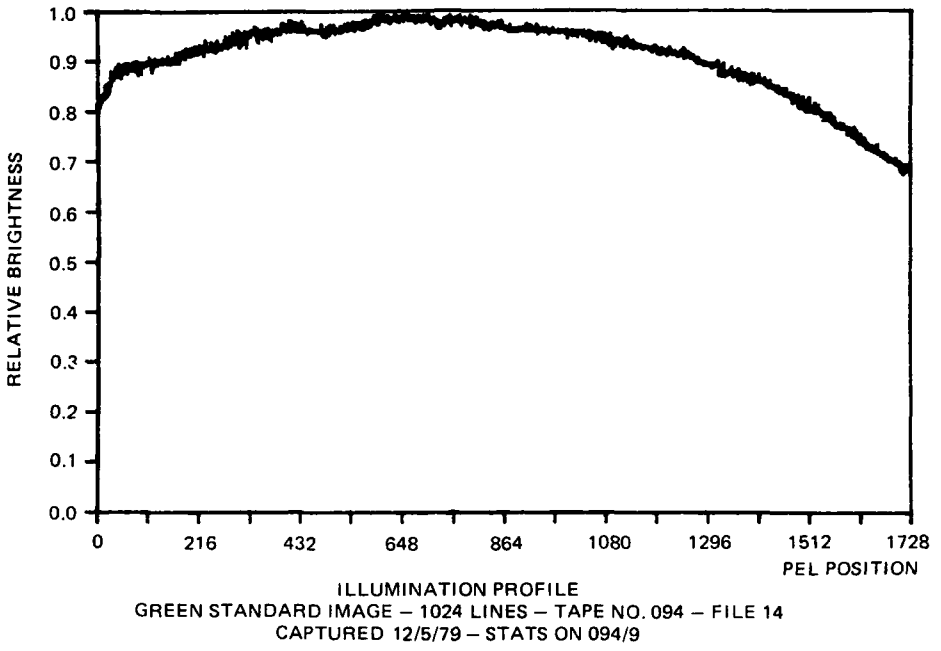

Figure B4.11D.

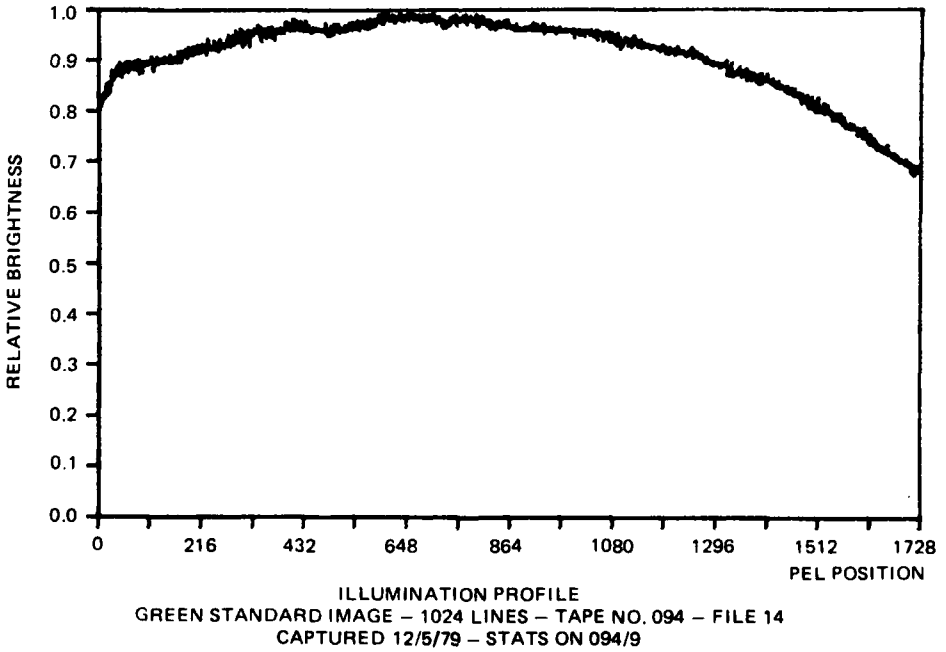

Figure B4.11E.

LEVEL	VALUE	LEVEL	VALUE	LEVEL	VALUE	LEVEL	VALUE
0	1024	16	0	32	0	48	20054
1	0	17	0	33	0	49	29167
2	0	18	0	34	0	50	36541
3	0	19	0	35	1	51	54198
4	0	20	0	36	1	52	102415
5	0	21	0	37	1	53	115550
6	0	22	0	38	3	54	70389
7	0	23	0	39	0	55	173021
8	0	24	0	40	8	56	228760
9	0	25	0	41	7	57	355977
10	0	26	0	42	14	58	282467
11	0	27	0	43	3926	59	204365
12	0	28	0	44	16758	60	404
13	0	29	0	45	20236	61	0
14	0	30	0	46	21535	62	0
15	0	31	0	47	32650	63	0

PEL BRIGHTNESS STATISTICS
BLUE STANDARD IMAGE – 1024 LINES – TAPE NO. 094 – FILE 15
CAPTURED 12/5/79 – STATS ON 094/11

Figure B4.12A.

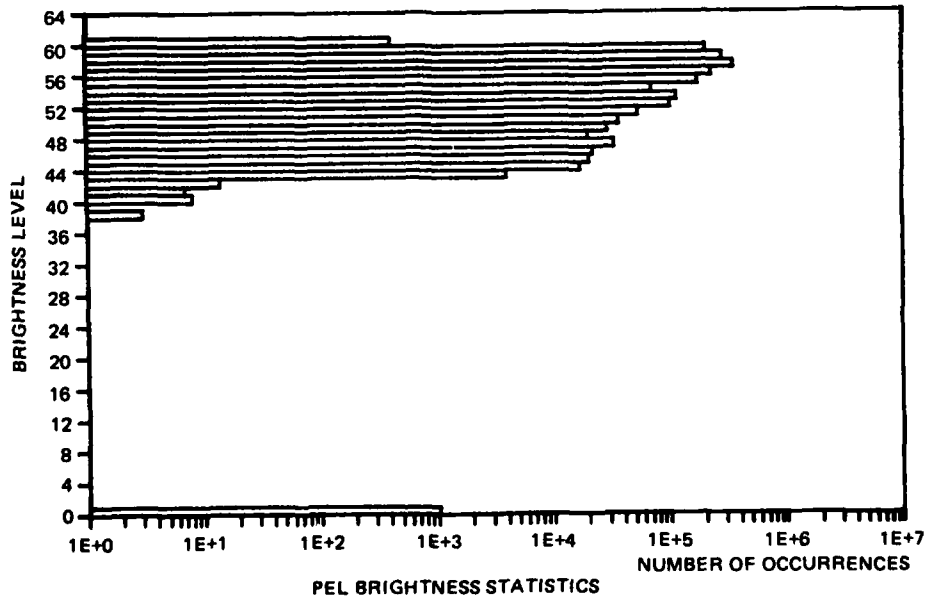

PEL BRIGHTNESS STATISTICS
BLUE STANDARD IMAGE – 1024 LINES – TAPE NO. 094 – FILE 15
CAPTURED 12/5/79 - STATS ON 094/10

Figure B4.12B.

STATISTICAL VALUES

FIRST ELEMENT	=	1
NUMBER OF ELEMENTS	=	1727
MAXIMUM VALUE	=	60505
RELATIVE LOCATION OF MAXIMUM	=	1034
MINIMUM VALUE	=	44362
RELATIVE LOCATION OF MINIMUM	=	1715
SUM OF ELEMENTS	=	97659291
ARITHMETIC MEAN	=	56548.6
MEAN DEVIATION	=	2722.8
STANDARD DEVIATION	=	3493.8
VARIANCE	=	12200969.1
QUADRATIC MEAN	=	56656.3

BLUE STANDARD IMAGE – 1024 LINES – TAPE NO. 094 – FILE 15
CAPTURED 12/5/79 – STATS ON 094/10

Figure B4.12C.

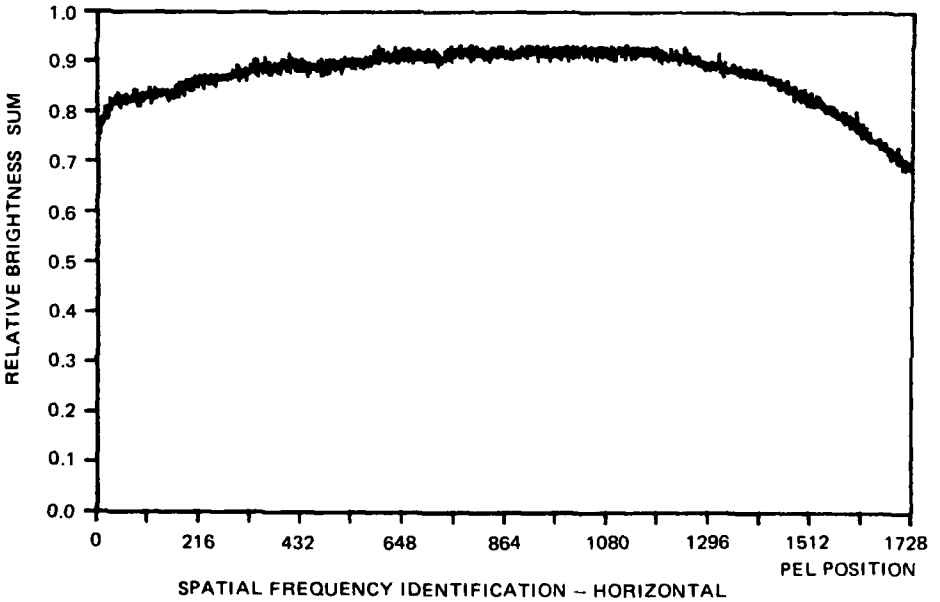

SPATIAL FREQUENCY IDENTIFICATION – HORIZONTAL
BLUE STANDARD IMAGE – 1024 LINES – TAPE NO. 094 – FILE 15
CAPTURED 12/5/79 – STATS ON 094/11

Figure B4.12D.

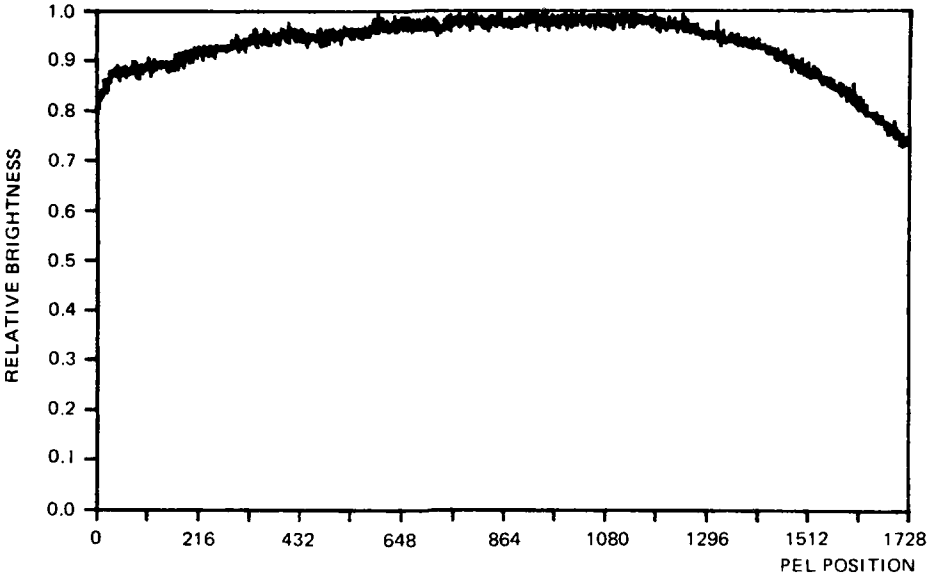

ILLUMINATION PROFILE
BLUE STANDARD IMAGE – 1024 LINES – TAPE NO. 094 – FILE 15
CAPTURED 12/5/79 – STATS ON 094/12

Figure B4.12E.

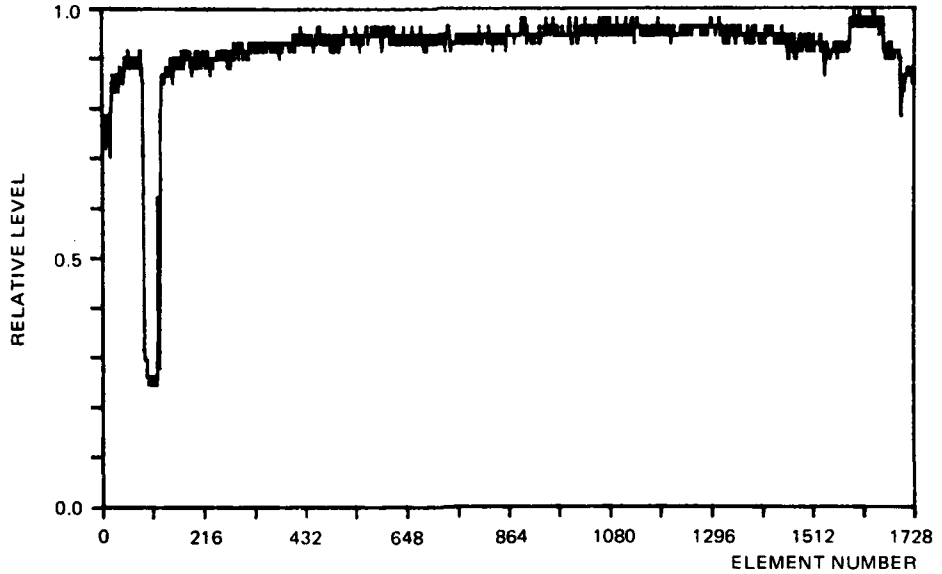

ARRAY VARIABLE PLOT – NORMALIZED TO MAXIMUM VALUE (61)
RED IMAGE – WTM TYPED PAGE – CORRECTED WITH WHITE STANDARD
TAPE 097 – FILE 0 – LINE 1800

Figure B4.13A.

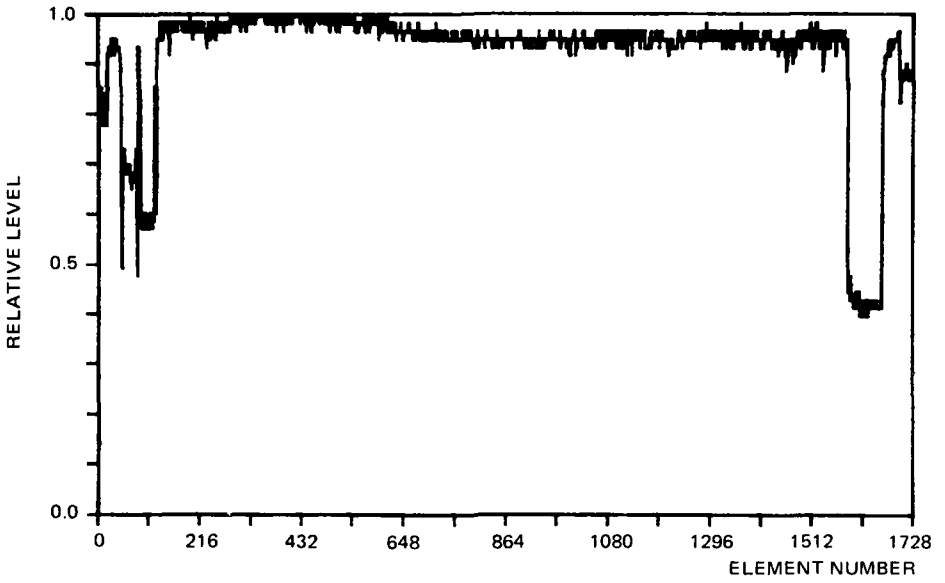

ARRAY VARIABLE PLOT – NORMALIZED TO MAXIMUM VALUE (63)
GREEN IMAGE – WTM TYPED PAGE – CORRECTED WITH WHITE STANDARD
TAPE 097 – FILE 1 – LINE 1800

Figure B4.13B.

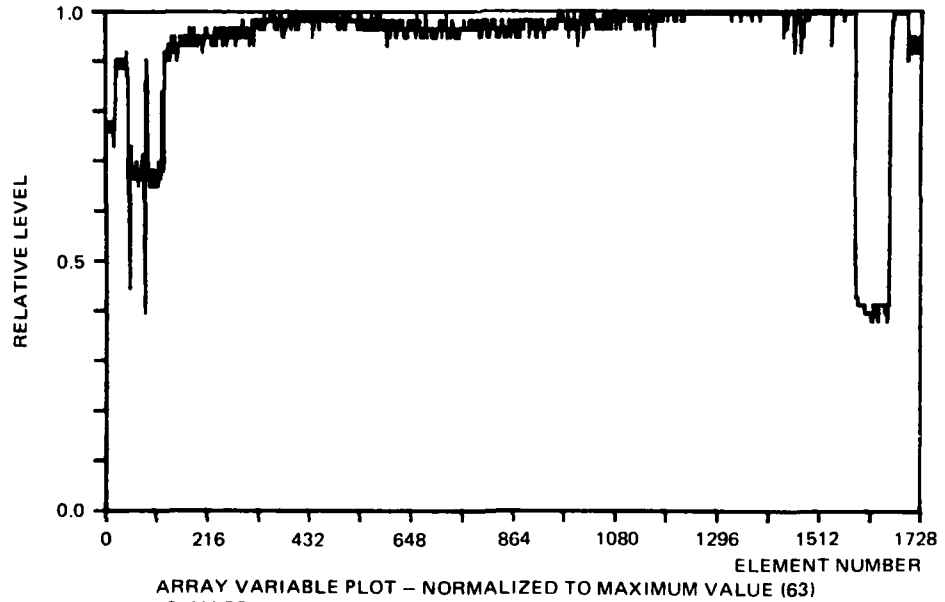

ARRAY VARIABLE PLOT – NORMALIZED TO MAXIMUM VALUE (63)
BLUE IMAGE – WTM TYPED PAGE – CORRECTED WITH WHITE STANDARD
TAPE 097 – FILE 2 – LINE 1800

Figure B4.13C.

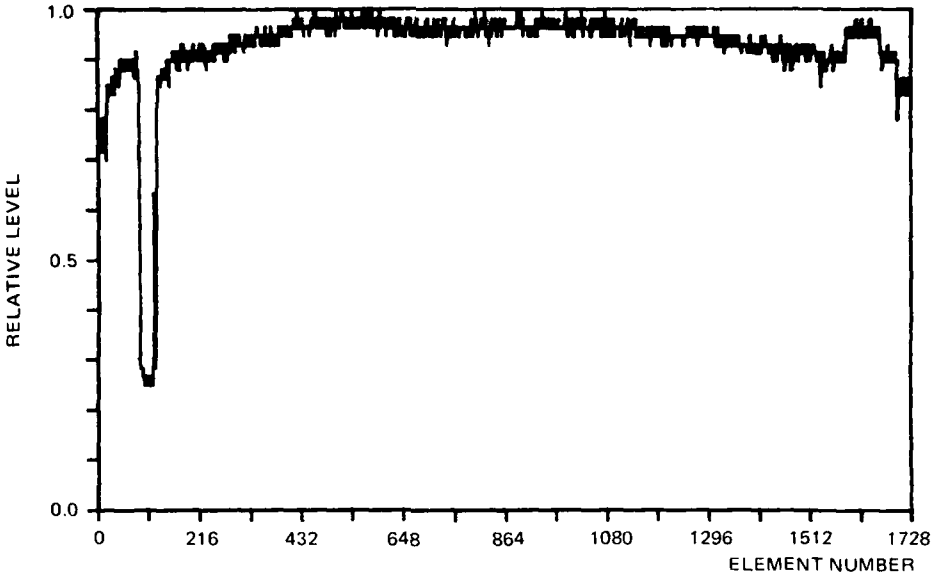

ARRAY VARIABLE PLOT – NORMALIZED TO MAXIMUM VALUE (60)
RED IMAGE – WTM TYPED PAGE – CORRECTED WITH RED STANDARD
TAPE 097 – FILE 3 – LINE 1800

Figure B4.14A.

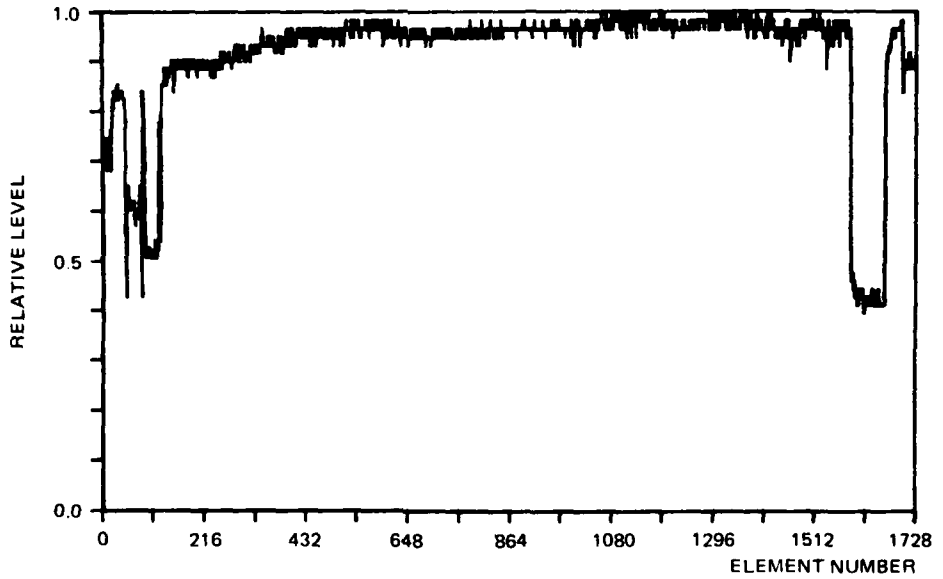

ARRAY VARIABLE PLOT – NORMALIZED TO MAXIMUM VALUE (63)
GREEN IMAGE – WTM TYPED PAGE – CORRECTED WITH GREEN STANDARD
TAPE 097 – FILE 4 – LINE 1800

Figure B4.14B.

AD-A089 436 NAVAL OCEAN SYSTEMS CENTER SAN DIEGO CA F/G 9/5
ADVANCED MAIL SYSTEMS SCANNER TECHNOLOGY, EXECUTIVE SUMMARY AND--ETC(U)
OCT 79 F C MARTIN, T R LITTLE, L A WISE
UNCLASSIFIED NOSC/TR-520 NL

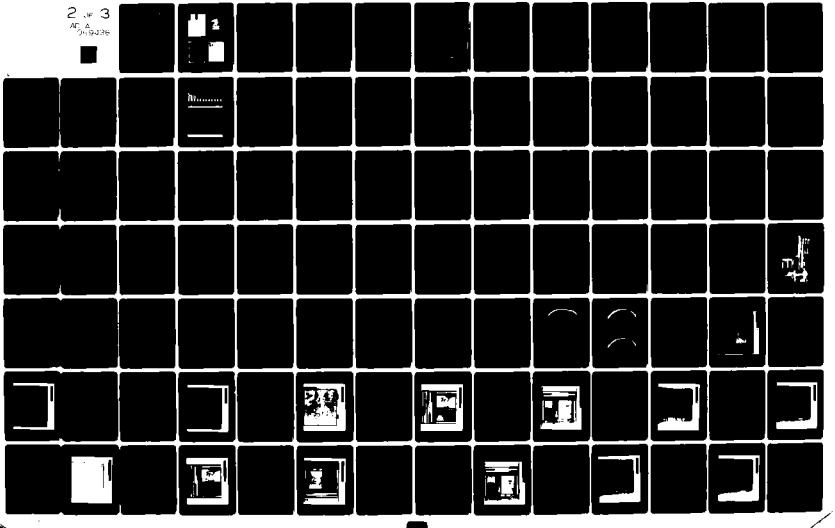

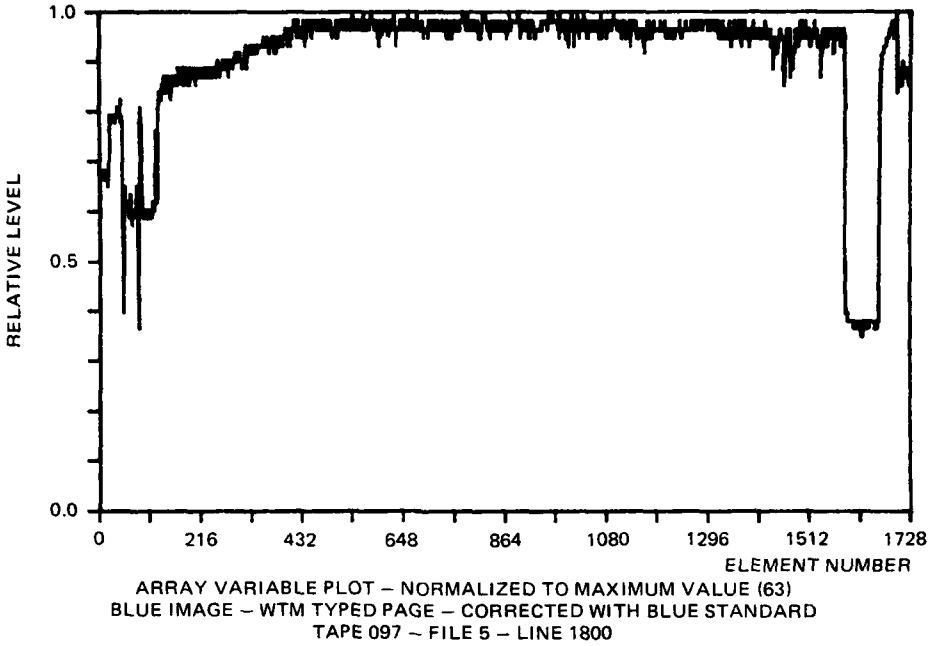

Figure B4.14C.

5.0 COLOR IMAGE TEST PATTERN

5.1 GREY SCALE STEP WEDGE

As an aid in the processing of photographic images it has become common practice to record a grey scale step wedge near the active image area. This acts as a source of calibration information for the printing process. Calibration information is necessary because the operator doing the photograph printing may not necessarily know what the correct intensity or color balance of the print should be. The grey scale wedge is generated by the computer by simply counting from the minimum to the maximum value, with an appropriate step size, and is printed for as many image lines as desired.

5.2 COLOR CALIBRATION TEST MATRIX

Although the whiteness of a grey scale test wedge is an excellent indicator of the color balance of a color image system, a color test matrix dramatically demonstrates the color capability of the system. In addition the color patches on prints or transparencies can be measured with appropriate optical instruments to determine the balance quantitatively. The color test matrix was generated by the computer much in the fashion in which the grey scale wedge had been generated. The color calibration test matrix is presented in figure B5.1A in reduced form. Figure B5.1 is the only color sample presented in this report, also shown as

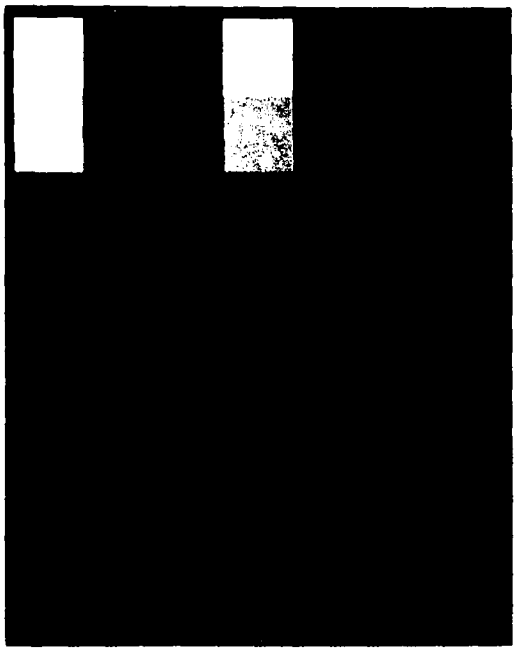

Figure B5.1A. Color test matrix.

Figure B5.1B. USPS logo.

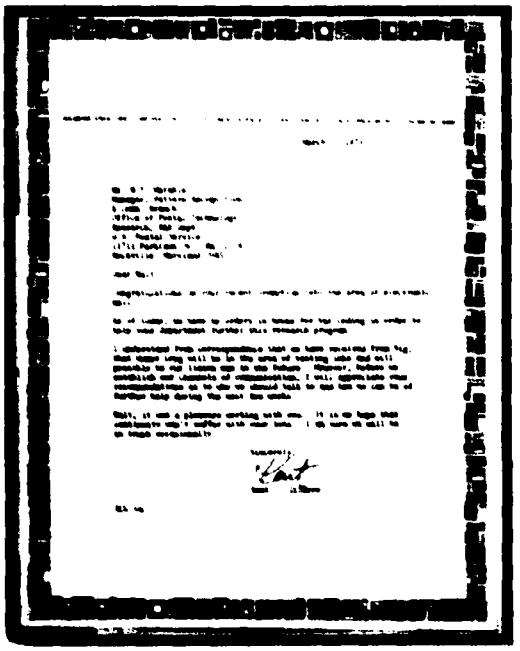

Figure B5.1C. WTM typed letter.

Figure B5.1D. Color photograph.

the frontispiece. The entire set of color prints used in the generation of the original Color Imaging Report is available at NOSC, Code 7323, for review.

6.0 TEST IMAGES

6.1 SELECTED DEMONSTRATION IMAGES

Seven test images were selected as typical examples of the type of material which might be transmitted via EMSS. The type of material selected is intended to demonstrate the color capability of the ICAS as well as some of the difficulties in acquiring and processing color images. The documents selected for acquisition, processing, and reproduction are the following:

1. Color test matrix (image 18-17)
2. The WTM typed letter (image 04-01)
3. USPS logo (image 18-15)
4. Newsweek ad (image 17-01)
5. Sample from Fairchild test deck (M-429)
6. A composite paste-up containing the NOSC logo, a grey scale wedge, a green oscilloscope trace, and a multicolor warning circular (image 18-18)
7. Color photograph (image 12-04)

These images were all acquired using the ICAS and large drum testbed as described in section 3 and color-corrected as described in section 4. The photographic prints were produced by photographically enlarging positive transparencies made on the Dicomed film recorder. The samples are intended to show the color capability and the associated problems of color image processing, and it was felt that accurate size reproduction was not essential. One sample serves as the frontispiece to this report. The others are available at NOSC, Code 7323.

6.2 COLOR TEST MATRIX

As previously described in section 5, a color test matrix was computer generated in order to aid in the evaluation of the color image reproduction process. Image 18-17 was produced from film made on the Dicomed image recorder directly from the computer-generated data. The original print was then placed on the large drum testbed and scanned as an original document. The rather unpleasant results of acquiring and printing are described in this section. There are two apparent problems that can be discussed here.

The most obvious deficiency is the fact that the overall brightness of the scanned image was far below that of the original. This is largely due to the fact that the page was acquired in prescan mode; that is, the illumination intensity was set up using a white standard photographic paper whose reflectance was higher than the print from which the image was acquired. The result is that the maximum brightness level acquired was in the 40 to 48 level range rather than 63 which was expected. The majority of this problem can be eliminated by a main scan setup of the illumination source to increase the overall brightness of the acquired image.

The second problem was noticed as an apparent imbalance of the three primary colors (red, green, and blue) in the magenta, cyan, and yellow portions of the reproduced image of the color test matrix. In investigating the source of this difficulty, a series of line plots through the image data were made. These plots should demonstrate a consistent brightness level for each of the color components used across the image. Specifically, four patches using a single primary color should show four identical brightness levels in the areas where that component color is present and three consistent zero levels where that component is not present. The figures that follow are actual line plots through the uncorrected (fig B6.1) and corrected (fig B6.2) images of the color matrix print. Referring back to the color test matrix in figure B5.1A, these line plots represent image lines through each of the top four rows of color patches in the matrix going from white, to cyan, to magenta, and on to red. The fact that these brightness levels are far from being uniform clearly indicates that the color balance of the original image scan was not correct. At this time, the cause of this deficiency is not yet fully understood.

6.3 COLOR IMAGE EXAMPLES

The color reproductions presented in this report represent a few of the early attempts at integrating color capability into the ICAS. The effects of many variables were studied, including illumination source, filters, illumination correction, and photographic processing and printing.

Figure B5.1 contains one computer-generated image and three reproductions of images after scanning and processing using the separate red, green, and blue illumination correction curves. As mentioned earlier the full-size original photographs produced of these and the other images mentioned in section 6.1 are available for review at NOSC, Code 7323.

RESULTS

1. Color images were successfully acquired with the ICAS.

2. Charge-coupled devices and fluorescent lamps proved satisfactory for color acquisition.

3. Methods were established to independently provide calibration of the input acquisition process and the output display and printing process.

4. Variations were discovered not only in illumination intensity across the scanned image but also in the color balance of the source.

CONCLUSIONS

1. The set of color separation filters, the Wratten 25, 58, and 47B, appears to be satisfactory for scanning color documents.

2. Very careful selection of neutral density filters or stop adjustments is required to maintain true color balance.

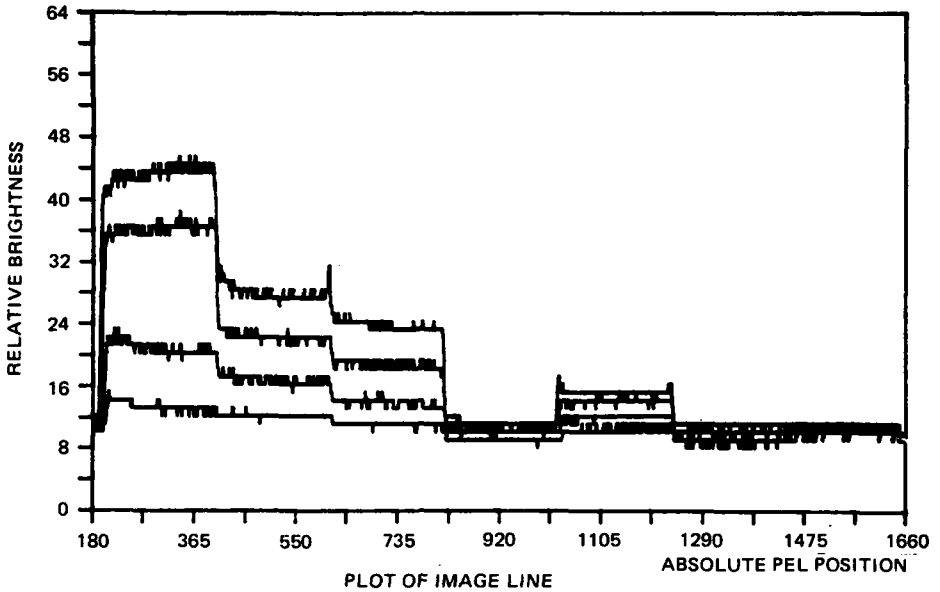

Figure B6.1A.

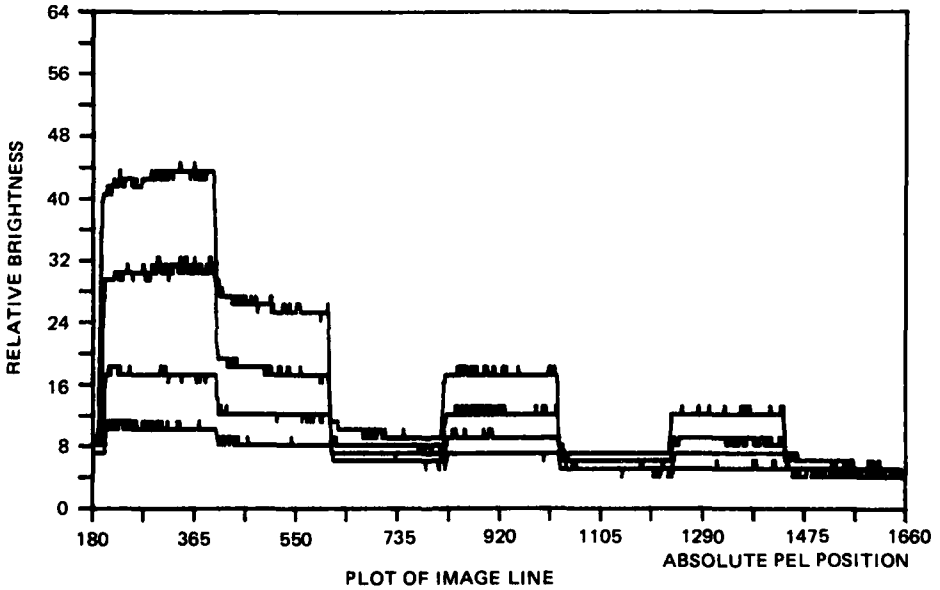

Figure B6.1B.

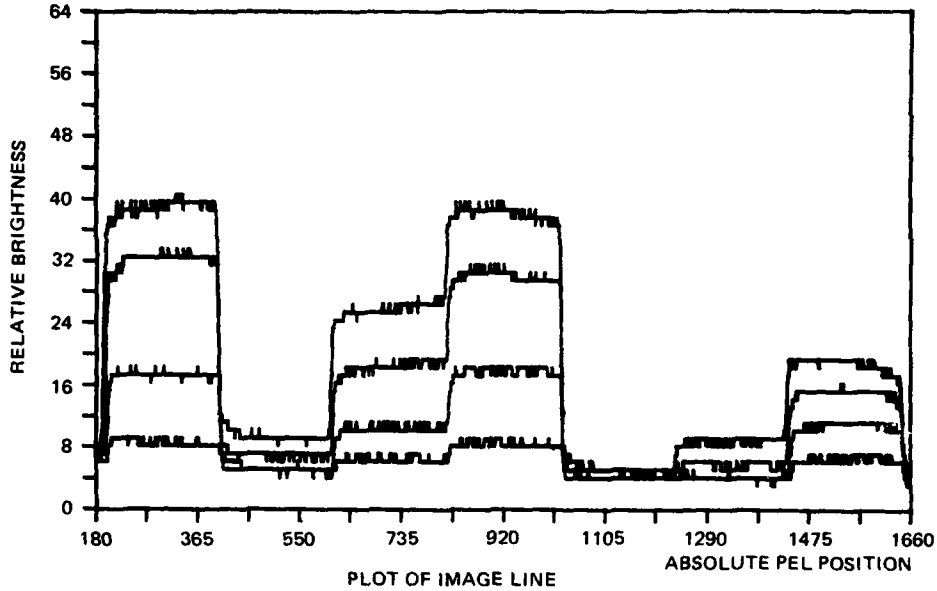

Figure B6.1C.

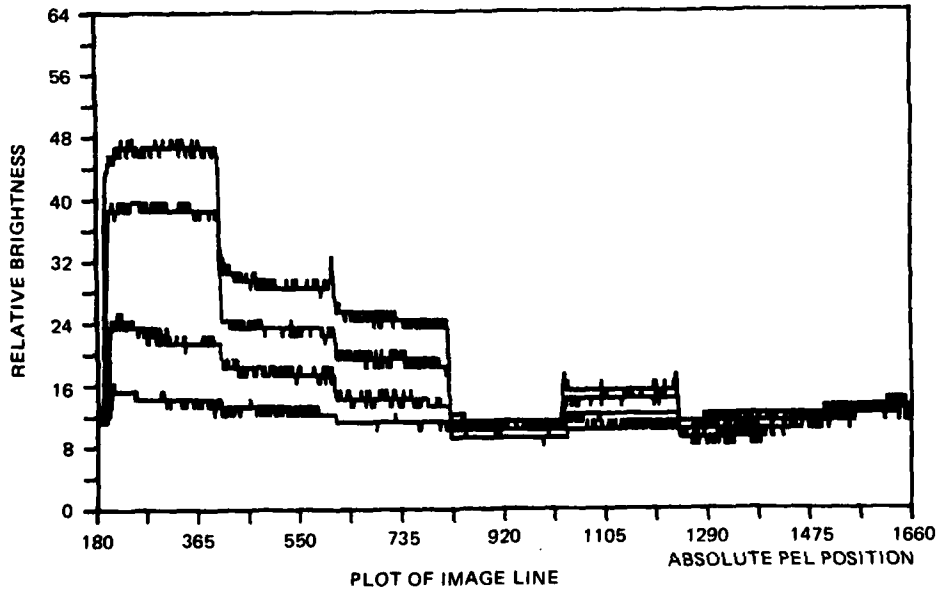

Figure B6.2A.

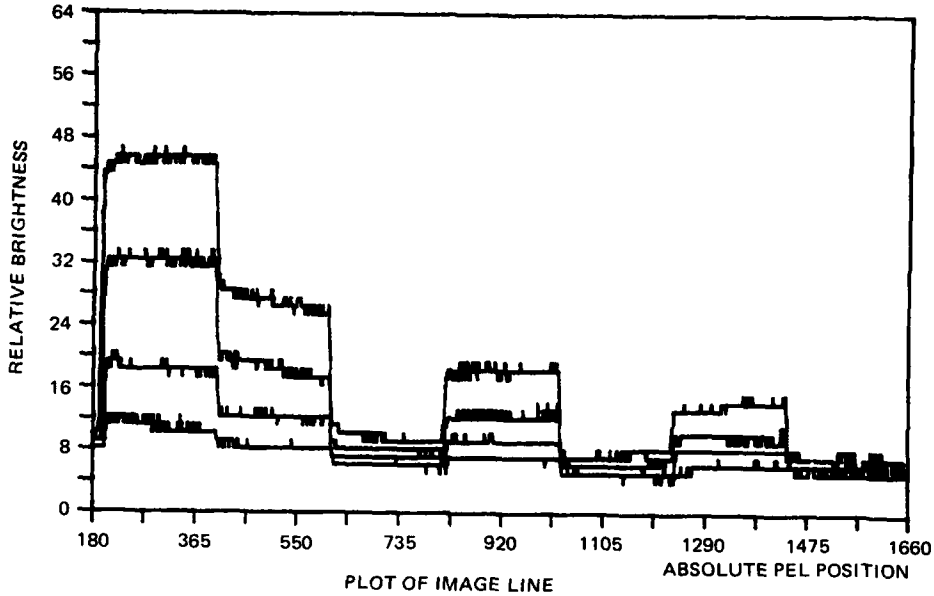

Figure B6.2B.

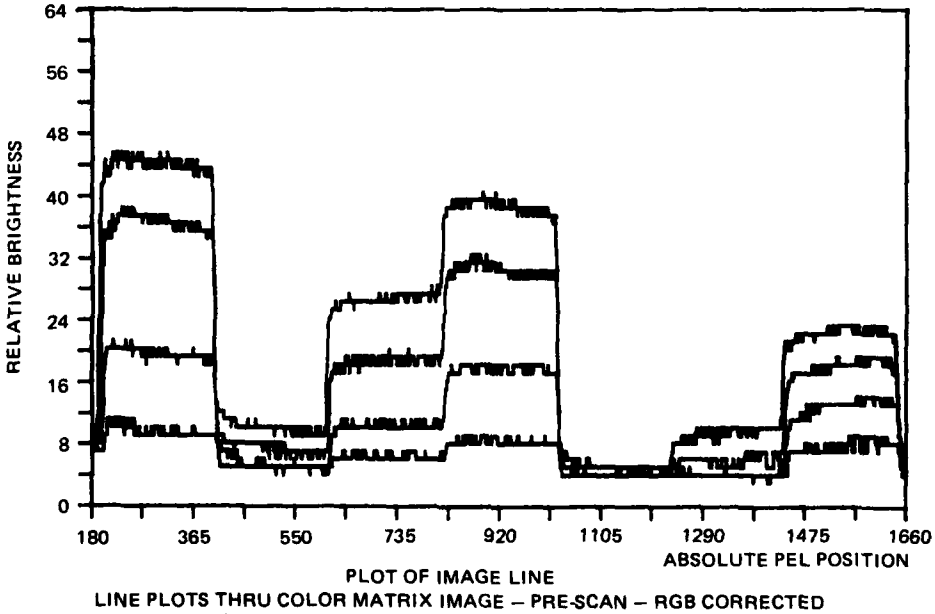

Figure B6.2C.

3. An illumination source very uniform in color temperature and intensity at the document surface is necessary to preclude the requirement for separate red, green, and blue standard corrections.

4. Registration, which might be a problem if three separate imager stations were used for tricolor acquisition instead of a single lens optical beamsplitter station, was not a problem when rescanning a color document affixed to the scanning drum.

APPENDIX C:

DATA DISPLAY SYSTEMS PERFORMANCE ANALYSES

by

WR Robinson

Code 8235

Naval Ocean Systems Center

CONTENTS

ILLUSTRATIONS

TABLES

INTRODUCTION

Appendix C presents and documents the quantitative performance data obtained in photometrically measuring AN/TMQ-29 generated test pattern film specimens received from the Naval Oceanography Command Facility (NOCF), formerly the Navy Weather Service Facility of San Diego (NWSF-SD). The standard configuration of a TMQ-29 utilizes a CRT to write on a wet process, after which it is developed matically. NOCF-SD has a TMQ-29 system that has been modified so that it can also write with a laser on either dry or wet process film. The laser wet process film is developed by the CRT film developer. The laser writing subsystem was developed and installed by the Harris Government Communications Systems Division of Melbourne, Florida. The film specimens received from NOCF-SD were made over a period of 5 months. Three configurations of the TMQ-29 were used for the purpose of quantifying the purported superiority of the laser writing process over the CRT writing process.

The TMQ-29 system at NOCF includes a computer which can be programmed to generate test pattern signals that can be printed in the same way the actual weather data are printed. The hard copies of a standardized test pattern made by the three different system configurations over the 5-month period are the primary data base for this report. Actual weather data printouts made over the same period with each configuration are the secondary data base used only for subjective analysis.

The film measurement procedures used in compiling the data for this report generally follow those specified by the Navy Space Systems Activity/Code 60, Los Angeles CA (NSSA), in their document titled "Evaluation of Laser Data Display System (LDDS) as part of the AN/SMQ-10 and AN/TMQ-29," dated 15 January 1979 (annex B), and, as revised, 15 June 1979 (annex C).* However, the instrumentation available at NOSC is quite different from that specified in the NSSA documents. The NSSA test procedures call for strictly analog measurement and recording equipment, whereas the NOSC equipment uses digital techniques. This difference results in not being able to fill in all the blanks in the NSSA procedure data sheets or obtaining all the data specified because of memory space. The digital technique, however, has the advantage that the measured data are stored on magnetic tape and can be retrieved at any time, reprocessed, and plotted again for comparison and analysis in different ways as new questions about the system arise.

When the systems evaluation program was started in March 1979, it was intended that a complete set of data would be generated every month for about 4 months. The purpose was to measure the performance of each subsystem at the beginning of the program and then watch for changes over the span of the program. This was a good plan; however, the equipments involved did not always cooperate and to some extent there was very likely human error. The details will be presented later; however, it can be said that considerably less usable data were received than had been expected. It was learned that there was a problem in getting the laser wet process film to feed into the TMQ-29's film developing subsystem because of excessive film curl. This resulted in losing most of the laser wet process film data.

* Available at NOSC, Code 7323

It should be noted that this author has very extensive experience with CRT systems and photometrics but no intimate familiarity with the equipments being evaluated. Therefore, any comments made on what the various subsystems may have been doing will be educated guesses based on this experience and what is found in the data. This lack of specific hardware familiarity precludes any comments on why there are gaps in the intended data base or what may have transpired at NOCF between data submissions. This report is based solely on the data submitted to NOSC. Table C1 is a complete tabulation of the data submitted and their quality. The presence of the letter U indicates there were functional problems somewhere in the TMQ-29 system that resulted in film specimens that would not produce useful microdensitometer data.

Table C1. Data submissions.

DATE OF RECORDING (Mon Day Yr)	LDDS					LWDS					CWDS					
	RES BARS	LIN PAT	64S GS	GS 32	MAPS	RES BARS	LIN PAT	64S GS	GS 32	MAPS	RES BARS	LIN PAT	64S GS	GS 32	MAPS	
Unknown											S	S	S	U		Sample of test pattern 1
3269	U	SS	S∅	S	S					S				U	S	
328										S						
3309									S							
4279															S	
4379											SU	SS	S∅			
5319	U		S	S	S	S		S	S	S	S		S	S	S	
6169					S					S					S	
7279															S	
7379					S											
7189					S					S						
8279					S										S	
8159	U	S	∅		S											
9679	S	S	S		S						SS	SS	SS		SS	One set of CW data was 2494 film.

S - good data
U - unusable data
∅ - data not used

PROCEDURES

The bulk of this appendix is based on the quantitative photometric data gathered from analyzing film specimens generated by the CRT printed wet process film subsystem (CWDS), the laser printed dry process film subsystem (LDDS), and the laser printed wet process film subsystem (LWDS). The NSSA test plan called for measurement of: (1) modulation transfer function (MTF), (2) step function density accuracy, (3) deflection linearity, and (4) grey shade 32 uniformity. The first three of these parameters are determined from the test pattern depicted in figure C1, which was generated by the computer associated with the TMQ-29 system at NOCF. The fourth parameter is determined from a film specimen that is generated by letting the printing head expose the film for several minutes at a selected static intensity that is defined as grey shade 32 (the system has a range of 64 shades).

All the quantitative data presented in this appendix were obtained with photometric equipment made by Gamma Scientific and controlled by a Hewlett-Packard 9825 programmable calculator. The prime piece of photometric hardware used was a Model 700-10-90 Scanning Microdensitometer (SMD) that was modified by the author to operate with the digitally controlled photometer. As different tests were performed, the stage scanning range, microscope optics, and microprojector optics and aperture were changed. The equipment in a typical setup is shown in annex A to this appendix.

A smaller portion of this appendix will deal with the actual weather data printouts received. Each of these printouts has a grey shade scale printed at the beginning as part of the title block. This scale was measured and recorded to aid in subjective evaluation (eyeball evaluation) of the film specimens.

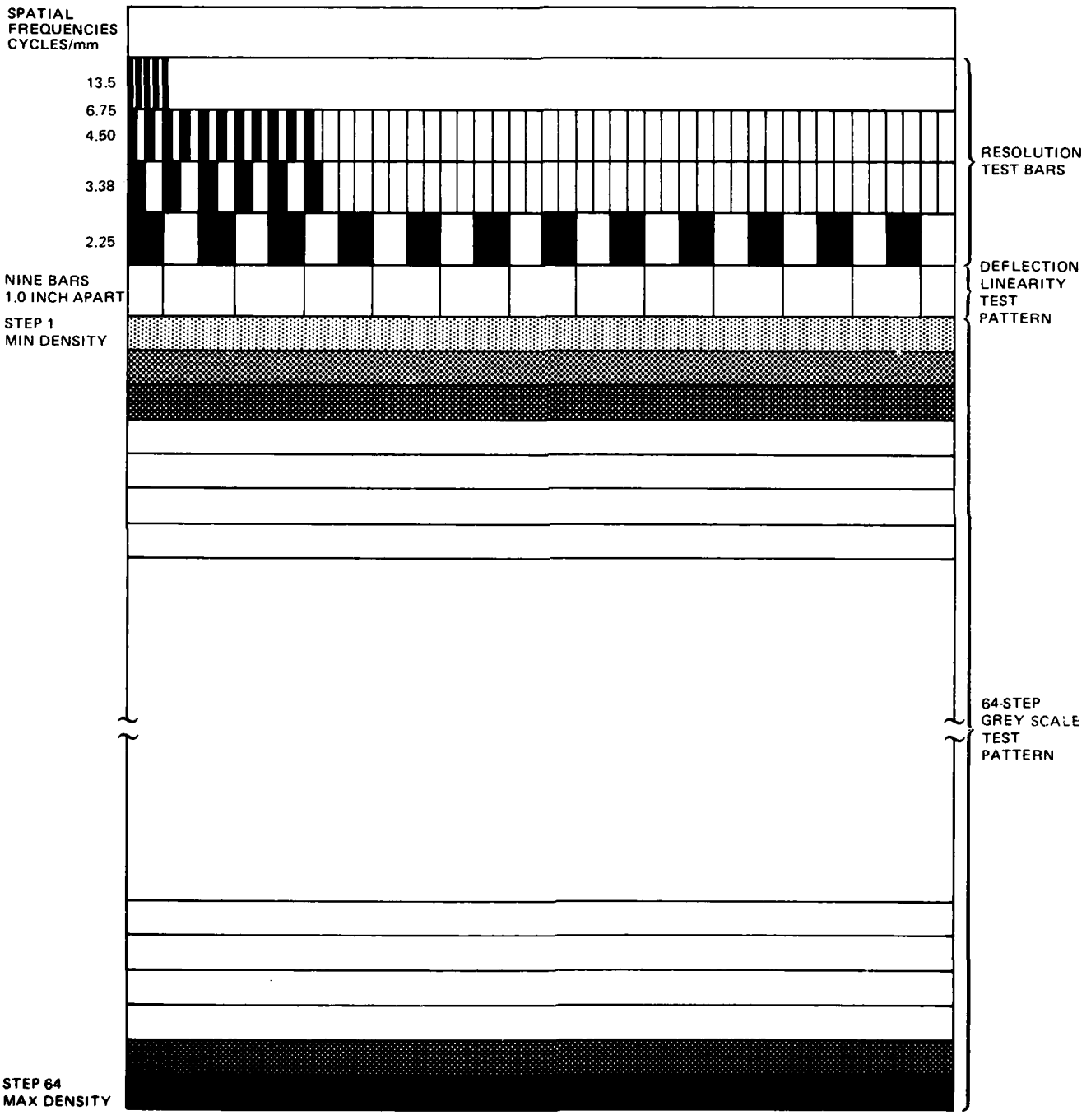

Figure C1. Test pattern (artist concept).

RESOLUTION

To measure the resolution with the SMD, the microprojector was set up with a 0.075-by-5.1-mm aperture and a 10X objective lens which gives an effective light slit width at the film of 7.5 micrometres, which is adequately narrow for measuring the highest spatial frequency of 13.5 cycles/mm where each half cycle is 37 μm wide. The sensor microscope was set up with a 0.075-by-2.5-mm aperture and a 5X objective to give a 15-by-500-μm pickup area. The stage drive was set for 1 to 1 ratio between stage lead screw and position transducer, and 4.00 volts was applied to the transducer. This setup allows the film to be moved past the sensor in increments as small as 6.3 μm. For the spatial frequencies in test pattern 1 (TP1), 2.25, 3.38, 4.50, 6.75 and 13.5 cycles/mm, stage movement increments of 152, 102, 76, 51, and 25 μm were used for each frequency, respectively. Eighty data points were measured for each frequency, which resulted in scanning approximately six cycles of each frequency. The TP1 resolution bars of each usable film specimen were scanned in the middle of the film and in an area 100 mm (4 in) off center on one side only. Only one side was measured because the film specimens were visually symmetrical. Tests similar to this were described in the NSSA test plan.

GREY SCALE ACCURACY

To measure the 64-step grey scale accuracy (step 1 is minimum density and 64 is maximum), the SMD was set up with a 5-mm aperture and 5X objective lens in the projector (the effective diameter is thus 1 mm), a 1250-μm aperture and X1 lens in the sensor microscope, 1 to 1 ratio between the stage lead screw and position transducer, and 1 volt on the transducer. The controller was programmed for two different tests:

(1) One hundred samples 1 mm in diameter and 1 mm apart were taken for a total scan of 100 mm (4 in). This was done for the 100 mm in the center of the total scan width of 21 mm (8.5 in) of grey shades (gs) 10, 20, 30, 40, 50, and 60. This test will be labeled 64S T1 on the data sheets. Also, the 100 mm to the left of gs32 center line and the 100 mm to the right of gs32 were measured. The film was manually repositioned for each 100 samples. This test will be labeled 64S T1a. The NSSA test plan does not describe a test of this nature.

(2) Eleven samples 1 mm in diameter and 1 mm apart were taken of each of the 64 gs steps. This test will be labeled 64S T2. A test similar to this is described in the NSSA test plan.

DEFLECTION LINEARITY

To measure the deflection linearity pattern on TP1, the SMD controller was programmed to drive the system plotter in a "digitize" mode. The plotter is actually an X-Y positioning device with 25-μm (0.001 in) accuracy. The film specimen to be measured is positioned in the plotter with the direction of film printer scan in the X axis. A special fiber optic probe is put into the plotter's penholder and positioned on top of each of the 1-inch deflection markers in turn. When the probe is accurately positioned over a test pattern mark, a controller key is pressed that causes the probe position to be read to the nearest 25 μm (0.001 in). The controller then prints out the plus or minus deviation in inches from the required position. A test very similar to this is described in the NSSA test plan.

GREY SHADE 32 UNIFORMITY

To measure the grey shade uniformity, the SMD was first set up with a large aperture, ie, 1 mm at the film plane, as called out in the NSSA test plan, and the controller was programmed for 160 samples 0.6 mm apart. Five 160-sample scans were made in the direction of film travel spaced 50 mm apart, and two scans were made end to end, thus scanning about 90% of the film width. Tests were run on three gs32 film specimens. The results were not deemed adequate -- particularly for the scans made in the direction of film travel. The filtering effect of the large aperture and increments with respect to the line-to-line film travel resulted in covering up the "periodic noise" in the direction of film travel. This noise will be discussed later. Suffice it to say at this time that it resulted in changing the measurement procedure.

The procedure adopted utilized a 0.075-by-5-mm light slit at the film plane and a 0.075-by-2.5-mm sensor aperture. The controller was programmed to read 800 points 0.1 mm apart in the direction of film travel and two scans end to end of 400 points 0.25 mm apart going across the film. The scan in the direction of film travel titled gs32 T1 was made approximately in the center of the film and covered a distance of 80 mm (which is about 1-1/2 minutes of film travel). The transverse scan covered about 90% of the film width and was titled gs32 T2.

The second procedure described above (which was used on all film specimens) resulted in too much noise, which also clouded the "periodic noise" alluded to above; however, it was possible to filter out some of this noise with a smoothing program in the controller. The smoothing process can be applied as many times as desired. Theoretically, running this smoothing program several times would have the same effect as using the large aperture initially described.

MAP DENSITY REFERENCE SCALE

To measure the map 64-step grey shade density reference scale, the SMD was set up with a 1-mm light spot at the film plane and a similar sensor aperture. The controller was programmed to take one reading at each density step. The map printouts received were in groups of three; ie, a X1 scaled map of some area and X2 and X4 blowups of an area near the center of the X1 map. The density reference scale was not measured on all the maps. The X1 scale was the one chosen unless it was obviously defective. Technically, the three scales should be identical, although no data were taken to prove the point. There is no procedure in the NSSA test plan similar to this test.

RESULTS

All the data obtained from the measurements described in the Procedures section were recorded on magnetic tape and then plotted on the four-color digital plotter that is part of the SMD controller system. All the data produced are contained herein. Each of the categories of tests will be described in detail below.

The data sheets are exactly as recorded by the plotter. The title on each is coded so as to fit within the allotted bytes assigned in the SMD controller programs. The first four letters identify the printing and film development process; ie, LDDS, LWDS, or CWDS. The next group of characters identifies the type of test and possibly a subset if there is a T1 or T2 present. The last four numbers are a date code for the date the film was recorded. The first digit is the month. The second and possibly the third digits are the day of the month the film was recorded. The last one or two digits are for the year, depending on the number of digits used by the day code. Thus, 79 appears in the last two digits if the day code used one digit, but only the 9 appears if the day code used two digits. The date shown in the right-hand corner of the data sheet is this same date code written in a more conventional manner.

The numbers following the word "maximum" on the data sheets are the maximum and minimum values attained by the particular trace associated with the color the numbers are written in. These numbers are optical densities, since the Y axis of the data sheets is optical density.

The X axis is labeled "Measurement No." These numbers indicate the actual number of data points recorded for each trace. They can be translated into spatial distance by checking the increments used for the test in question. The plotting program was not sophisticated enough to present the data in terms of distance. In the detailed discussion of results the spatial increments will be correlated.

RESOLUTION

Of all the tests described, this one is probably the most crucial in determining the best printing subsystem; however, it was the test that was the most difficult to get good data from, as evidenced by the U's in table C1 in the RES BARS columns. There was only one other U for all the other data. The U was assigned to the data because of line synchronization problems -- particularly with the data submitted that were laser printer originated. This sync problem makes a SMD test useless.

There were eight usable resolution data submissions during the program, three of which came from the laser printer. Of these three, two were on dry process film and one on wet process film. It should be noted that there was only one TP1 from LWDS submitted during the entire program. The results of the SMD scans are shown in figures C10 through C17.

In the Procedures section it was stated that there were five special test frequencies ranging from 2.25 to 13.5 cycles/mm; however, in figures C10 through C17, the frequencies appear to be all about equal. This is the result of the different SMD stage travel increments used to maximize the volume of data gathered. The only information being sought in this test was modulation amplitude, so the X axis distortion did not result in losing any data.

Table C2 presents the modulation amplitudes achieved in the eight film specimens. Figures C2 and C3 show the data of table C2 plotted as modulation transfer functions for the CRT and the laser configurations, respectively. The upper half of each figure is the response at the center of the film and the lower half is the response at the edge of the film (more precisely, 100 cm from the center). The different curves are identified by their date code.

Analyzing the data of figures C2 and C3 and table C2 produces the following facts:

(1) The ORIG (original) sample of CWDS was the best ever received from any configuration in terms of the maximum modulation response at the higher frequencies.

(2) The ORIG sample of CWDS had the best edge response, which indicates the best adjustment of the CRT focus and astigmatism controls.

(3) The center-of-film responses of all CWDS samples were quite consistent and nearly equal, whereas the edge responses were relatively inconsistent.

(4) The last CWDS film specimen, 9679, had the poorest edge response of any CW specimen.

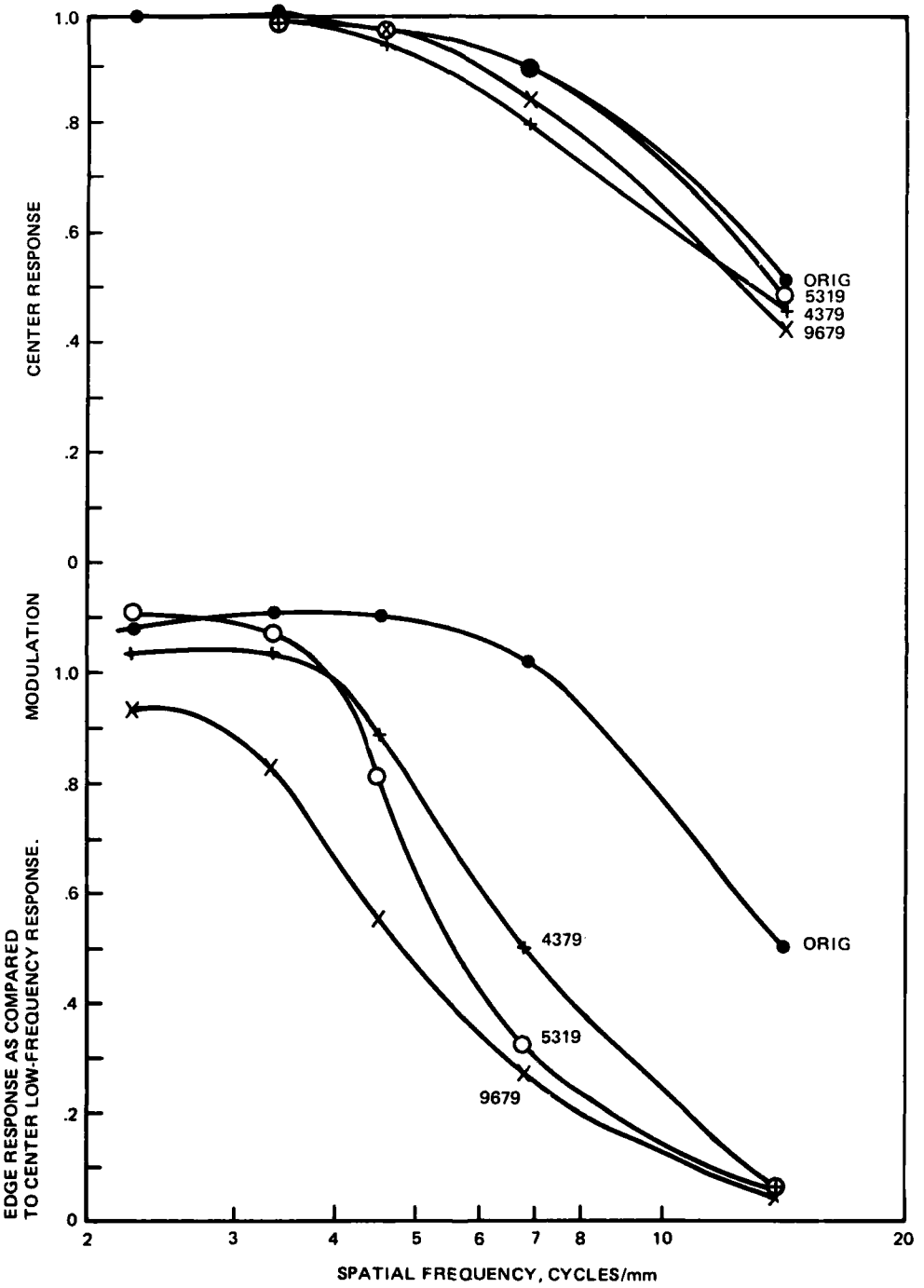

Figure C2. CWDS modulation transfer functions.

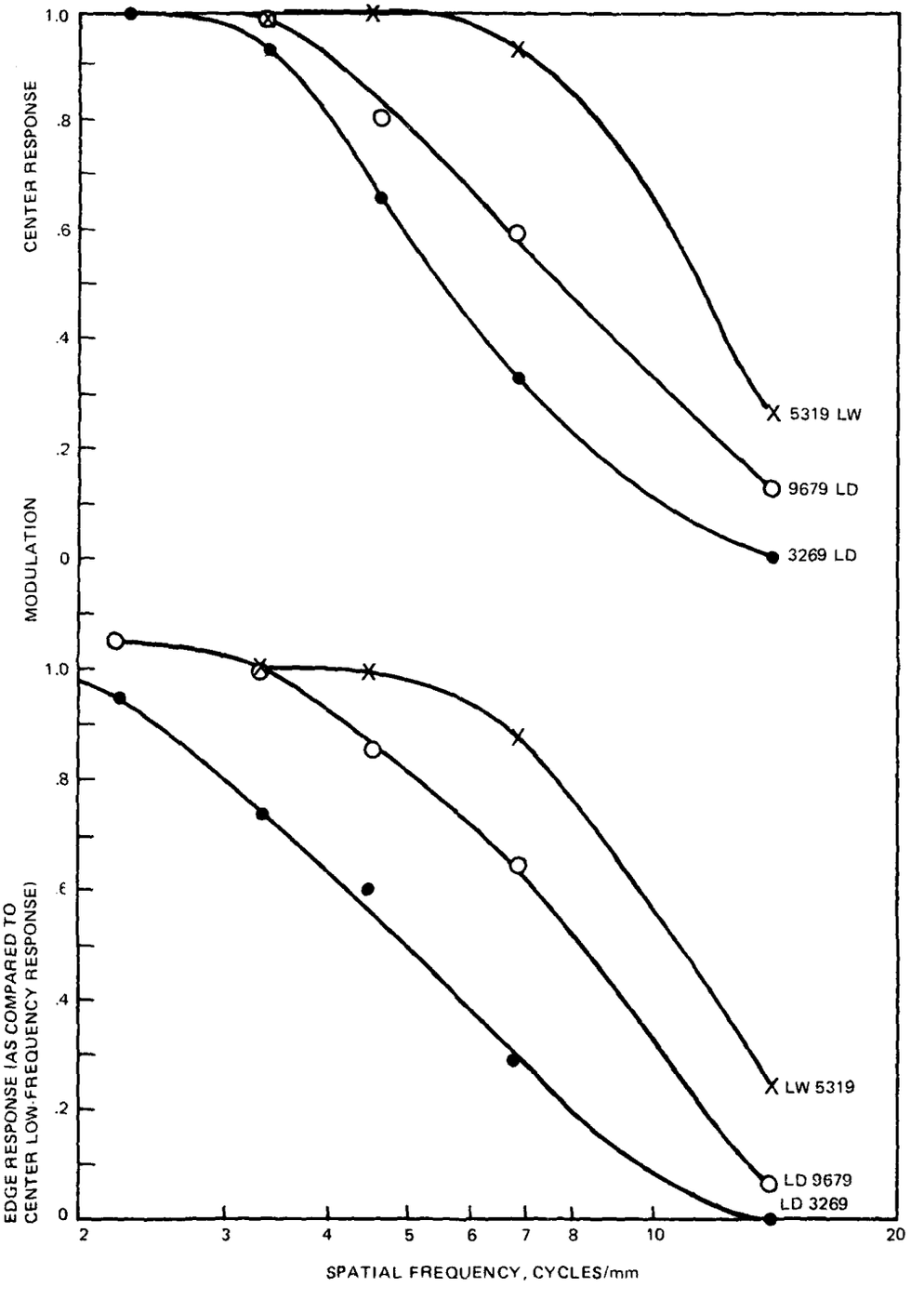

Figure C3. LDDS and LWDS modulation transfer functions.

Table C2. Film density modulation as a function of frequency.

Date Code		SPATIAL FREQUENCY, cycles/mm																				
		2.25			3.38			4.50			6.75			13.5			Low Frequency Avg Shift			High Frequency Avg Shift		
		LD	LW	CW	LD	LW	CW	LD	LW	CW	LD	LW	CW	LD	LW	CW	LD	LW	CW	LD	LW	CW
Unknown	C			1.56			1.57			1.52			1.32			.79			1.13			1.37
	E			1.70			1.73			1.72			1.61			.79			1.25			1.44
3269	C	1.18			1.10			.79			.39			.00			1.00			1.01		
	E	1.12			.88			.71			.34			.00			.97			1.04		
4379	C			1.60			1.58			1.53			1.44			.75			1.09			1.40
	E			1.66			1.67			1.43			.80			.11			1.23			1.80
5319	C		1.27	1.34		1.26	1.32		1.28	1.31		1.18	1.20		.33	.66		.90	1.41		.93	1.10
	W		1.27	1.49		1.28	1.44		1.26	1.09		1.10	.43		.31	.10		.90	1.10		.93	1.52
9679	C	.73		1.76	.72		1.75	.58		1.71	.43		1.48	.09		.77	.70		1.54	.64		2.07
	E	.78		1.64	.73		1.47	.63		.98	.48		.48	.05		.10	.74		1.71	.70		2.31
9679 (2494 Film)	C			2.98			3.00			3.02			2.60			1.17			2.17			3.01
	E			3.13			2.76			1.78			.74			.00			2.36			3.48

C = center response
E = edge response as compared to center low frequency

(5) The edge responses of the laser specimens tended to be quite similar and nearly equal to the center-of-film responses.

(6) The last LDDS specimen, 9679, had significantly poorer response than the 5319 LWDS specimen.

(7) The 2494 type of film tried with the CWDS system on 9679 produced significantly more film density than the 2491 type of film used for all other CWDS specimens.

(8) The average value of the film density increased with frequency for the CRT system whereas it remained constant for the laser printer.

GREY SCALE ACCURACY

The NSSA test plan implies that the hardware should be able to produce 64 distinct, evenly spaced shades of grey spanning a density range of at least 1.5D and starting at a density level of no more than 0.2D. This starting point is essentially the film fog level. The NSSA acceptance criterion requires that the film specimens meet the above criterion and also that no step shall vary from its absolute value more than 0.15D.

Figures C18 through C26, 64S T2 data, were used to compile table C3, which summarizes the performance of the printer systems during the course of the program; however, it does not convey the whole picture. Three types of nonlinear performance were exhibited:

(1) General nonlinear performance from minimum to maximum density such as exemplified in each printer operational configuration by figures C18, C21, and C22.

(2) Very poor linearity during the first 5 to 10 steps followed by relatively linear performance as exemplified by the CWDS performance shown in figures C23 through C26.

(3) Two segments of performance which was linear but with different average density step sizes as exemplified by the LDDS performance shown in figure C19.

Analyzing the data in table C3 and figures C18 through C26 produces these facts about the grey scale test 64S T2:

(1) The system in general produced a higher base fog level than NSSA considers acceptable (the existing equipment did not meet the acceptance criterion).

(2) The change in density over the 64-step range was greater than the minimum acceptable 1.5D except for one LDDS sample that was considerably lower.

(3) The CRT system appears to be capable of a wider density range than the laser printer.

(4) The new film (type 2494) tried with the CWDS system on 9-6-79 appears to have an even greater dynamic range.

(5) Neither printer met the linearity requirement of NSSA.

The large density variation on each step at the high density end of a scan such as exemplified in figure C18 is difficult to detect or correlate with what is seen by the eye when looking directly at the film; therefore, the series of tests labeled 64S T1 and 64S T1a was instituted. The results of the 64S T1 scanning are shown in figures C27 through C34 and the results of the 64S T1a scanning are shown in figures C35 through C42.

Table C3. Sixty-four-step grey scale accuracy performance.

Date	Step 1 Density			64-Step Density Range			Max deviation from line through end dens points			Approx Number of steps within .15D max deviation		
	LD	LW	CW	LD	LW	CW	LD	LW	CW	LD	LW	CW
Orig			.28			1.80			.42			42
3269	.22			1.61			.28			55		
4379			.16			2.05			.32			58
5319	.28	.20	.27	2.31	1.69	1.98	.62	.31	.27	50	52	62
9679	.25		.86	1.09		2.40	.25		.85	50		55
9679 2494 Film		1.26				3.37			1.2			55

The major differences between the T2 and T1/T1a tests are the amount of film scanned and the scan to plot ratios. The T2 test scans about 10 mm and plots it in 3.5 mm whereas the T1 test scans about 100 mm and plots it in 235 mm and the T1a test scans about 200 mm and plots it in 235 mm.

In figure C27, the scan to plot expansion of T1 shows the relatively large variations in film density for what should have been constant density steps in the 64S T2 scan, figure C18. Conversely, the traces on figure C28 are much straighter and have less amplitude deviation, which is in keeping with the smaller variations in each step of the trace in figure C19. There is a similar correlation between all the 64S T1 and 64S T2 scans.

The 64S T1a scans were made for reference purposes and are not used in any significant way in this report. The test was a scan across the width of the film at gs32 of the 64-step pattern.

DEFLECTION LINEARITY

The data obtained in measuring the deflection linearity test pattern part of TP1 are given in table C4. As a check on the instrumentation system accuracy, a machinist's scale was also measured and these data are included. It can be said that the technique is subject to a sighting error of about plus or minus 0.002 inch because the fiber optic positioning marker dot is too large as compared to the lines on the film. However, the technique was quite adequate for the present task.

Figure C4 summarizes the deflection linearity results. As in the resolution testing, here again the original sample specimen exhibited better performance than anything that followed from the CWDS. This performance of that specimen and an average of the other four CWDS specimens are plotted in figure C4. Also, the LDDS average performance of the four specimens was plotted. It can be seen on figure C4 that the LDDS error plot is essentially a straight line, which says that the deflection was not adjusted for exactly 8.0 inches. If the width correction were made, the absolute position errors would be essentially zero.

Table C4. Deflection linearity test data.

SYSTEM	DATE	DISTANCE FROM ABSOLUTE POSITION thousandths of an inch							
		IN* 1	2	3	4	5	6	7	8
	ORIG	- 25	- 29	- 24	- 11	9	19	27	20
	4379	- 44	- 51	- 32	9	58	81	82	8
CWDS	4379	- 45	- 53	- 34	5	49	78	78	2
	9679	- 47	- 55	- 34	5	48	77	75	0
	9679	- 47	- 54	- 38	3	46	73	70	0
Average of last four dates		- 46	- 53	- 34	6	50	77	76	2
	3269	9	16	24	34	43	51	59	65
LDDS	3269	9	16	28	37	44	51	62	68
	8159	7	16	23	32	40	47	56	67
	9679	0	16	26	36	43	52	59	70
Average		6	16	25	35	42	50	59	68
Browne & Sharpe Rule	1019	0	0	0	- 2	- 4	- 2	0	- 1

* inches from an edge

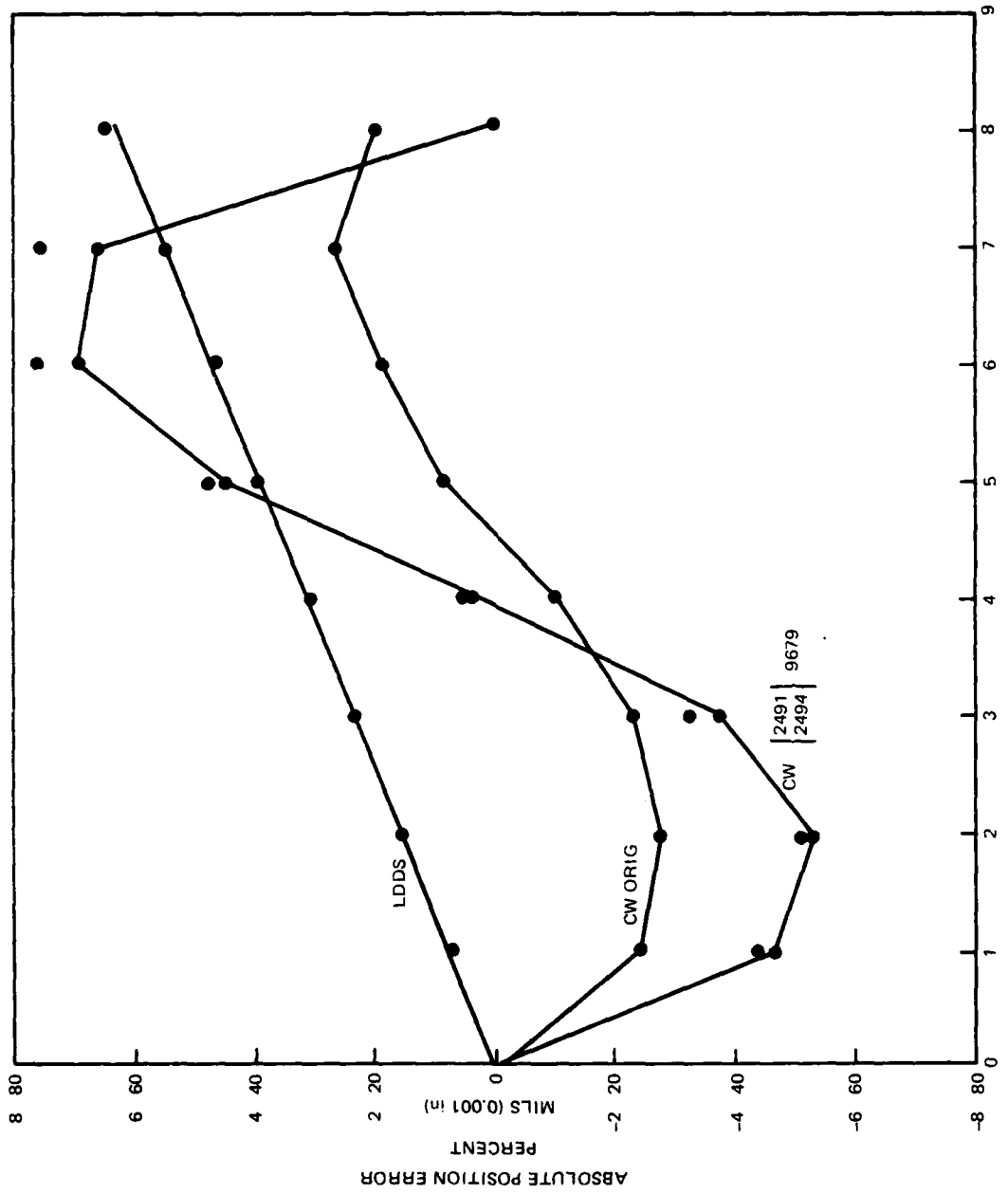

Figure C4. LDDS and CWDS deflection linearity.

GREY SHADE 32 UNIFORMITY

The data obtained in measuring grey shade 32 variations are shown in figures C43 through C54 and the peak-to-peak variations in table C5. The NSSA test plan acceptance criterion is 0.25D maximum peak-to-peak variation per inch of film. It should be noted that the acceptance criterion is 0.25D per inch whereas the data in table C5 are over the range of scan, which was about 3.2 inches for length and 8.0 inches for width.

The analysis of the data obtained is summarized with the following facts:

(1) Five of six specimens showed a length variation of 0.1D and the sixth, a laser printout, was 0.19; thus, all were better than required by NSSA in this direction of film travel.

(2) The two CWDS specimens showed deviations of more than 0.25D, but when put in terms of per inch, they also meet the requirements.

(3) The laser printed specimen that was poor in length is also poor in width.

(4) The laser printing exhibited better performance than CRT printing.

Analyzing the six film specimens with the eye and 50X microscope produces these facts:

(1) The two CWDS and three of the four laser printed specimens exhibited a periodic pattern that repeated with film travel. The periods ranged from about 20 to 40 mm but are not exactly constant on the same piece of film.

(2) The periodic density variations on the laser printed specimens appear to be caused only by intensity modulation variations.

(3) The periodic density variations on the CRT printed specimens appear to be caused by intensity modulation, focus modulation, and transport variations.

(4) The CWDS exhibited periodic density variations going across the film that are synchronized with the line rate or nearly so.

(5) The laser printer did not appear to produce any density variations that were synchronized to the line rate.

(6) The two specimens designated LDDS have density variations that appear to be the result of interference patterns possibly caused by stray light reflections.

(7) The correlation of the above observations with the measured performance leads to the conclusion that the periodic intensity variations are no greater than 0.1D.

Table C5. Grey shade 32 peak-to-peak density variations.

SYSTEM	DATE	P-P DENSITY VARIATION	
		Length Scan (GS32T1)	Width Scan (GS32T2)
CWDS	3269	.11	.27
	5319	.10	.28
LDDS	3269	.10	.15
	5319	.19	.24
LWDS	3309	.10	.12
	5319	.10	.10

MAP ANALYSIS

It was stated in the Procedures section that the map analysis would be primarily subjective; however, as a point of reference, the 64-step reference grey scale that is part of each map heading data was measured. Figures C55 through C60 show the results of these measurements. The video can be contoured in several ways before it is printed by either the laser or CRT system. The maps received at NOSC had been recorded with NORM (linear), LOG, and LOW (between NORM and LOG) contouring. The figures show this grey scale contouring for the three subsystem configurations.

The facts learned from analyzing the grey scale reference data include:

(1) The normal contour seems to wander all over from somewhat logarithmic to exponential, as exemplified in figures C55 and C56.

(2) The log contours showed relatively good repeatability; however, the laser printer contouring was different from the CRT contouring. See figures C57 and C58.

(3) The laser low contour showed good consistency whereas the CRT low contours were quite different. See figures C59 and C60.

(4) The laser printer generally produced much smoother contouring than did the CRT printer.

(5) The laser printer, with wet or dry film, produced a starting density between 0.2D and 0.3D whereas the CRT printer produced starting densities from about 0.3D to almost 1.6D.

In subjectively analyzing the actual weather maps, the following points are made:

(1) The apparent loss of high-frequency response never seemed to be a problem.

(2) The periodic noise in the direction of film travel usually was present although it was a minimum about the middle of the program.

(3) The periodic noise did not seem to interfere with map data but could be a problem in other applications.

(4) The laser interference pattern noise was usually present but did not interfere with map data. It could be a problem in other applications.

(5) The latitude printed per inch of film differed by 1 to 2% between the laser and CRT printing systems for all film specimens received through July. In August the laser apparently was adjusted to produce the same performance as the CRT system. The performance was maintained with the last specimens received in September.

(6) In general, it was not practical to try to correlate the actual map data quality with the map density reference scales (figures C55 to C60) because the dynamic range of the map was frequently significantly different from the range of the reference scale.

(7) The only times there was much of a problem in reading the map data occurred with the last CWDS maps when the density got very high (possibly because of developing problems) and with the laser system when the dynamic range of the picture was concentrated at the low-density end of the dynamic range and the video contour was logarithmic.

(8) The LDDS and LWDS maps seemed always to be more pleasing to view than the CWDS maps. They seemed to be more crisp, which suggested the resolution of the laser system was actually better than the measured data suggest.

CONCLUSIONS

The conclusion of this investigator/author concerning the foregoing evaluation program is: The laser printer system tested at NOCF is superior to the CRT printer system at NOCF. The quantitative data gathered during the course of the program only marginally support this conclusion; however, personal experience and knowledge coupled with the qualitative observations of the film specimens submitted lead unequivocally to the stated conclusion. The following paragraphs explain in more detail the basis for the conclusion reached.

It was stated in the Introduction that the plan was to print TP1 with each of the subsystems at least once a month for 4 or 5 months with the idea in mind of determining the actual performance of each and watching for long-term deterioration. This plan fell far short of its goal as can be seen from table 1. Many maps were generated whereas relatively few usable test patterns, the more important pieces of data, were generated. This sparsity of test pattern data precluded any attempt at looking for system deterioration over the life of the program. Another point that would make such an attempt worthless is the reported breakdown of the systems at various times during the program. There were sufficient data, however, to make reasonably good assessments about the performance of the systems.

The following statements are the conclusions reached by the author based on the data presented for quantitative measurement:

(1) There were not sufficient data to pass judgment on a possible superiority of the laser dry or the laser wet process. On the basis of the data submitted, the performances are deemed to be equal; therefore, there will be no further distinction made between these two subsystems.

(2) Figure C3 shows the laser resolution, at its best, to be essentially equal to the resolution of a properly focused CRT system as presented in figure C2. There are, however, extenuating conditions to this statement:

(a) The CRT always performed about the same in the middle of the film,

(b) During the program, the CWDS never produced a specimen with good edge resolution such as was demonstrated by the sample of unknown origin received at the beginning of the program,

(c) The poor laser response at the higher special frequencies for any sample chosen, including those that were not suitable for measurement, was the result of poor modulator response, insufficient laser power, or a combination of both -- not the result of reaching the limits of system resolution, and

(d) The laser performance at the edge of the film was always about the same as in the center of the film.

Given these facts, the laser system that was installed at NOCF yielded a performance about equal to that of the CRT but could produce much better performance with some changes in the modulation system.

(3) The 64-step grey scale accuracy test was essentially a draw. Neither system produced performance considered acceptable in the NSSA test plan. The test actually tells more about the correction factors that are implemented in the video circuitry than about the printing techniques. Film properties did not appear to affect the results at any time except possibly the inability to meet the minimum density specification. It was reported that the computer program that generated TP1 had to be manually loaded, which possibly accounts for the random shape of the density curves in figures C18 through C26.

(4) The laser system was unquestionably superior to the CRT system in the deflection linearity test. The deflection width of the laser printer was not set at exactly 8 inches, but the linearity was nearly perfect given the test procedure used.

(5) The results of the grey shade 32 uniformity test seemed to favor the laser technique; but, as with the 64-step gs accuracy test, the results speak to the quality of hardware implementation rather than the technique used to expose the film. Table C5 shows the CRT system to be producing more "noise" going across the film than the laser did. Actually both systems met the acceptance criterion of the NSSA test plan, but both systems would need to be much better in other applications. The grey shade uniformity subject is discussed further in the following statements concerning the subjective analysis.

The subjective analysis of the data presented has resulted in the following conclusions:

(1) The periodic noise, random noise, and interference pattern noise noted in the gs32 uniformity testing did not seem to be detrimental in reading the weather maps; however, in other applications it would be unacceptably excessive.

(2) The laser printed maps were more pleasing to look at than the CRT printed maps, which suggests that the resolution was better than the measured data indicated, although there was no detectable loss of required resolution in any of the maps submitted.

(3) Most of the maps appeared to be quite satisfactory for weather analysis use (the observation of one not trained in aerology). There were, however, a few maps on which the dynamic range of the data was in the lower density end of the printer dynamic range when the video contouring was logarithmic, which resulted in unquestionably poor data. These instances of poor printouts were generated by the laser printer, but that does not mean the printer technique was at fault.

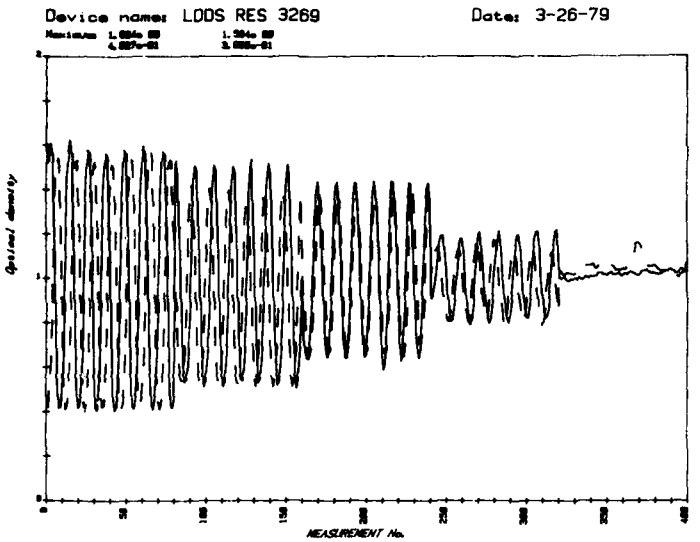

Figure C10.

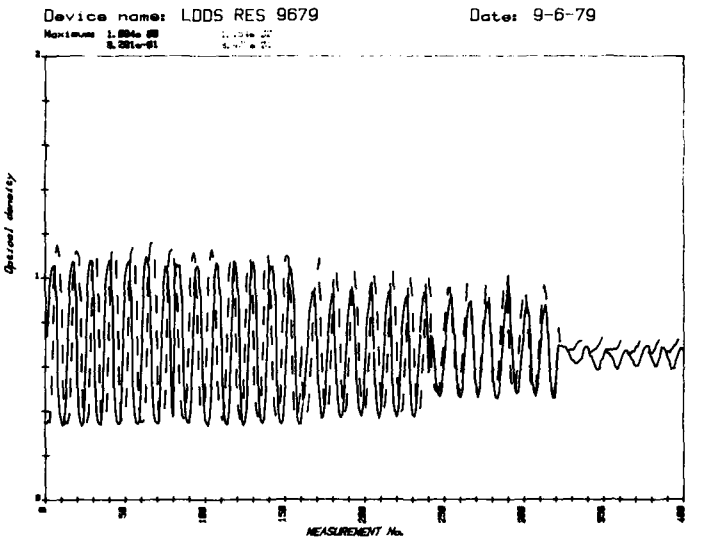

Figure C11.

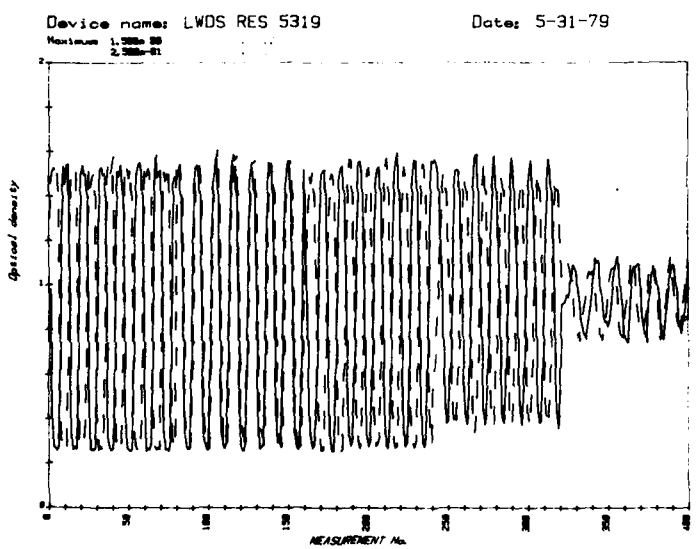

Figure C12.

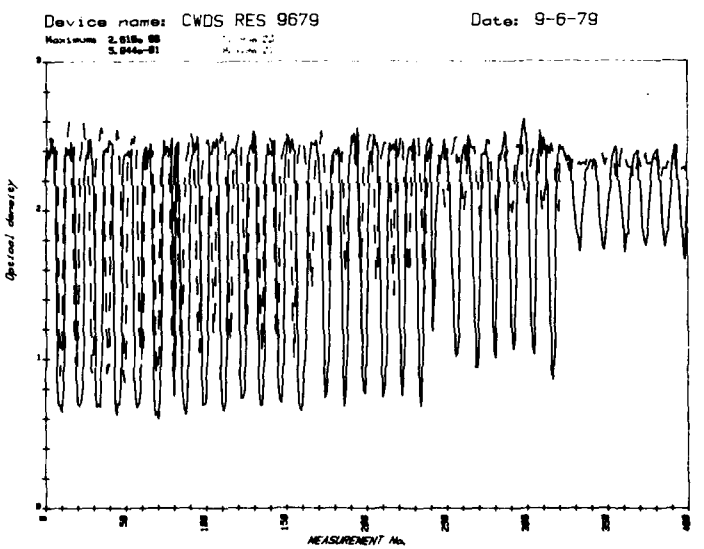

Figure C13.

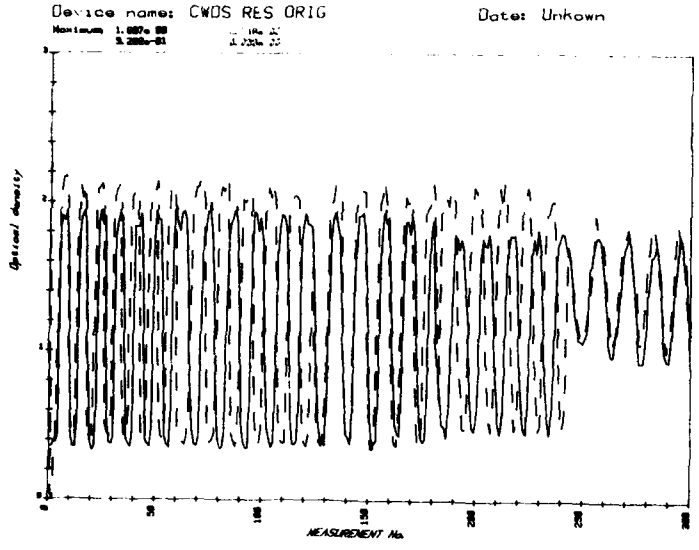

Figure C14.

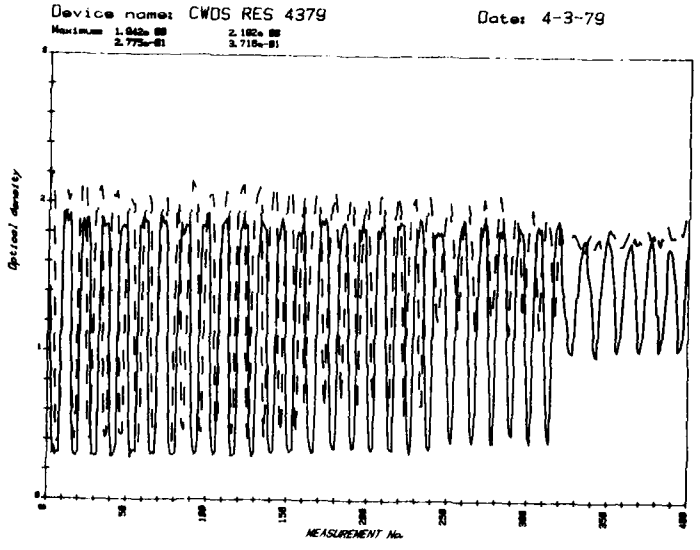

Figure C15.

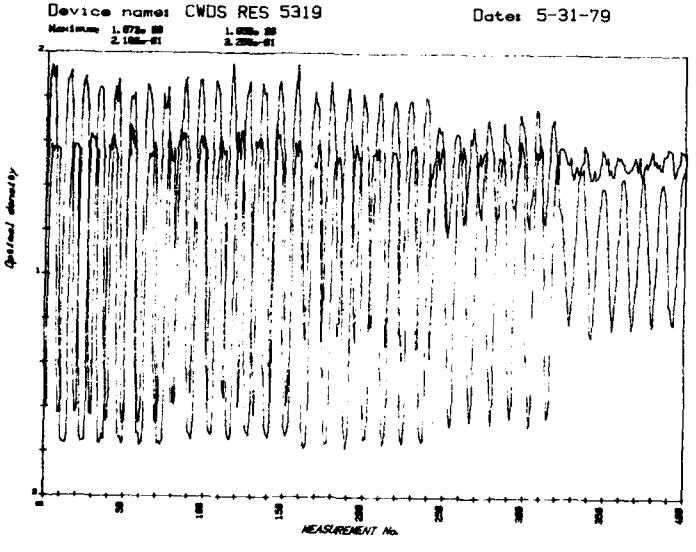

Figure C16.

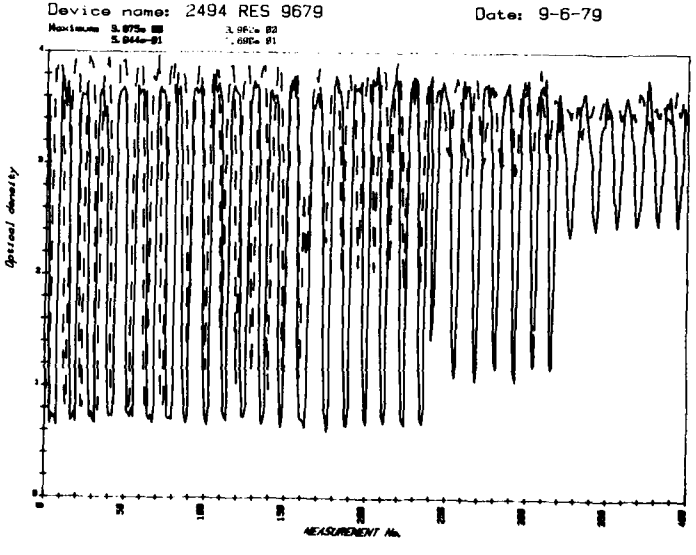

Figure C17.

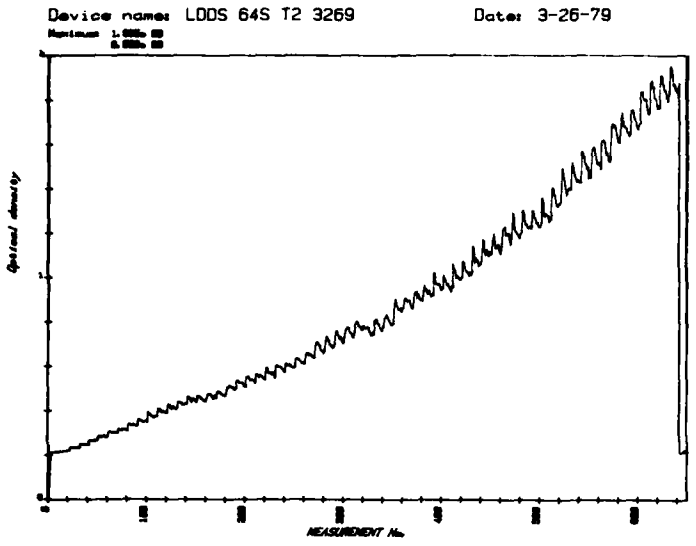

Figure C18.

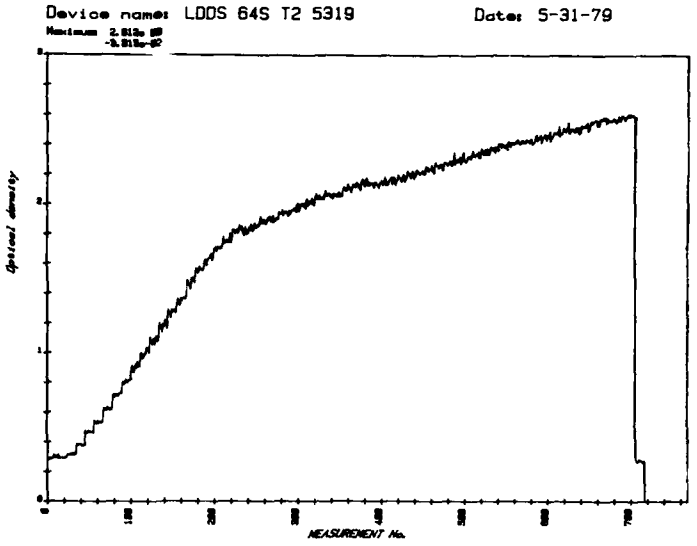

Figure C19.

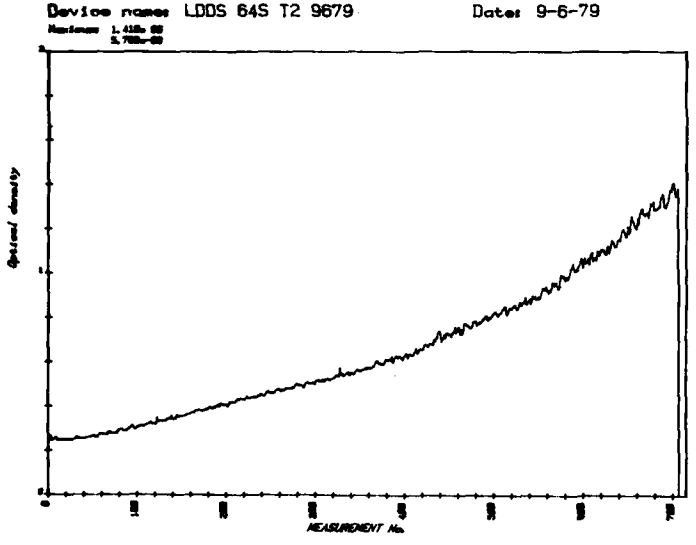

Figure C20.

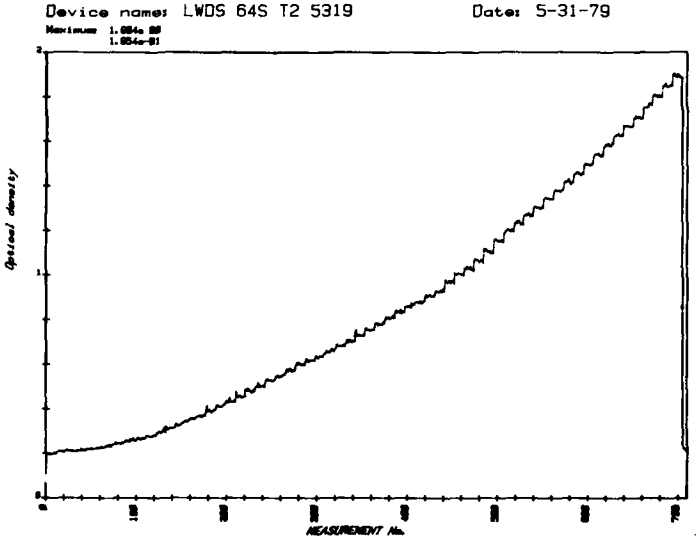

Figure C21.

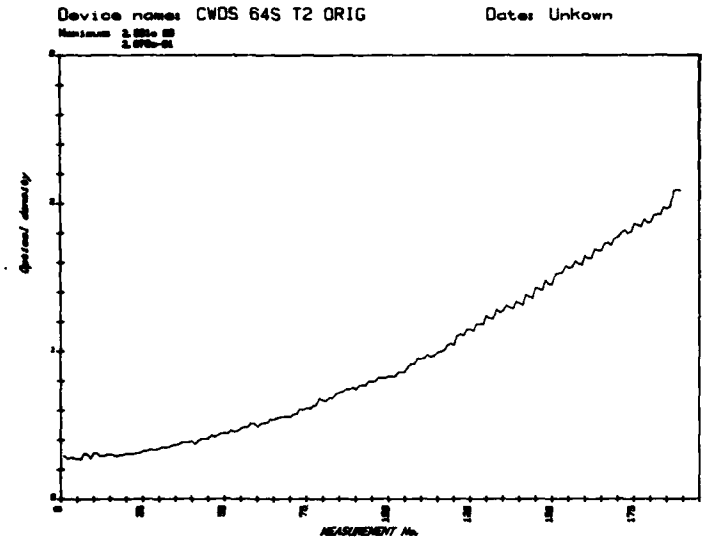

Figure C22.

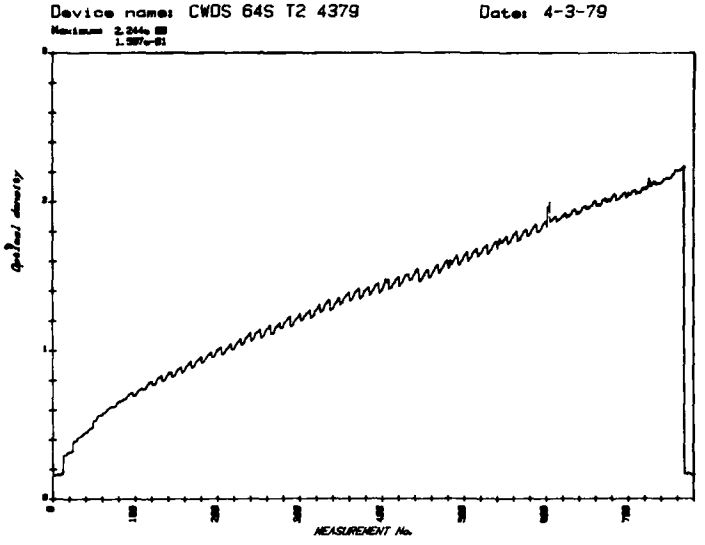

Figure C23.

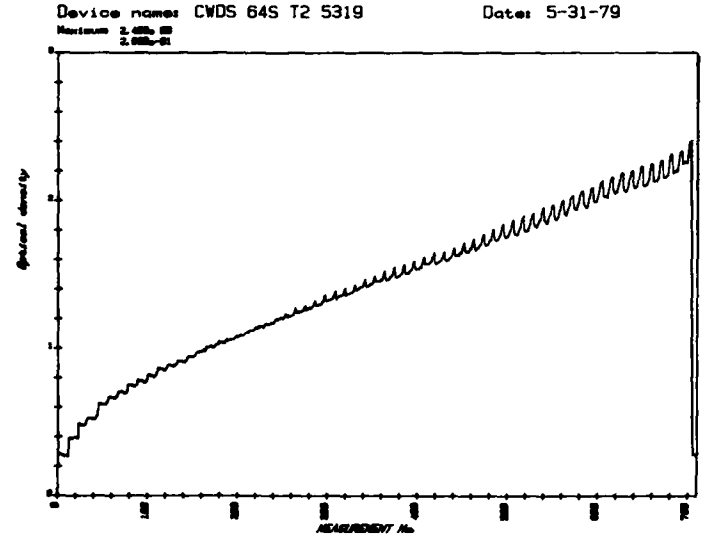

Figure C24.

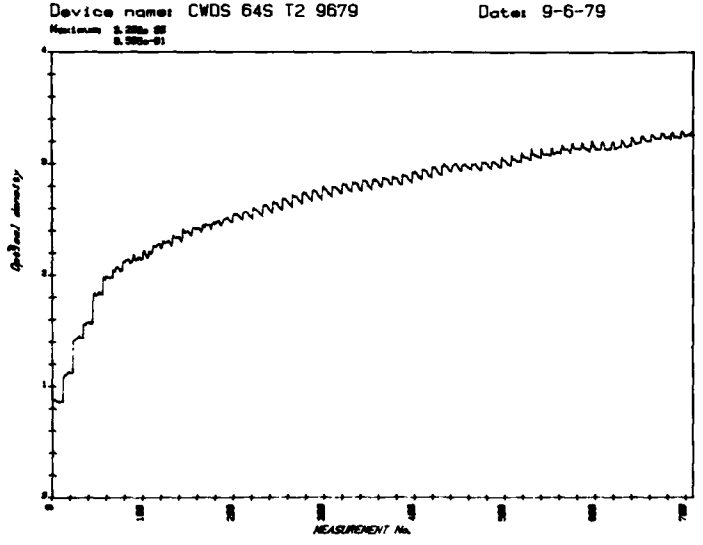

Figure C25.

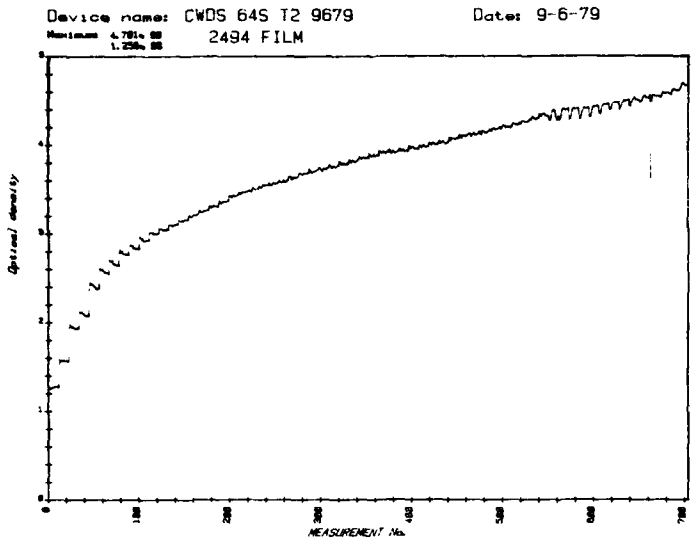

Figure C26.

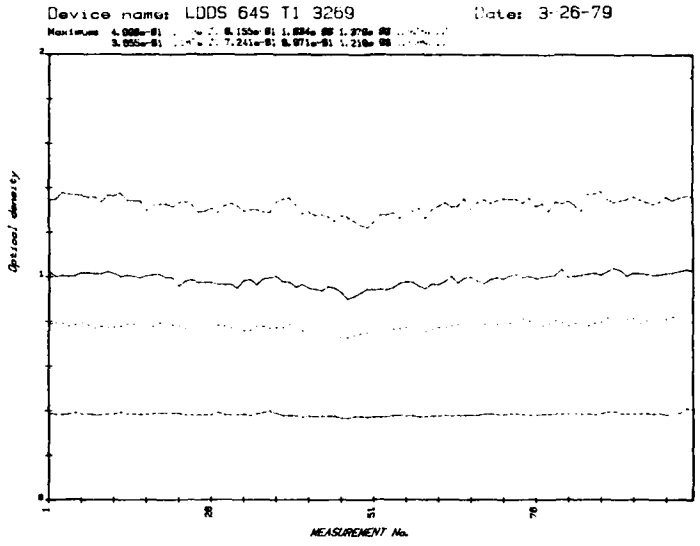

Figure C27.

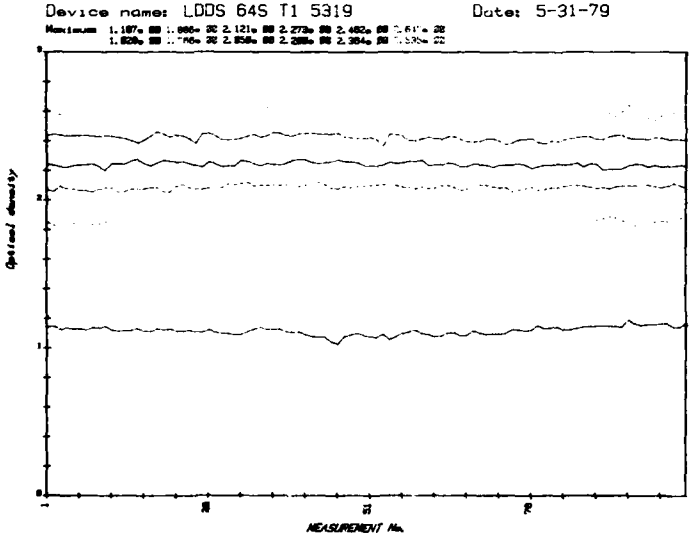

Figure C28.

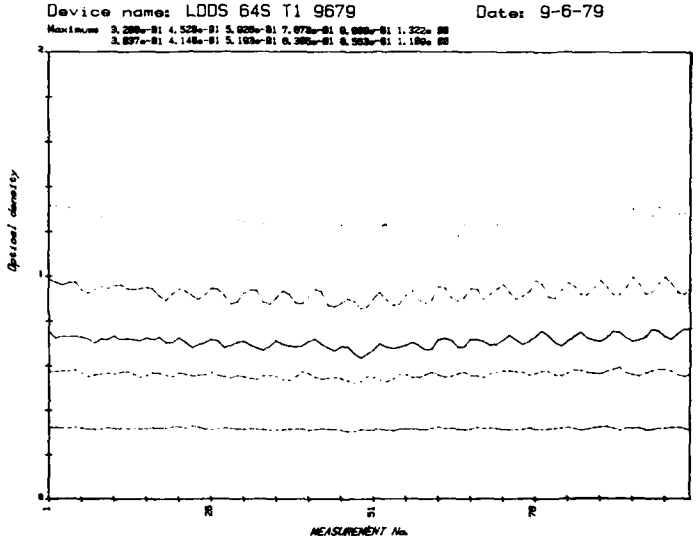

Figure C29.

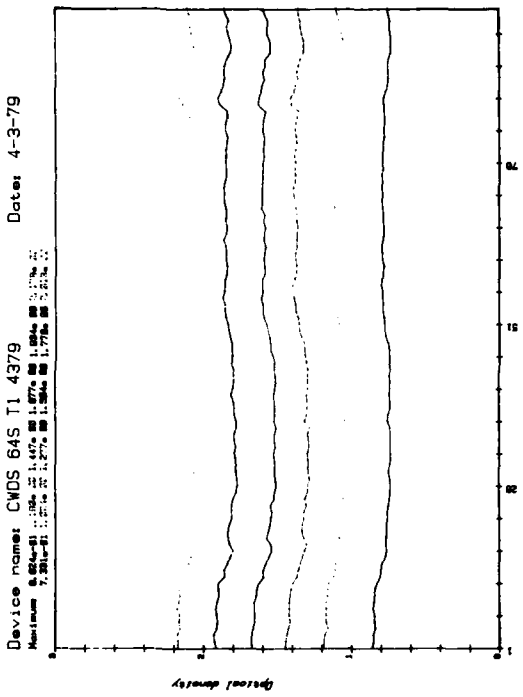

Figure C31.

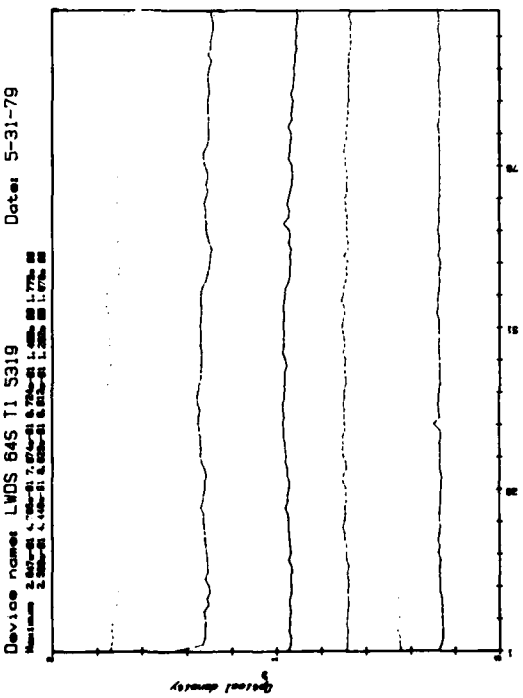

Figure C30.

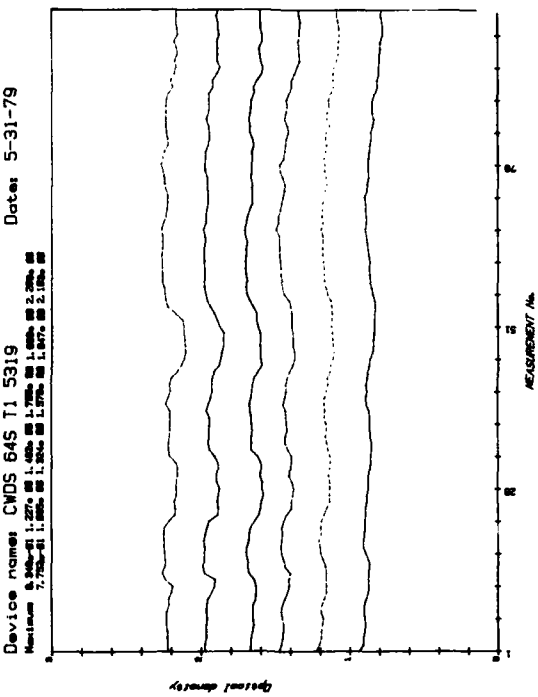

Figure C33.

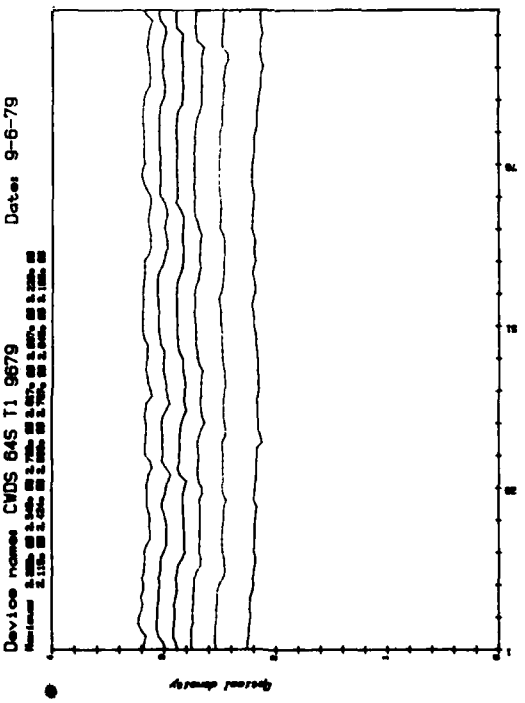

Figure C32.

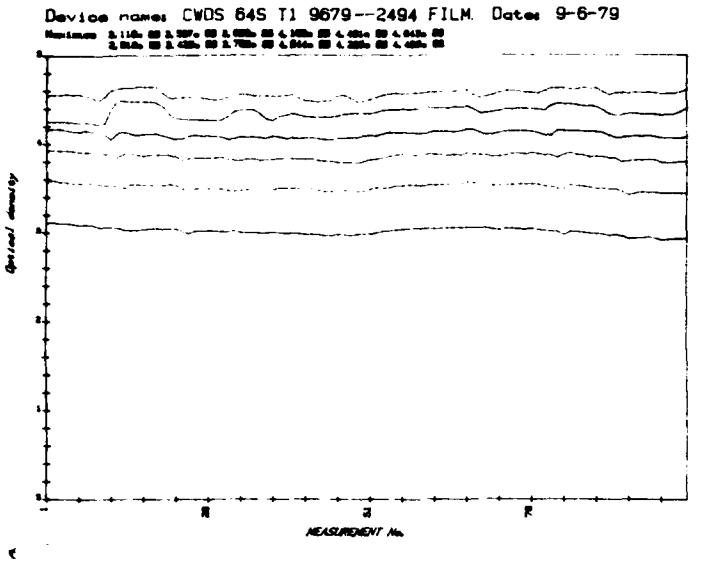

Figure C34.

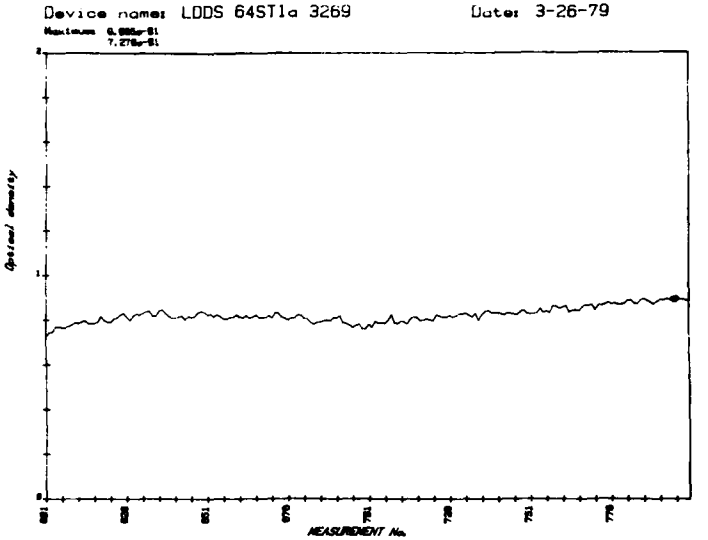

Figure C35.

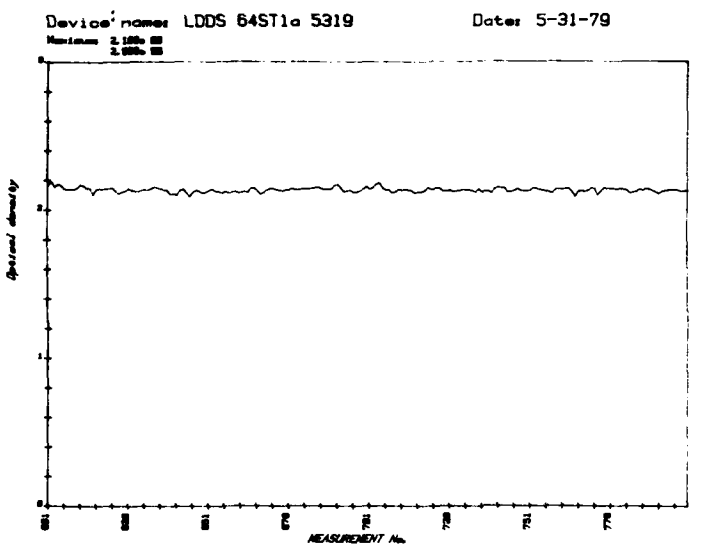

Figure C36.

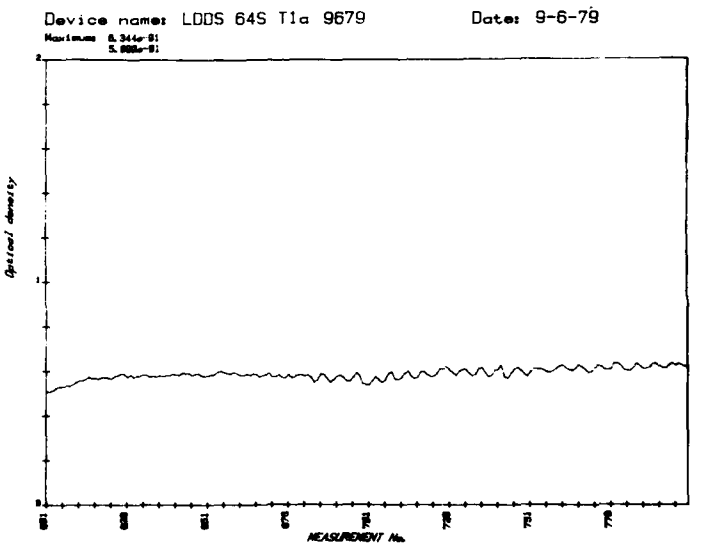

Figure C37.

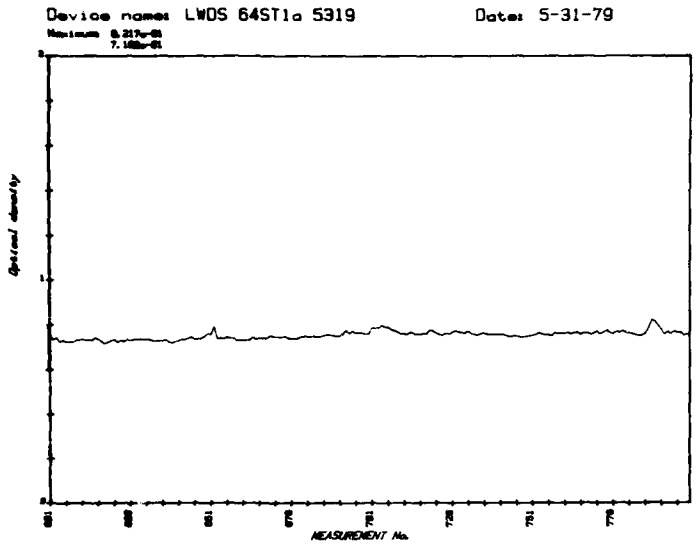

Figure C38.

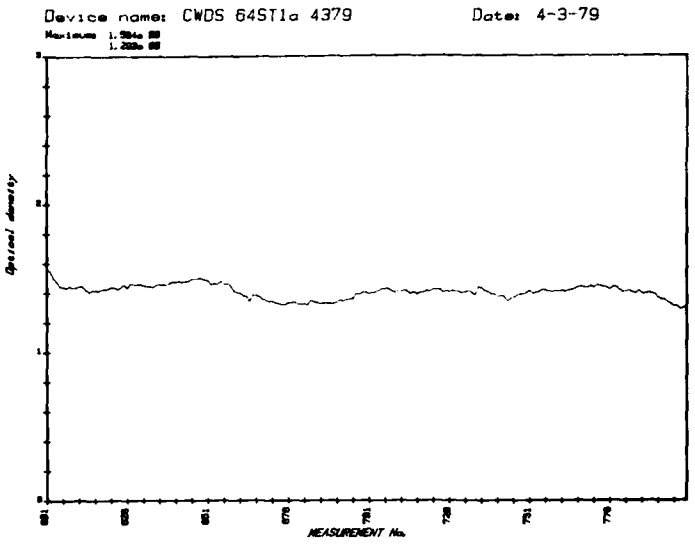

Figure C39.

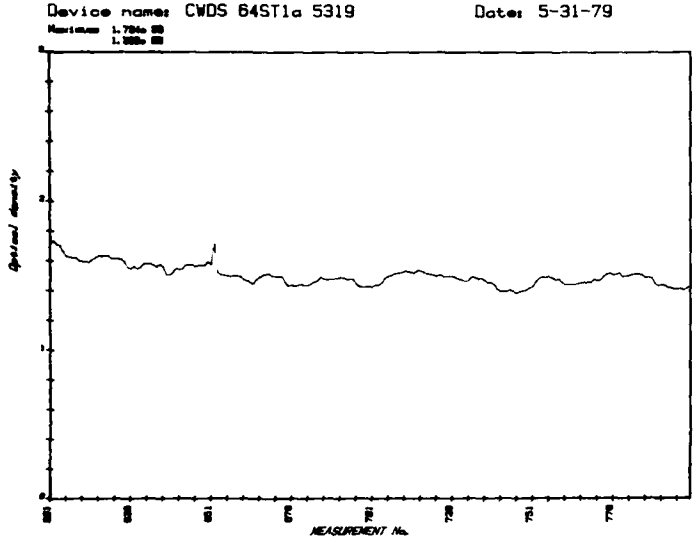

Figure C40.

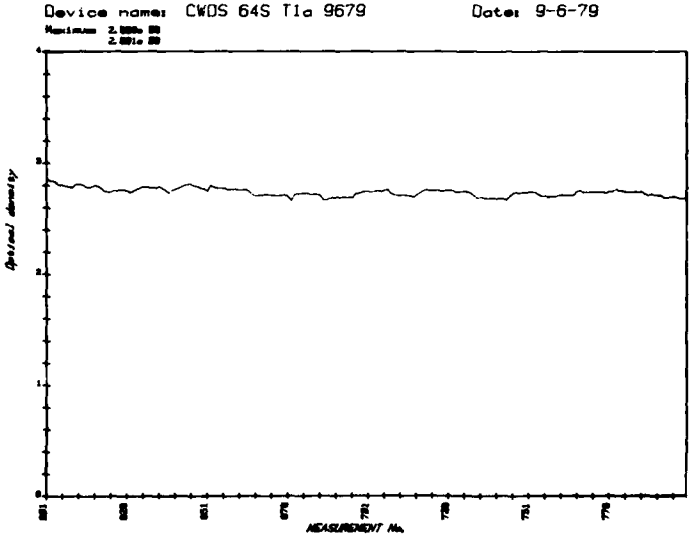

Figure C41.

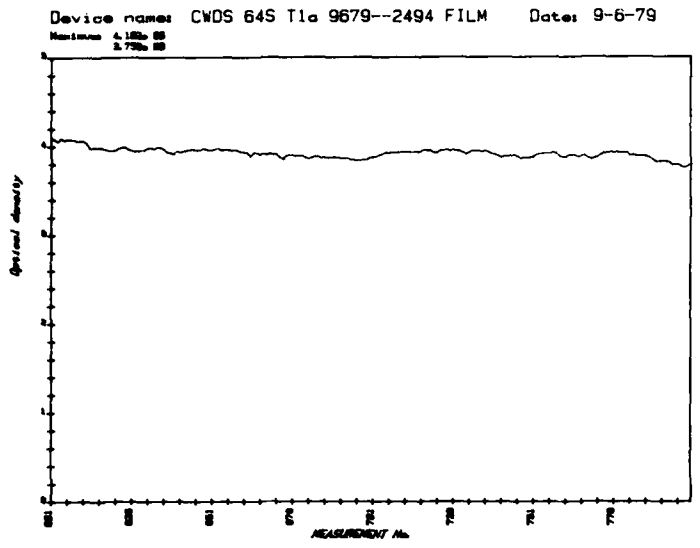

Figure C42.

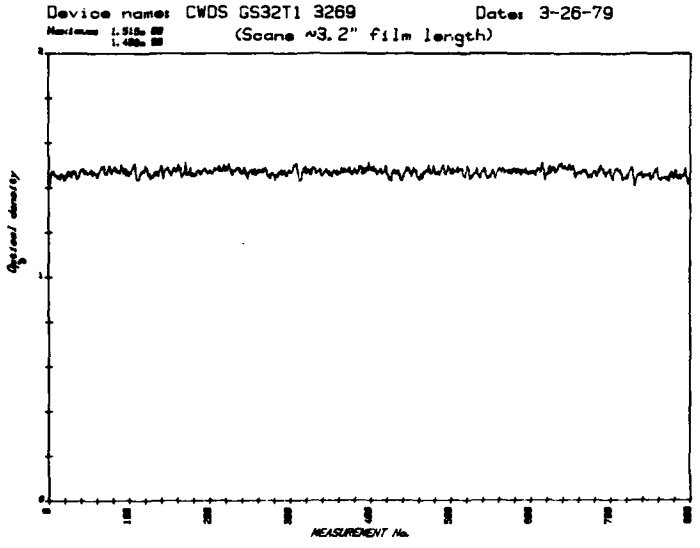

Figure C43.

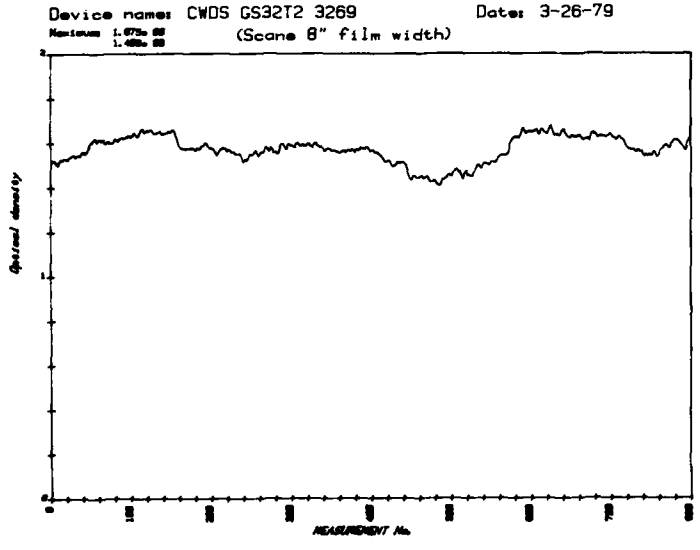

Figure C44.

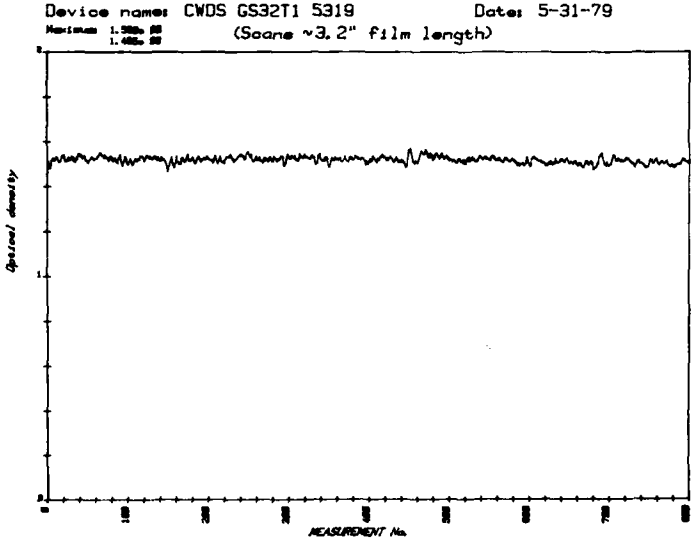

Figure C45.

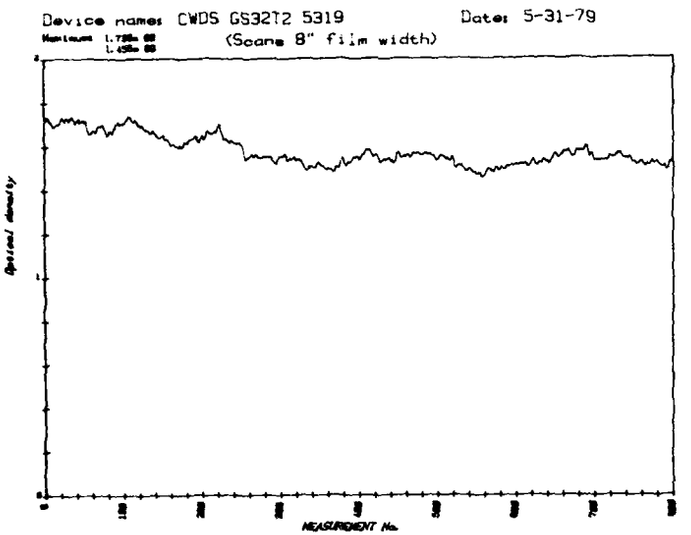

Figure C46.

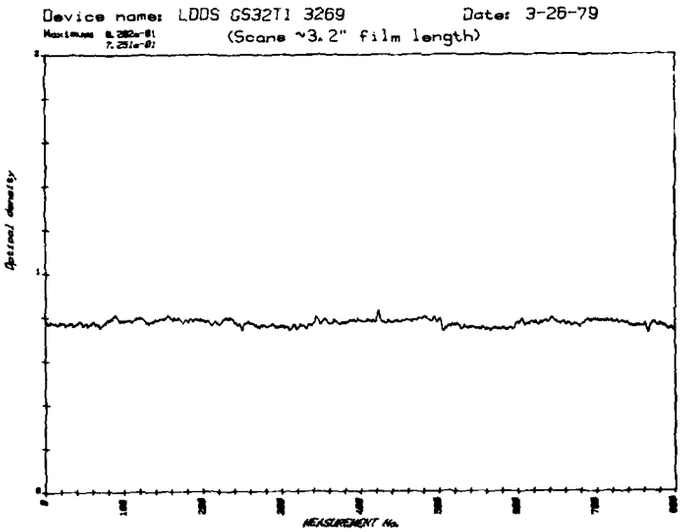

Figure C47.

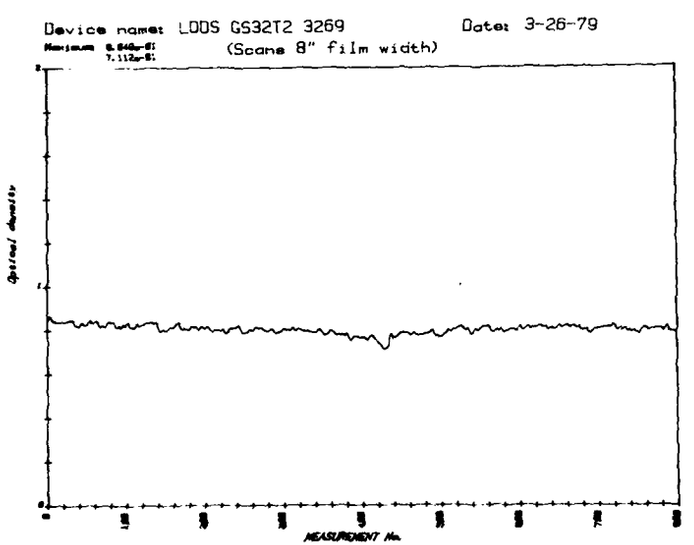

Figure C48.

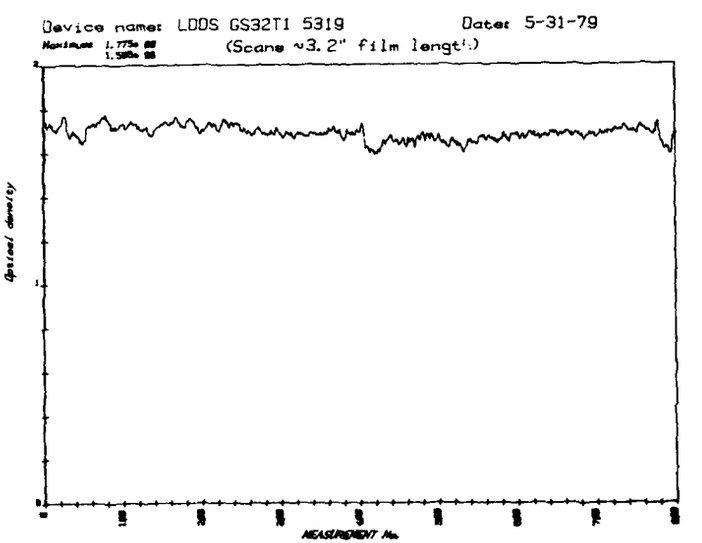

Figure C49.

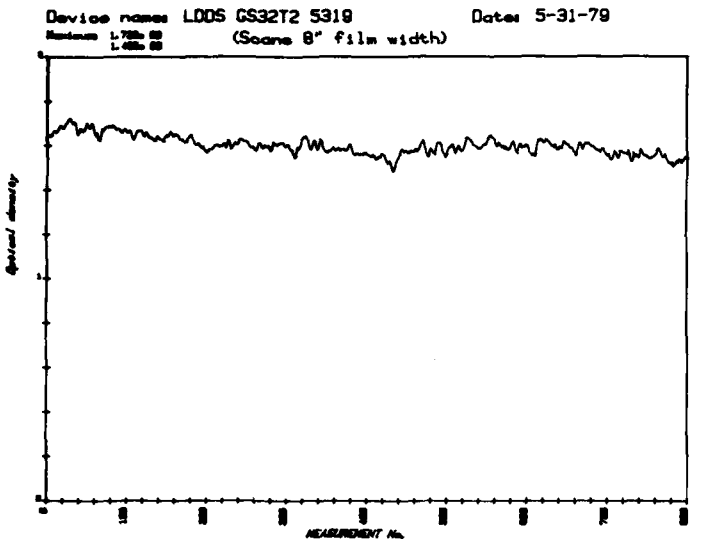

Figure C50.

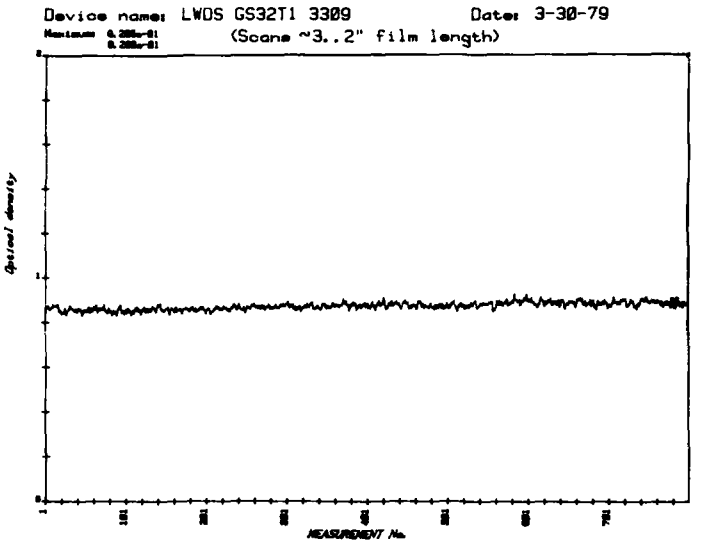

Figure C51.

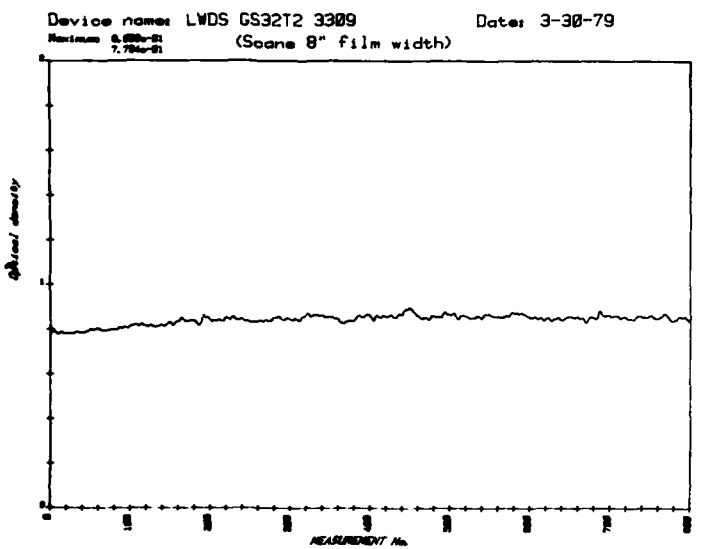

Figure C52.

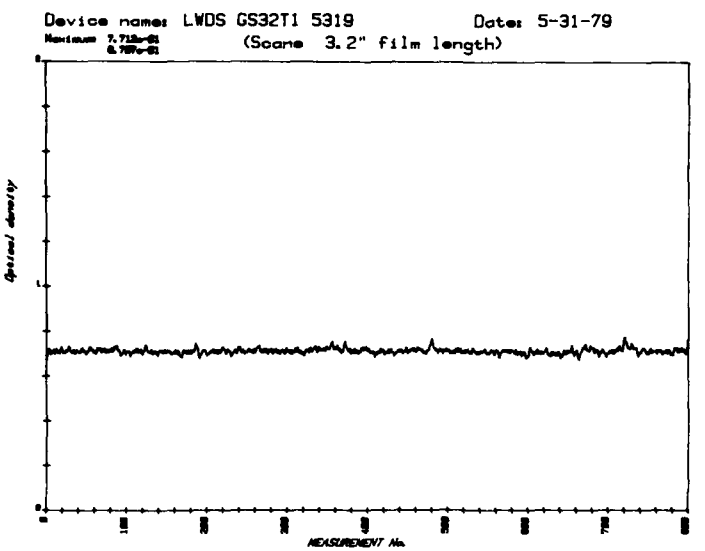

Figure C53.

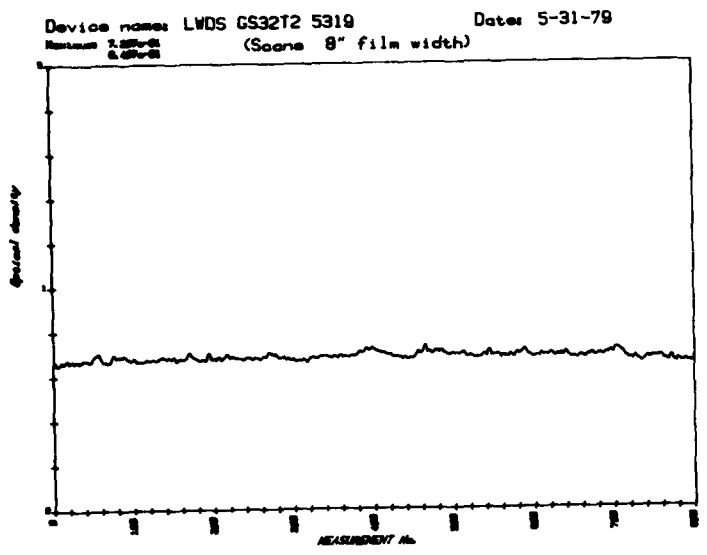

Figure C54.

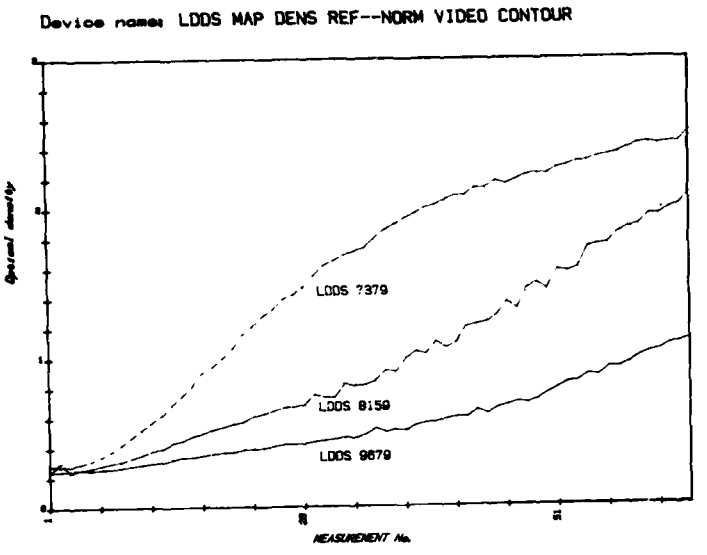

Figure C55.

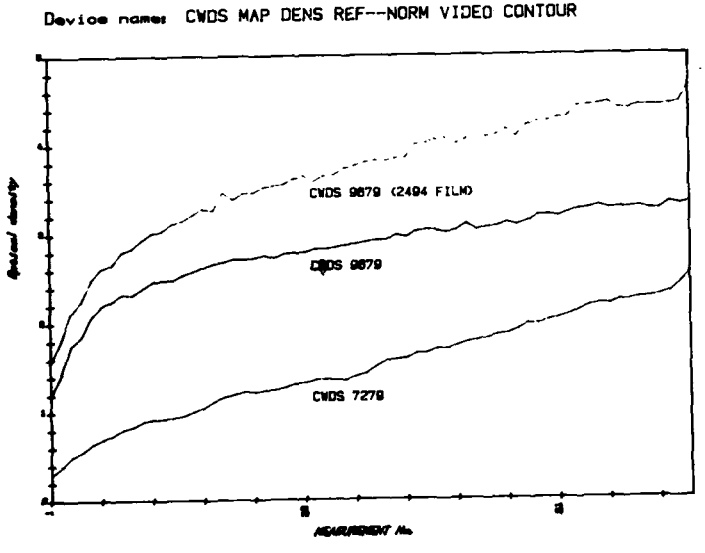

Figure C56.

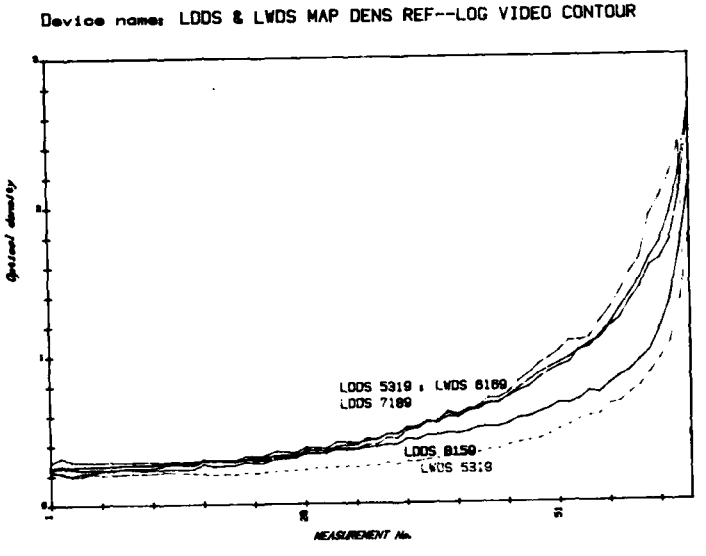

Figure C57.

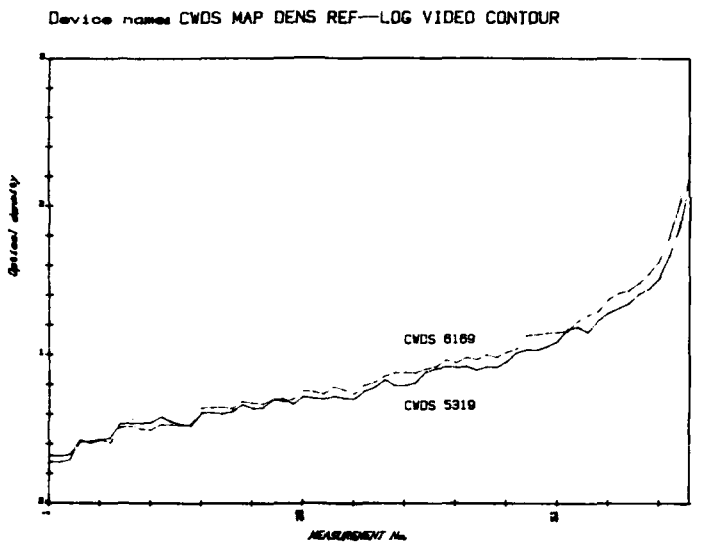

Figure C58.

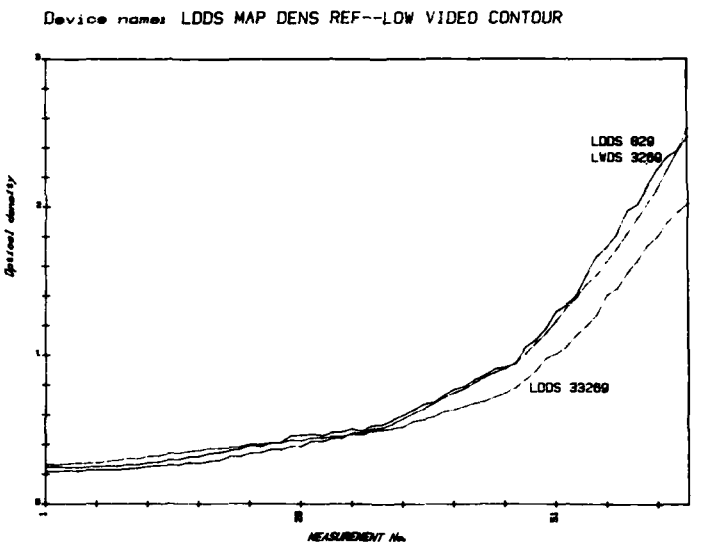

Figure C59.

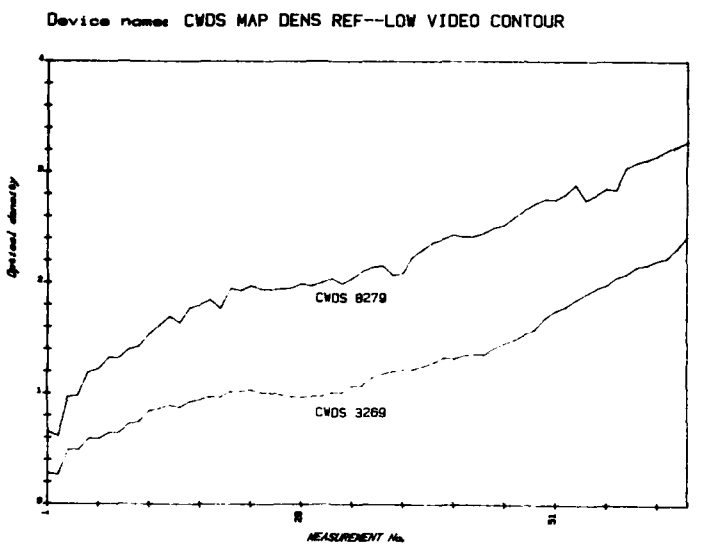

Figure C60.

ANNEX A TO APPENDIX C

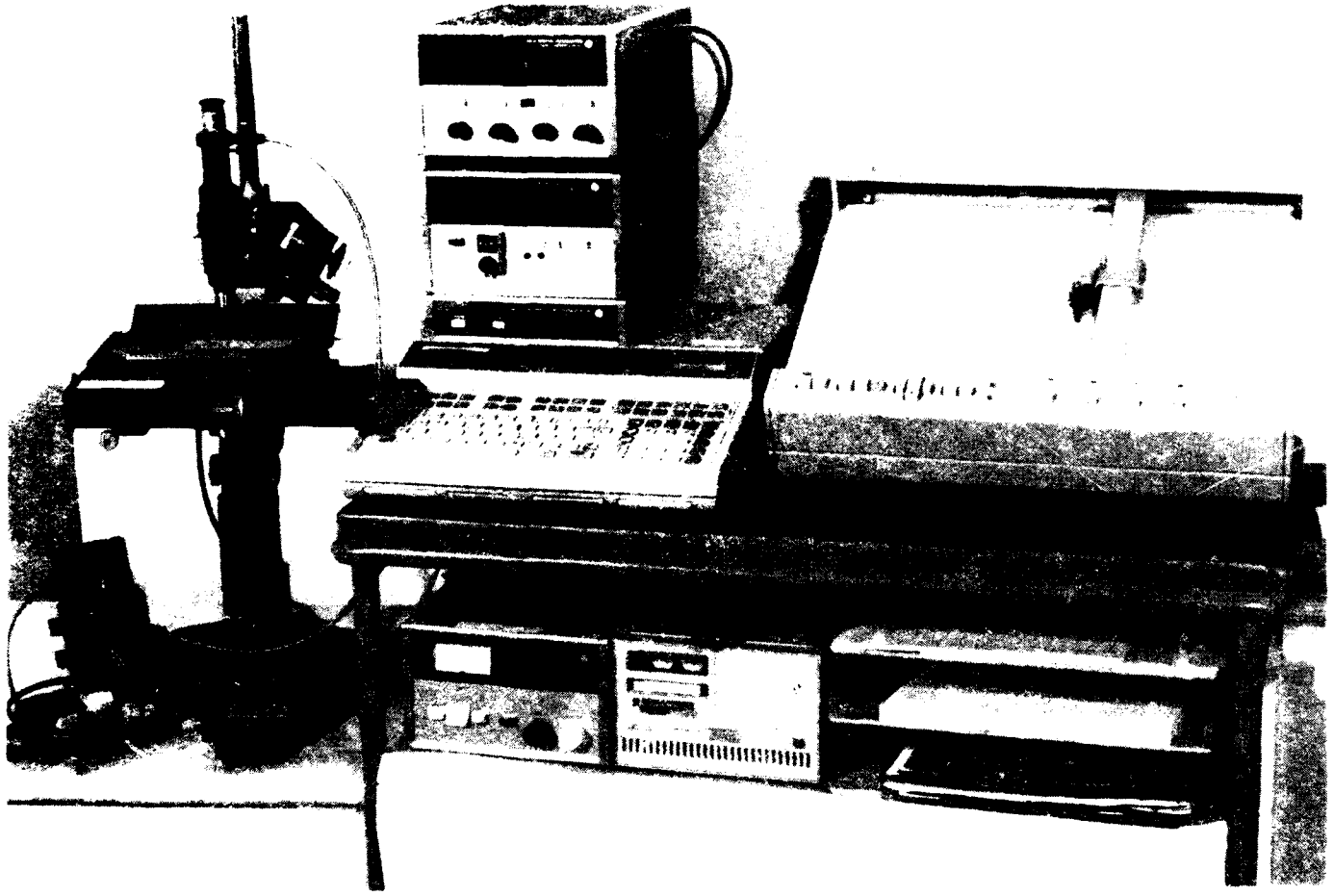

The typical setup of the Gamma Scientific computer controlled scanning microdensitometer system used in gathering data for this report.

APPENDIX D:
EDM HARDWARE EVALUATION

by

LA Wise
Code 7323
Naval Ocean Systems Center

CONTENTS

INTRODUCTION

A contract was awarded to Fairchild Imaging Systems Syosset, NY, by the US Postal Service Design Division, Rockville, MD, to design and fabricate a scanner subsystem for the USPS Electronic Message Service System (EMSS). NOSC representatives participated in the formulation of technical portions of the specifications, RFP, and SOW. USPS contract 104230-77-D-0463 (Fairchild job 6157) resulted in a 16-month, four-part development and fabrication program. NOSC representatives participated as consultants in design reviews throughout the program. The equipment was completed June 1978 and was interfaced with an input paper handling equipment developed by Pitney Bowes in Stamford, CT. Plans are being made to install a number of equipments relevant to the EMSS including the Fairchild scanner, the Pitney Bowes paper handling input and output equipments, and the Versatec printer at the USPS Development Laboratories in Rockville, MD.

PURPOSE

Further improvements in the scanner subsystem are contemplated for the future. For this reason it was felt that characterization of one of the two identical scan-head assemblies and the spare card file will lead to other potential applications and recommendations for future improvements for an advanced scanner subsystem.

Interconnection of the Fairchild scanner to the NOSC ICAS offers numerous opportunities to evaluate performance parameters of both equipments heretofore untested. Some of the major tests are:

1. Operation of the Fairchild scanner/NOSC ICAS interface including the confirmation of the personality module. It evaluates the performance of the scanner operating at full speed, 10 pages per second, and the ICAS at half speed. It also provides experience and information for future interconnection of the RCA Princeton time-delay-and-integration (TDI) imager now under development.

2. Evaluation of the Fairchild high-performance analog signal conditioning circuits, especially with regard to ability to accommodate images having grey scale.

3. Characterization of the Fairchild type CCD 131 imaging devices, with both daylight and special phosphor Sylvania slit-aperture lamps.

4. A pel-by-pel comparison of the analog Fairchild threshold algorithm to the digital NOSC equivalent with several types of images.

SCOPE

This appendix encompasses the results of tests made at NOSC between 28 June, when the interface debugging was complete, and 31 July, at which time the equipment was disassembled for shipment to the Rockville, MD, US Postal Service Laboratories via Fairchild Imaging Systems, Syosset, NY.

The only components of the Fairchild scanner involved in the test were the card file and the scan head itself. The page memories and control computer were not needed, since the ICAS provided control and storage of the image data.

Video signals were sampled from five sources along the scanner video chain, starting with the raw video. The final sample point was the thresholded (bilevel) signal output, which

would normally constitute the input signal to the digital frame-store (page) memories in the Fairchild equipment. A discussion of the characteristics of the signals taken at each point is included in this appendix.

A relatively small number of documents were used in the tests, because each document was run several times in order to compare outputs from each of the five sources along the video path. A portion of the Fairchild color document deck was run with both the special and standard daylight bulbs. Images were acquired at speeds of 4.0 and 8.77 pages per second during the tests.

INTERFACE

MECHANICAL

A special large drum testbed was fabricated at NOSC in line with the same general concepts that guided the building of the NOSC testbed. The drum provided was made 11.2 inches wide to accommodate the scanning of 8½-by-11-inch paper along the 11-inch axis. The drum is driven by a 900-rpm hysteresis synchronous motor through one or two, depending on the speed required, polyurethane round belts. Step pulleys were provided that could generate many different scanning rates. The drum is supported by two precision ball bearings (class 5) that were mounted in a way that produces no side load on them. Removable dust covers were included with the bearing mounts to facilitate the adding of a drop of oil to the bearings once or twice a year.

The Fairchild scan-head assembly was supported on the testbed by a three-point technique that was considerably different from the mounting concept used on the Pitney Bowes equipment. The NOSC technique utilized two rigid pivot points tangent to the drum surface and a third point directly under the focal plane assembly. The pivot points utilized the holes in the scan-head assembly that were intended for drum alignment. The NOSC mounting concept assumed that the fabrication precision precluded a further alignment requirement.

The testbed, as originally designed, utilized two aluminum rails with a cross section 1¼ by 2 inches to tie the scan-head support point to the drum assembly. These rails were replaced, at the request of Fairchild, with rails that had a cross section 1/2 by 8 inches before any testing was started. No other modifications were made during the course of the program.

ELECTRICAL

Control

The scan head and the card file were interfaced to ICAS as shown in the block diagram in figure D1. Images mounted on the drum were acquired by the scanner at a resolution of approximately 200 by 200 pels per inch. Raw video from the scanner assembly was input to the card file for further processing and digitization. Video signals from five different points in the processing chain were input to the four-channel A/D in ICAS for testing. The shaft encoder produced the page and line sync signals for the scanning operation. The interface circuits, designed specifically for this application, used the shaft encoder signals to generate the required control signals for both the scanner and the ICAS.

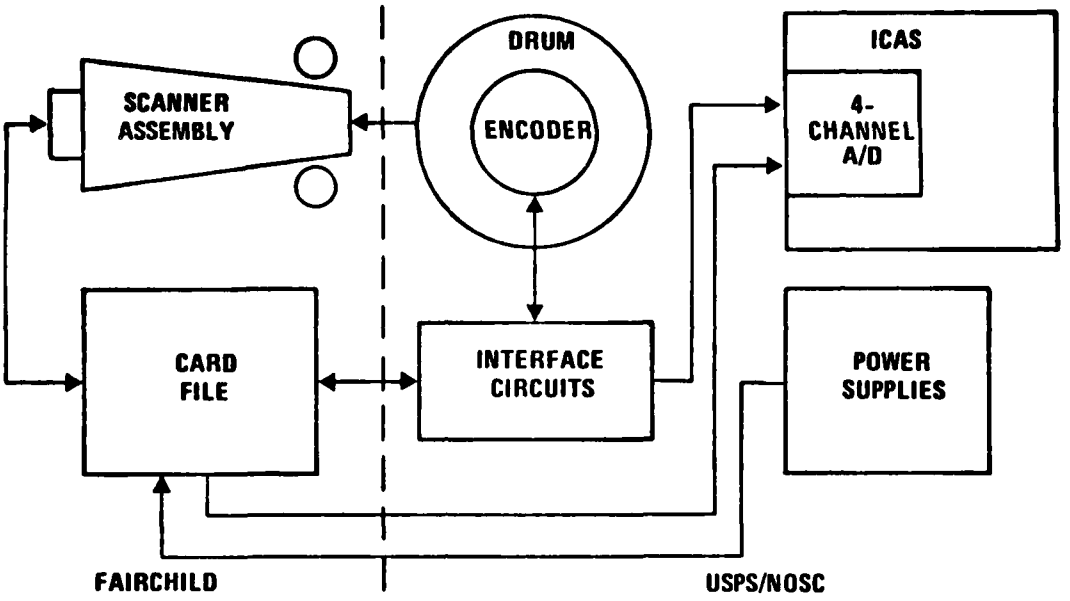

Figure D1. NOSC/Fairchild interface.

The control signals generated in the interface circuits are shown in figure D2. The signals on the left of the figure are ICAS and encoder controls, while those on the right are scanner interface signals.

The Drum Sync and 5-mil Clock, generated by the shaft encoder, provide start-of-page and line sync information to the interface. The remainder of the signals on the left side of the figure are control signals sent to ICAS. The Data Available and Page True signals go true at the start of the page and false after 1700 lines have been scanned. The Page Present signal is a single pulse which occurs at the start of the page, and the Kth Line signal is a single pulse at the start of the tenth line of the image.

The control signals output from the scanner subsystem include the 21-MHz clock and the Video Valid signal. The 21-MHz clock divided by 2 is used for sample commands for the four A/D converters. Variable delays for each of these clocks are necessary so that each may be adjusted to sample its respective analog signal at the optimum instant in time. The Video Valid signal is true for the active line time, during which the accumulated charge packets are shifted out of the imager. The timing of this signal is set for the digital video outputs, which is not correct for any of the analog video test points. The actual delays in the scanner subsystem video processing channels are, with respect to the raw video outputs:

Matched filter outputs	100 ns
Multiplexed video	180 ns
Digitized video	280 ns

In place of the Video Valid signal, a Data Gate signal was generated which has a programmable delay to compensate for the different video delays through the system. Any misalignment of this signal results in an improper abutment of the two halves of the image.

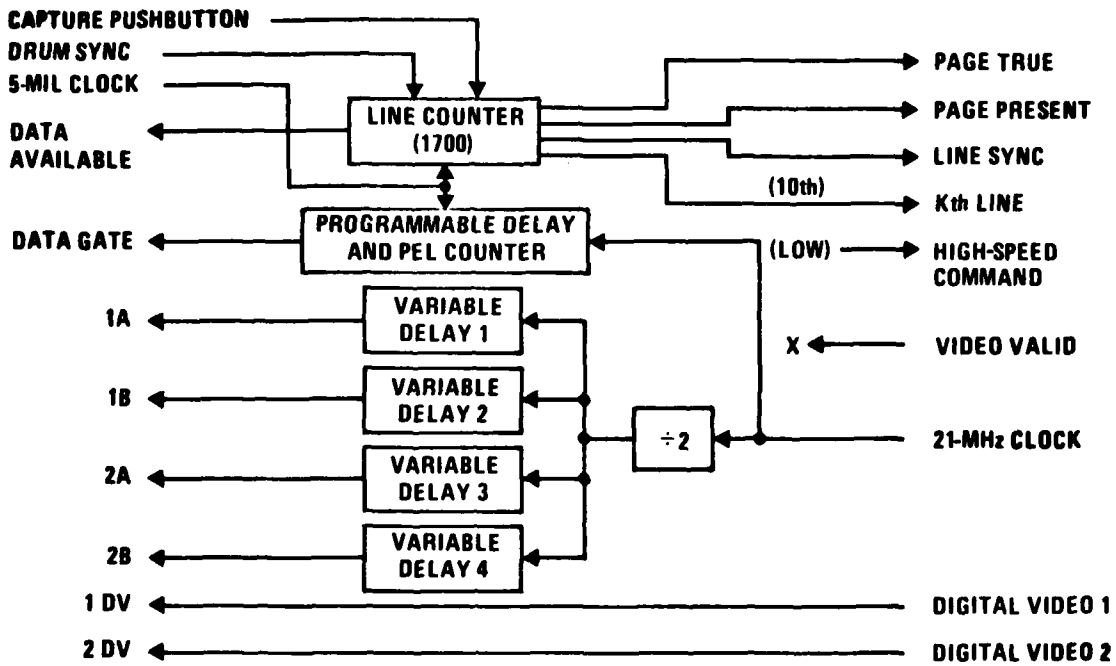

Figure D2. ICAS/Fairchild scanner interface.

Raw Video Outputs

Figure D3* is a block diagram of the video data flow through one of the two channels of the scanner subsystem. The first test point used for characterization is the raw video output, labeled A Video Out and B Video Out. Annex A contains the Fairchild Setup and Test Visit Report, in which there is a series of scope photographs taken during the initial setup of the scanner subsystem at NOSC. Photographs 2 through 5 show the four raw video outputs with the alignment test target in place and the line integration time adjusted to 131.5 μs, equivalent to a four-page-per-second scan rate. A problem was encountered here that could not easily be overcome for the characterization. The peak-to-peak amplitude swing of the raw video outputs was not great enough to cover the full dynamic range of the ICAS input, even with the gain and level circuits set on maximum gain. The peak-to-peak swing referred to is excursion of the negative-most portion of the waveform shown in the photographs and is seen to be on the order of 100 mV. Because of this, all the continuous-tone photographs taken from the raw video outputs will appear to have low contrast.

Matched Filter Outputs

Referring back to figure D3, the matched filter outputs are shown, labeled A S/H Video and B S/H Video. These outputs are the results of the raw video signals passing through the matched filter and sample-and-hold function. The waveshapes are shown in

*Figure D3 is reprinted from Fairchild's Technical Manual for Scanner Subsystem of the U.S. Postal Service Electronic Message Service System, vol I.

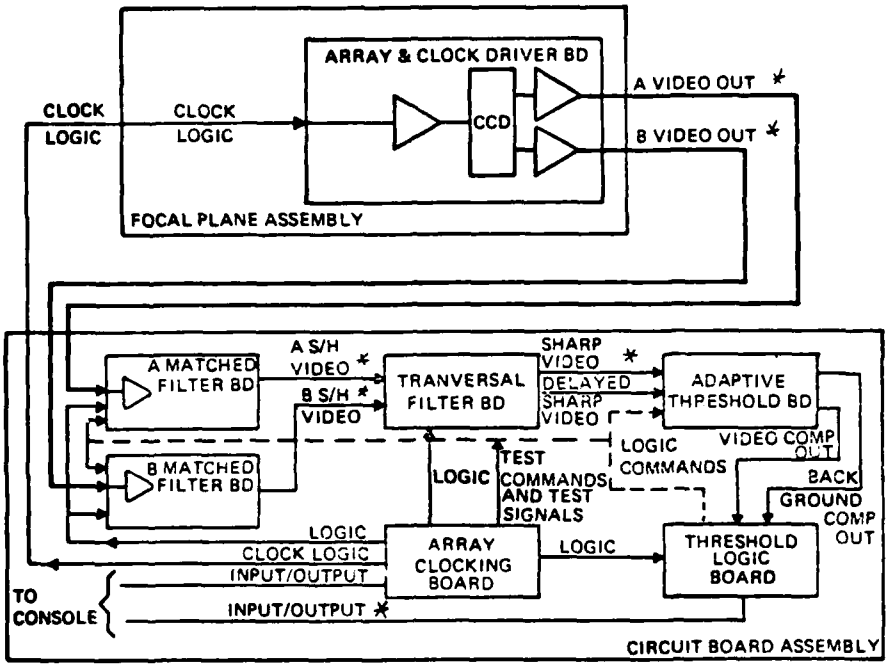

*Buffered outputs for characterization

Figure D3. One channel video data flow.

photographs 6 through 9 in annex A. The polarity has been reversed from the raw video, and the peak-to-peak amplitude is now about 400 mV, enough for full dynamic range on the ICAS input.

Multiplexed Outputs

The multiplexed output from one of the two channels is labeled SHARP VIDEO in figure D3. The multiplexed video at this point in the signal flow is a single pel stream (for each channel) at a 21-MHz rate, which is then input to the thresholding circuitry. The waveforms at these outputs are shown in photographs 10 and 11 in annex A and are seen to have a peak swing of 1 to 1.5 volts.

For input to ICAS, these two signals, and the rest of the signals described below, are double buffered and input to two each of the four ICAS input channels. The delays for the sample commands for each pair of signals were adjusted to sample alternating pels, thus effectively performing a demultiplexing function to satisfy the four-channel requirement of the "personality" card set in ICAS.

Reference Level Outputs

In order to examine the adaptive thresholding circuitry, as implemented, the actual threshold reference voltage was made available for each channel of the scanner subsystem. For this test, only one channel of the scanner could be examined at a time. The reference

voltage was input to two channels of ICAS and the multiplexed video output from the same channel of the scanner was input to the other two channels.

With this input configuration, a split image is captured in memory both halves of which contain data obtained from the same half of the image on the drum during the same scan (ie, two different outputs from the same channel in the scanner). In viewing these images, one side of the image appears to be a mirror image of the other.

Using the resultant split image, the threshold algorithm, as simulated in NOSC software, can be used to process the 6-bit half image, storing the threshold level in image memory instead of the thresholded image data. A direct comparison can then be made of the two reference levels for the same lines of the image acquired during the same scan. Photographs of the reference level outputs are numbers 12 and 13 in annex A.

Digital Video

There are two emitter-coupled logic (ECL) level digital video outputs from the scanner subsystem. These are shown in the top traces of photographs 15 and 16 in annex A. For the characterization, one channel will be examined at a time, just as for the reference level described above. The ECL digital video was input to two channels of the ICAS, and the multiplexed output from the same scanner channel was input to the other two channels of the ICAS. For this test the NOSC adaptive threshold algorithm was used unmodified to threshold the 6-bit image for a direct comparison of the two versions of the digitized image.

ACQUISITIONS

The principal images used for most of the analog and digital image acquisitions were the IEEE Facsimile Test Chart, the 8½-by-8½-inch version of the WJ Miller letter, and a continuous-tone photograph of Point Loma. A NOSC Research Library cover sheet was used to test the operation of the thresholding circuitry on a white-on-black document. Also, a selection of several documents from the Fairchild test deck was used in a test of the color response of the scanner using the two different sets of fluorescent lamps in the scanner.

A chart is presented in figure D4 identifying the principal images used in the evaluation and the test points in the scanner subsystem from which they were obtained. Within each block in the matrix are the image type (continuous-tone or bilevel) and the figure number in which the image is presented. In the remainder of this section, the images identified in figure D4 will be presented in column format. All the continuous-tone prints (CTPs) were analyzed and the pel brightness statistics (PBS) and first difference statistics (FDS) for each CTP are included immediately following the respective image.

ILLUMINATION PROFILE

The illumination profiles presented here are obtained by scanning a sheet of white photographic paper and numerically averaging and normalizing 256 lines of the resulting image to obtain a characteristic profile of the total system response across the active scanning area. This profile includes such contributions as illumination nonuniformity, lens roll-off, imager nonuniformity, and video amplifier responses.

The first illumination profile is shown in figure D5. The label on figure D5, A-1, denotes where that figure fits into the matrix in figure D4. This curve was captured at a page

IMAGE / IMAGE SOURCE	ACQN SPEED, P/S	(1) WHITE STANDARD ILLUM PROFILE	(2) RAW VIDEO OUTPUTS	(3) MATCHED FILTER OUTPUTS	(4) MULTI-PLEXED VIDEO OUTPUTS	(5) THRES-HOLDED VIDEO	(6) ILLUM. CORRECTED FROM (3) OR (4)	(7) DIGITAL EQUIVALENT THRES-HOLDED VIDEO
IEEE FACSIMILE (A) TEST CHART 8½" LEADING 11" LEADING	8.8	D5*	NA	CTP D20 NA	CTP D35 D38	NA	CTP D56 D59	BLP D74 NA
IEEE FACSIMILE (B) TEST CHART 11" LEADING	4	D6	CTP D8	CTP D23	CTP D41	NA	CTP D62	NA
WJ MILLER (C) LETTER TOP LEADING LEFT LEADING	4	D7 D6	CTP D11 D14	CTP D26 D29	CTP D44 D47	BLP D53 D54	CTP D65 D68	BLP D75 NA
POINT LOMA (D) PHOTOGRAPH	4	D7	CTP D17	CTP D32	CTP D50	NA	CTP D71	NA
NOSC (E) LIBRARY COVER	4	NA	NA	NA	NA	D55	NA	NA

CTP: CONTINUOUS-TONE PRINT

BLP: BILEVEL PRINT

NA: NOT AVAILABLE

* FIGURE NUMBER

Figure D4. Principal images evaluated.

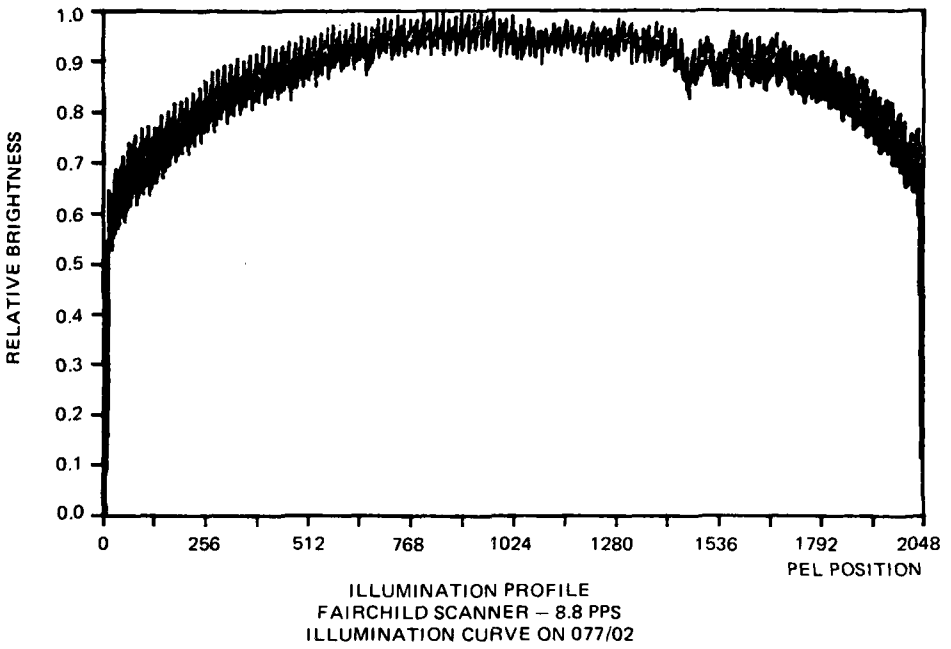

Figure D5. A-1 (fig D4, row A, column 1).

rate of 8.8 pages per second with the video signals from the matched filter input to ICAS. The width of the "envelope" of the curve is primarily due to the mismatch of the two gain and level amplifiers used for each half of the image. There is also a contribution due to clocking noise in the scanner outputs which is much more pronounced at the higher scanning rate. There is a slight mismatch at the center of the curve due both to mismatch of the two sets of scanner outputs and to mismatch of the gain and level amplifiers. There are two rather pronounced dips in this and all other curves at approximately pel position 1400. It is believed that these are caused by dust or dirt on one of the imaging devices. Unfortunately, it was not possible to clean the imager without having to go through the mechanical alignment procedure afterwards.

At either end of this curve can be seen several values that are significantly lower than the rest of the curve. The abutment philosophy used in the scanner calls for an overlap of approximately three pels in the physical alignment of the two imaging devices. The four-port digital interface that NOSC designed requires exactly 2048 pels per line to be stored in memory. This meant that the timing signal, Data Gate, had to be adjusted so that the first pel captured actually preceded the valid video information by about three pels. The net result of this is several invalid values at each end of the scan line. The Fairchild frame-store memory controls suppress those invalid pels at each end of the line and store only about 2042 pels per line.

Figures D6 and D7 contain similar illumination profiles, all of which were taken at a page rate of four per second. The effects of the dust particles are more pronounced in these figures. The differences in these two figures are due to the different times at which they were generated and different attempts at aligning the gain and level amplifiers.

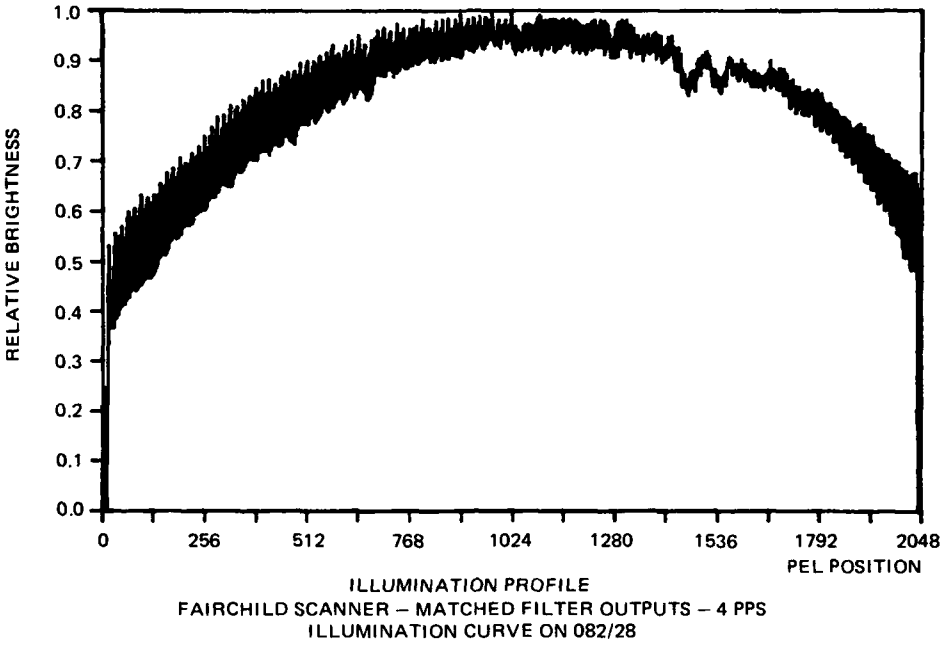

Figure D6. C-1A.

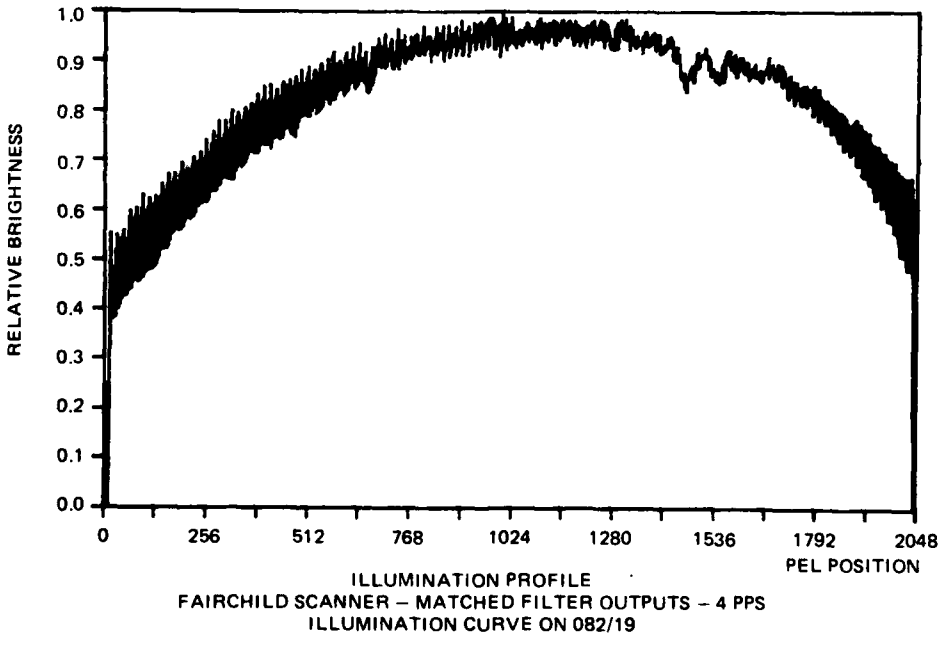

Figure D7. C-1B and D-1.

In generating these illumination profiles, the ICAS gain and level amplifiers were adjusted for 0 codes with no light (zero reflectance) input and a few 63 codes with a high-reflectance white standard in place on the drum. This adjustment procedure was done for all video test points except for the raw video signals which did not have enough amplitude for a full-scale output. Figures D6 and D7 indicate that the scanner system response falls off to about 50% at each end of the field of view. This, of course, includes the effects not only of illumination falloff but of lens response as well.

RAW VIDEO

Because of the relatively low signal level at the raw video test points in the scanner, no useful images could be captured on the ICAS at the 8.8-page-per-second rate. Thus, there is no entry in the image matrix for A-2.

Figure D8 is the first of the continuous-tone prints (CTP) presented in this report. This and all other photographs presented here are printed on 4-by-5-inch sheet film using a Dicomed model D-47 film recording system. The D-47 prints a 4096-by-4096-dot matrix in a 3.39-inch-square area on the film. This results in a printing resolution capability of 1210 dots per inch. However, for the photographs in this report, the D-47 was used at half the maximum resolution, printing a 2-by-2-dot matrix for each pel scanned. The negatives are then printed at about 2X magnification for a print at 65% of original size. The eight-step grey scale printed outside the image area is computer-generated and used to maintain linearity in the photographic process. The photographs are then screened with a 120-line-per-inch screen for reproduction. NOSC, Fairchild, and USPS have original photographs for reference purposes.

Figure D8 is a photograph of the IEEE Facsimile Test Chart scanned with the 11-inch edge leading and using the raw video outputs from the scanner. The scanning rate was four pages per second. As mentioned earlier, the output signal amplitude at the raw video test point was only about 100 mV. With the gain and level amplifiers set on maximum gain, the 100-mV signal produced only up to 62% of the full dynamic range. This is the reason that all images from the raw video outputs appear to have low contrast.

Figure D9 contains the pel brightness statistics (PBS) for the image in figure D8. These and all other PBS are computed on only the portion of the image representing the document being scanned, cutting off the invalid pels at the end of each line as well as any pels that represent the scanner drum reflectance. Figure D9 shows that for this image all pels fall between levels 24 and 63.

Figure D10 shows the first difference statistics (FDS) for figure D8. The FDS describe the distribution of the magnitudes of the differences between each pel and its predecessor. These statistics are accumulated only in the direction of scan, not in the direction of paper motion. The larger difference values are an indicator of how the system responds to large step changes in reflectance on the document scanned. Here, the term "system" includes the entire video processing chain, both in the scanner and in ICAS. Figure D10 says that there were no changes from one pel to the next greater than 22 levels.

The next of the raw video test images is in figure D11. This is an example of a typed page scanned parallel to the lines of type. Although the imager abutment is very nearly optimum, a difference in the relative focus of the two imagers is quite evident, the left side showing the better focus. Following that image are the PBS and FDS in figures D12 and D13, respectively.

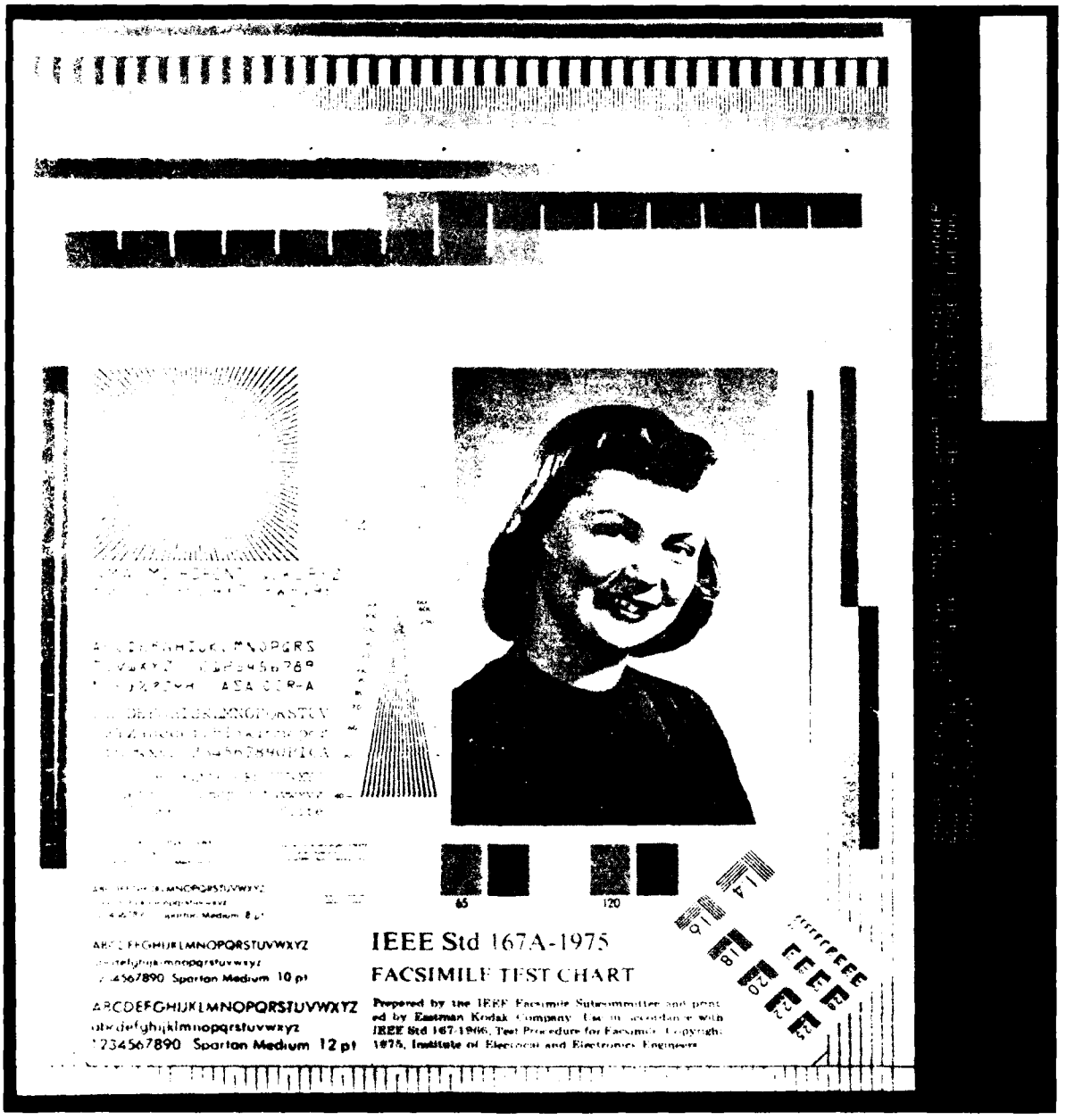
IEEE Std 167A-1975
FACSIMILE TEST CHART
ABCDEFGHIJKLMNOPQRSTUVWXYZ
4567890 Sparton Medium 10 pt
ABCDEFGHIJKLMNOPQRSTUVWXYZ
1234567890 Sparton Medium 12 pt
65
120

Figure D8. B-2.

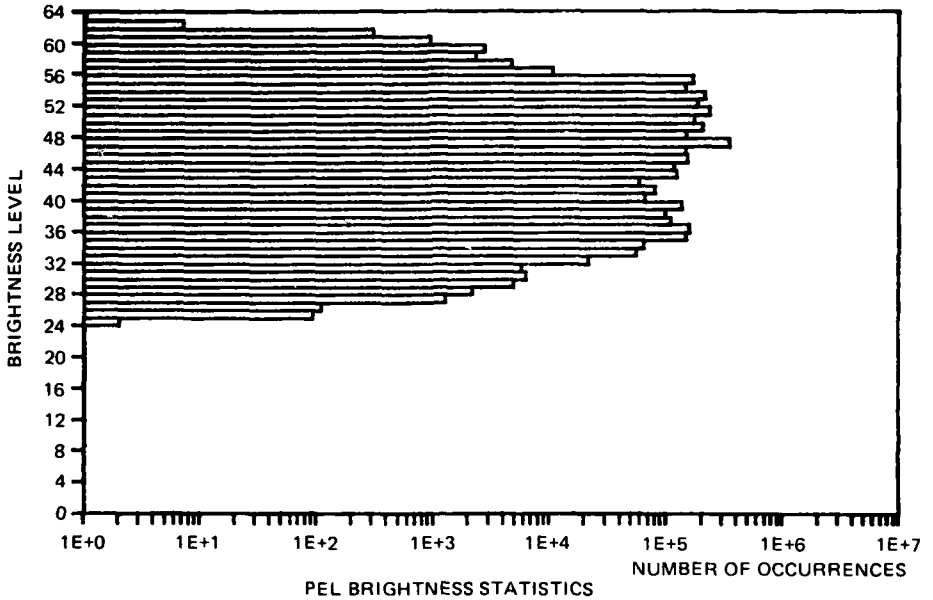

PEL BRIGHTNESS STATISTICS
IEEE FACSIMILE TEST CHART – FAIRCHILD SCANNER – RAW VIDEO OUTPUTS – 4 PPS
IMAGE (13-01) ON 080/02 – STATS ON 087/03

Figure D9. B-2.

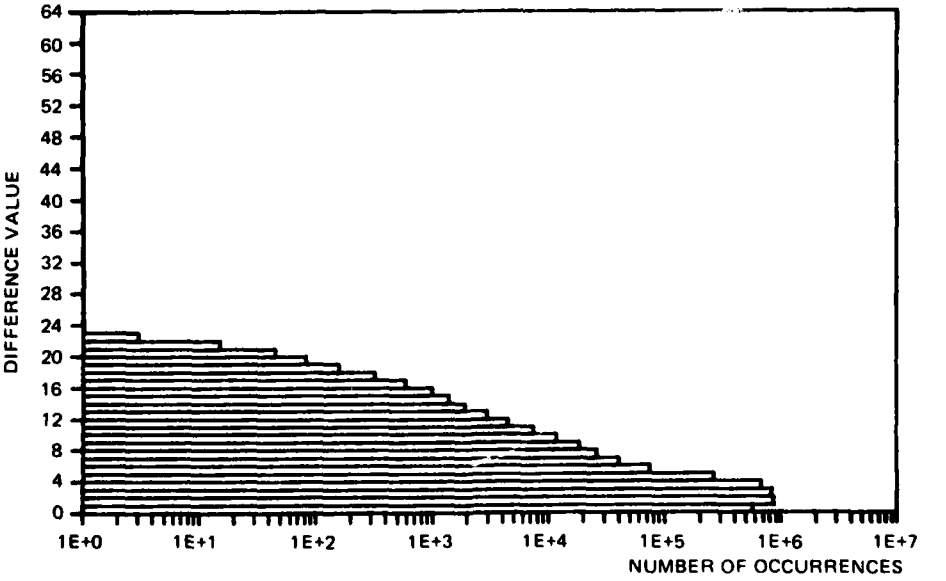

FIRST DIFFERENCE STATISTICS
IEEE FACSIMILE TEST CHART – FAIRCHILD SCANNER – RAW VIDEO OUTPUTS – 4 PPS
IMAGE (13-01) ON 080/02 – STATS ON 087/03

Figure D10. B-2.

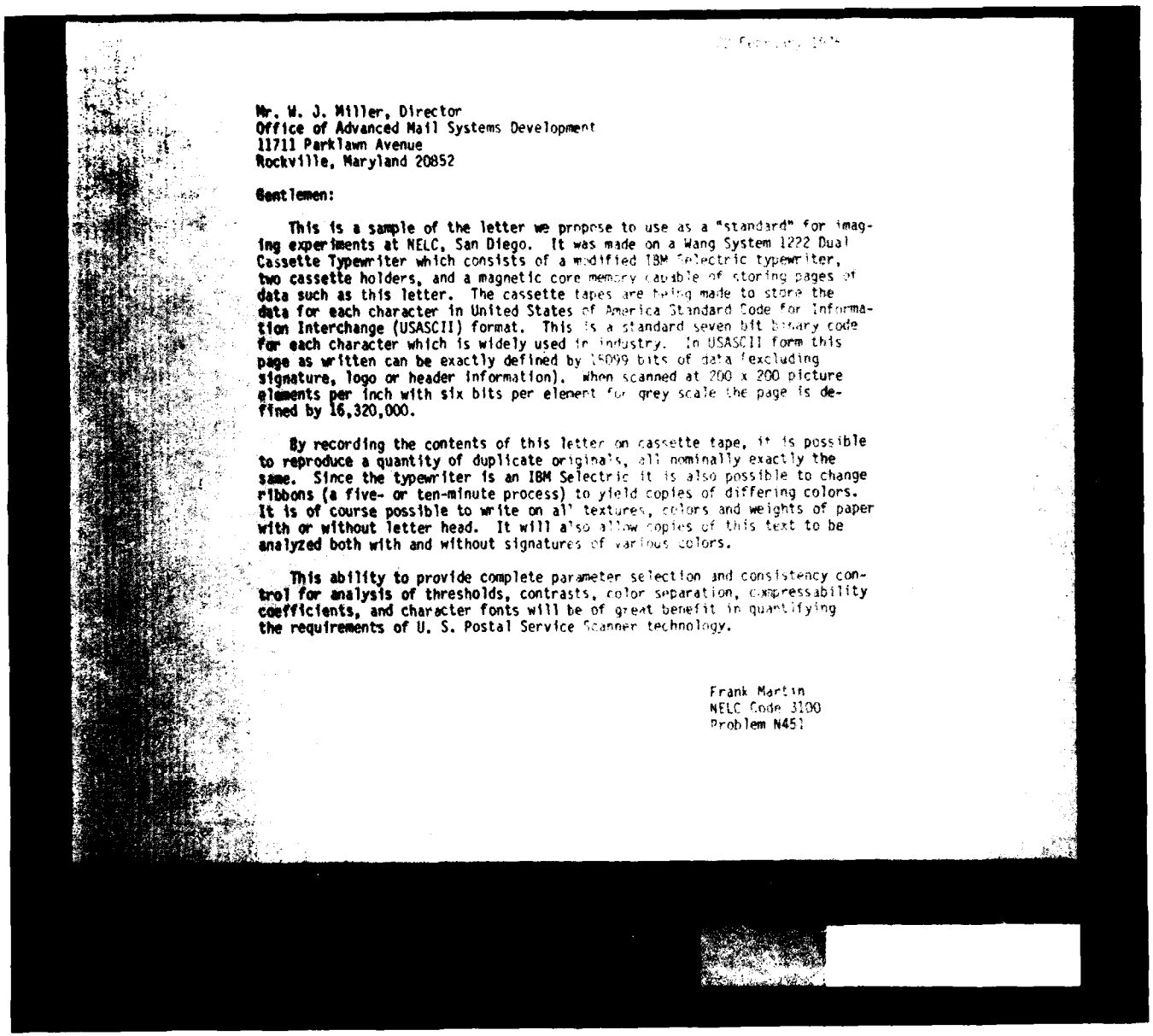

Mr. W. J. Miller, Director
Office of Advanced Mail Systems Development
11711 Parklawn Avenue
Rockville, Maryland 20852

Gentlemen:

This is a sample of the letter we propose to use as a "standard" for imaging experiments at NELC, San Diego. It was made on a Wang System 1222 Dual Cassette Typewriter which consists of a modified IBM Selectric typewriter, two cassette holders, and a magnetic core memory capable of storing pages of data such as this letter. The cassette tapes are being made to store the data for each character in United States of America Standard Code for Information Interchange (USASCII) format. This is a standard seven bit binary code for each character which is widely used in industry. In USASCII form this page as written can be exactly defined by 15099 bits of data (excluding signature, logo or header information). When scanned at 200 x 200 picture elements per inch with six bits per element for grey scale the page is defined by 16,320,000.

By recording the contents of this letter on cassette tape, it is possible to reproduce a quantity of duplicate originals, all nominally exactly the same. Since the typewriter is an IBM Selectric it is also possible to change ribbons (a five- or ten-minute process) to yield copies of differing colors. It is of course possible to write on all textures, colors and weights of paper with or without letter head. It will also allow copies of this text to be analyzed both with and without signatures of various colors.

This ability to provide complete parameter selection and consistency control for analysis of thresholds, contrasts, color separation, compressability coefficients, and character fonts will be of great benefit in quantifying the requirements of U. S. Postal Service Scanner technology.

Frank Martin
NELC Code 3100
Problem N451

Figure D11. C-2.

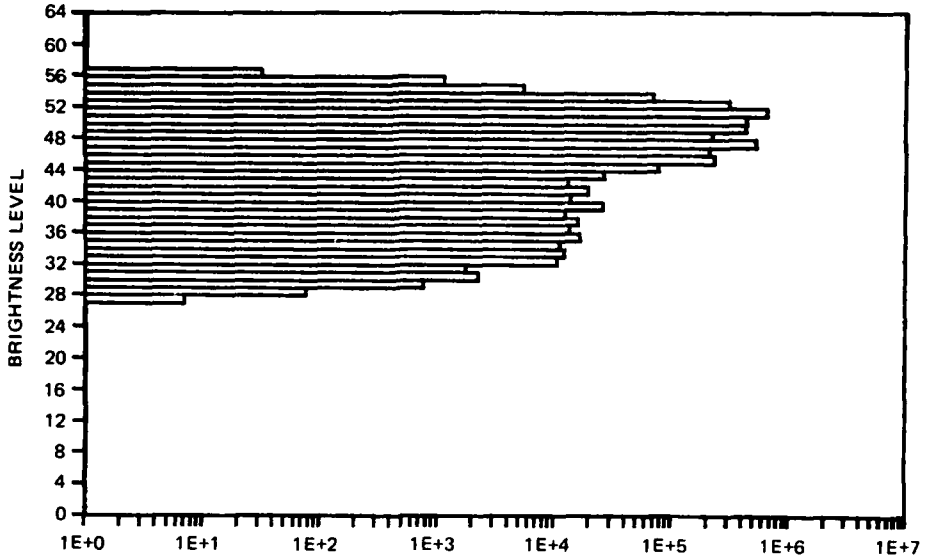

PEL BRIGHTNESS STATISTICS
WJM TYPED PAGE – FAIRCHILD SCANNER – RAW VIDEO OUTPUTS – 4 PPS
IMAGE (8 1/2 X 8 1/2 – TOP EDGE LEADING) ON 080/06 – STATS ON 087/06

Figure D12. C-2.

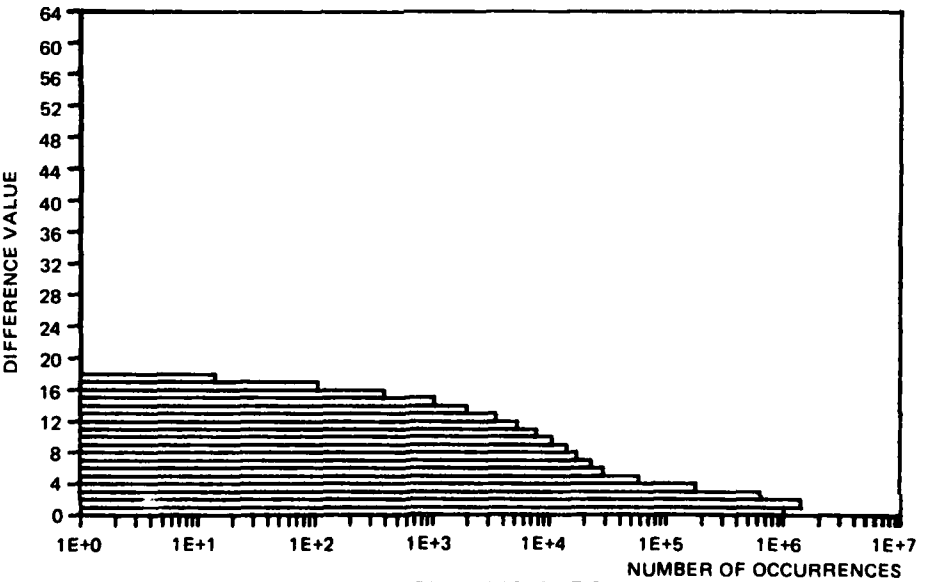

FIRST DIFFERENCE STATISTICS
WJM TYPED PAGE – FAIRCHILD SCANNER – RAW VIDEO OUTPUTS – 4 PPS
IMAGE (8 1/2 X 8 1/2 – TOP EDGE LEADING) ON 080/06 – STATS ON 087/06

Figure D13. C-2.

Figure D14 is of the typed page scanned perpendicular to the lines of type, as would be the normal configuration in the Pitney Bowes Printer and Paper Handling Equipment Input Unit (PPHE/IU). This figure and its statistics in figures D15 and D16 can be compared to the previous figure to determine any differences in image quality due to scan direction. It can be seen that the PBS and FDS for the two images are very nearly the same.

An example of a continuous-tone photograph, an aerial view of Point Loma, is shown in figure D17. The effects of the uneven focus are pronounced in this photograph. The PBS and FDS follow in the next two figures.

MATCHED FILTER OUTPUTS

Figure D20 is the first of the images acquired from the matched filter outputs. At this point in the scanner analog video processing chain there is sufficient amplitude to cover the full dynamic range of the ICAS input. This is evidenced by the higher contrast in the photograph and also in the PBS of figure D21. This image was acquired at an equivalent rate of 8.8 pages per second. A certain amount of noise can be seen showing up as vertical striations mostly noticeable in the darker areas of the image. However, there is no real loss of information in the image. The FDS in figure D22 indicates that there are step changes in the image from one pel to the next of up to 28 intensity levels.

The next image, figure D23, is the IEEE Facsimile Test Chart, this time with the 11-inch edge leading, and an acquisition rate of four pages per second. The vertical noise patterns are still visible but not quite as pronounced, because of the increased integration time at the slower speed. In this image a considerable fall-off in the illumination on the document can be noticed as it was scanned. The PBS in figure D24 show that this image does utilize the full dynamic range of the ICAS with a small amount of saturation at either end of the brightness range. The FDS in figure D25 show a problem that is very likely caused by the gain and level amplifiers in the ICAS. The peaking circuits in those amplifiers were adjusted for imager outputs which were "return-to-zero" waveforms. The matched filter and multiplexed outputs from the scanner are sample-and-hold waveforms which are non-return-to-zero. The net effect is overshoot in the analog input to the A/D converters which can be seen upon close examination of the photograph. This overshoot is what caused the relatively large differences shown in figure D25.

The next two images, figures D26 and D29, are of the typed page scanned in both directions. The comments made on the previous image also apply here. Additionally, the difference in focusing can easily be seen as well as the vertical streaking in the same pel positions as the two dips mentioned in the discussion of figure D5 at pel position 1400.

The last of the images from the matched filter outputs is the continuous-tone photograph shown in figure D32. The original photograph contains many dark areas which, with the illumination fall-off, produced a very dark image after scanning.

MULTIPLEXED OUTPUTS

The images in column 4 of the matrix in figure D4 are captured using the multiplexed outputs from the scanner. Figures D35 and D38 are images of the IEEE Facsimile Test Chart scanned in both directions at a page rate of 8.8 pages per second. The image in figure D38 shows a peculiar intensity modulation in the lower left portion of the image. The source of this is not known, but it does appear as if the illumination source was modulated momentarily.

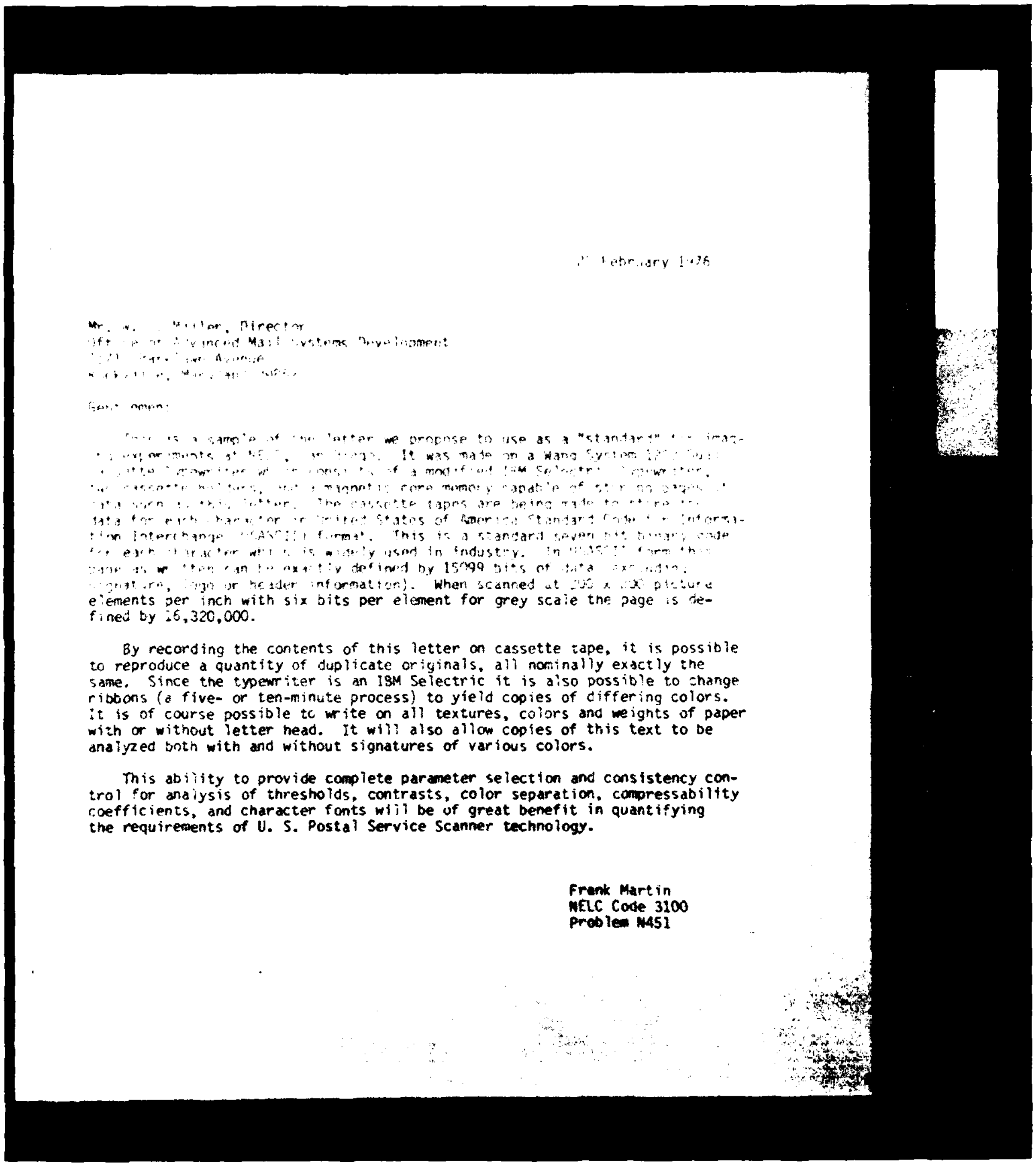

[illegible] February 1976

Mr. [illegible] Miller, Director
Office of Advanced Mail Systems Development
[illegible] Avenue
[illegible], Maryland [illegible]

Gentlemen:

[illegible] is a sample of the letter we propose to use as a "standard" for imag[illegible] experiments at NELC, [illegible]. It was made on a Wang System [illegible] typewriter which consists of a modified IBM Selectric typewriter, two cassette holders, and a magnetic core memory capable of storing pages of data such as this letter. The cassette tapes are being made to store the data for each character in United States of America Standard Code for Information Interchange (USASCII) format. This is a standard seven bit binary code for each character which is widely used in industry. In USASCII form this page as written can be exactly defined by 15099 bits of data (excluding signature, logo or header information). When scanned at 200 x 200 picture elements per inch with six bits per element for grey scale the page is defined by 16,320,000.

By recording the contents of this letter on cassette tape, it is possible to reproduce a quantity of duplicate originals, all nominally exactly the same. Since the typewriter is an IBM Selectric it is also possible to change ribbons (a five- or ten-minute process) to yield copies of differing colors. It is of course possible to write on all textures, colors and weights of paper with or without letter head. It will also allow copies of this text to be analyzed both with and without signatures of various colors.

This ability to provide complete parameter selection and consistency control for analysis of thresholds, contrasts, color separation, compressability coefficients, and character fonts will be of great benefit in quantifying the requirements of U. S. Postal Service Scanner technology.

Frank Martin
NELC Code 3100
Problem N451

Figure D14. C-2.

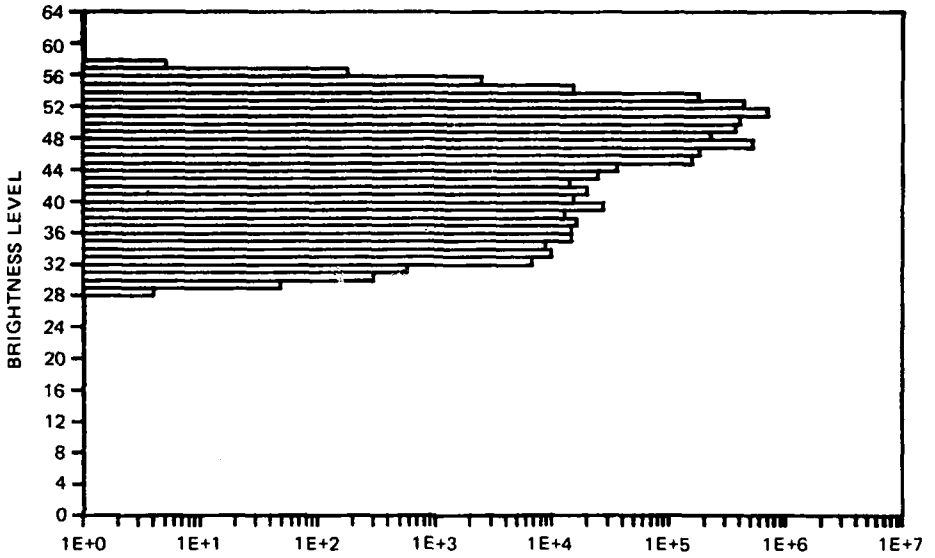

PEL BRIGHTNESS STATISTICS
WJM TYPED PAGE – FAIRCHILD SCANNER – RAW VIDEO OUTPUTS – 4 PPS
IMAGE (8 1/2 x 8 1/2 – LEFT EDGE LEADING) ON 080/07 – STATS ON 087/07

Figure D15. C-2.

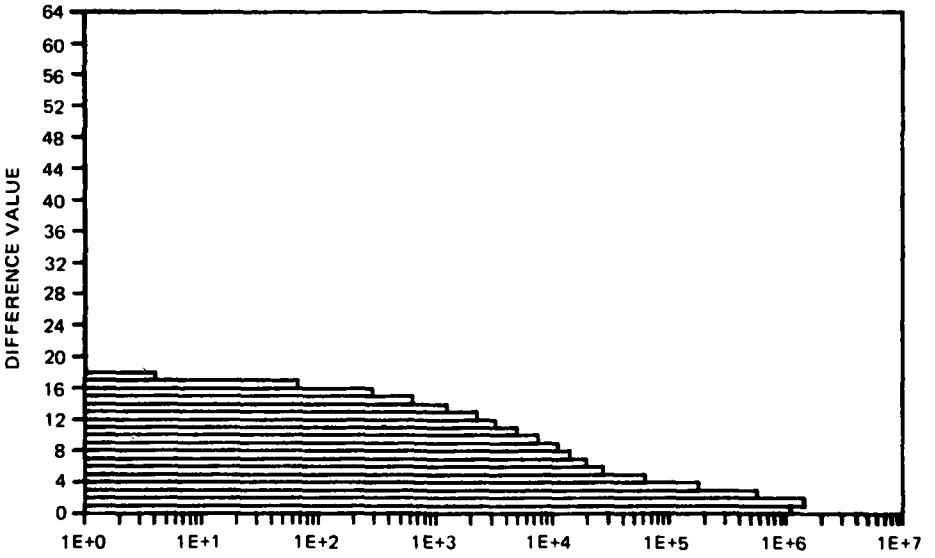

FIRST DIFFERENCE STATISTICS
WJM TYPED PAGE – FAIRCHILD SCANNER – RAW VIDEO OUTPUTS – 4 PPS
IMAGE (8 1/2 x 8 1/2 – LEFT EDGE LEADING) ON 080/07 – STATS ON 087/07

Figure D16. C-2.

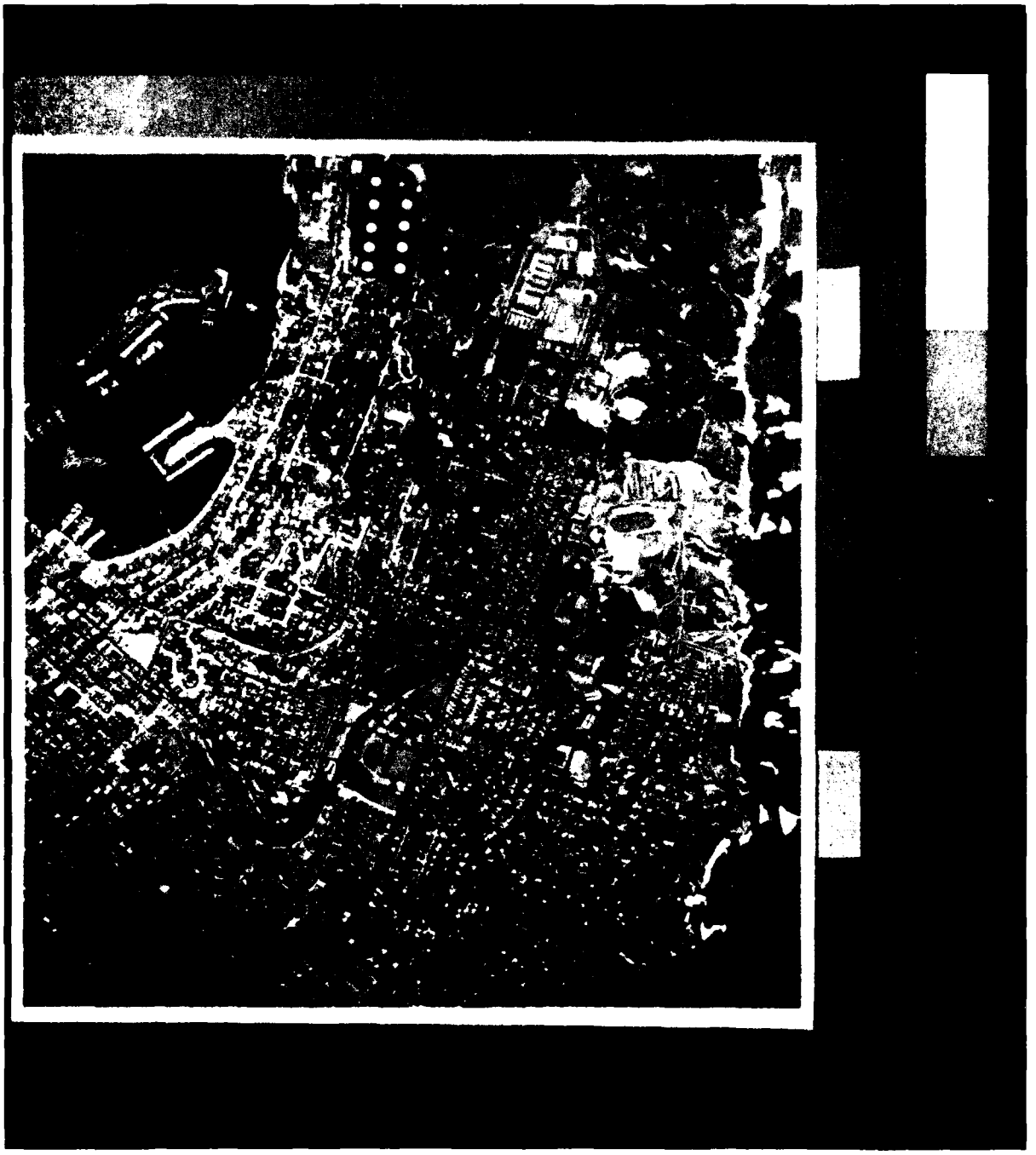

Figure D17. D-2.

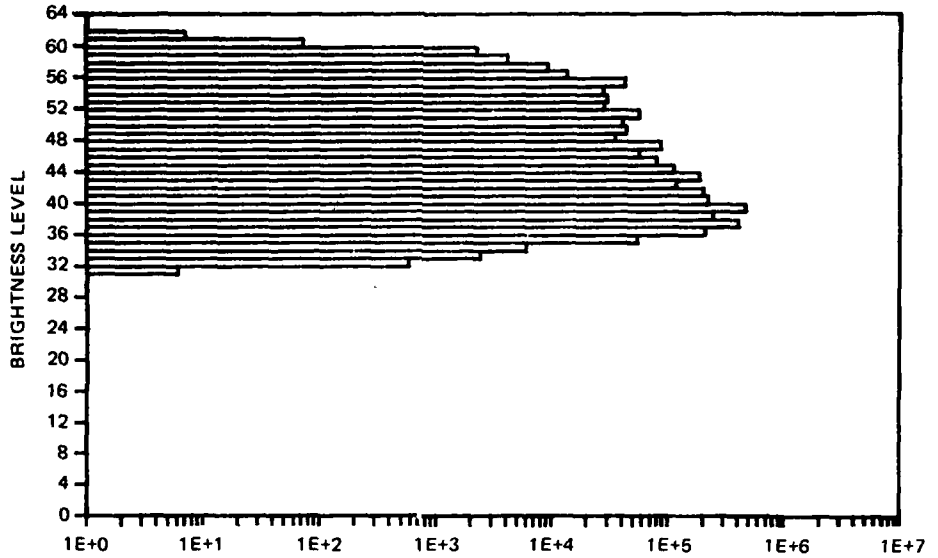

PEL BRIGHTNESS STATISTICS
POINT LOMA PHOTO – FAIRCHILD SCANNER – RAW VIDEO OUTPUTS – 4 PPS
IMAGE (11-06) ON 080/04 – STATS ON 087/05

Figure D18. D-2.

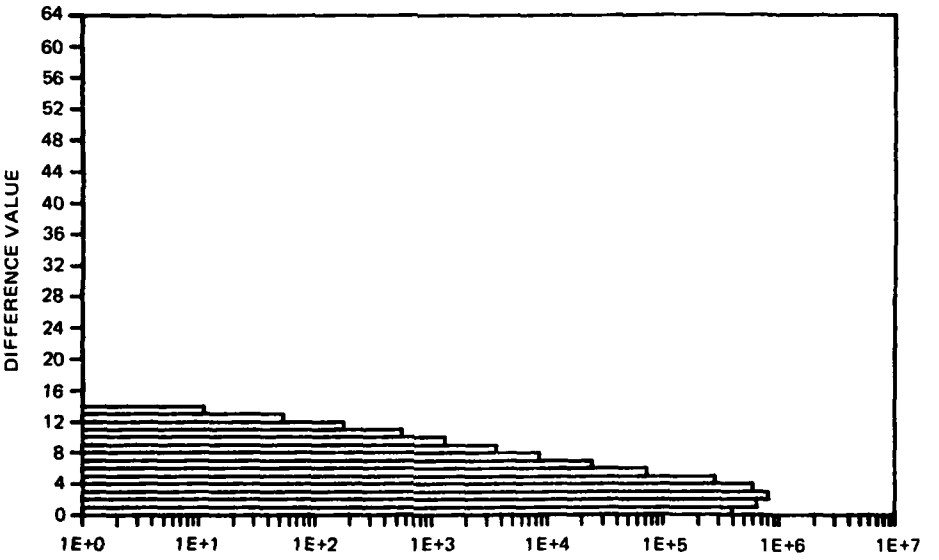

FIRST DIFFERENCE STATISTICS
POINT LOMA PHOTO – FAIRCHILD SCANNER – RAW VIDEO OUTPUTS – 4 PPS
IMAGE (11-06) ON 080/04 – STATS ON 087/05

Figure D19. D-2.

Figure D20. A-3.

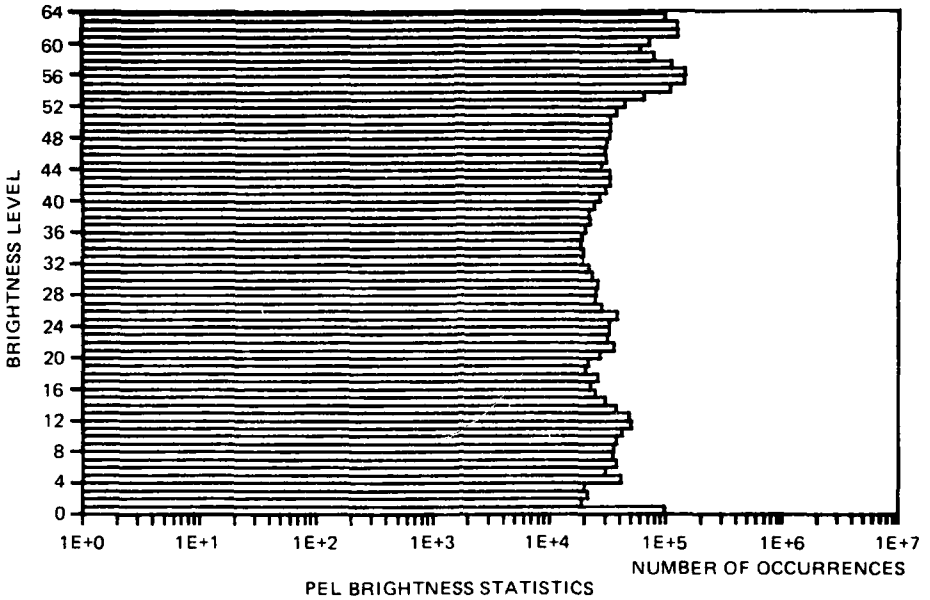

PEL BRIGHTNESS STATISTICS
IEEE FAX TEST CHART – FAIRCHILD SCANNER – MATCHED FILTER OUTPUTS – 8.77 PPS
IMAGE (13-01) ON 075/06 – STATS ON 087/04

Figure D21. A-3.

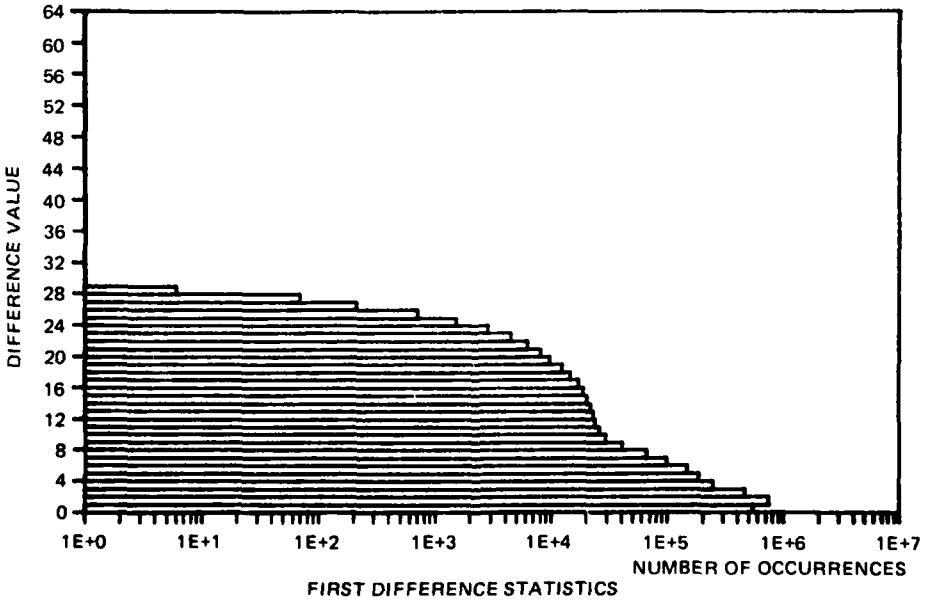

FIRST DIFFERENCE STATISTICS
IEEE FAX TEST CHART – FAIRCHILD SCANNER – MATCHED FILTER OUTPUTS – 8.77 PPS
IMAGE (13-01) ON 075/06 – STATS ON 087/04

Figure D22. A-3.

Figure D23. B-3.

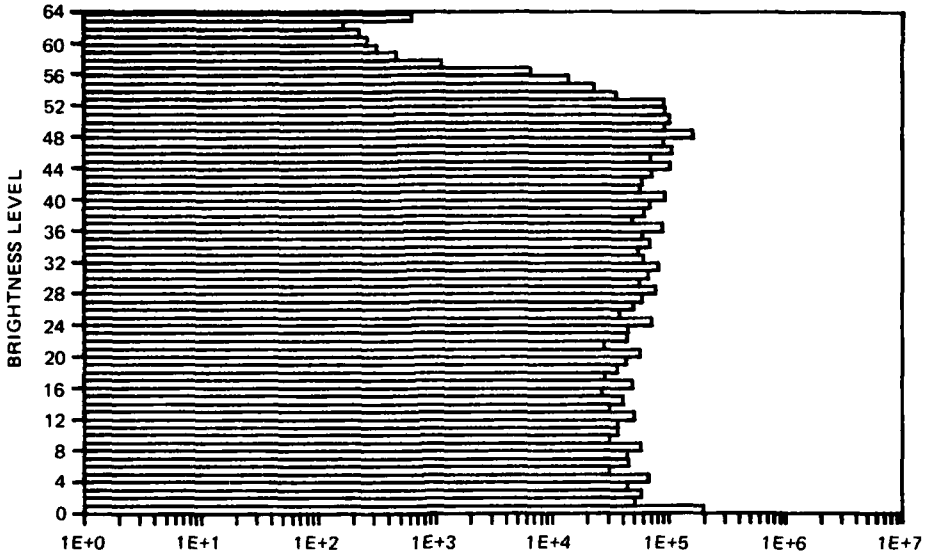

PEL BRIGHTNESS STATISTICS
IEEE FAX TEST CHART – FAIRCHILD SCANNER – MATCHED FILTER OUTPUTS – 4 PPS
IMAGE (13-01) ON 080/13 – STATS ON 080/14

Figure D24. B-3.

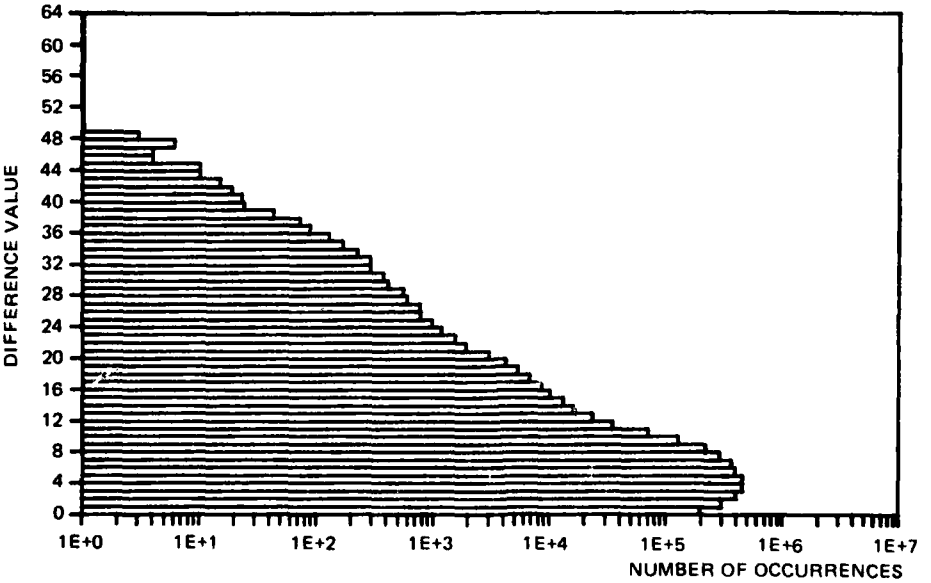

FIRST DIFFERENCE STATISTICS
IEEE FAX TEST CHART – FAIRCHILD SCANNER – MATCHED FILTER OUTPUTS – 4 PPS
IMAGE (13-01) ON 080/13 – STATS ON 080/14

Figure D25. B-3.

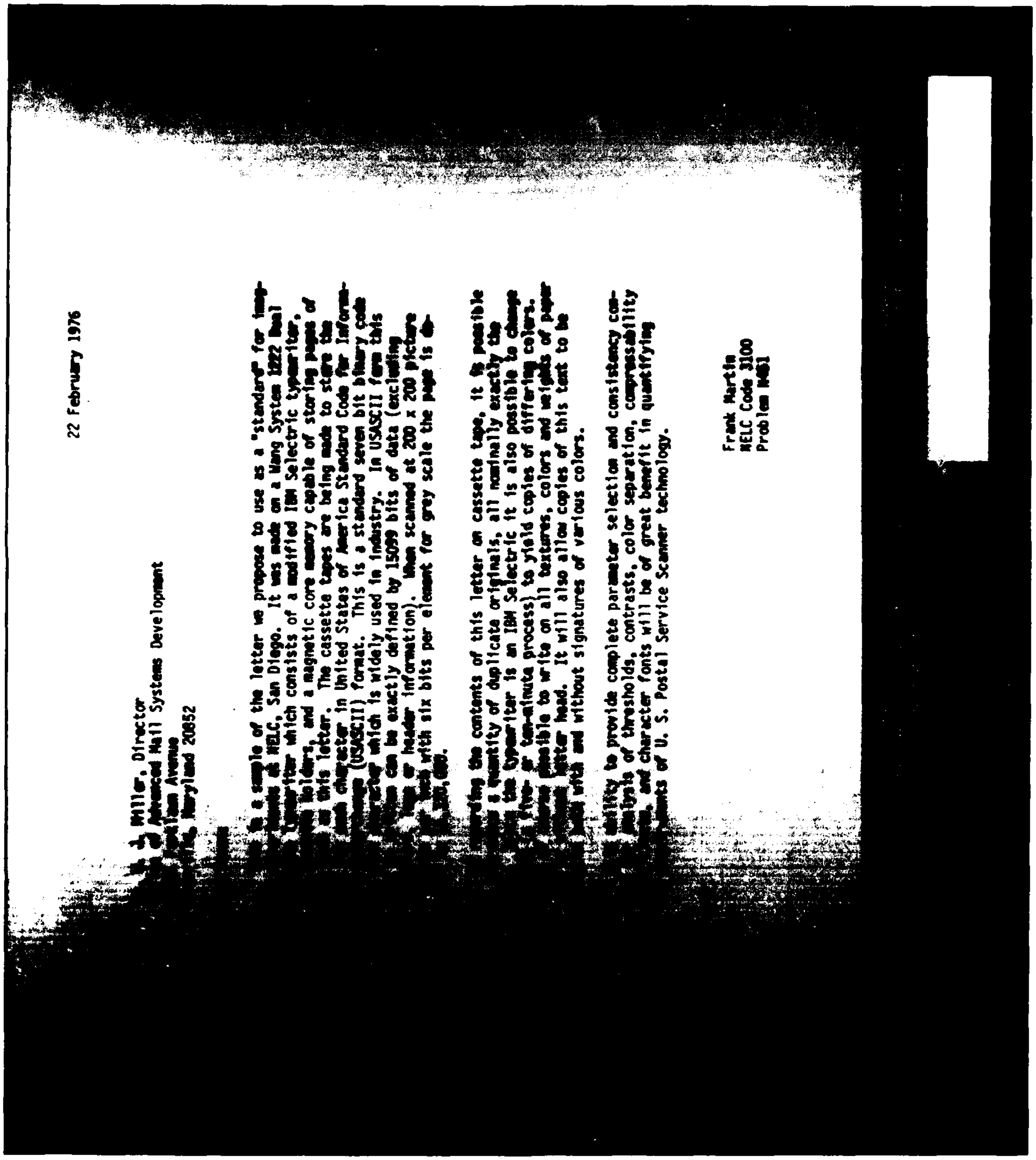
22 February 1976

[illegible] J. Miller, Director
[illegible] of Advanced Mail Systems Development
[illegible] Avenue
[illegible], Maryland 20852

[illegible] is a sample of the letter we propose to use as a "standard" for imag-
[illegible] at NELC, San Diego. It was made on a Wang System 1222 Dual
[illegible] Typewriter which consists of a modified IBM Selectric typewriter,
[illegible] holders, and a magnetic core memory capable of storing pages of
[illegible] as this letter. The cassette tapes are being made to store the
[illegible] character in United States of America Standard Code for Informa-
[illegible] (USASCII) format. This is a standard seven bit binary code
[illegible] which is widely used in industry. In USASCII form this
[illegible] can be exactly defined by 15099 bits of data (excluding
[illegible] or header information). When scanned at 200 x 200 picture
[illegible] with six bits per element for grey scale the page is de-
[illegible].

[illegible] the contents of this letter on cassette tape, it is possible
[illegible] a quantity of duplicate originals, all nominally exactly the
[illegible] the typewriter is an IBM Selectric it is also possible to change
[illegible] five- or ten-minute process) to yield copies of differing colors.
[illegible] possible to write on all textures, colors and weights of paper
[illegible] letter head. It will also allow copies of this text to be
[illegible] with and without signatures of various colors.

[illegible] ability to provide complete parameter selection and consistency com-
[illegible] analysis of thresholds, contrasts, color separation, compressability
[illegible], and character fonts will be of great benefit in quantifying
[illegible] of U. S. Postal Service Scanner technology.

Frank Martin
NELC Code 3100
Problem N461

Figure D26. C-3.

PEL BRIGHTNESS STATISTICS
WJM TYPED PAGE – FAIRCHILD SCANNER – MATCHED FILTER OUTPUTS – 4 PPS
IMAGE (8 1/2 x 8 1/2 – TOP EDGE LEADING) ON 080/10 – STATS ON 087/10

Figure D27. C-3.

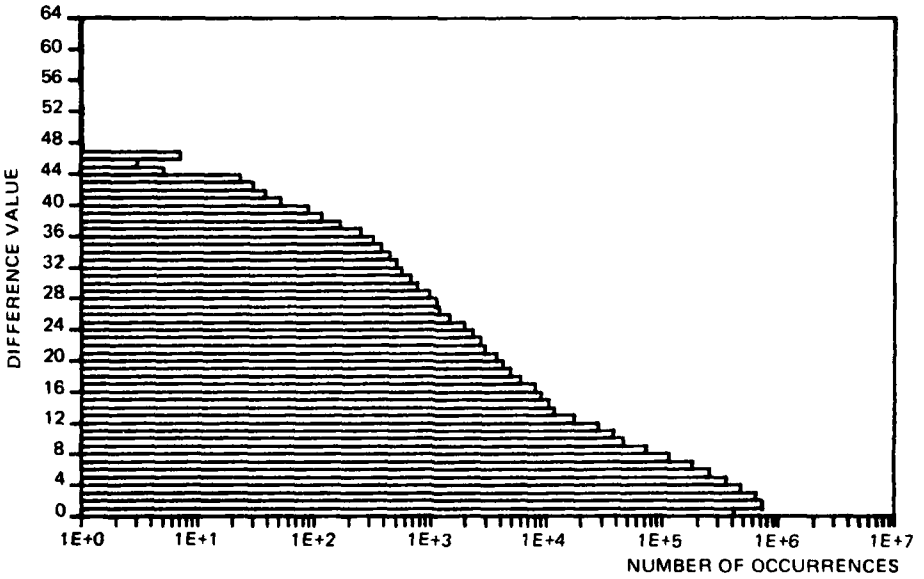

FIRST DIFFERENCE STATISTICS
WJM TYPED PAGE – FAIRCHILD SCANNER – MATCHED FILTER OUTPUTS – 4 PPS
IMAGE (8 1/2 x 8 1/2 – TOP EDGE LEADING) ON 080/10 – STATS ON 087/10

Figure D28. C-3.

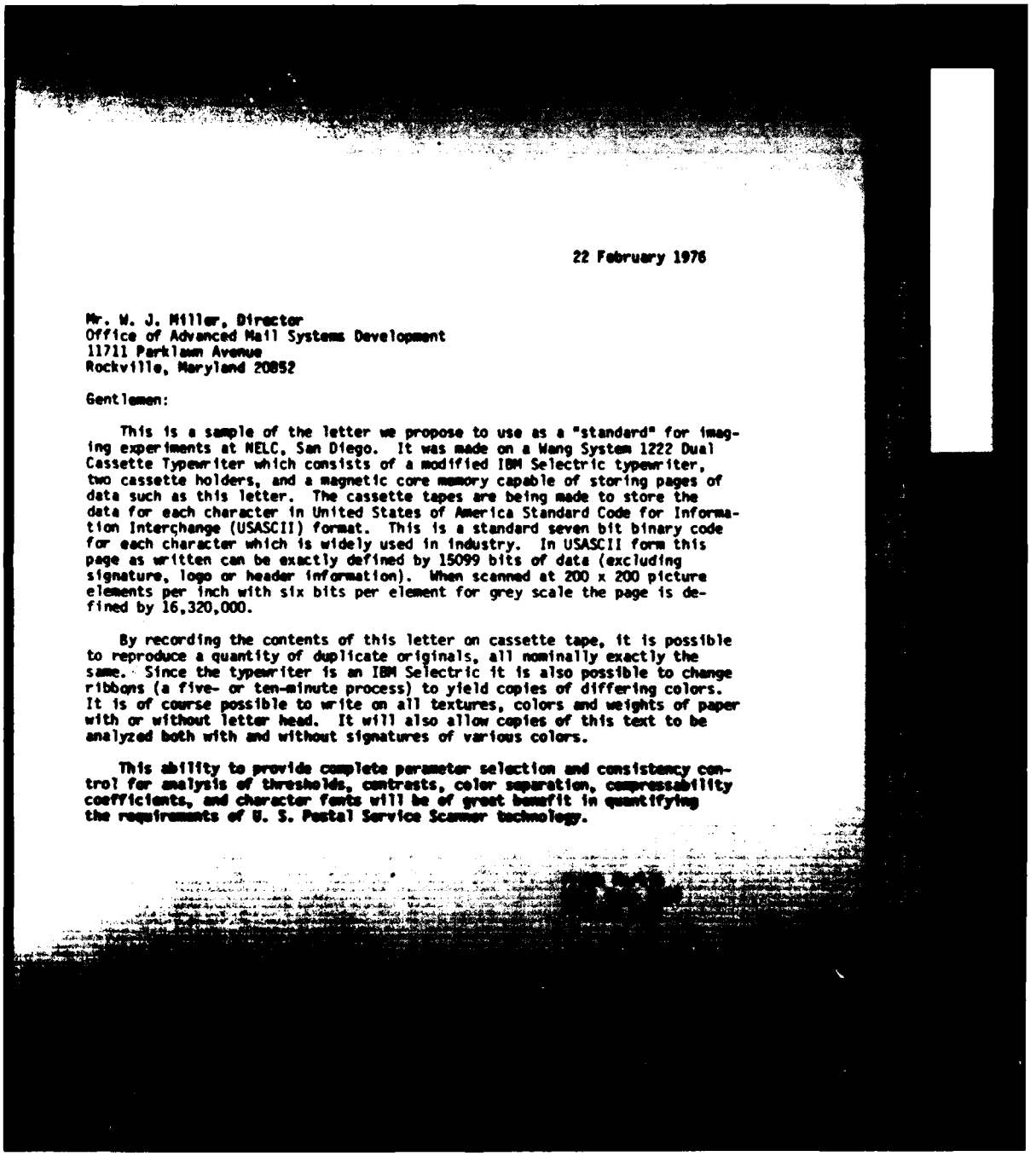

22 February 1976

Mr. W. J. Miller, Director
Office of Advanced Mail Systems Development
11711 Parklawn Avenue
Rockville, Maryland 20852

Gentlemen:

This is a sample of the letter we propose to use as a "standard" for imaging experiments at NELC, San Diego. It was made on a Wang System 1222 Dual Cassette Typewriter which consists of a modified IBM Selectric typewriter, two cassette holders, and a magnetic core memory capable of storing pages of data such as this letter. The cassette tapes are being made to store the data for each character in United States of America Standard Code for Information Interchange (USASCII) format. This is a standard seven bit binary code for each character which is widely used in industry. In USASCII form this page as written can be exactly defined by 15099 bits of data (excluding signature, logo or header information). When scanned at 200 x 200 picture elements per inch with six bits per element for grey scale the page is defined by 16,320,000.

By recording the contents of this letter on cassette tape, it is possible to reproduce a quantity of duplicate originals, all nominally exactly the same. Since the typewriter is an IBM Selectric it is also possible to change ribbons (a five- or ten-minute process) to yield copies of differing colors. It is of course possible to write on all textures, colors and weights of paper with or without letter head. It will also allow copies of this text to be analyzed both with and without signatures of various colors.

This ability to provide complete parameter selection and consistency control for analysis of thresholds, contrasts, color separation, compressability coefficients, and character fonts will be of great benefit in quantifying the requirements of U. S. Postal Service Scanner technology.

Figure D29. C-3.

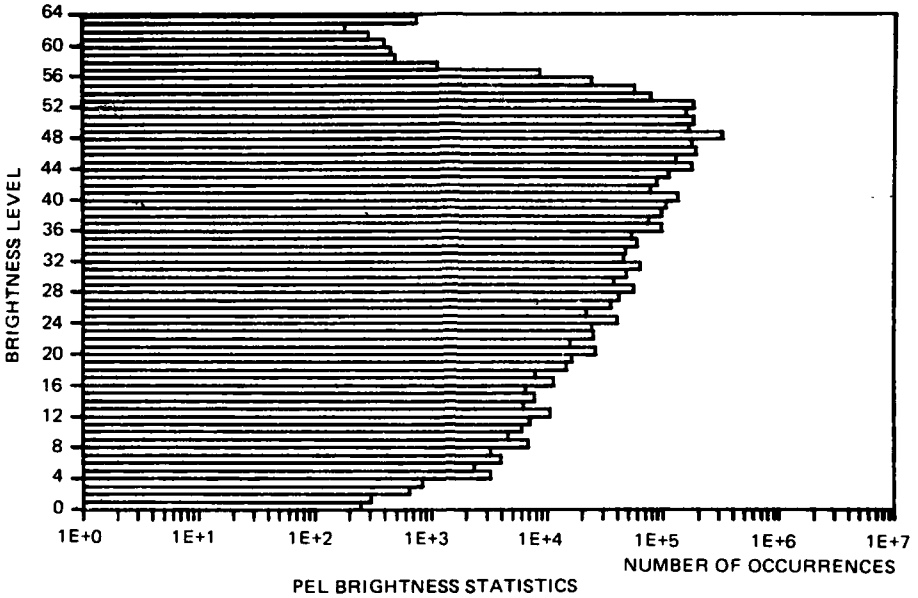

PEL BRIGHTNESS STATISTICS
WJM TYPED PAGE – FAIRCHILD SCANNER – MATCHED FILTER OUTPUTS – 4 PPS
IMAGE (8 1/2 x 8 1/2 – LEFT EDGE LEADING) ON 080/12 – STATS ON 087/11

Figure D30. C-3.

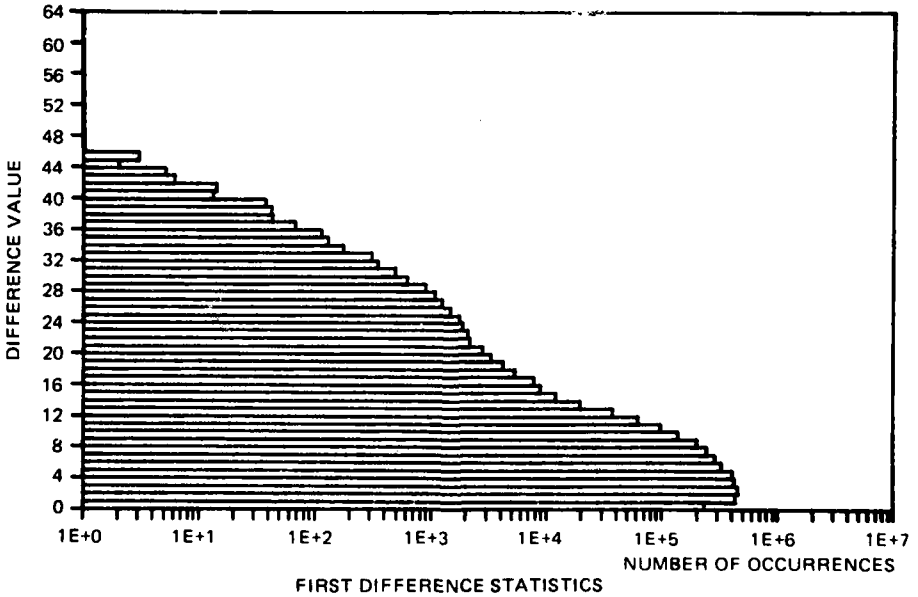

FIRST DIFFERENCE STATISTICS
WJM TYPED PAGE – FAIRCHILD SCANNER – MATCHED FILTER OUTPUTS – 4 PPS
IMAGE (8 1/2 x 8 1/2 – LEFT EDGE LEADING) ON 080/12 – STATS ON 087/11

Figure D31. C-3.

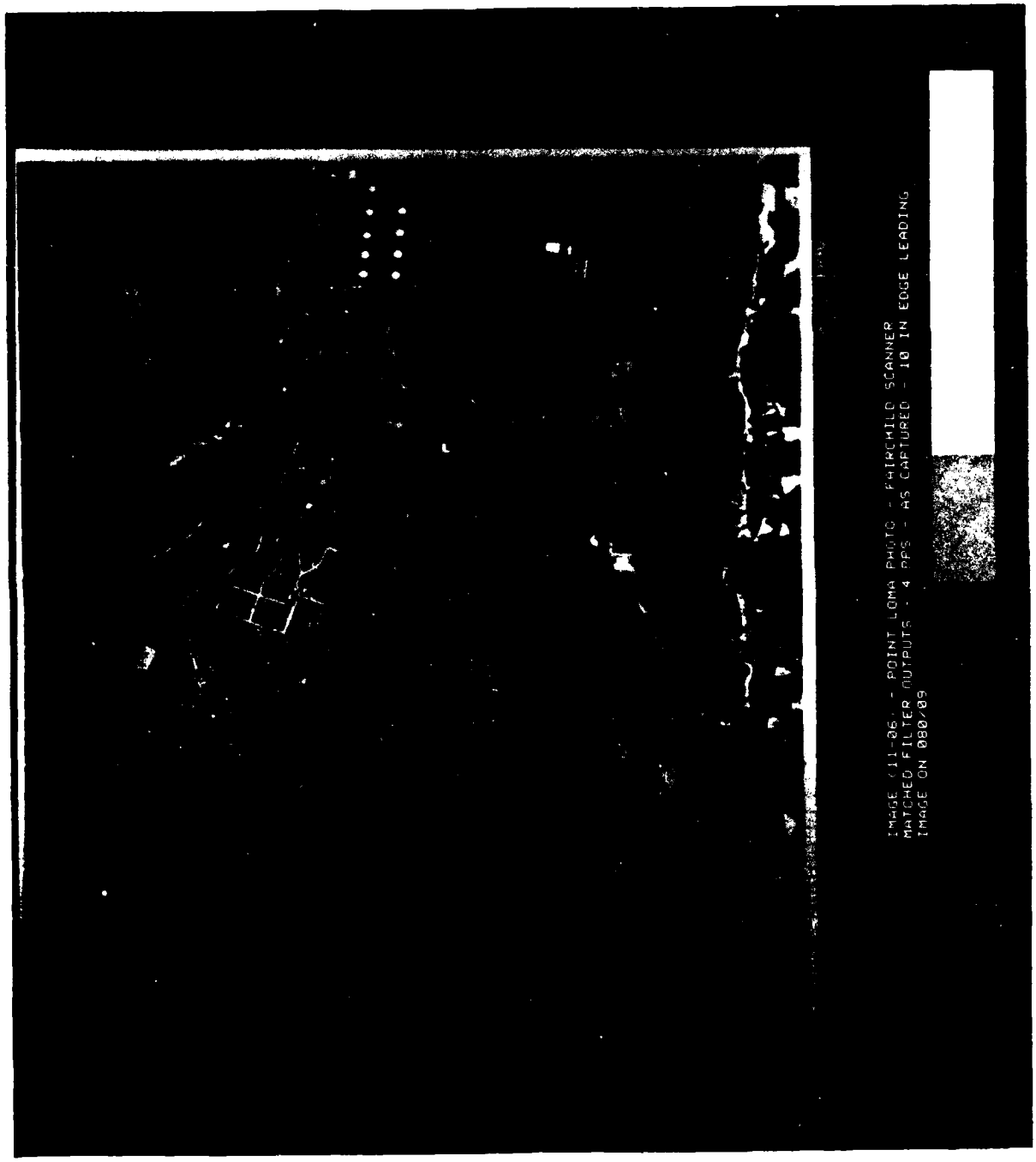

Figure D32. D-3.

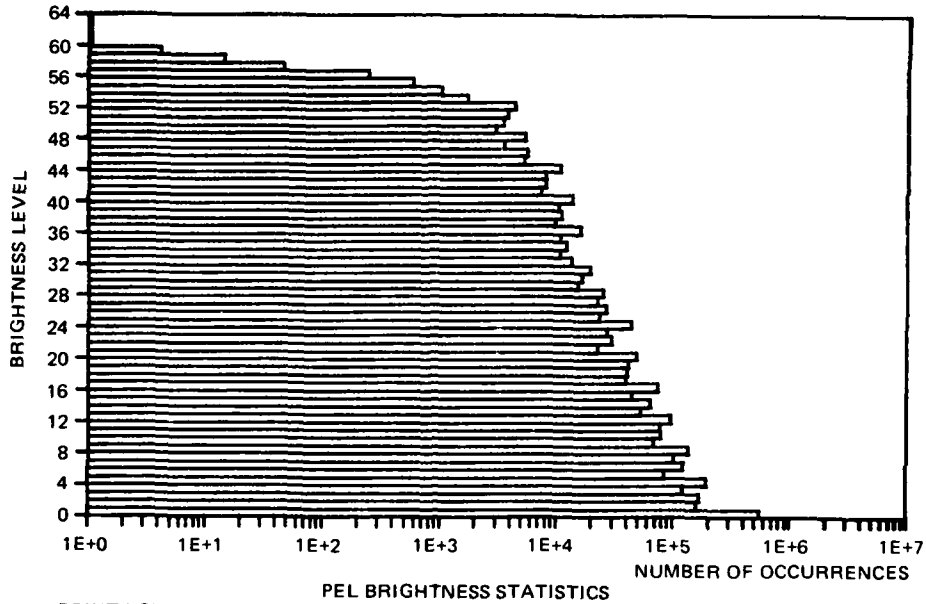

PEL BRIGHTNESS STATISTICS
POINT LOMA PHOTO – FAIRCHILD SCANNER – MATCHED FILTER OUTPUTS – 4 PPS
IMAGE (11-06) ON 080/09 – STATS ON 087/08

Figure D33. D-3.

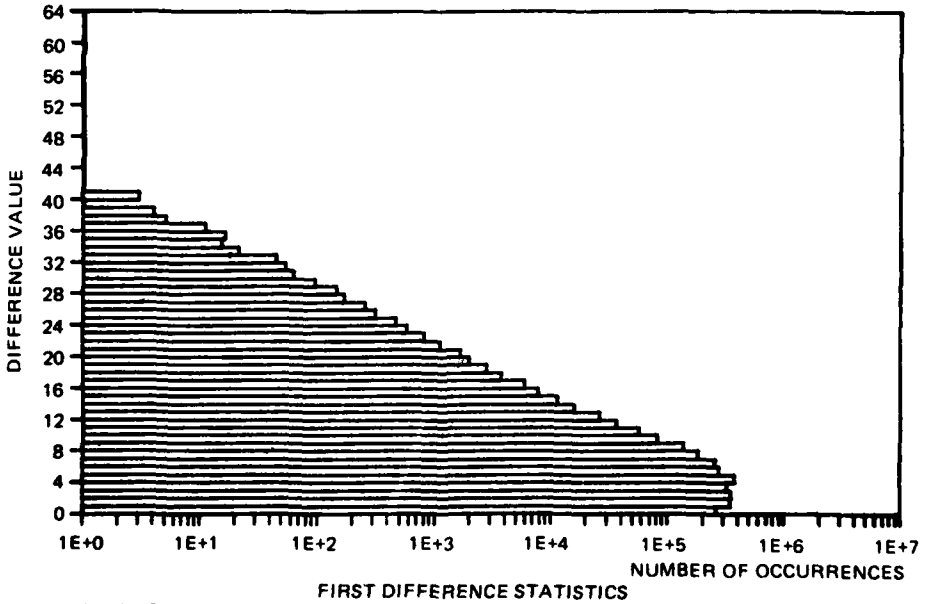

FIRST DIFFERENCE STATISTICS
POINT LOMA PHOTO – FAIRCHILD SCANNER – MATCHED FILTER OUTPUTS – 4 PPS
IMAGE (11-06) ON 080/09 – STATS ON 087/08

Figure D34. D-3.

Figure D35. A-4.

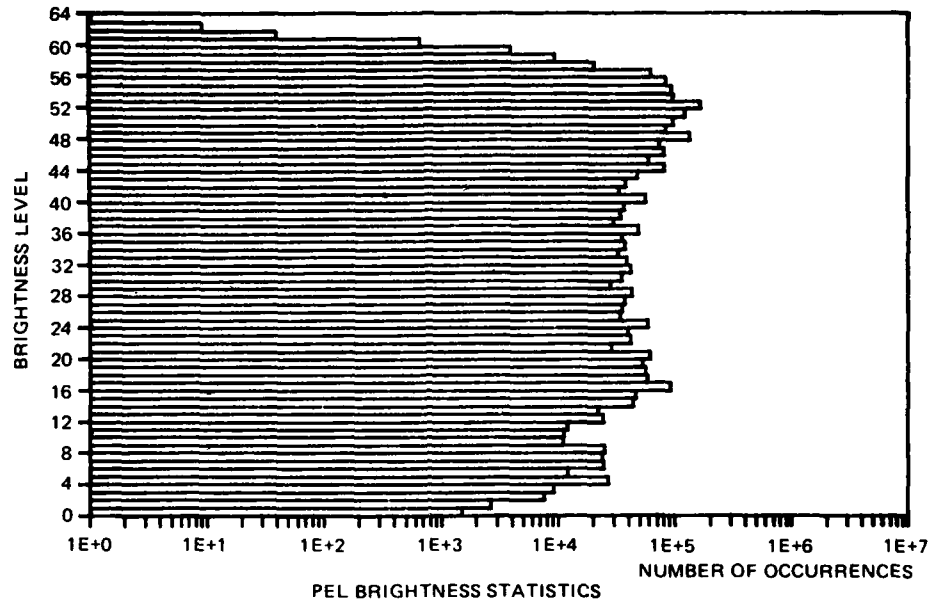

PEL BRIGHTNESS STATISTICS
IEEE FAX CHART – FAIRCHILD SCANNER – MUX'ED OUTPUTS – 8.77 PPS
IMAGE (31-01) ON 077/05 – STATS ON 077/16

Figure D36. A-4.

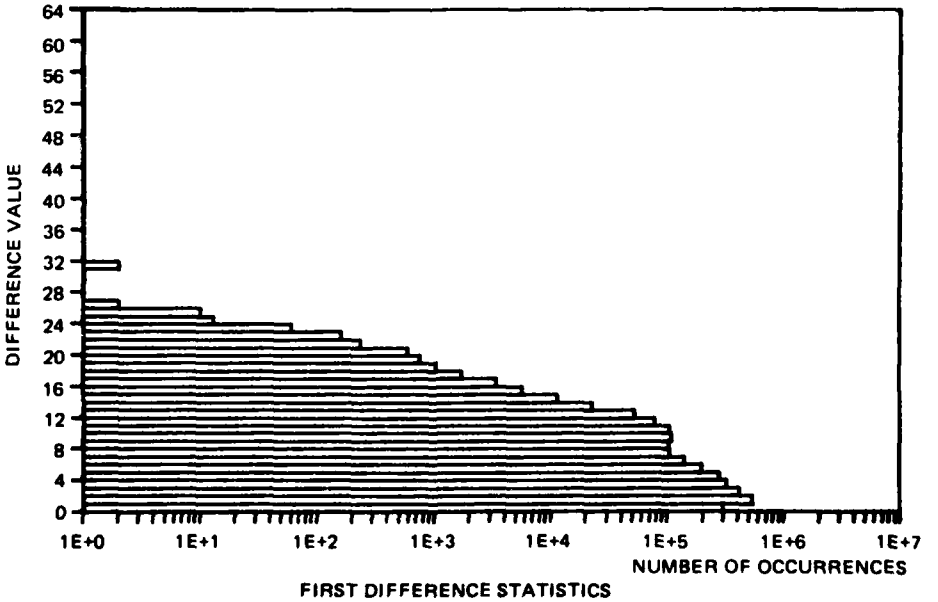

FIRST DIFFERENCE STATISTICS
IEEE FAX CHART – FAIRCHILD SCANNER – MUX'ED OUTPUTS – 8.77 PPS
IMAGE (31-01) ON 077/85 – STATS ON 077/16

Figure D37. A-4.

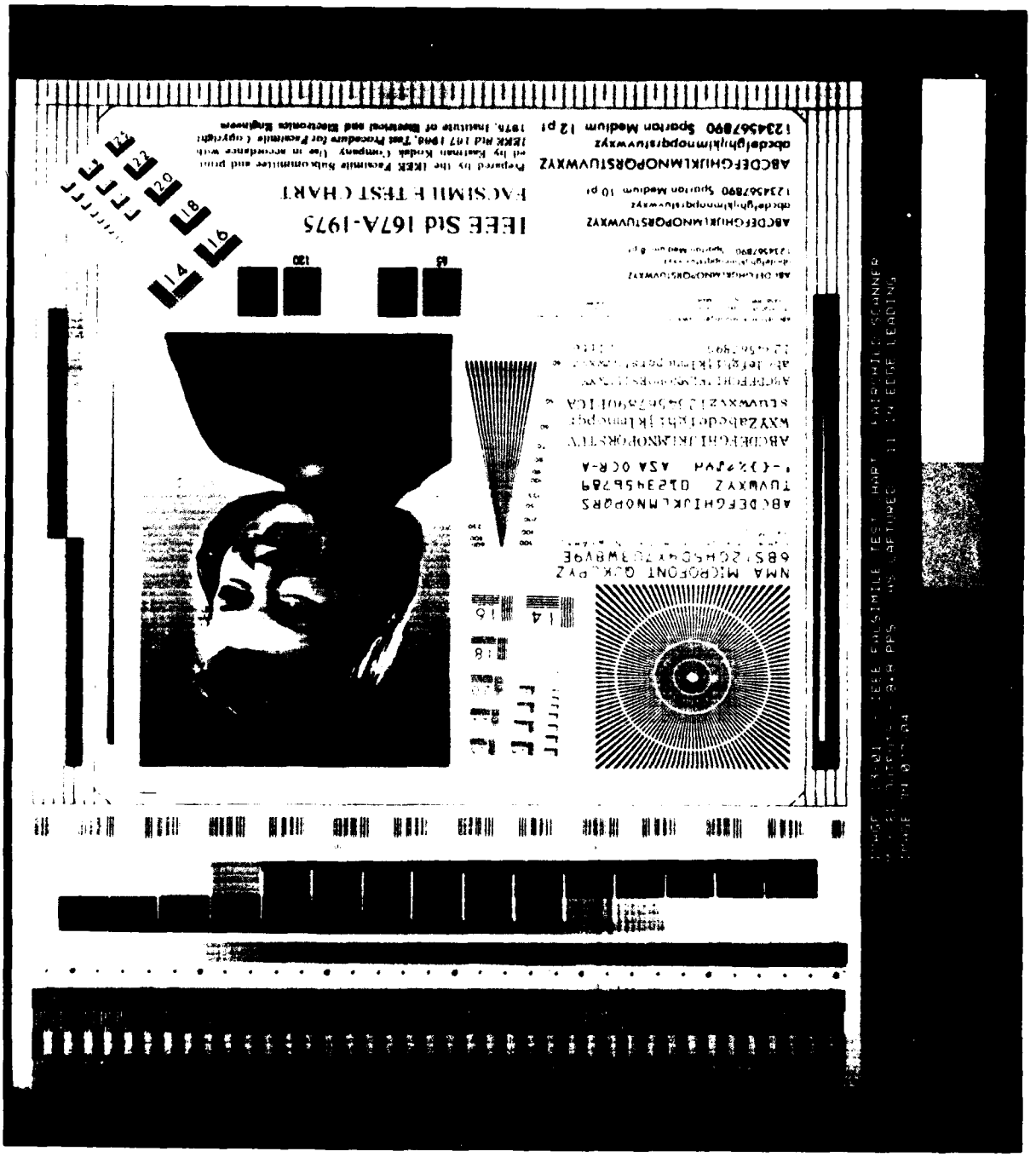

Figure D38. A-4.

Figure D41 is next, scanned at four pages per second. Following that image are two images of the typed page in figures D44 and D47. In comparing these images with the corresponding images from the matched filter outputs, it can be seen that the image quality is very nearly the same after the multiplexing circuitry in the scanner. The last of the multiplexed output images is figure D50, the continuous-tone photograph. A mismatch can be seen in the two halves of this image, the right side being at a higher level. This is most likely due to a loss of alignment in the ICAS gain and level amplifiers.

THRESHOLDED VIDEO

Since NOSC was requested to return half of the analog processing circuit boards to Fairchild midway through the characterization of the scanner, the thresholded images were acquired in the following manner. The channel 2 digital video output was input to the two ICAS inputs corresponding to the right half of image memory. Since scanner channel 2 is the left half of the image, this information appears as a mirror image in the resultant output. The inputs to the left half image in ICAS were from the multiplexed video output from the same channel in the scanner. In this way a direct comparison could be made between the thresholding algorithm as implemented in hardware and as implemented in software during a single scan of an image.

Figures D53 and D54 are of the typed page scanned in two directions. The scanner digitized output on the right exhibits a small amount of smearing on the far right edge of the image, while the NOSC thresholded version on the left contains a vertical black bar along the left edge of the image. These effects will be analyzed further in the following section.

Figure D55 is an example of a white-on-black page of information. Both halves of this image pair provide a good facsimile of the input document. However, the scanner hardware provides smoother character edges than the NOSC algorithm.

ILLUMINATION-CORRECTED VIDEO

The images presented in this section have been illumination-corrected using the illumination profiles shown earlier in this section. Figures D56 and D59 show the IEEE Facsimile Test Chart after illumination correction. These can be compared to figures D35 and D38 before correction. It can be seen that there is a reduced amount of clocking noise after the correction. Also, the PBS show that the average background reflectance is more uniform; ie, there is a more noticeable peaking in the statistics at the higher intensity levels.

Figure D62 is another example of the IEEE Facsimile Test Chart, this time scanned at four pages per second. The illumination curve shown in figure D6 was used for this correction. The NOSC algorithm for illumination correction uses a multiplication look-up table to generate the corrected pel outputs. In generating and using this look-up table, an assumption was made that the calibration values (ie, the values in the illumination curve) would never fall below 50% of full scale. This allows the size of this table to be cut in half in order to conserve memory. Now, examination of figure D6 reveals that this curve does fall below 50% at either end. This caused two bands on either side of figure D62 which were incorrectly computed. This problem will be seen in all subsequent photographs that have been illumination-corrected; ie, all the entries in figure D4, column 6, except figures D56 and D59.

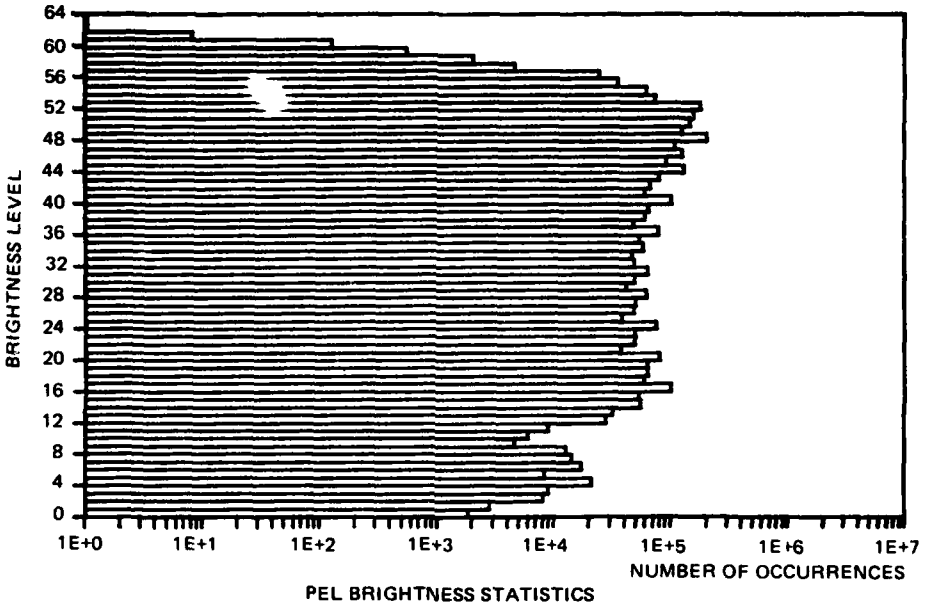

PEL BRIGHTNESS STATISTICS
IEEE FAX CHART – FAIRCHILD SCANNER – MUX'ED OUTPUTS – 8.77 PPS
IMAGE (31-01) ON 077/07 – STATS ON 077/15

Figure D39. A-4.

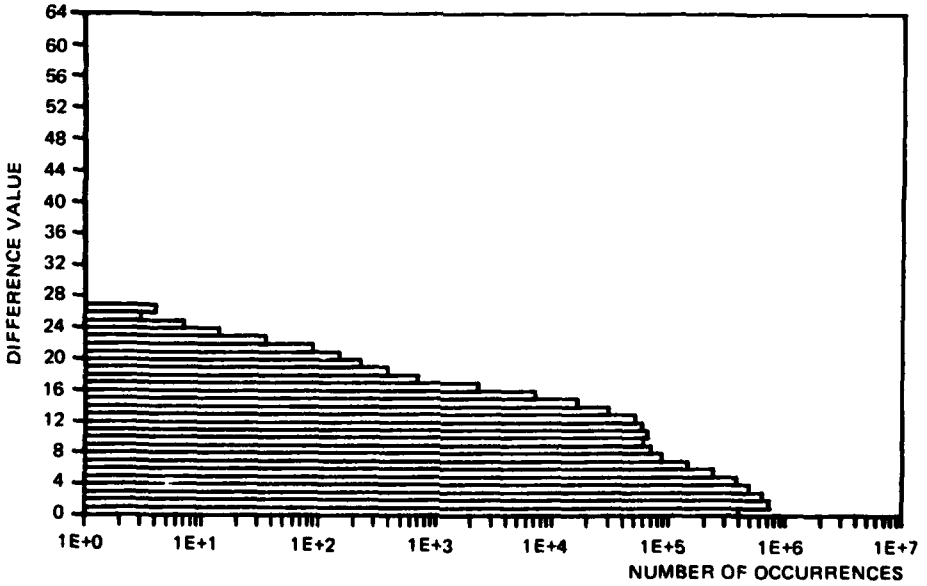

FIRST DIFFERENCE STATISTICS
IEEE FAX CHART – FAIRCHILD SCANNER – MUX'ED OUTPUTS – 8.77 PPS
IMAGE (31-01) ON 077/07 – STATS ON 077/15

Figure D40. A-4.

Figure D41. B-4.

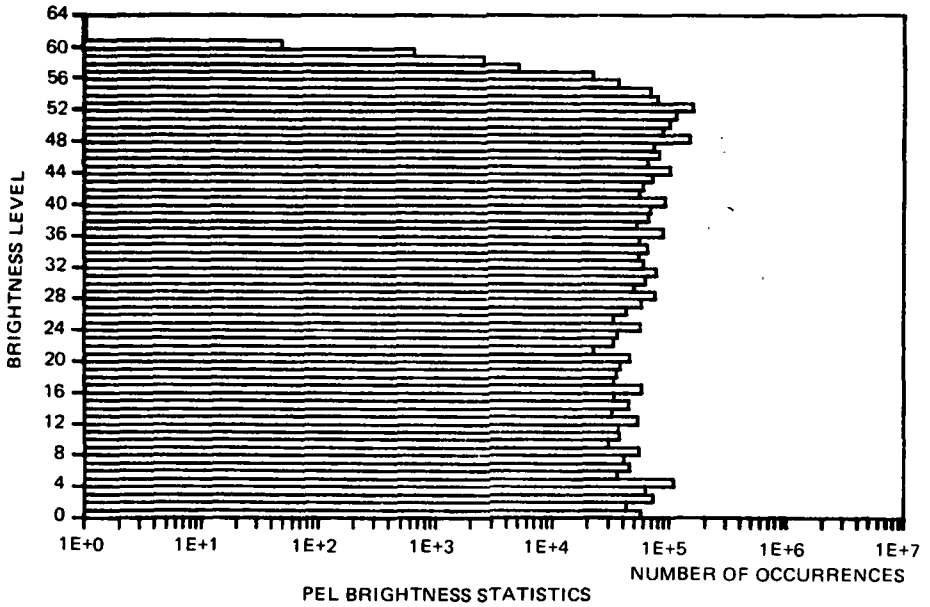

PEL BRIGHTNESS STATISTICS
IEEE FAX TEST CHART – FAIRCHILD SCANNER – MUX'ED OUTPUTS – 4 PPS
IMAGE (13-01) 11" LEADING – IMAGE ON 081/10 – STATS ON 087/14

Figure D42. B-4.

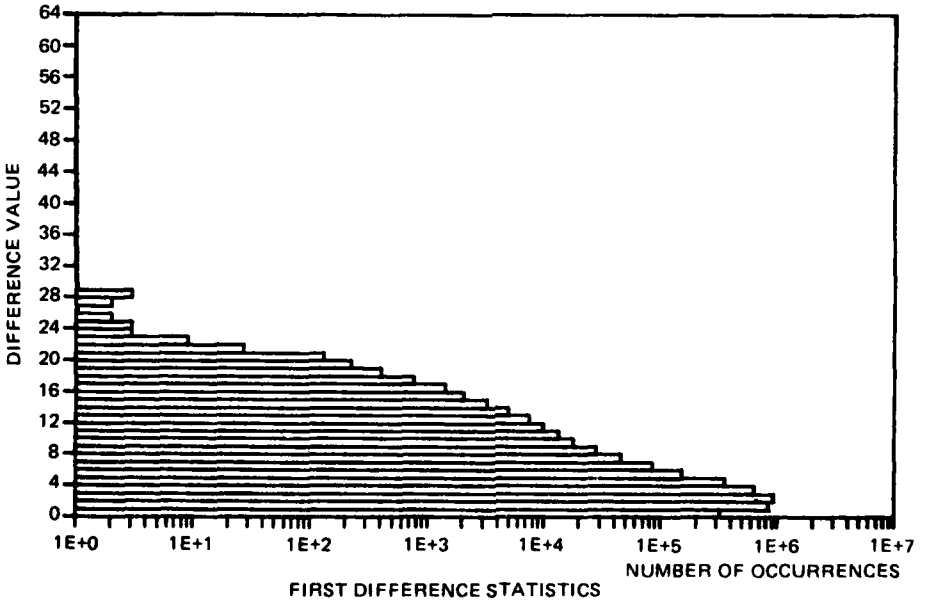

FIRST DIFFERENCE STATISTICS
IEEE FAX TEST CHART – FAIRCHILD SCANNER – MUX'ED OUTPUTS – 4 PPS
IMAGE (13-01) 11" LEADING – IMAGE ON 081/10 – STATS ON 087/14

Figure D43. B-4.

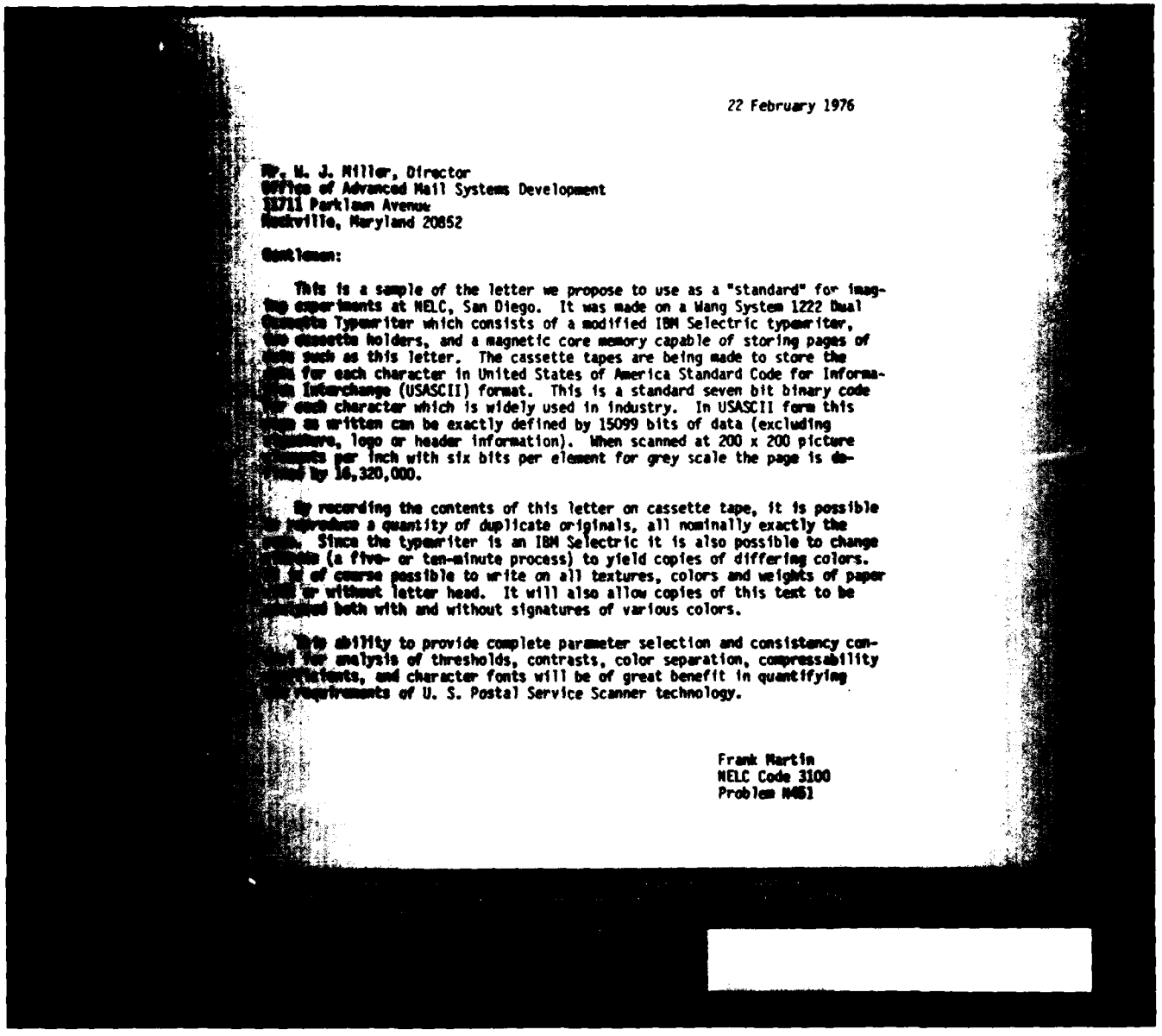

22 February 1976

Mr. W. J. Miller, Director
Office of Advanced Mail Systems Development
13711 Parklawn Avenue
Rockville, Maryland 20852

Gentlemen:

This is a sample of the letter we propose to use as a "standard" for imaging experiments at NELC, San Diego. It was made on a Wang System 1222 Dual Cassette Typewriter which consists of a modified IBM Selectric typewriter, two cassette holders, and a magnetic core memory capable of storing pages of data such as this letter. The cassette tapes are being made to store the data for each character in United States of America Standard Code for Information Interchange (USASCII) format. This is a standard seven bit binary code for each character which is widely used in industry. In USASCII form this page as written can be exactly defined by 15099 bits of data (excluding signature, logo or header information). When scanned at 200 x 200 picture elements per inch with six bits per element for grey scale the page is defined by 16,320,000.

By recording the contents of this letter on cassette tape, it is possible to reproduce a quantity of duplicate originals, all nominally exactly the same. Since the typewriter is an IBM Selectric it is also possible to change typefaces (a five- or ten-minute process) to yield copies of differing colors. It is of course possible to write on all textures, colors and weights of paper with or without letter head. It will also allow copies of this text to be reproduced both with and without signatures of various colors.

The ability to provide complete parameter selection and consistency control for analysis of thresholds, contrasts, color separation, compressability requirements, and character fonts will be of great benefit in quantifying the requirements of U. S. Postal Service Scanner technology.

Frank Martin
NELC Code 3100
Problem N481

Figure D44. C-4.

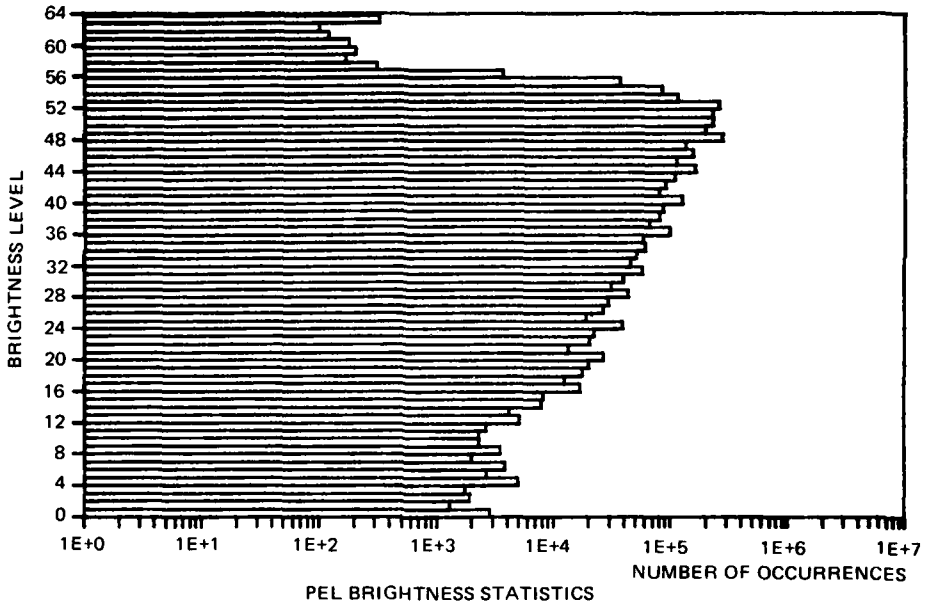

PEL BRIGHTNESS STATISTICS
WJM TYPED PAGE – FAIRCHILD SCANNER – MUX'ED OUTPUTS – 4 PPS
IMAGE (8 1/2 X 8 1/2 – TOP EDGE LEADING) ON 081/06 – STATS ON 087/12

Figure D45. C-4.

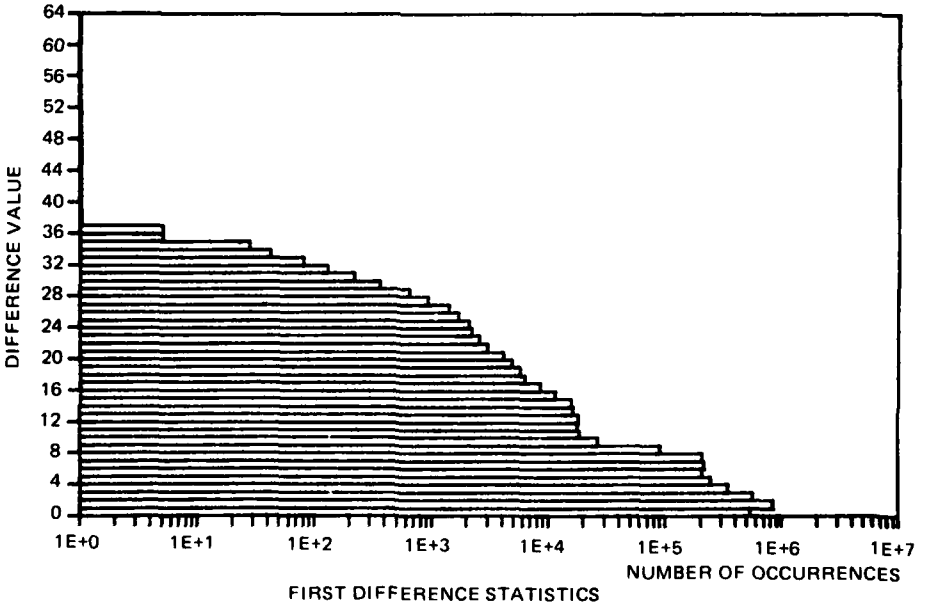

FIRST DIFFERENCE STATISTICS
WJM TYPED PAGE – FAIRCHILD SCANNER – MUX'ED OUTPUTS – 4 PPS
IMAGE (8 1/2 X 8 1/2 – TOP EDGE LEADING) ON 081/06 – STATS ON 087/12

Figure D46. C-4.

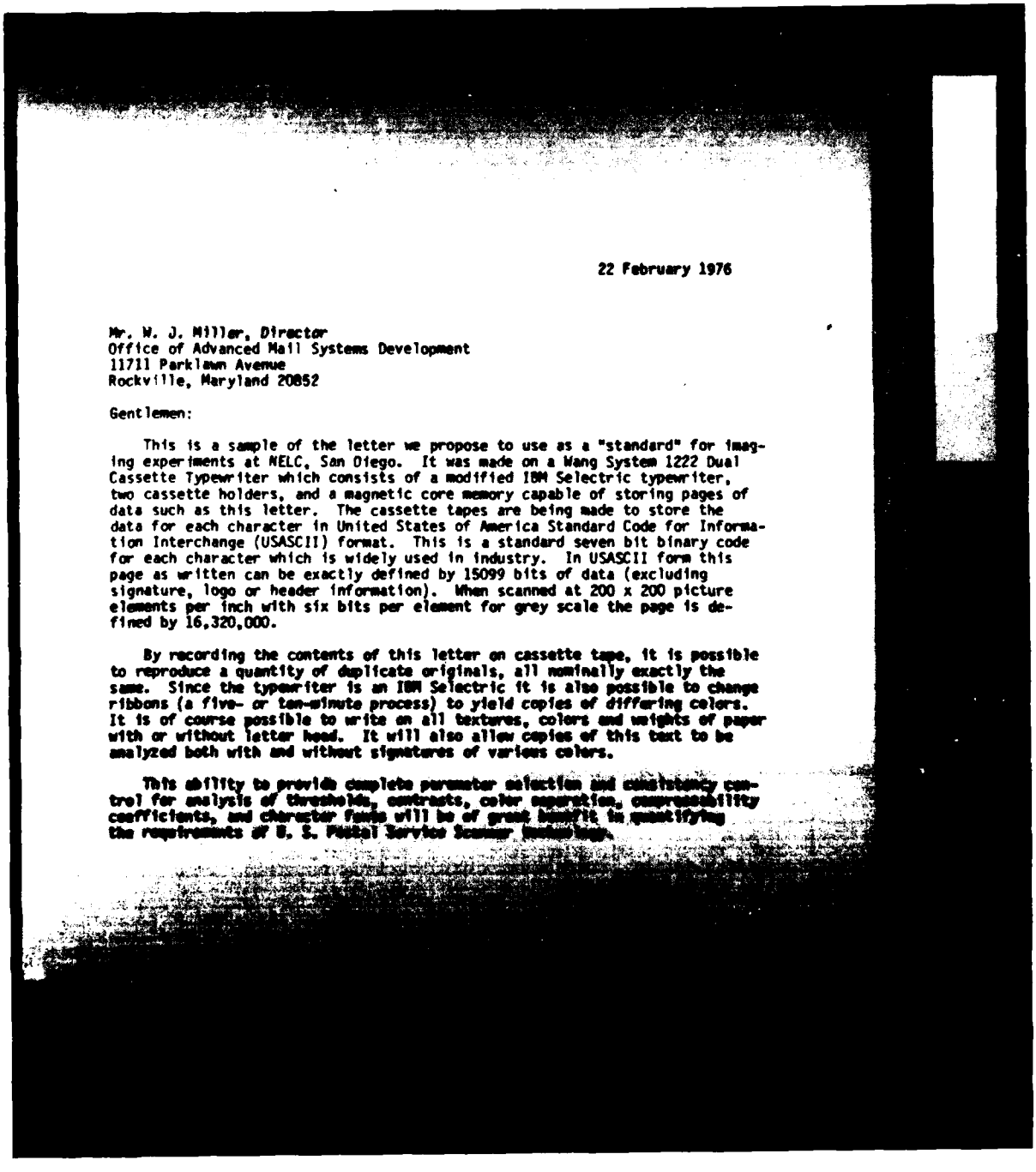

22 February 1976

Mr. W. J. Miller, Director
Office of Advanced Mail Systems Development
11711 Parklawn Avenue
Rockville, Maryland 20852

Gentlemen:

This is a sample of the letter we propose to use as a "standard" for imaging experiments at NELC, San Diego. It was made on a Wang System 1222 Dual Cassette Typewriter which consists of a modified IBM Selectric typewriter, two cassette holders, and a magnetic core memory capable of storing pages of data such as this letter. The cassette tapes are being made to store the data for each character in United States of America Standard Code for Information Interchange (USASCII) format. This is a standard seven bit binary code for each character which is widely used in industry. In USASCII form this page as written can be exactly defined by 15099 bits of data (excluding signature, logo or header information). When scanned at 200 x 200 picture elements per inch with six bits per element for grey scale the page is defined by 16,320,000.

By recording the contents of this letter on cassette tape, it is possible to reproduce a quantity of duplicate originals, all nominally exactly the same. Since the typewriter is an IBM Selectric it is also possible to change ribbons (a five- or ten-minute process) to yield copies of differing colors. It is of course possible to write on all textures, colors and weights of paper with or without letter head. It will also allow copies of this text to be analyzed both with and without signatures of various colors.

This ability to provide complete parameter selection and consistency control for analysis of thresholds, contrasts, color separation, compressability coefficients, and character fonts will be of great benefit in quantifying the requirements of U. S. Postal Service Scanner technology.

Figure D47. C-4.

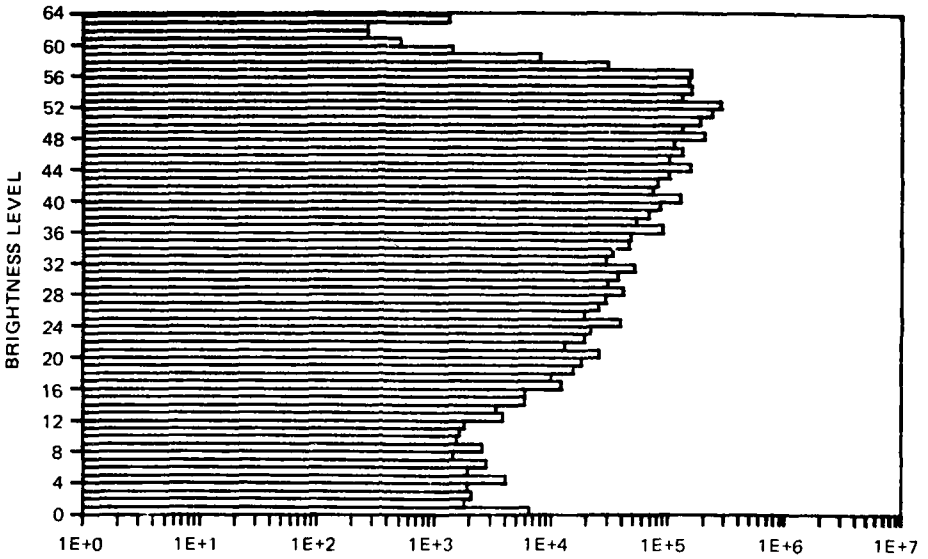

PEL BRIGHTNESS STATISTICS
WJM TYPED PAGE – FAIRCHILD SCANNER – MUX'ED OUTPUTS – 4 PPS
IMAGE (8 1/2 x 8 1/2 – LEFT EDGE LEADING) ON 081/07 – STATUS ON 087/13

Figure D48. C-4.

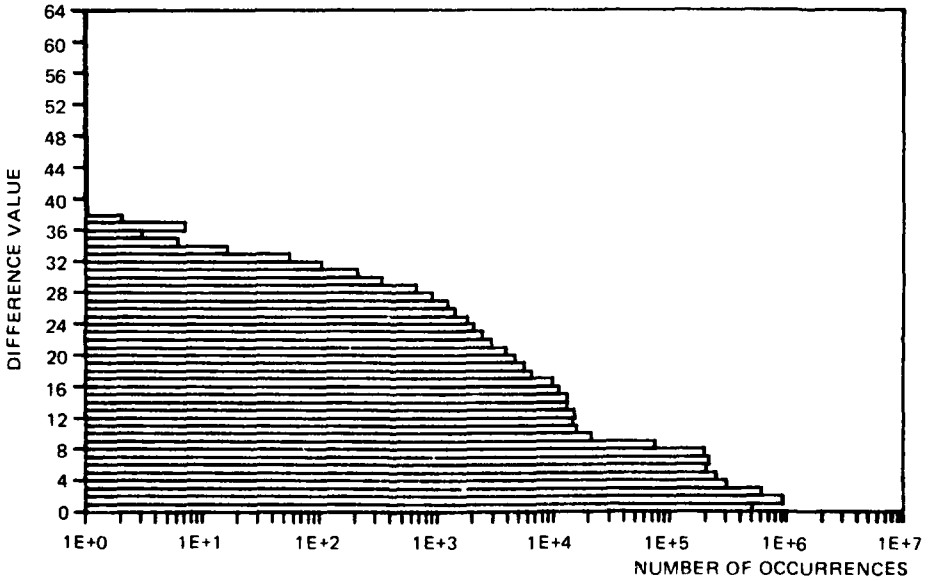

FIRST DIFFERENCE STATISTICS
WJM TYPED PAGE FAIRCHILD SCANNER – MUX'ED OUTPUTS – 4 PPS
IMAGE (8 1/2 x 8 1/2 – LEFT EDGE LEADING) ON 081/07 – STATS ON 087/13

Figure D49. C-4.

AD-A089 436 NAVAL OCEAN SYSTEMS CENTER SAN DIEGO CA F/G 9/5
ADVANCED MAIL SYSTEMS SCANNER TECHNOLOGY, EXECUTIVE SUMMARY AND--ETC(U)
OCT 79 F C MARTIN, T R LITTLE, L A WISE
UNCLASSIFIED NOSC/TR-520 NL

3 OF 3

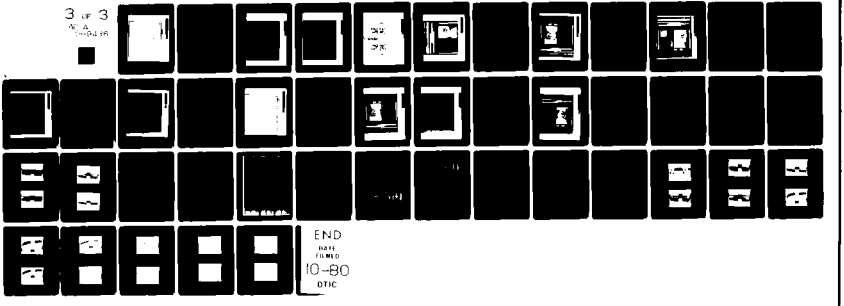

END
DATE FILMED
10-80
DTIC

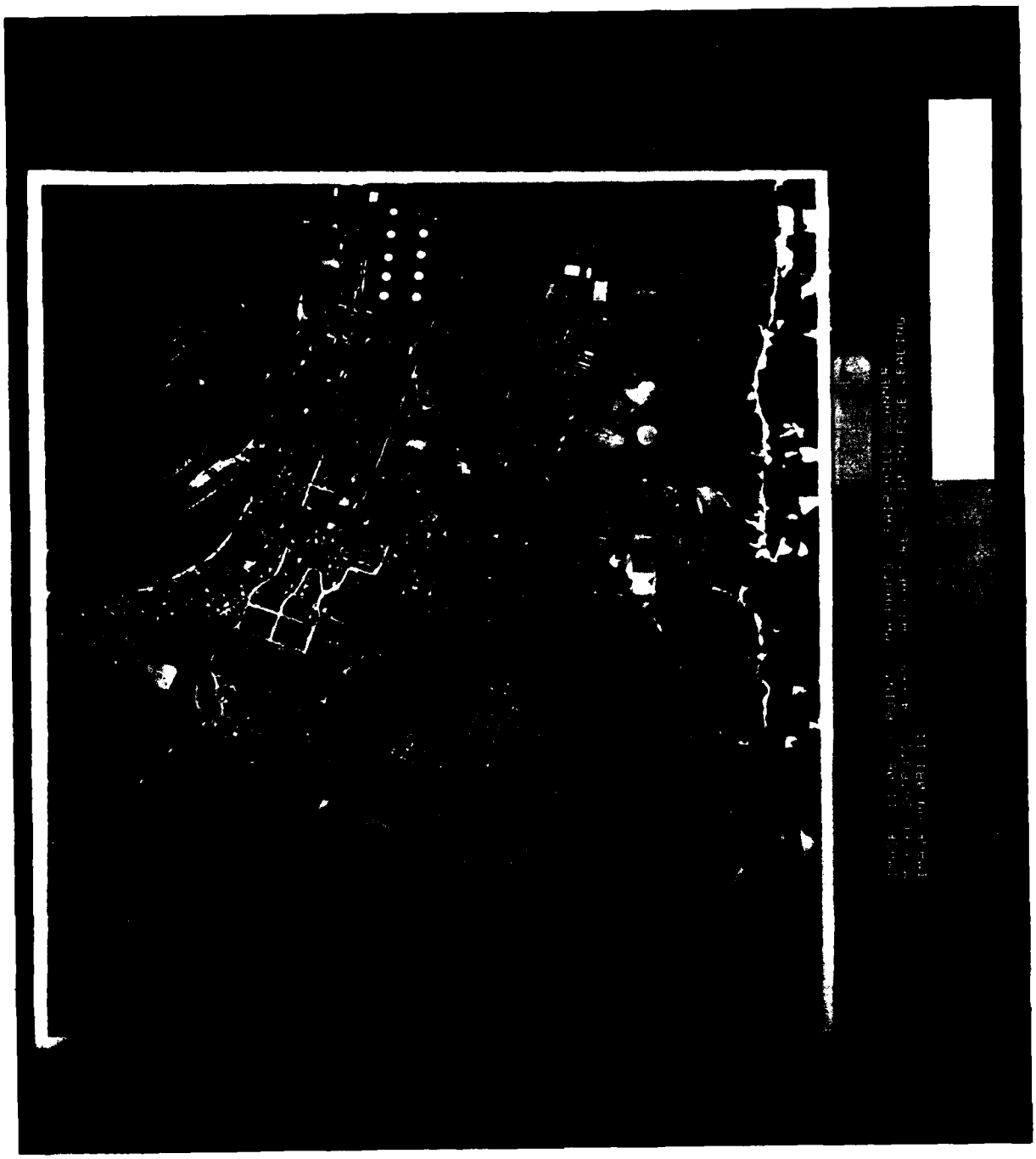

Figure D50. D-4.

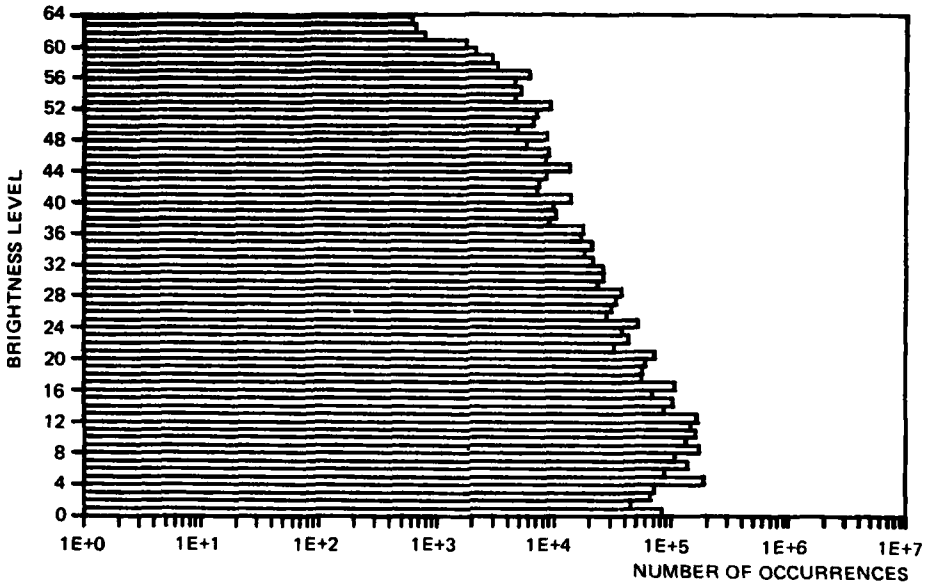

PEL BRIGHTNESS STATISTICS
PT. LOMA PHOTO – FAIRCHILD SCANNER – MUX'ED OUTPUTS – 4 PPS
IMAGE (11-06) ON 081/11 – STATS ON 087/15

Figure D51. D-4.

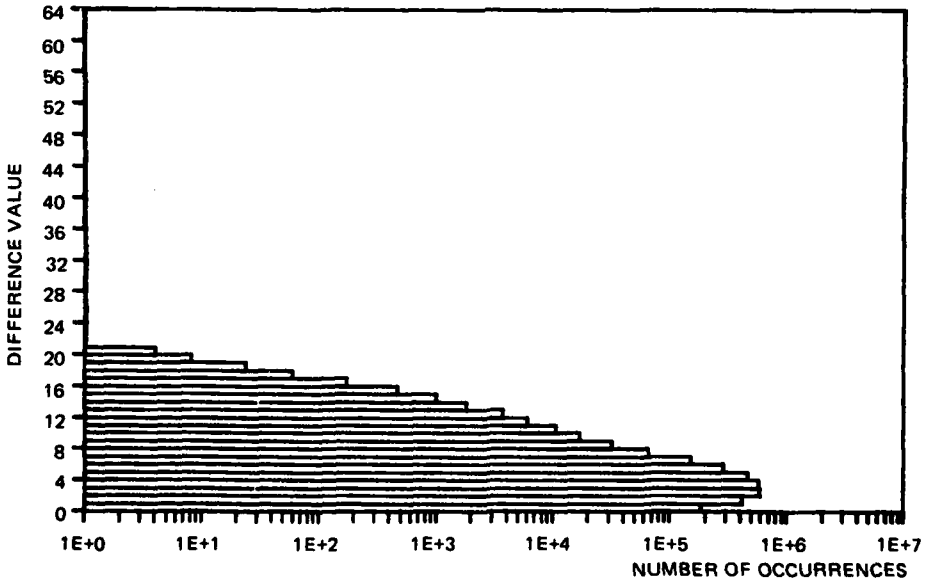

FIRST DIFFERENCE STATISTICS
PT. LOMA PHOTO – FAIRCHILD SCANNER – MUX'ED OUTPUTS – 4 PPS
IMAGE (11-06) ON 081/11 – STATS ON 087/15

Figure D52. D-4.

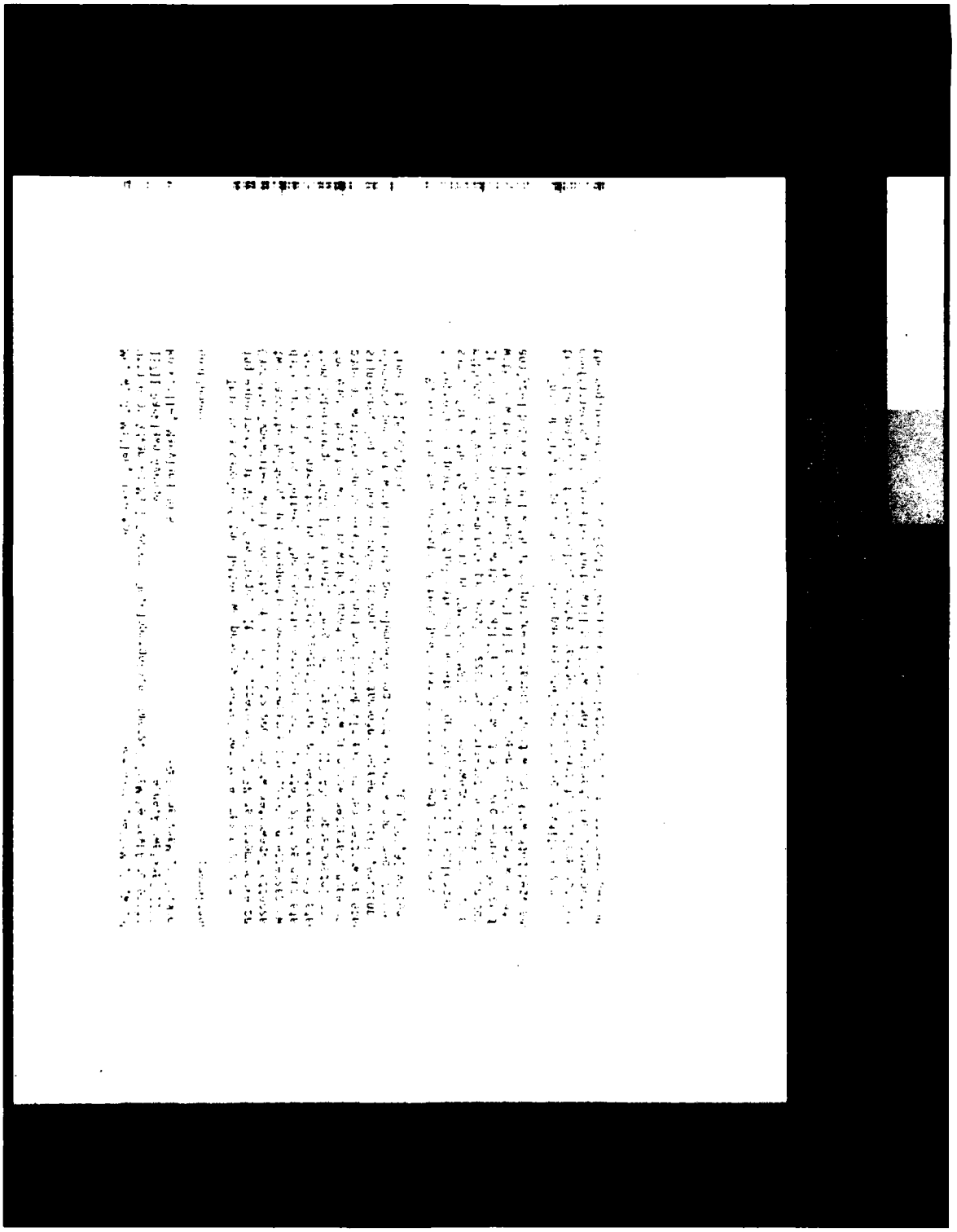

Figure D53. C-5.

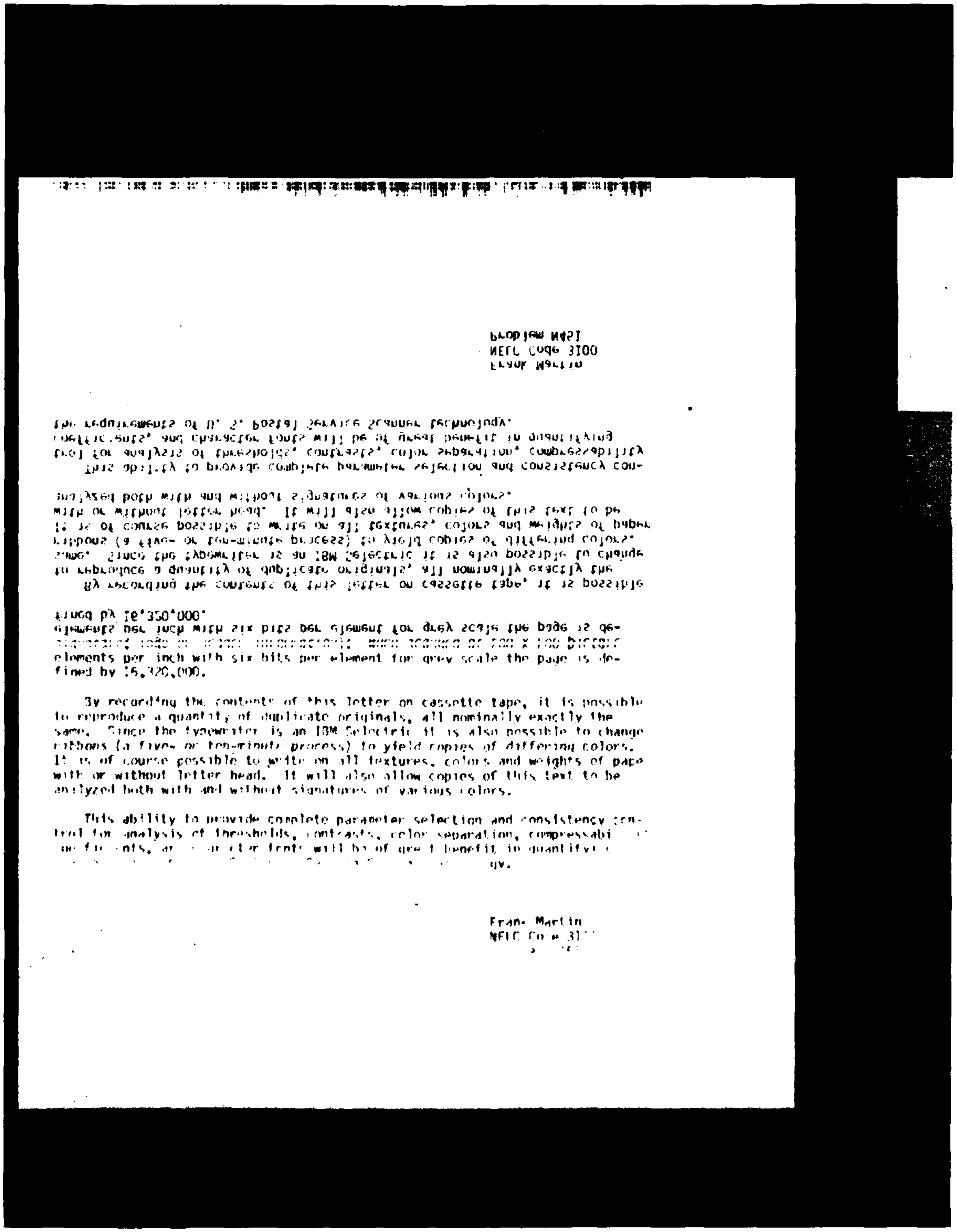

elements per inch with six bits per element for grey scale the page is defined by 16,320,000.

By recording the contents of this letter on cassette tape, it is possible to reproduce a quantity of duplicate originals, all nominally exactly the same. Since the typewriter is an IBM Selectric it is also possible to change ribbons (a five- or ten-minute process) to yield copies of differing colors. It is of course possible to write on all textures, colors and weights of pape with or without letter head. It will also allow copies of this text to be analyzed both with and without signatures of various colors.

This ability to provide complete parameter selection and consistency control for analysis of thresholds, contrasts, color separation, compressabi [illegible] [illegible] will be of great benefit in quantify [illegible] gy.

Frank Martin
NELC Code 31[illegible]

Figure D54. C-5.

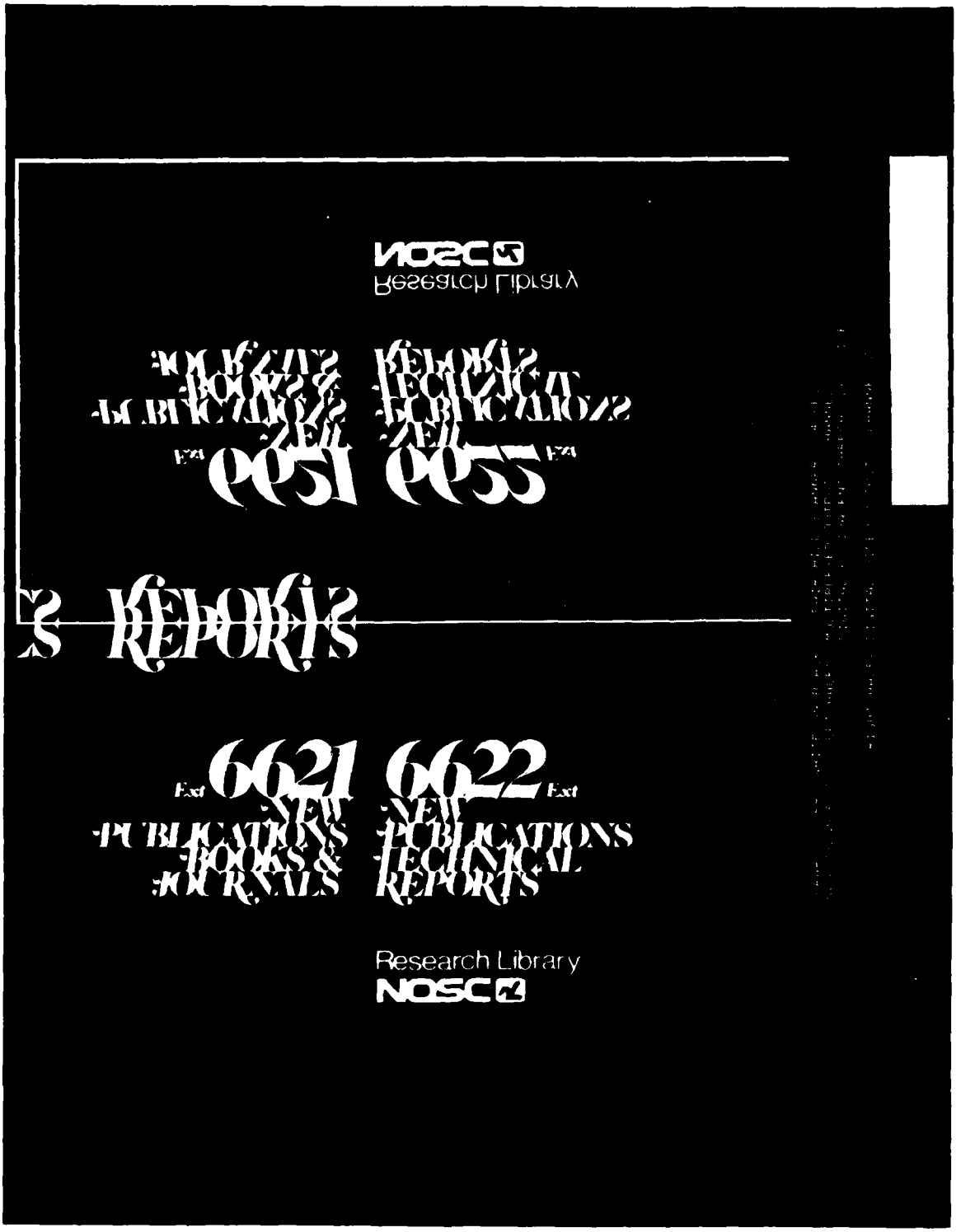

Figure D55. E-5.

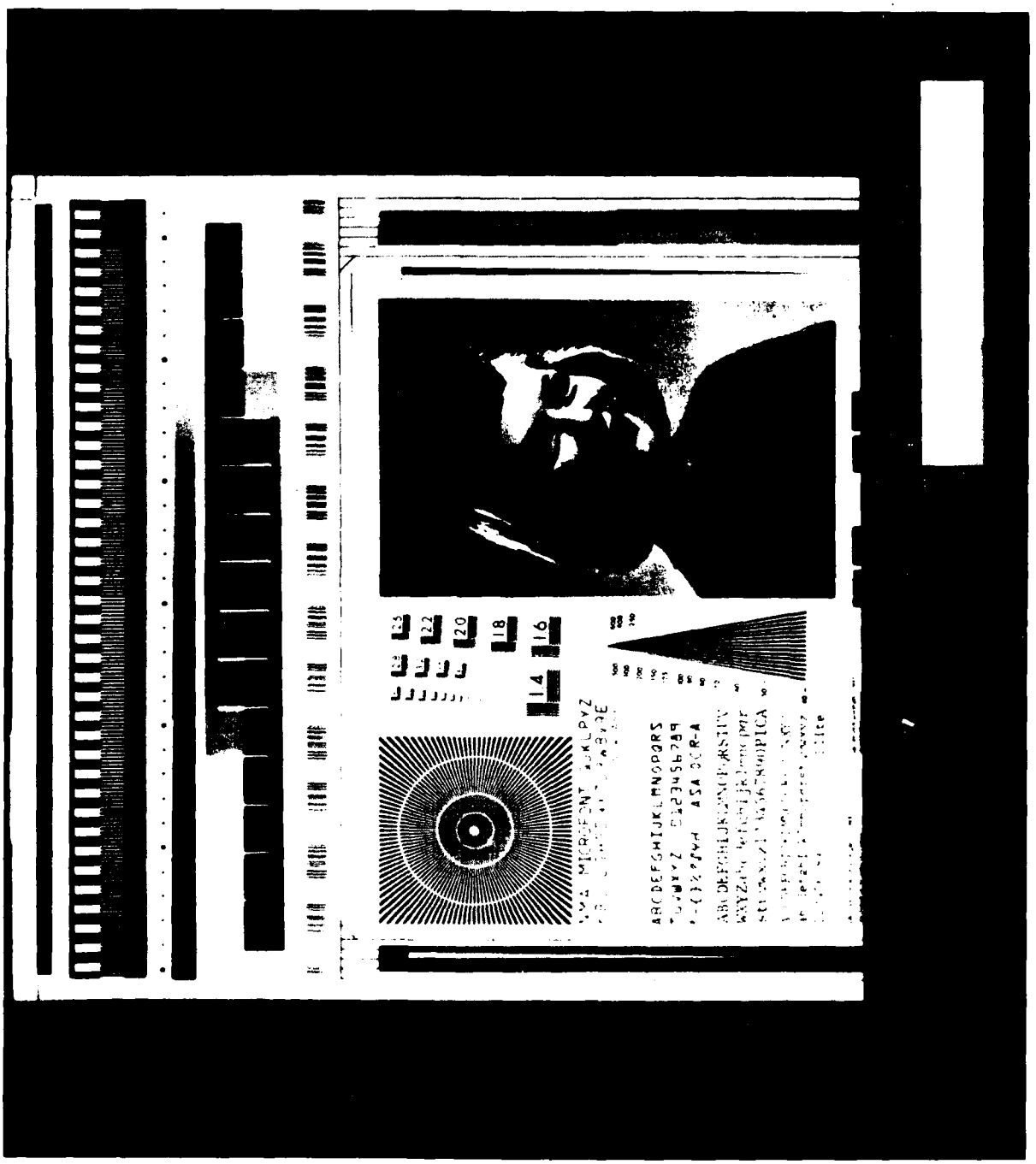

Figure D56. A-6.

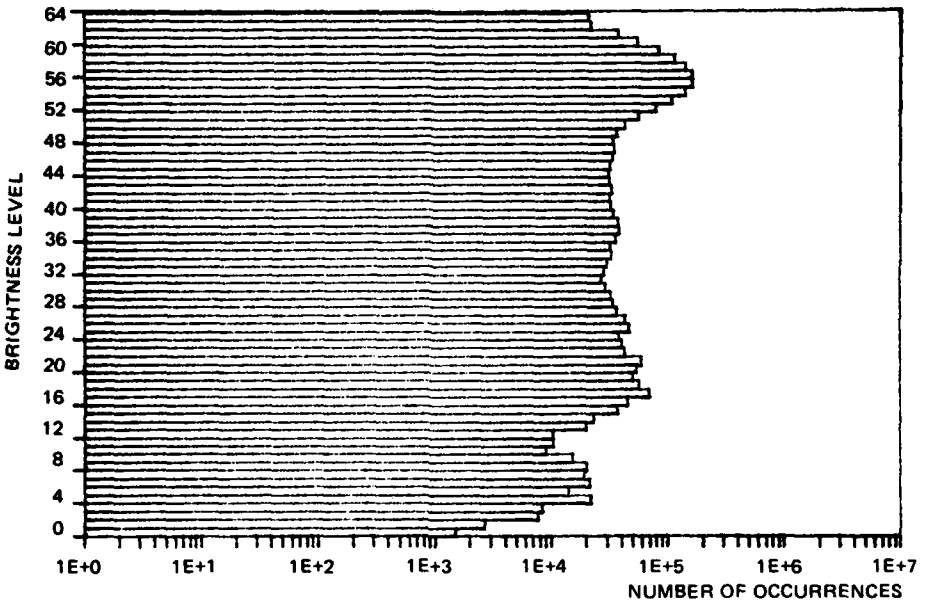

PEL BRIGHTNESS STATISTICS
IEEE FAX CHART – FAIRCHILD SCANNER – MUX'ED OUTPUTS – CORRECTED – 8.77 PPS
IMAGE (13-01) ON 077/06 – STATS ON 077/12

Figure D57. A-6.

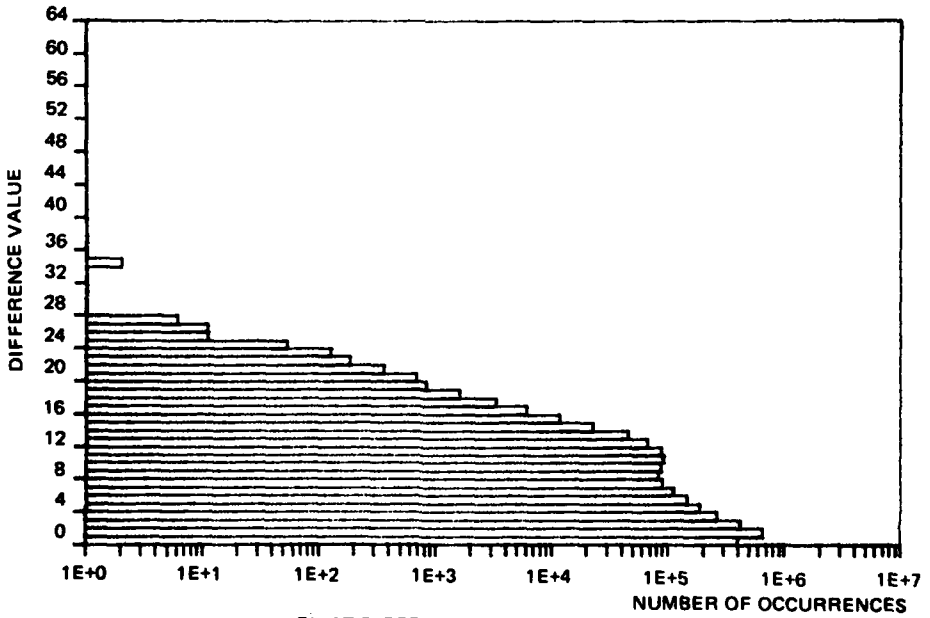

FIRST DIFFERENCE STATISTICS
IEEE FAX CHART – FAIRCHILD SCANNER – MUX'ED OUTPUTS – CORRECTED – 8.77 PPS
IMAGE (13-01) ON 077/06 – STATS ON 077/12

Figure D58. A-6.

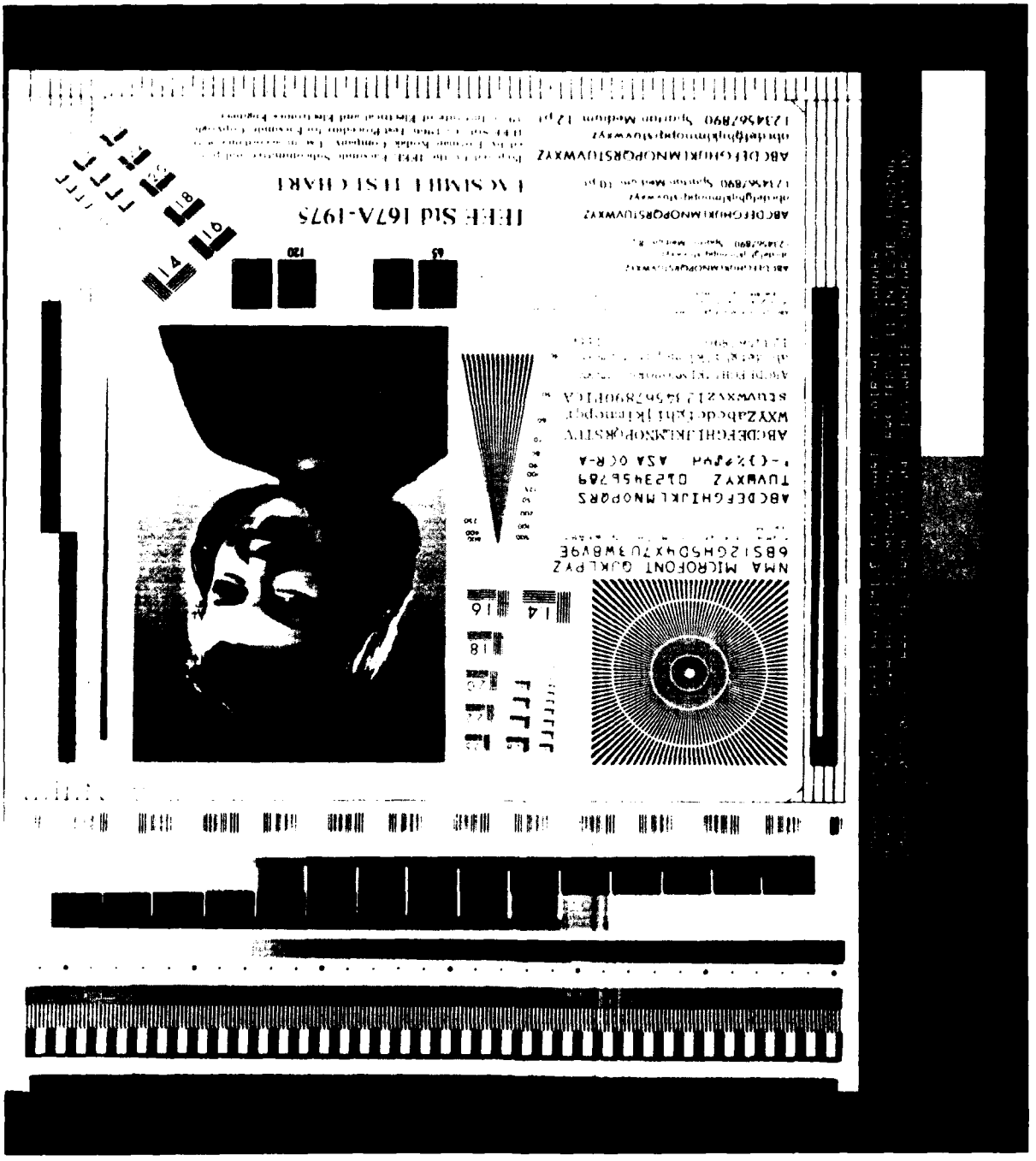

Figure D59. A-6.

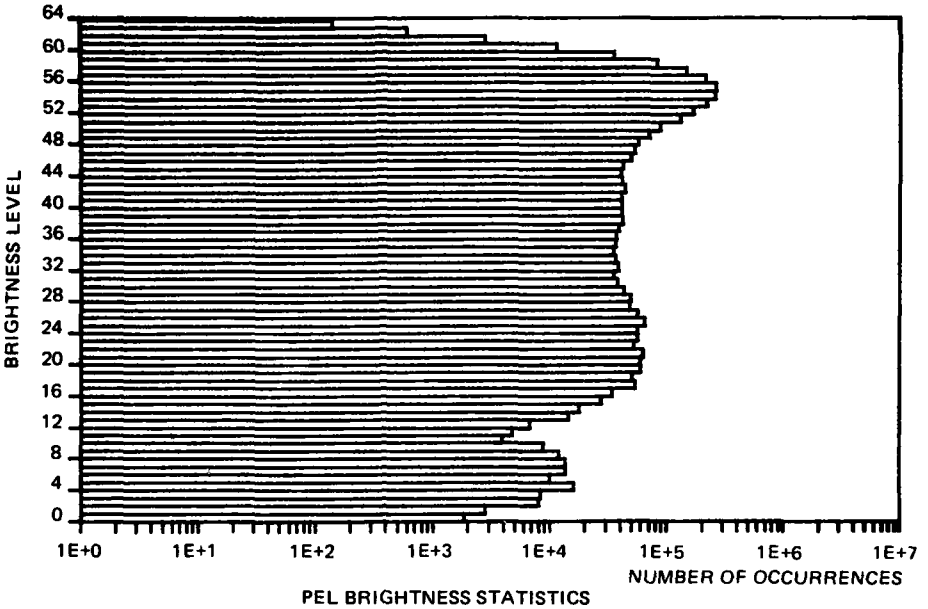

PEL BRIGHTNESS STATISTICS
IEEE FAX CHART – FAIRCHILD SCANNER – MUX'ED OUTPUTS – CORRECTED – 8.77 PPS
IMAGE (31-01) ON 077/08 – STATS ON 077/09

Figure D60. A-6.

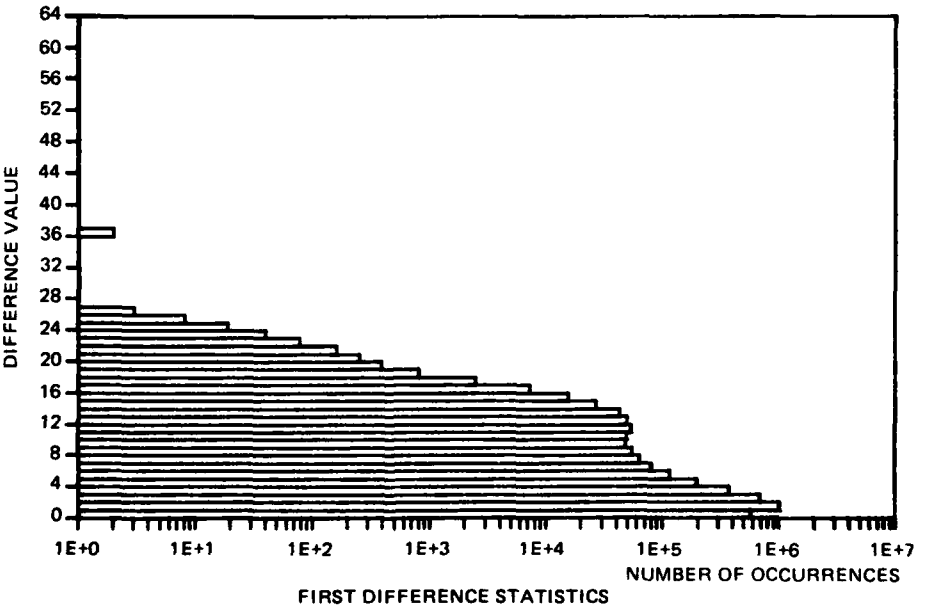

FIRST DIFFERENCE STATISTICS
IEEE FAX CHART – FAIRCHILD SCANNER – MUX'ED OUTPUTS – CORRECTED – 8.77 PPS
IMAGE (31-01) ON 077/08 – STATS ON 077/09

Figure D61. A-6.

Figure D62. B-6.

Figures D65 and D68 are of the typed page scanned in two directions after illumination correction. When these images and their respective PBS are compared to the uncorrected images and their PBS, a striking improvement can be noticed. The uniformity of the paper background in the image, except for the correction errors, is greatly improved. The PBS reflect this improvement in a narrowing of the peak in the curve around level 54.

The continuous-tone photograph after illumination correction is shown in figure D71 along with its PBS and FDS in figures D72 and D73.

DIGITAL EQUIVALENT THRESHOLDED VIDEO

Two representative images were chosen to demonstrate the NOSC thresholding algorithms as applied to the entire image. The images chosen were those in figures D35 and D44. The resultant thresholded images are shown in figures D74 and D75.

The actual application of the algorithm to these two images is different from the hardware implementation in the scanner. The scanner, which uses two imaging devices, has two completely independent processing channels, each of which operates on half the image. The two channels each scan or process image data from the edge of the page toward the center. This means that, during thresholding, reference voltage level is carried from the end of one line in the center of the page to the beginning of the next line at the edge of the page. Due to the drop in system response at the edge of the page, the background level at the edge of the page is sometimes lower than the threshold level, causing background levels to be interpreted as information.

In the two examples in figures D74 and D75, the software algorithm was applied to the image as a single entity. That is, the thresholding was performed clear across each line, not just half way. Ideally, if the system response were symmetrical about the centerline, there would not be the problem of mismatch in carrying a threshold level from the end of one line to the beginning of the next. However, as can readily be seen in figure D75, such is not the case. There are still many image lines in which the last time the threshold level is updated occurs in the middle of a line. Then, at the end of that line and at the beginning of the next, the background level falls below the threshold level, causing the smearing at the edges of the image. This points to a need to flatten the system response.

CHARACTERIZATION

FOUR-CHANNEL OPERATION

The interface of the Fairchild Scanner Subsystem to the NOSC ICAS provided the first opportunity to test the four-channel operation of ICAS. The ICAS was designed to accommodate an effective 20-page-per-second input rate. The digital processing portions, including the personality chassis, the memory interface unit, and the frame-store memory, all operated satisfactorily at up to about half the design speed, 8.8 pages per second. The ICAS gain and level amplifiers presented a considerable amount of difficulty in operating four channels simultaneously. It was not possible to maintain stabilized alignment of the four amplifiers so that they tracked one another for any reasonable length of time. This problem requires further investigation at NOSC.

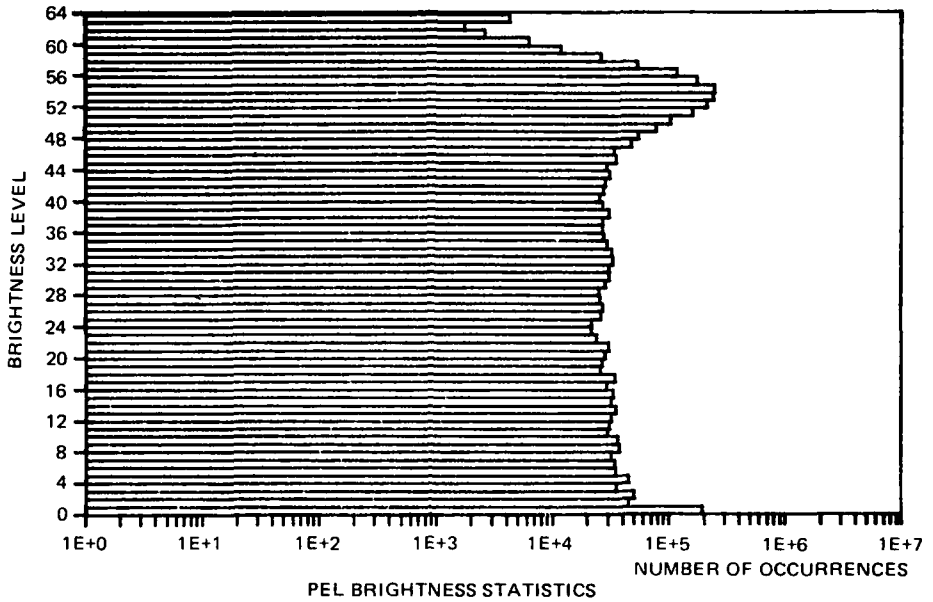

PEL BRIGHTNESS STATISTICS
IEEE FAX CHART – FAIRCHILD – MATCHED FILTER – ILLUM. CORRECTED – 4 PPS
IMAGE (13-01 11 IN EDGE LEADING) ON 082/33 – STATS ON 087/19

Figure D63. B-6.

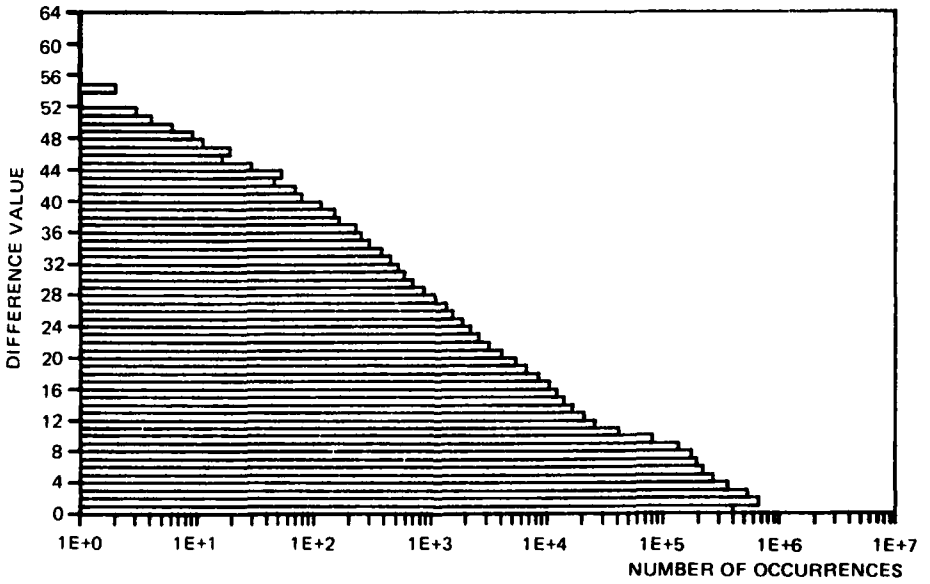

FIRST DIFFERENCE STATISTICS
IEEE FAX CHART – FAIRCHILD – MATCHED FILTER – ILLUM. CORRECTED – 4 PPS
IMAGE (13-01 11 IN EDGE LEADING) ON 082/33 – STATS ON 087/19

Figure D64. B-6.

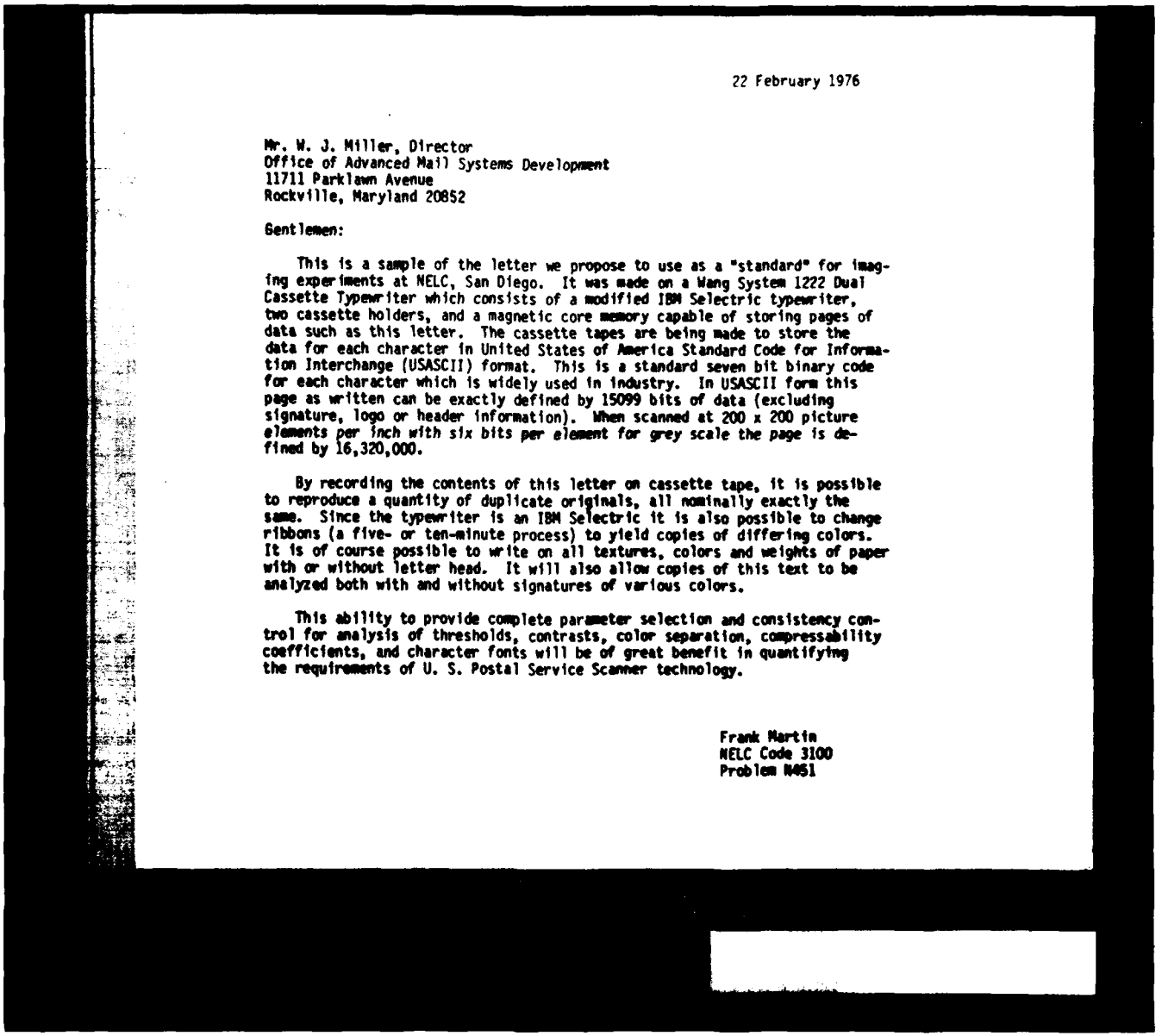

22 February 1976

Mr. W. J. Miller, Director
Office of Advanced Mail Systems Development
11711 Parklawn Avenue
Rockville, Maryland 20852

Gentlemen:

This is a sample of the letter we propose to use as a "standard" for imaging experiments at NELC, San Diego. It was made on a Wang System 1222 Dual Cassette Typewriter which consists of a modified IBM Selectric typewriter, two cassette holders, and a magnetic core memory capable of storing pages of data such as this letter. The cassette tapes are being made to store the data for each character in United States of America Standard Code for Information Interchange (USASCII) format. This is a standard seven bit binary code for each character which is widely used in industry. In USASCII form this page as written can be exactly defined by 15099 bits of data (excluding signature, logo or header information). When scanned at 200 x 200 picture elements per inch with six bits per element for grey scale the page is defined by 16,320,000.

By recording the contents of this letter on cassette tape, it is possible to reproduce a quantity of duplicate originals, all nominally exactly the same. Since the typewriter is an IBM Selectric it is also possible to change ribbons (a five- or ten-minute process) to yield copies of differing colors. It is of course possible to write on all textures, colors and weights of paper with or without letter head. It will also allow copies of this text to be analyzed both with and without signatures of various colors.

This ability to provide complete parameter selection and consistency control for analysis of thresholds, contrasts, color separation, compressability coefficients, and character fonts will be of great benefit in quantifying the requirements of U. S. Postal Service Scanner technology.

Frank Martin
NELC Code 3100
Problem N451

Figure D65. C-6.

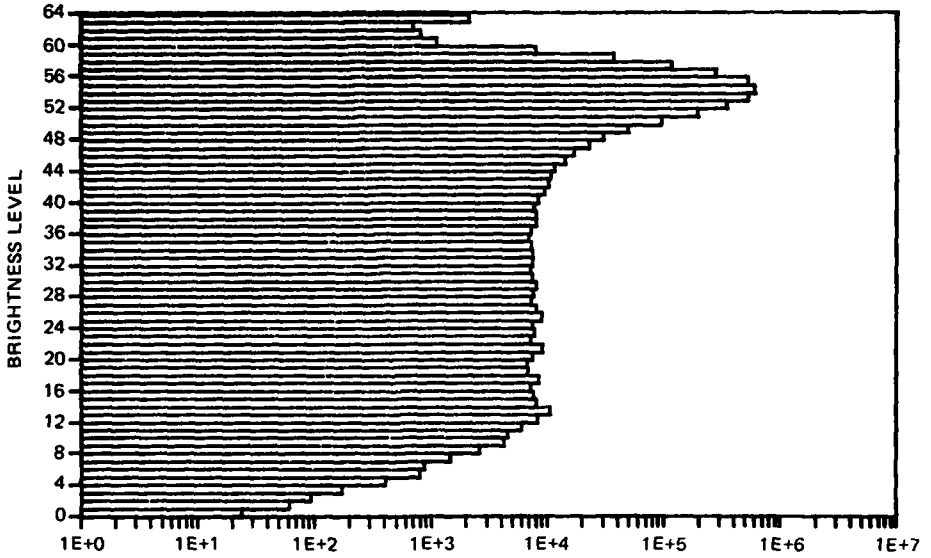

PEL BRIGHTNESS STATISTICS
WJM TYPED PAGE – FAIRCHILD – MATCHED FILTER – ILLUM. CORRECTED – 4 PPS
IMAGE (8 1/2 X 8 1/2 – TOP EDGE LEADING) ON 082/24 – STATS ON 087/17

Figure D66. C-6.

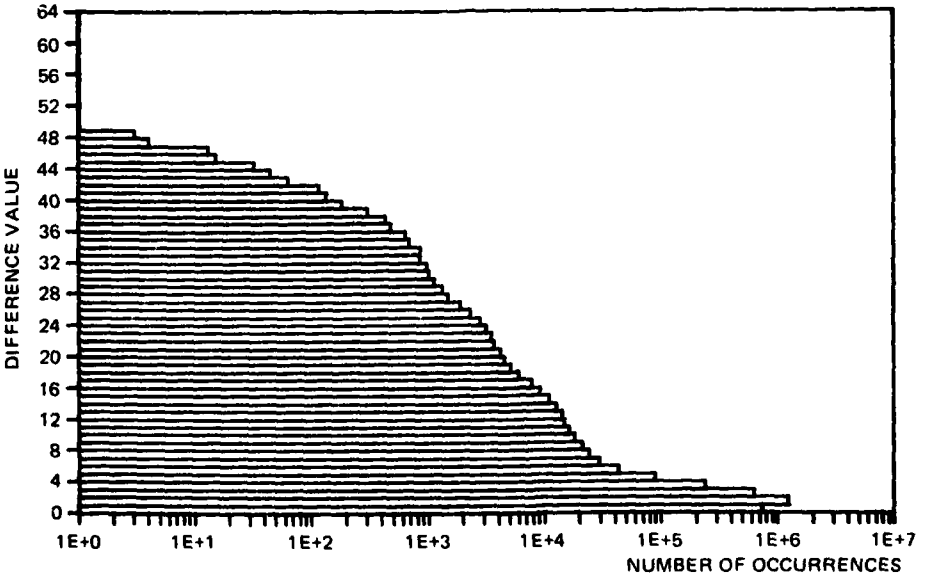

FIRST DIFFERENCE STATISTICS
WJM TYPED PAGE – FAIRCHILD – MATCHED FILTER – ILLUM. CORRECTED – 4 PPS
IMAGE (8 1/2 X 8 1/2 – TOP EDGE LEADING) ON 082/24 – STATS ON 087/17

Figure D67. C-6.

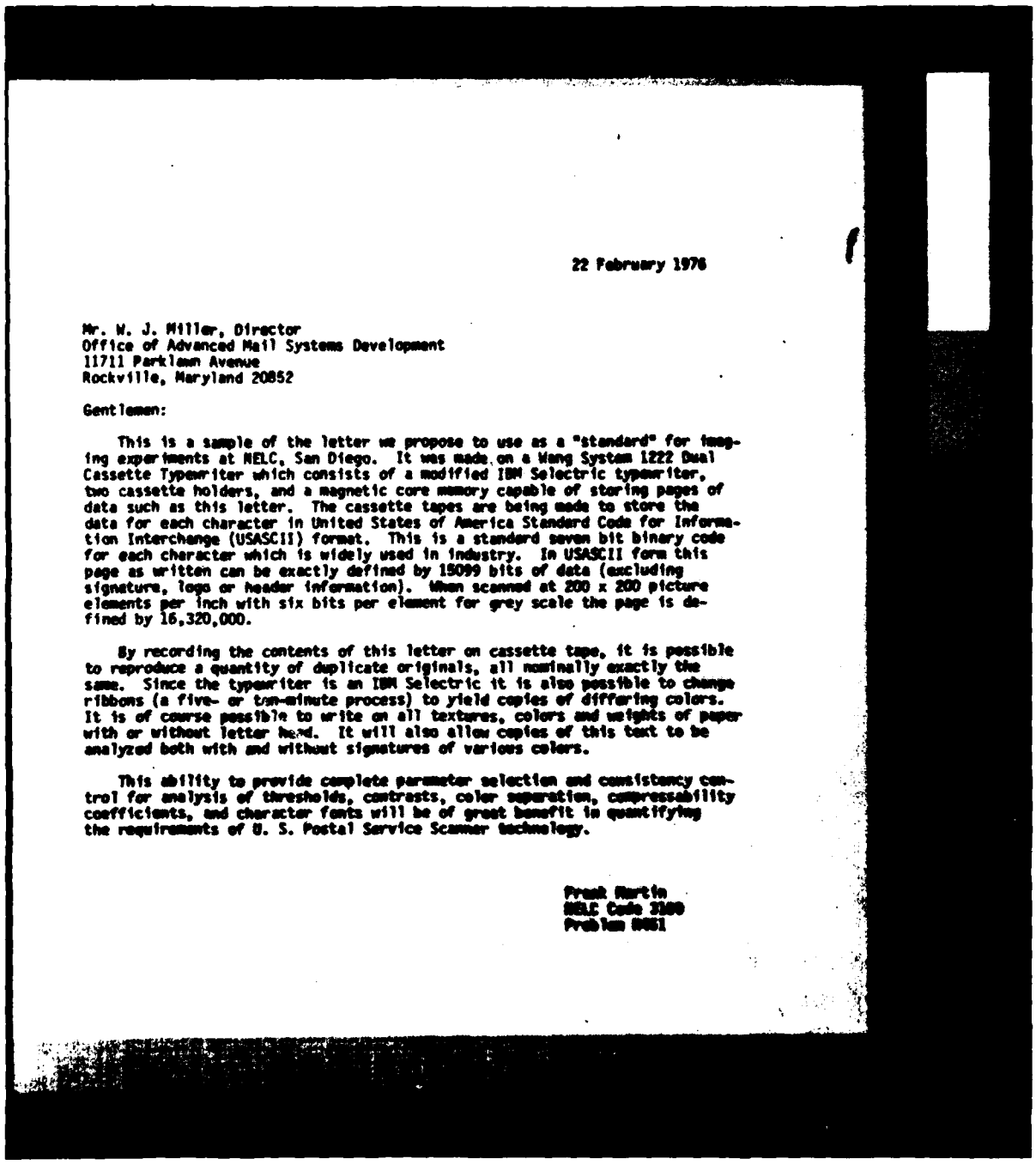

22 February 1976

Mr. W. J. Miller, Director
Office of Advanced Mail Systems Development
11711 Parklawn Avenue
Rockville, Maryland 20852

Gentlemen:

This is a sample of the letter we propose to use as a "standard" for imaging experiments at NELC, San Diego. It was made on a Wang System 1222 Dual Cassette Typewriter which consists of a modified IBM Selectric typewriter, two cassette holders, and a magnetic core memory capable of storing pages of data such as this letter. The cassette tapes are being made to store the data for each character in United States of America Standard Code for Information Interchange (USASCII) format. This is a standard seven bit binary code for each character which is widely used in industry. In USASCII form this page as written can be exactly defined by 15099 bits of data (excluding signature, logo or header information). When scanned at 200 x 200 picture elements per inch with six bits per element for grey scale the page is defined by 16,320,000.

By recording the contents of this letter on cassette tape, it is possible to reproduce a quantity of duplicate originals, all nominally exactly the same. Since the typewriter is an IBM Selectric it is also possible to change ribbons (a five- or ten-minute process) to yield copies of differing colors. It is of course possible to write on all textures, colors and weights of paper with or without letter head. It will also allow copies of this text to be analyzed both with and without signatures of various colors.

This ability to provide complete parameter selection and consistency control for analysis of thresholds, contrasts, color separation, compressability coefficients, and character fonts will be of great benefit in quantifying the requirements of U. S. Postal Service Scanner technology.

Frank Martin
NELC Code 3100
Problem 6661

Figure D68. C-6.

PEL BRIGHTNESS STATISTICS
WJM TYPED PAGE – FAIRCHILD – MATCHED FILTER – ILLUM. CORRECTED – 4 PPS
IMAGE (8 1/2 X 8 1/2 – LEFT EDGE LEADING) ON 082/29 – STATS ON 087/18

Figure D69. C-6.

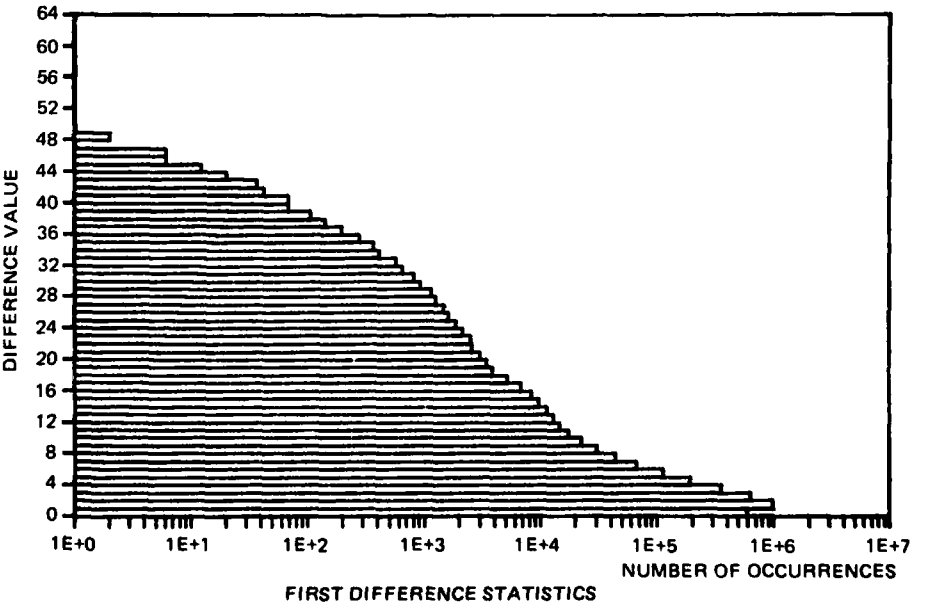

FIRST DIFFERENCE STATISTICS
WJM TYPED PAGE – FAIRCHILD – MATCHED FILTER – ILLUM. CORRECTED – 4 PPS
IMAGE (8 1/2 X 8 1/2 – LEFT EDGE LEADING) ON 082/29 – STATS ON 087/18

Figure D70. C-6.

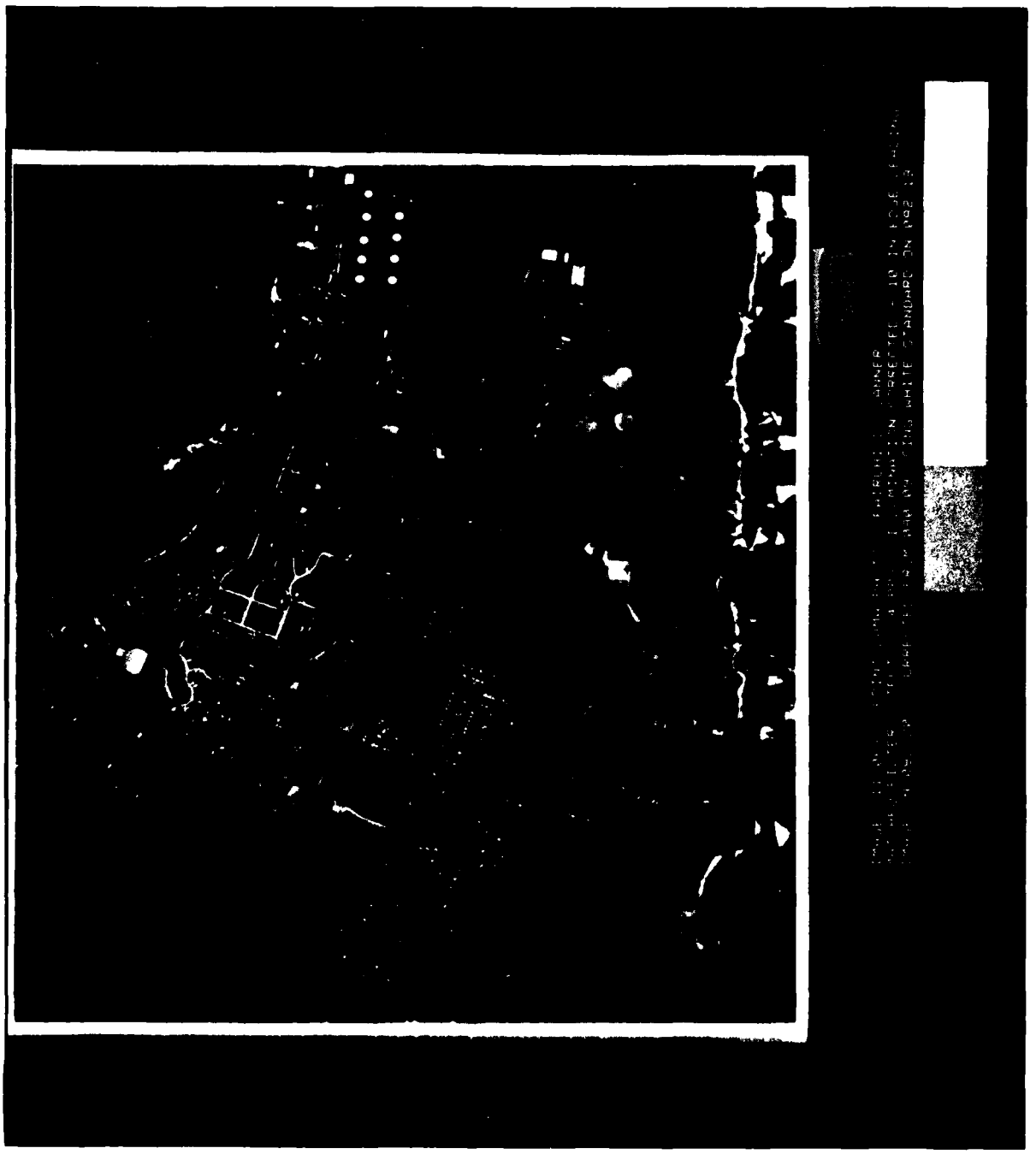

Figure D71. D-6.

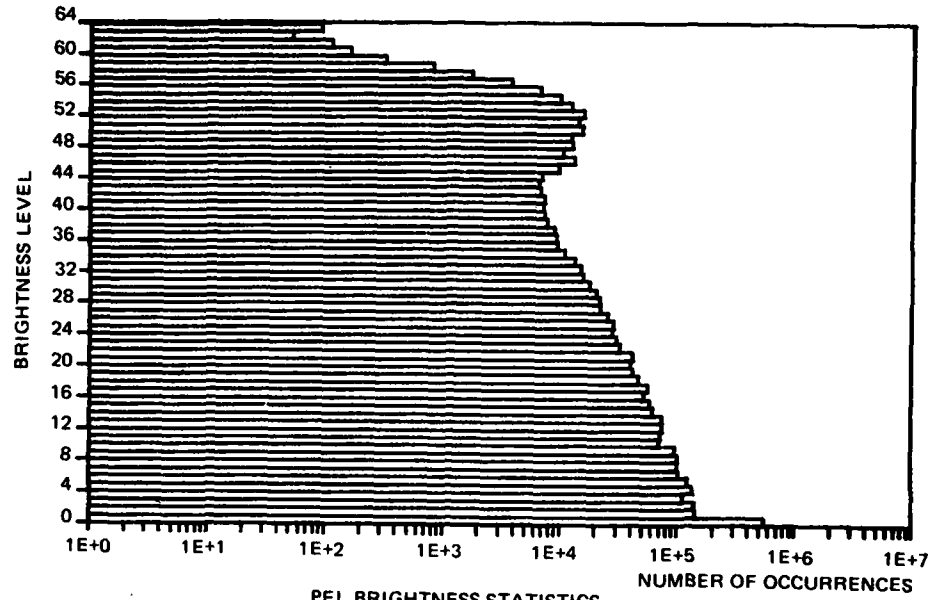

PEL BRIGHTNESS STATISTICS
PT. LOMA PHOTO – FAIRCHILD SCANNER – MATCHED FILTER OUTPUTS – 4 PPS
IMAGE (11-06) – ILL. CORRECTED – IMAGE ON 082/20 – STATS ON 087/16

Figure D72. D-6.

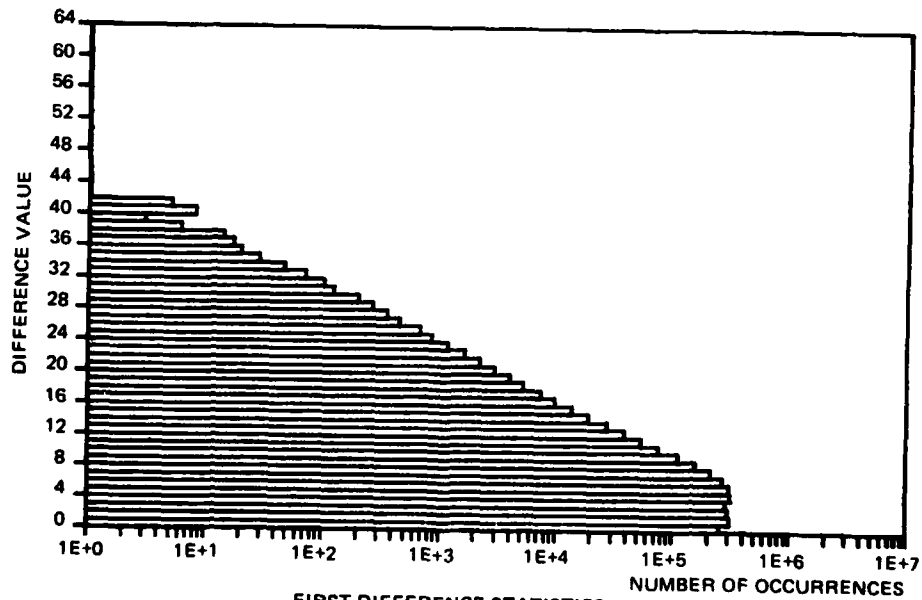

FIRST DIFFERENCE STATISTICS
PT. LOMA PHOTO – FAIRCHILD SCANNER – MATCHED FILTER OUTPUTS – 4 PPS
IMAGE (11-06) – ILL. CORRECTED – IMAGE ON 082/20 – STATS ON 087/16

Figure D73. D-6.

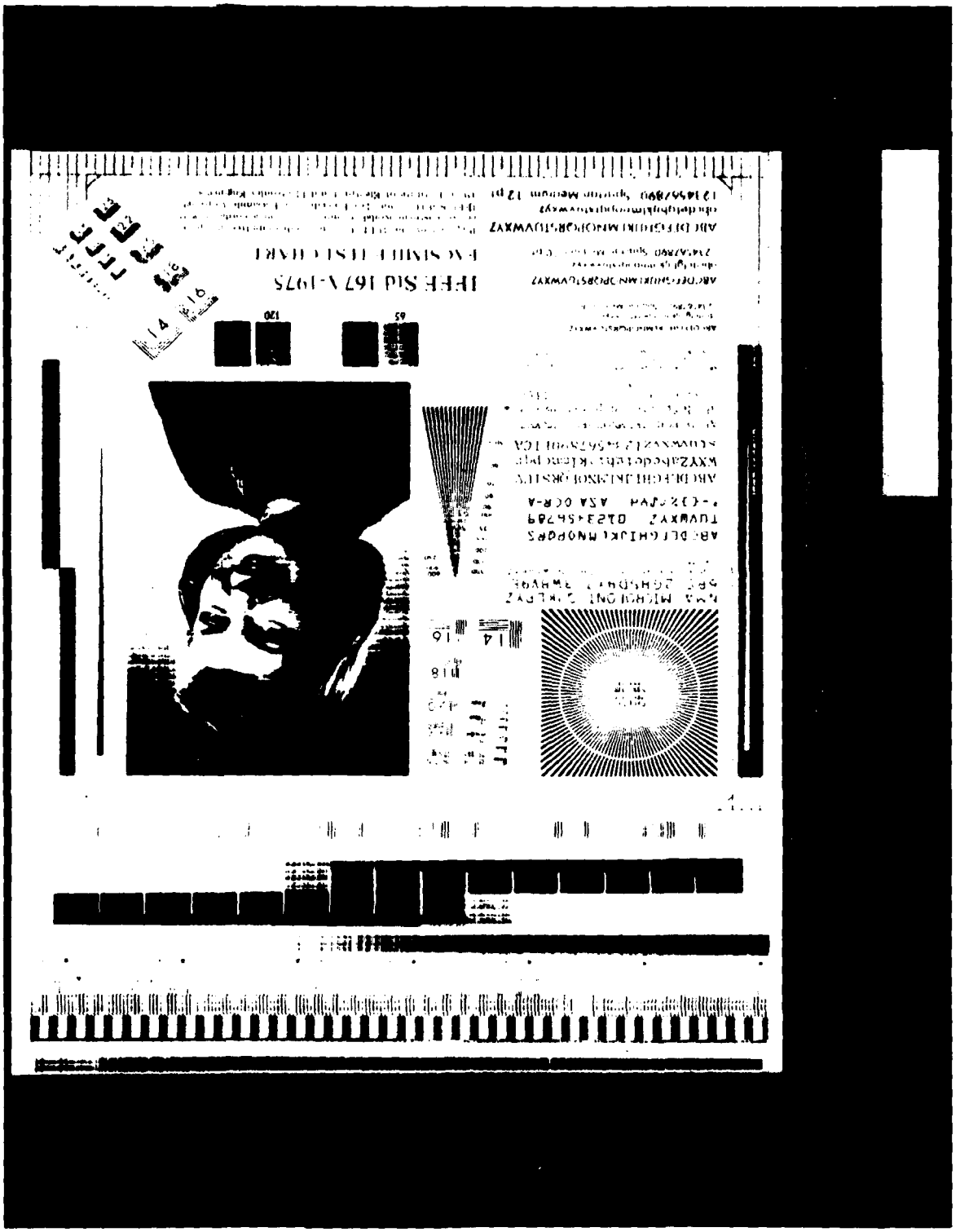

Figure D74. A-7.

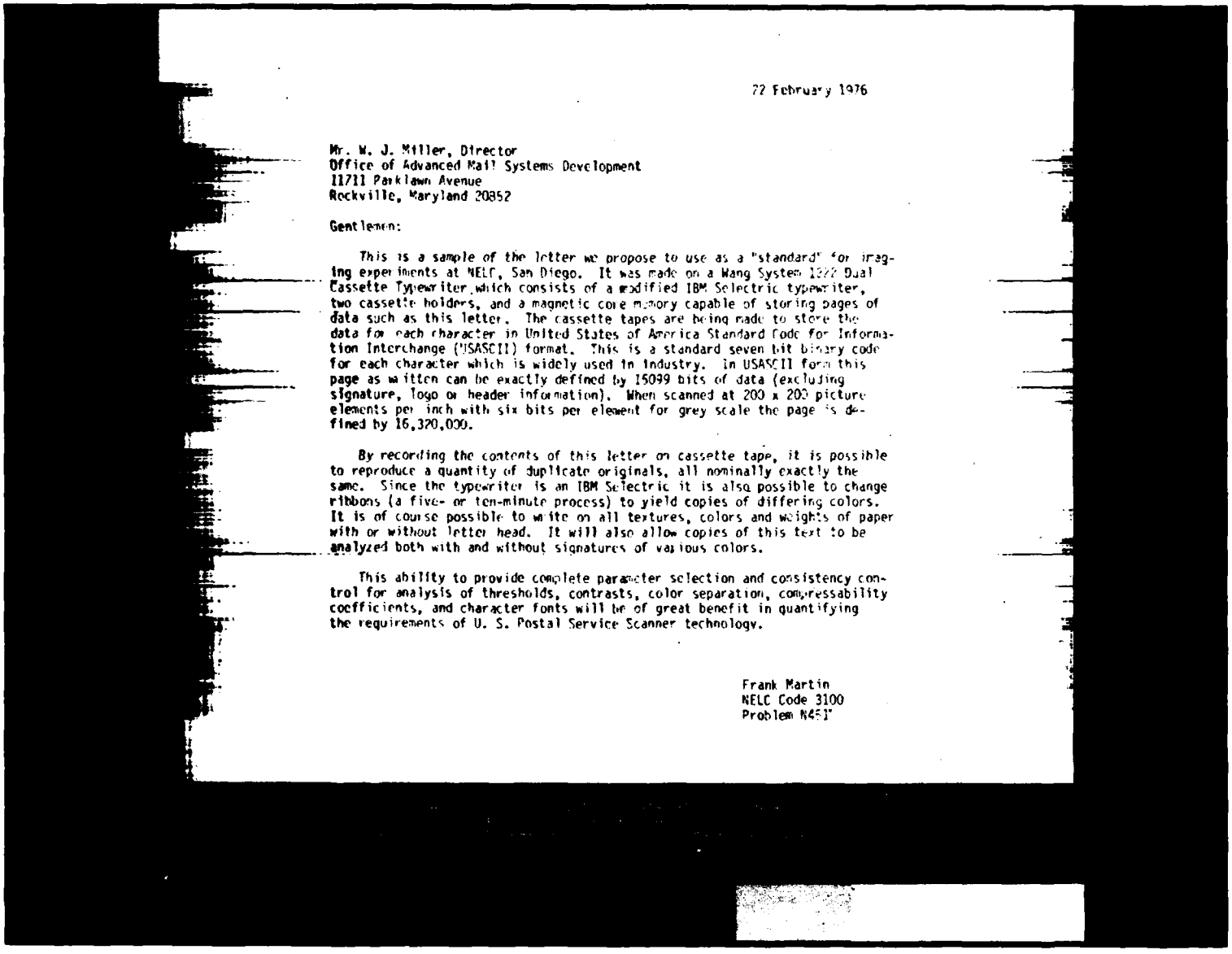

22 February 1976

Mr. W. J. Miller, Director
Office of Advanced Mail Systems Development
11711 Parklawn Avenue
Rockville, Maryland 20852

Gentlemen:

This is a sample of the letter we propose to use as a "standard" for imaging experiments at NELC, San Diego. It was made on a Wang System 1222 Dual Cassette Typewriter which consists of a modified IBM Selectric typewriter, two cassette holders, and a magnetic core memory capable of storing pages of data such as this letter. The cassette tapes are being made to store the data for each character in United States of America Standard Code for Information Interchange (USASCII) format. This is a standard seven bit binary code for each character which is widely used in industry. In USASCII form this page as written can be exactly defined by 15099 bits of data (excluding signature, logo or header information). When scanned at 200 x 200 picture elements per inch with six bits per element for grey scale the page is defined by 16,320,000.

By recording the contents of this letter on cassette tape, it is possible to reproduce a quantity of duplicate originals, all nominally exactly the same. Since the typewriter is an IBM Selectric it is also possible to change ribbons (a five- or ten-minute process) to yield copies of differing colors. It is of course possible to write on all textures, colors and weights of paper with or without letter head. It will also allow copies of this text to be analyzed both with and without signatures of various colors.

This ability to provide complete parameter selection and consistency control for analysis of thresholds, contrasts, color separation, compressability coefficients, and character fonts will be of great benefit in quantifying the requirements of U. S. Postal Service Scanner technology.

Frank Martin
NELC Code 3100
Problem N451

Figure D75. C-7.

The scanner operated as expected at the 4-page-per-second rate, but the thresholding circuitry did not function at 8.8 pages per second. All analog output ports operated normally at both page rates, since the data are always shifted out of the imaging devices at the same rate of 10.5 MHz on each of the four channels. The images presented in figures D8 through D50 are 6-bit images acquired when operating in a four-channel configuration. Even though there are only two multiplexed video outputs from the scanner, each of these was double buffered and input to two of the ICAS input channels. Referring to figure D4, these 6-bit images are shown in columns 2, 3, 4, and 6.

The images from the raw video outputs, column 2 in figure D4, appear to be of low contrast because of the low signal level at those outputs. At the acquisition rate of 8.8 pages per second there was just not enough signal level for ICAS to obtain any quality image at all. For the images from all other test points there was sufficient amplitude to utilize the full dynamic range of the ICAS.

Because of the differences in dynamic range, it is difficult to evaluate the relative image quality before and after the matched filter circuitry. To facilitate this comparison, the image in figure D23 was compressed in dynamic range to match the dynamic range of the image in figure D8. This image is shown in figure D76. In comparing these two images, the most obvious difference is in the maximum resolution obtainable in the test patterns. See figure D77 for the pattern definitions. In the images presented, the microcopy resolution pattern 14A can be used to verify the resolution in the direction of scan. In figure D8 the highest resolution is about 150 lines/inch, while in figure D76 the resolution is just over 100 lines/inch. However, upon examination of figure D20, which was scanned at a page rate of 8.8 pages/second, the matched filter outputs exhibit a resolution of about 150 lines/inch. One possible cause of this is that one or more amplifiers in the matched filter are saturated with the increased signal level at the lower page rates. Thus, in this scanner, the matched filter appears to operate satisfactorily with no appreciable bandwidth reduction at relatively low signal levels. At higher signal levels there is a slight loss of bandwidth. In considering the scanner's use in a continuous-tone application, or in a situation in which the video is converted to multibit digital information for processing prior to thresholding, the real need for the matched filter circuitry is questionable. This statement is supported by the small qualitative differences in the digitized images before and after the matched filter.

Using figure D20, the modulation transfer function (MTF) was estimated for the system in both the direction of scan and the direction of paper motion. Keep in mind that the curves presented in figure D78 do include possible effects of the ICAS gain and level amplifiers and A/D converters. This information was calculated using the modulation of the 10-line/inch pattern, pattern 3 in figure D77, as the 100% point. Then the modulation of the horizontal and vertical resolution bars in pattern 14A was measured and the percentage difference between those figures and the modulation of the 10-line/inch pattern was plotted in figure D78. These curves are somewhat lower than the predicted best phasing MTF, which is 31% at the Nyquist limit, for the scanner subsystem only.

To observe any possible degradation of image data due to the two-to-one multiplexer in each channel of the scanner, figures D20 and D35 are samples of before and after, respectively. Pattern 14A shows a slight degradation in resolution, but this small difference may be partially attributable to the ICAS gain and level amplifiers. The net result is that there is not much, if any, degradation due to the multiplexers in the scanner.

One additional measurement made was the actual magnification through the scanner. A bilevel image was printed on the NOSC Versatec printer and comparative measurements indicated a magnification of 0.96X in the direction of scan. This is only a verification of previous measurements made on the system.

Figure D76. Dynamic range compressed.

IEEE Std 167A-1975
Facsimile Test Chart

Pattern Descriptions

The pattern number given in the following description may be identified from Figure 1. This chart is designed for scanning in either direction, horizontally across the page.

IEEE Std 167-1966, Test Procedure for Facsimile was based on previous issues of the IEEE Test Chart.

Patterns 1 and 2. 96 lines per inch (3.78 lines per millimeter) consisting of 48 dark and 48 light lines, substantially equal in width. In pattern 1, the black corresponds approximately to step 2 and gray to step 7 of pattern 8. In pattern 2, white represents paper white and gray to approximately step 11. These patterns are intended for generating low-modulation high-frequency signals at both ends of the density scale— useful for testing modulation characteristics at edges of band in a frequency shift system.

Patterns 3, 4, and 5. *Vertical bar patterns at* 10, 50, and 96 lines per inch (0.394, 1.97, and 3.78 lines per millimeter) of substantially equal width — useful for square-wave testing at several keying frequencies.

Pattern 6. A continuous density wedge designed so that at equal intervals of distance across the page, the variation in reflectance will be roughly equally perceptible to the eye. Reading left-to-right across the page, the relative reflection density values at the heavy dots are approximately as shown in Table 1. Pattern 6 is useful for cases where intermediate reflection densities are needed between the steps in Patterns 7 and 8.

Table 1
Pattern 6 Density Values

Dot	1	2	3	4	5	6	7
Density	1.95	1.75	1.23	0.73	0.38	0.14	0.03

Patterns 7 and 8. Reversed step tablets of 15 steps with reflection densities corresponding the approximately equal perceptibility modified to provide smaller low density increments. Consistent with conventional practice, paper white is understood to be equal to 0.00 in density (approximately 0.07 on an absolute scale). For patterns 7 and 8 the relative reflection densities are shown in Tables 2 and 3 respectively.

These patterns will assist in appraising gradient and absolute scale. They are useful for checking half-tone characteristics. Reversed sequences are used since the dynamic halftone characteristics may differ for a rising density or a falling density scale.

Pattern 9. National Bureau of Standards (NBS) type repeating tri-bar resolution test pattern. Twelve complete sets of three-line patterns are repeated across the sheet. Alternate groups are of different line spacing. Density values are shown in Table 4. This pattern is useful for checking definition.

Pattern 10. Rectangle with 45° diagonal marks at each corner — useful for checking index of cooperation, skew, and paper-feed error.

Patterns 11 and 17. White wedge on black background and black wedge on white background, 0.07 in (1.78 mm) to zero — useful for checking single-line definition.

Pattern 12. W. and L. E. Gurley type Pestrecov Star pattern. Outer circle 50, second circle 100, and third circle 200 lines per inch (1.97, 3.94, and 7.87 lines per millimeter).

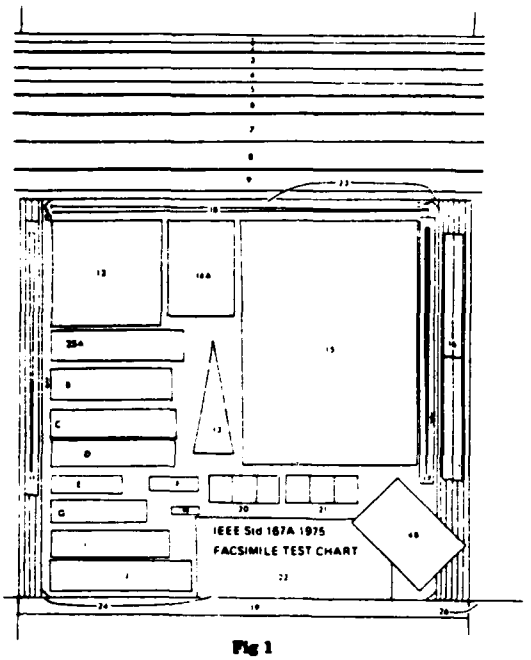

Fig 1
Pattern Arrangement

Pattern 13. Truncated fan-type multiple-line test pattern.Calibrated in lines per inch—useful for checking multiple-line definition along scanning line, envelope delay distortion, and ringing.

Patterns 14A and 14B. NBS type Microcopy Resolution test pattern. Numerals indicate the number of cycles (one black plus one white *line) per millimeter (that is, line pairs)—useful* in checking high definition systems.

Pattern 15. Photograph with detail in highlight and shadow. The limiting densities of the photograph approximate those of test patterns 7 and 8.

Pattern 16. *Vertical gray steps with relative* reflection densities of approximately 0.95 and 0.27 — useful in testing rising and falling transient characteristics and level variations.

Pattern 18. Horizontal "V" pattern with 0.13 in (3.3 mm) opening. Number of scanning line crossings of both lines, multiplied by 7.7 will equal number of lines per inch (multiply by 0.3 for number of lines per millimeter).

Pattern 19. "Fence" pattern with 0.01 in (0.254 mm) lines 0.10 in (2.54 mm) apart—useful for checking jitter and measuring available line length.

Patterns 20 and 21. Halftone dot screens. Reproduced in approximately 10, 50 and 90 percent black, left to right and at 65 dots per inch (2.56 dots per millimeter) at a 45° angle for pattern 20, and 120 dots per inch (4.72 dots per millimeter) for pattern 21.

Pattern 22. Title and credit box. Three sizes of Times Roman type font.

Patterns 23 and 24. Fiducial dots forming a 3, 4, 5 *right triangle—useful for indicating* the presence of skew by comparing the hypotenuse of the two patterns.

Pattern 25. Type faces as indicated—useful for checking readability.

Pattern 26. Extension lines to permit measurement of *available line and useful length of* copy.

Table 2
Pattern 7 Density Test*

Step	1	2	3	4	5	6	7	8	9	10	11	12	13	14	15
Density	0.01	0.03	0.08	0.16	0.26	0.36	0.46	0.60	0.72	0.89	1.07	1.22	1.43	1.64	1.80

Table 3
Pattern 8 Density Values*

Step	1	2	3	4	5	6	7	8	9	10	11	12	13	14	15
Density	1.67	1.51	1.32	1.14	0.98	0.85	0.70	0.59	0.48	0.38	0.28	0.18	0.09	0.04	0.02

*Preliminary values for first batch of test charts.

Table 4
Pattern 9 Density Values

	Group A						Group B					
	1	2	3	4	5	6	1	2	3	4	5	6
Lines per Inch	61.0	86.4	122	173	244	345	406	284	203	142	102	71.1
Lines per Millimeter	2.40	3.40	4.80	6.81	9.60	13.6	16.0	11.2	7.99	5.59	4.02	2.80

NOTE: Group A has coarse lines starting at the left. Group B has coarse lines starting at the right.

Figure D77.

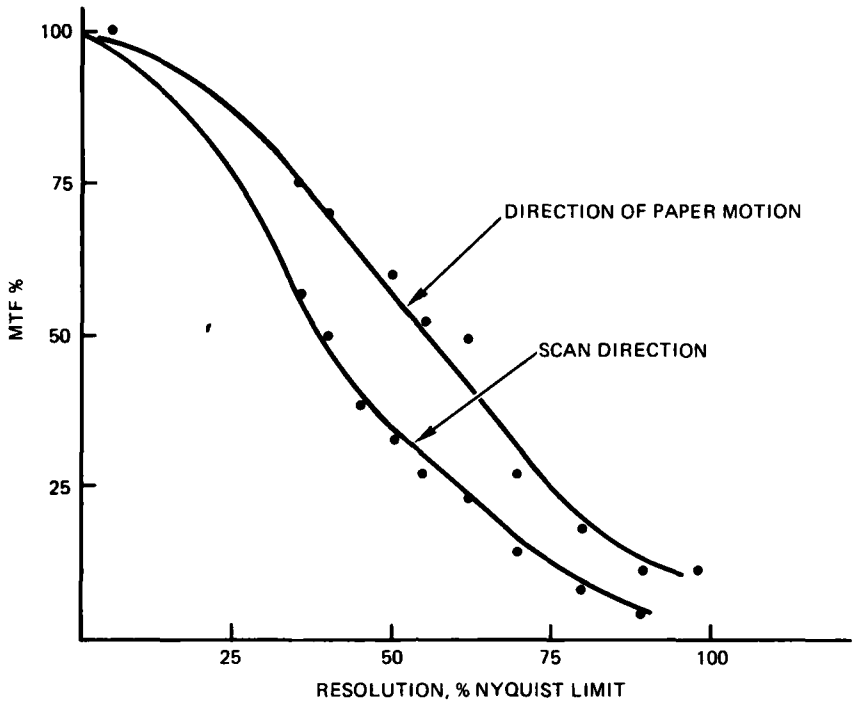

Figure D78. Modulation transfer function.

IMAGER ABUTMENT

The images captured using the Fairchild scanner all contain several pels at each end of every line that are substantially lower in value than the rest of the image. The reason for this is the abutment philosophy used in the scanner. As it is understood, the scanner Data Valid control signal is generated in a manner such that the first pels stored in the Fairchild frame-store memory are actually about the first valid pels shifted out of each imager. The mechanical alignment is then done to provide optimum abutment of the two image halves at a point several pels from the end of each imager. This means that there are not a full 2048 valid pels on a line but something on the order of 2042. This is all the Fairchild system actually stores in the frame-store memory for each line of an image. The NOSC interface, on the other hand, stores a full 2048 pels per line, which means that several pels are stored before the valid information is shifted out of each imager. Measurements on the NOSC stored images indicate that the number of invalid pels at each end of a line is on the order of 8 to 10 pels, not the 3 indicated by Fairchild. The reason for this method of imager abutment is not entirely clear. One possible reason might be that the photosite response nonuniformity increases in the several photosites at the ends of the imager.

Another point of concern in the two-imager design is the relative focus of the two imagers. In all the 6-bit images obtained from the scanner it is seen that the right half image is not focused as well as the left half. With all the degrees of freedom designed into the focal plane assembly, attempts at focusing the imager did not improve the resultant images. Figure D26 exemplifies the problem.

ILLUMINATION

The illumination source for this type of scanner is, of course, of prime importance in producing accurate copies of the input material. There are two areas that merit attention in this characterization, uniformity and spectral content. Figures D5 and D7 illustrate the problem of lack of uniformity. The system response is seen to fall off about 50% at either end of the field of view, most of which is due to the illumination source.

Even though the dynamic thresholding circuitry was designed to follow variations in the illumination across the page, this much droop in the illumination can cause large numbers of errors in thresholded data. The reason is that for each of the two threshold circuits in the scanner the last value of the reference voltage level on one line is used as the starting point for the next line. Since each threshold circuit operates on half the scan line, from the edge to the center of the image, the last value of the reference voltage is nominally 30% below the background level at the point of highest response. Now, when this value of the reference level is used as the threshold at the beginning of the next line, the background level will likely be below the threshold level and will be stored as information bits incorrectly. This will occur until the background level rises above this threshold or until information in the image causes the reference voltage level to be updated according to the rules of the algorithm.

A potential problem would still exist even if a future scanner used a single threshold circuit which operated on a full scan line. If data in a scanned image ended in the center of the scan line, causing no further updating of the reference voltage during that line, the background could again be interpreted as information if there were sufficient droop in the illumination at the edges of the image area. Because of this, it seems imperative that, if this type of adaptive threshold circuit is used, the system response must be flattened to within the percentage established as the minimum PCR, which is currently 30%.

The next test performed is a comparison of the two sets of fluorescent lamps supplied with the scanner. The lamps normally used on the scanner contain the standard daylight phosphor, the spectral distribution for which is shown in figure D79. It has strong lines in both the blue and the green portions of the visible spectrum. The second set of fluorescent tubes contains a special phosphor blend similar to that used in the ICAS. The blend consists of six to eight parts blue, two parts green, and one part red phosphor. The relative spectral content of this phosphor blend is shown in figure D80. Photographs of the channel 2 raw video outputs are shown in figures D81 through D84, comparing the amplitudes of those signals with the two different phosphors. The alignment test target was mounted on the scanner for these photographs. Notice that for channel 2A the daylight phosphor produces a slightly greater signal amplitude while the opposite is true for channel 2B. It is therefore assumed that there is not a significant difference in the actual overall intensity of the two sets of lamps.

In order to more fully characterize the two phosphors, 10 images were chosen from the Fairchild test deck to be scanned using both sets of fluorescent lamps. These images are of the tricolor test document printed on different colors of paper. All these images had indicated PCRs of substantially greater than the required minimum of 30%. There is, however, some question as to the exact measurement procedure, since both the scanner hardware and the NOSC thresholding software produced very poor results on all these images, as will be shown.

The PCRs notwithstanding, the 10 images were scanned with each set of lamps and a comparison was made by visually examining each segment of each image. The images consist of three segments printed with red, green, and blue inks from top to bottom, respectively.

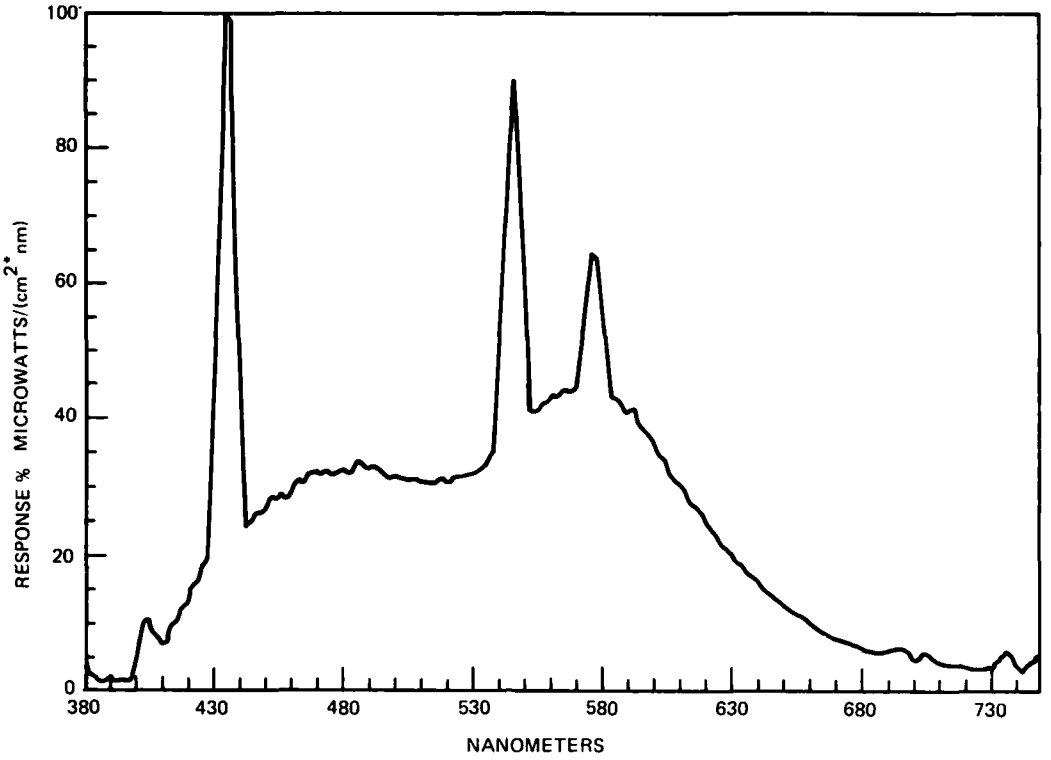

Figure D79. Daylight phosphor spectral distribution.

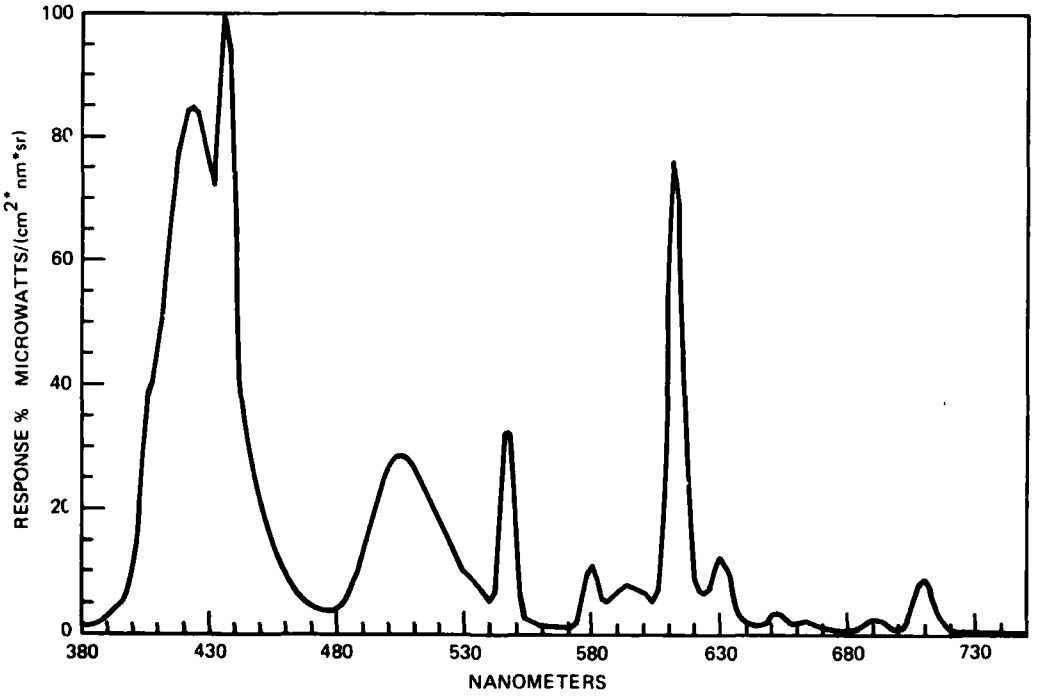

Figure D80. Special phosphor spectral distribution.

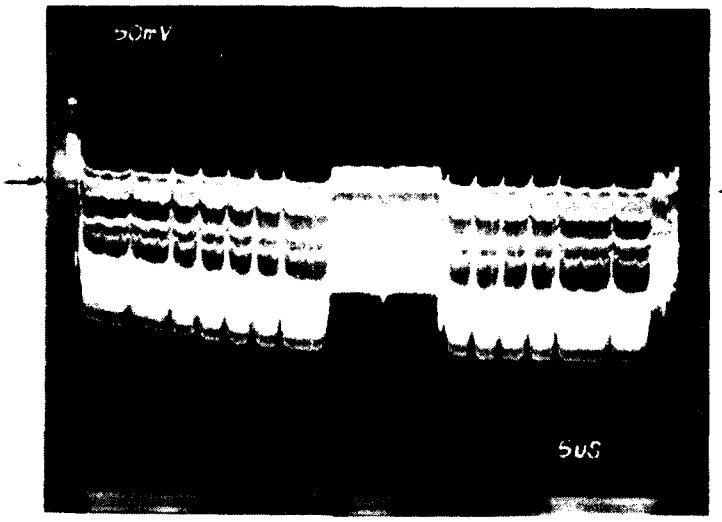

Figure D81. Raw video channel 2A daylight phosphor.

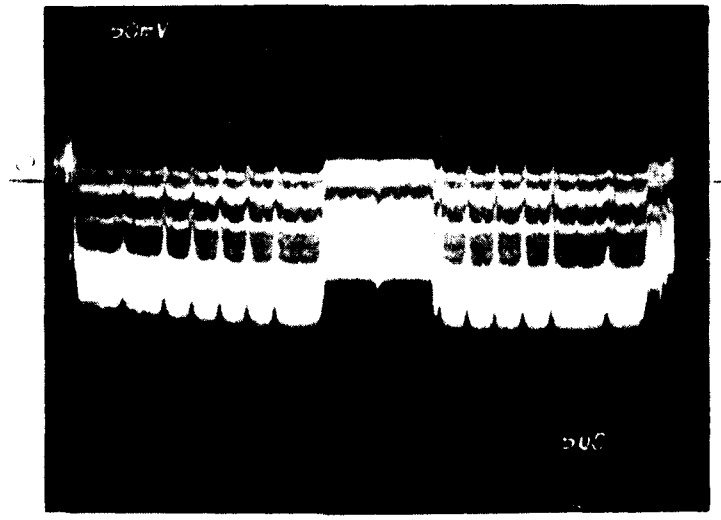

Figure D82. Raw video channel 2A special phosphor.

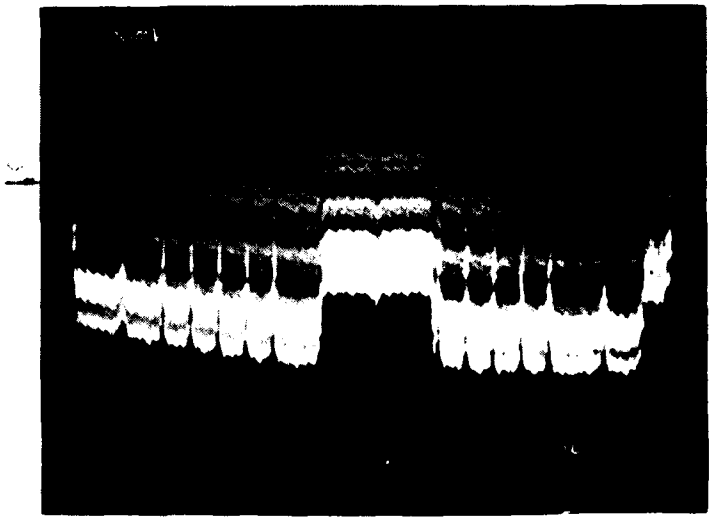

Figure D83. Raw video channel 2B daylight phosphor.

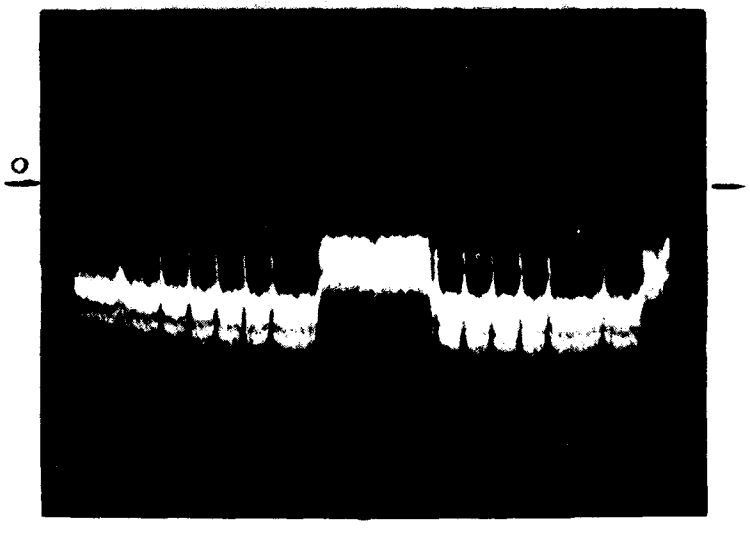

Figure D84. Raw video channel 2B special phosphor.

Each image segment scanned with the two phosphors was examined, and the phosphor which produced the thresholded image with the higher accuracy was selected and tabulated. Figures D85 and D86 are two thresholded images of test document B426 scanned using the daylight phosphor and the special phosphor, respectively. These images are acquired in the manner described for the threshold images in column 5 of figure D4; that is, the segments on the right side are from the digitized video output from the scanner and the segments on the left are the results of the NOSC thresholding algorithm. As can be seen, there is fair agreement between the two outputs. However, for the purposes of this comparison only the scanner's digitized output will be used. The result of this comparison is presented in figure D87. The document number is shown in the leftmost column, followed by the paper color. The polarity, in the next column, indicates whether the printing is dark on light (positive) or light on dark (negative). Next, there are two sets of entries, one for each phosphor, containing the NOSC tape and file number of each image and a box for each of the three ink colors. The boxes marked indicate which phosphor produced the more accurate thresholded image. These results indicate that the special phosphor blend produces better results with the single-color inks.

THRESHOLDING

The image data obtained from the digitized video outputs from the scanner are shown in the images from column 5 in figure D4. These images show a comparison of the thresholding circuitry in the scanner with the NOSC implementation of the thresholding algorithm in software operating on digitized image data. Analyzing figures D54 and D55 closely, it appears that the hardware implementation of the thresholding algorithm outperforms the software version by producing, in general, thicker character strokes which contain fewer voids.

Another comparison of the thresholding algorithm is shown by plotting the actual reference level across half a line of an image. Several images were captured storing the reference voltage in one half of the image memory and the 6-bit image in the other half. The NOSC threshold algorithm was then run on the 6-bit image portion but storing the threshold level in memory instead of the image data. A plot of the threshold values across half an image line is shown in figure D88. The upper trace is of the NOSC algorithm reference level across 1024 pels of a line of image through a column of typed characters. The lower trace is of the scanner's reference voltage digitized to 6 bits across the same line of image data acquired on the same pass over the typed page. As can be seen, there is not very much agreement between the two traces.

Figure D89 is a superposition of the scanner-acquired reference voltage on the 6-bit image data for the same line. Note that in this figure there is no implied calibration of the reference voltage level with respect to the image line. This figure is presented only to compare the shape of the reference voltage to the image line. Figure D90 shows the NOSC-generated reference superimposed on the same image line. In this figure the reference level is an accurate indication of exactly where the threshold is at all points across the line, except for the first 16 pels on the line.

As shown in figures D89 and D90, the major problem with the threshold circuitry is due to the fall-off in system response from the center of the image area to each edge. When the reference voltage level is carried from the center of the image area to the edge for the succeeding line, any drop in system response greater than the minimum PCR will cause thresholding errors. This shows up as smearing along the right edge of figures D53, D54,

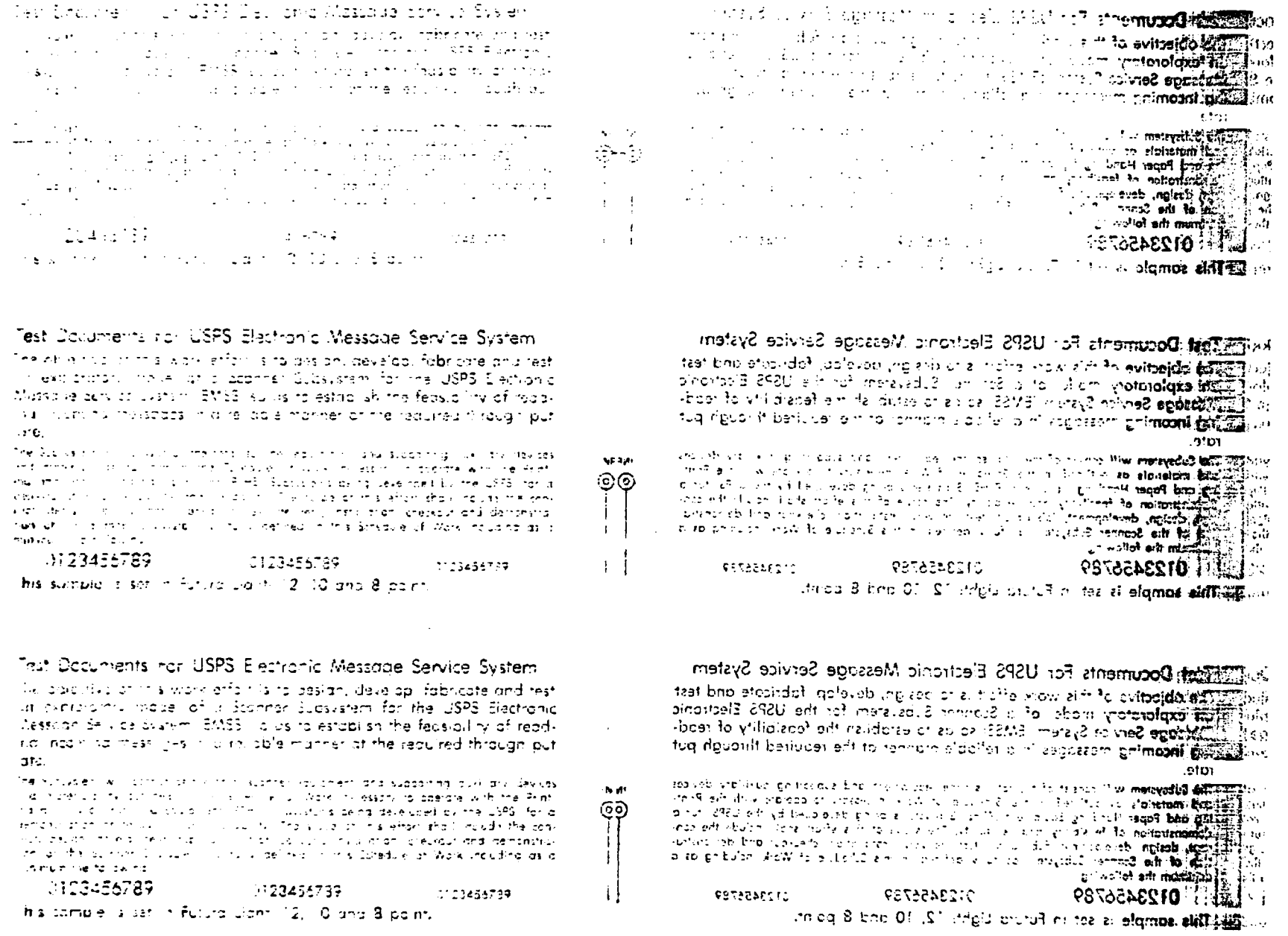

Figure D85. Image B426 scanned with daylight phosphor.

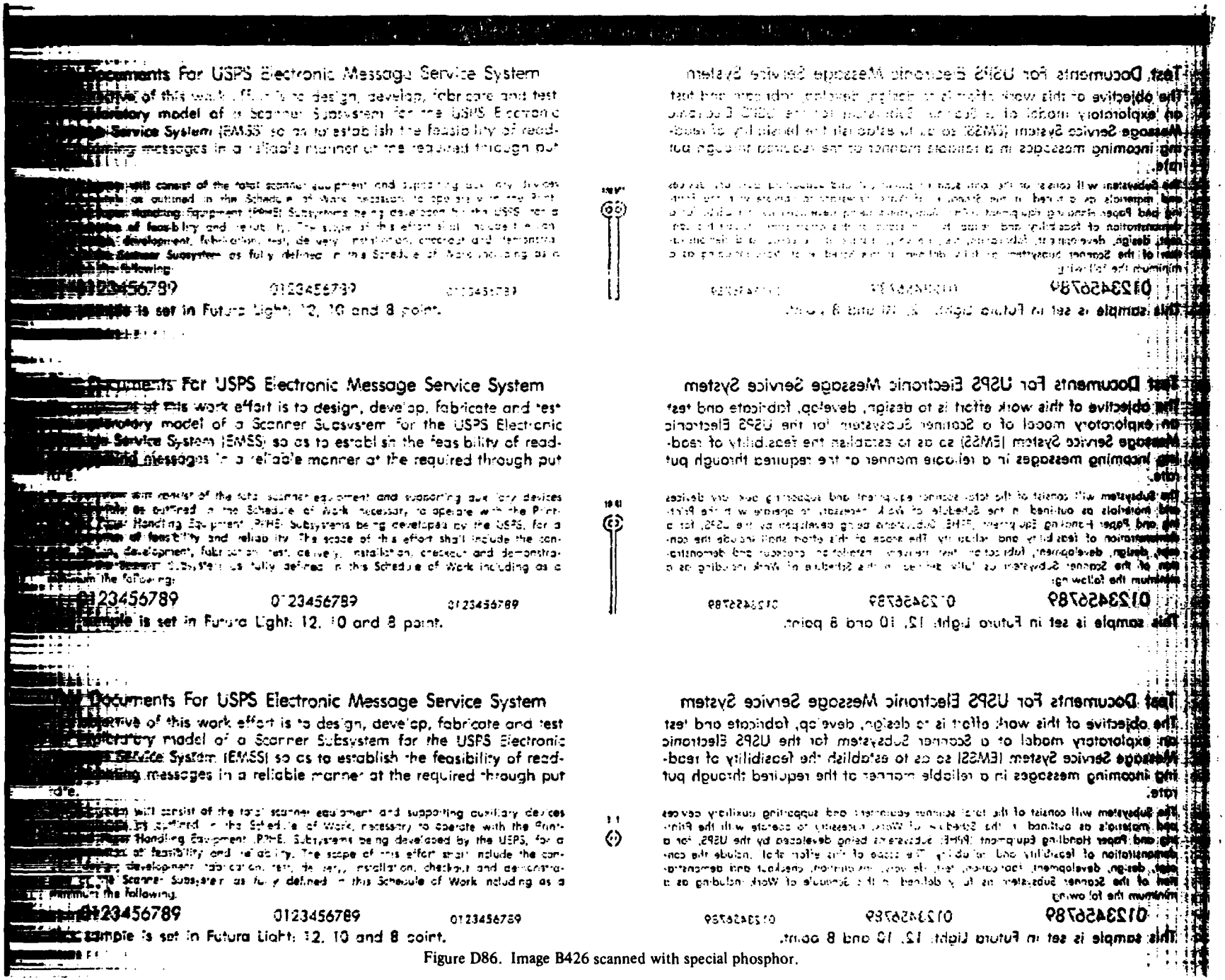

Figure D86. Image B426 scanned with special phosphor.

IMAGE	BACKGROUND COLOR	POLARITY POS/NEG	DAYLIGHT PHOSPHOR				SPECIAL PHOSPHOR BLEND			
			TAPE/FILE	RED	GREEN	BLUE	TAPE/FILE	RED	GREEN	BLUE
A452	WHITE	P	85/03				86/06	X	X	X
B426	BEIGE	P	84/06				86/01	X	X	X
C431	GOLD	P	84/07				86/02	X	X	X
E424	PINK	P	84/08			X	86/03	X	X	
G434	GREEN	P	84/09				86/10	X	X	X
H426	BLUE	P	84/10				86/09	X	X	X
I429	GREY	P	85/01				86/08	X	X	X
J416	PURPLE	P	85/02		X	X	86/07	X		
K079	WHITE	N	85/04				86/05	X	X	X
L079	YELLOW	N	85/05		X	X	86/04	X		

Figure D87. Comparison of phosphors using Fairchild test deck.

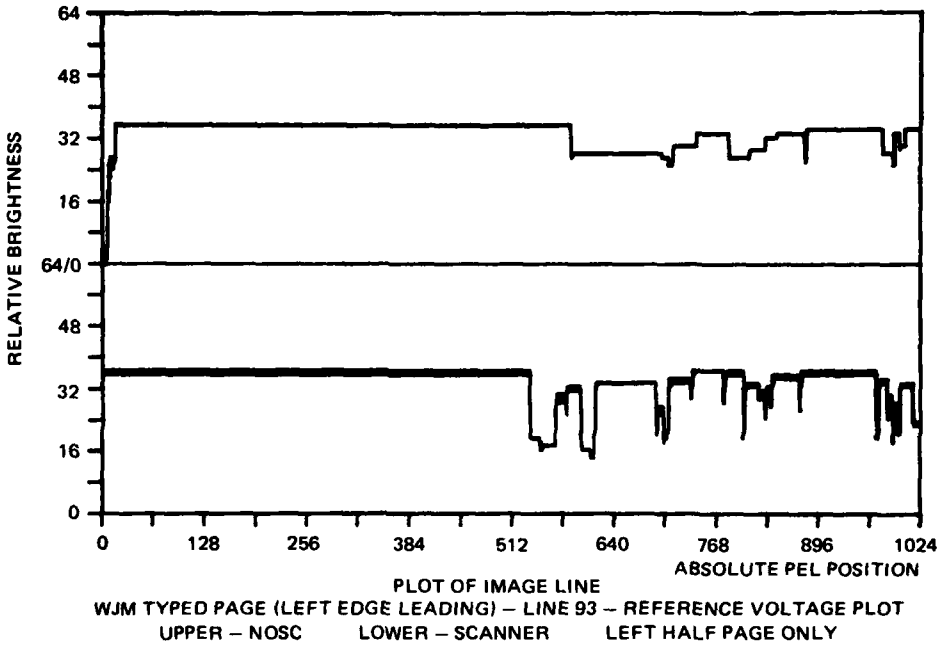

Figure D88. Threshold comparison.

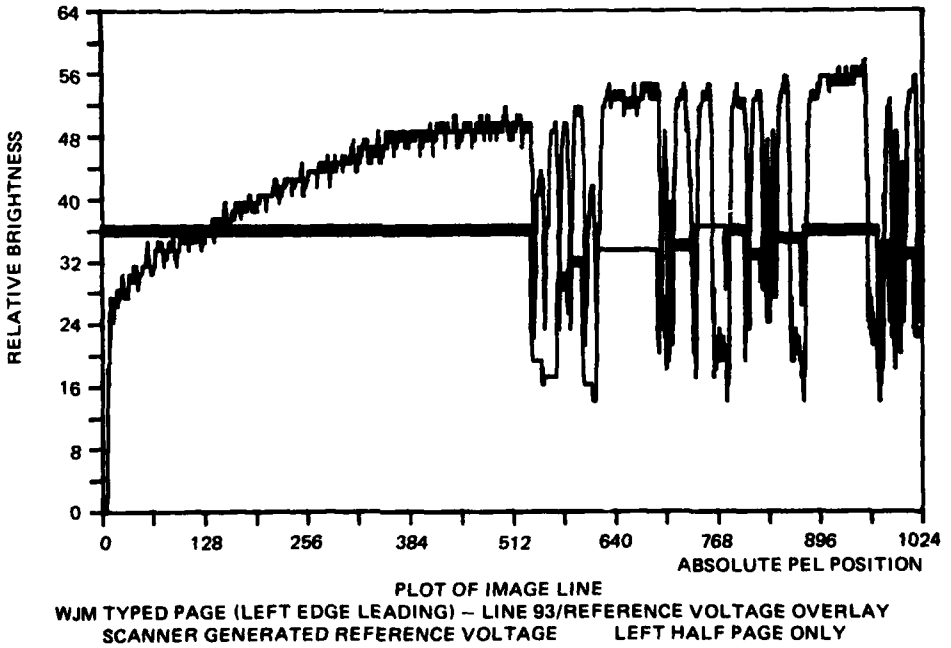

Figure D89. Threshold comparison.

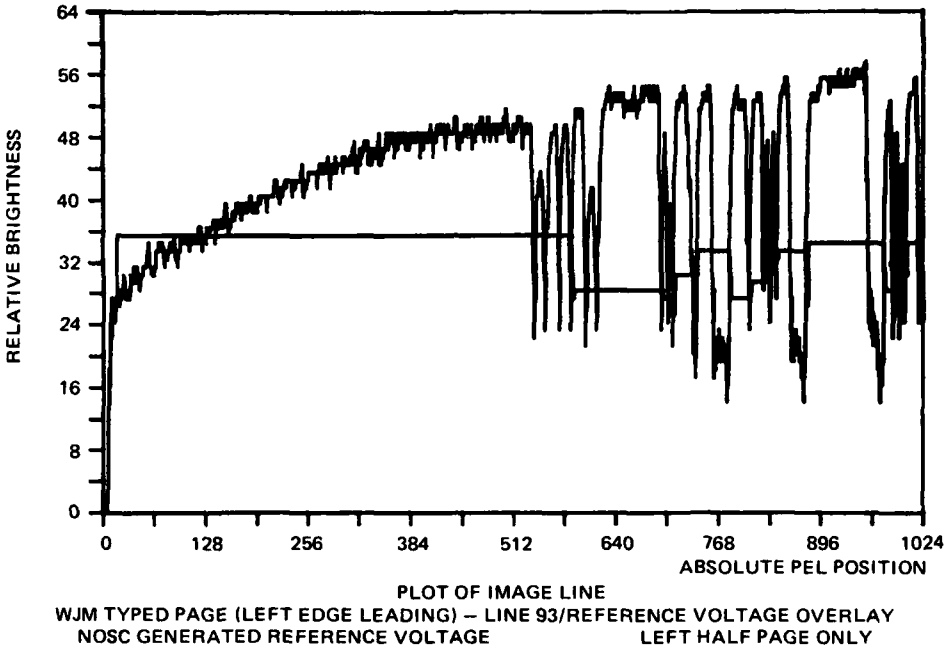

Figure D90. Threshold comparison.

D85, and D86. The left side of these images does not contain the smearing referred to, because of another problem. The several pels of overlap at the abutment of the two imaging devices caused the ICAS to store several invalid pels at the beginning of each line of data. These pels are of very low value, which caused the reference voltage to be updated to a similarly low value at the beginning of every line of data thresholded. This in turn caused the first few pels of the first character encountered on each line of typing to be missed. The invalid pels at the beginning of every line show up in the images as a black vertical line at the left side of the images.

If the overall system response can be flattened to within 30%, or whatever is established as the minimum PCR, this thresholding circuitry should be able to produce accurate results.

CONCLUSIONS

Application of this type of scanner for possible continuous-tone imaging shows considerable promise. The 6-bit images presented in this report at the two acquisition speeds of 4 and 8.8 pages per second contain noticeable clocking noise in the direction of scan. The clocking noise is of course more pronounced at the higher scan rate because of the reduced signal level. However, the imagery produced is very readable.

The highest resolution obtainable with the system is between 130 and 150 lines/inch. At these resolutions the system MTF is measured at about 15% in the direction of scan and 25% in the direction of paper motion.

When operating with the 6-bit A/D converters, there does not appear to be any significant difference in image quality before and after the matched filter circuitry. This

may be an important consideration in the event that in a later-version scanner it is decided to convert the video to digital data as early as possible and do all further processing digitally.

The method of abutting the two imaging devices is questionable because of the number of pels that are essentially lost because of overlapping. Analysis of images captured on the ICAS indicates that there are five to eight invalid pels at each end of every scan line. It seems that there should be enough adjustment latitude to allow abutting the end pels of each imager so as not to lose any useful pels from the imagers.

The most significant problem area is the illumination source. The 50% drop in the overall system response does cause significant smearing of the image data. In tests run on the Fairchild Test Deck samples, the smearing did make many characters which were close to the edge of the page unreadable. Also, in analyzing the data from the test deck, it is evident that the special phosphor blend fluorescent lamps produced slightly higher accuracy in scanning the documents with single-color inks.

The mechanical design of the focal plane assembly apparently did not allow sufficient adjustment capability to properly focus both imagers. Attempts at focusing one of the imagers while the scanner was at NOSC proved unsuccessful. Also, the scanner has no capability for adjusting for different focal length lenses, and hence the magnification of the image was in error by about 4%.

RECOMMENDATIONS

The following recommendations are presented for consideration and possible inclusion in future scanner design tasks.

A more uniform system response is needed across the scanner's field of view. The best means of achieving this is by judiciously shaping the illumination source to provide a relatively flat response across the active image area. If the same thresholding circuitry is used, it is felt that the response should be flat within the limits of the minimum PCR percentage desired to be read. This uniformity of response may not be so critical if the video data are digitized and processed digitally prior to thresholding.

A method should be provided for adjusting for different focal length lenses in order to obtain the proper scanning resolution.

If multiple imagers are used in the future, less-sensitive adjustments should be provided for both abutment and relative focusing of the devices. An alternative to this might be to redesign the imagers to allow close abutment of two imaging devices on one substrate. This would preclude the need for relative positioning and for a beamsplitter.

ANNEX A TO APPENDIX D

FAIRCHILD SETUP AND TEST VISIT REPORT PERIOD MAY 8–10 1979

INTRODUCTION

Under the provisions of USPS contract 104320-79-Z-0475, job 6275, three personnel from Fairchild Imaging Systems, Syosset, NY, visited NOSC for the purpose of verification of operation and interfacing between the Fairchild scanner system and NOSC ICAS system. Those personnel from Fairchild in attendance were: Mr Stanley W Roth, Program Manager, Mr Dan Barber, Project Engineer, and Mr Mike Wolf, Project Engineer. The expected results of this visit were established at an interface meeting held at NOSC on 26 and 27 February 1979 and attended by Mr Roth and Mr Barber. The basic goals to be achieved during this visit were (1) operational verification of the focal-plane and the card file assemblies, (2) a complete electrical alignment and mechanical alignment of the card file and focal-plane assembly, and (3) a series of baseline tests to document the performance of the equipment after the interfacing was complete.

OPERATIONAL VERIFICATION

1. Interface Verification. On 8 May, the power and interface signals from the NOSC equipment to the Fairchild equipment were connected and verified. Power levels, signal polarity, and timing were checked and found to be acceptable. Some wiring was necessary on the Fairchild digital logic boards in order to provide a cable interface not previously completed. By the end of 8 May, this was completed and light response in the video output was verified.

2. Electrical Alignment. Since the particular analog cards in the card cage assembly had never operated with this particular focal-plane assembly, all electrical alignment adjustments were necessary. On the morning of 9 May, the large drum assembly was removed from the Fairchild scanner hardware and the alignment target installed. At this time Fairchild performed the necessary electrical alignment to properly interface the focal-plane assembly to the analog cards.

3. Focus and Mechanical Alignment. The lens focus, mechanical alignment of the focal-plane assembly, and relative alignment of the arrays themselves, as well as the alignment of the light sources, were completed by the end of Wednesday 9 May. At this point it was decided the scanner system was operating appropriately and it was reasonable to proceed to baseline testing.

BASELINE TESTING

The baseline testing required made use of the Fairchild alignment target as the source and oscilloscope photographs of scanner output waveforms as the performance verification recording medium. Reference to the February interface meeting indicates that the test will be performed at a line integration time of 131.5 microseconds, which corresponds to four pages per second. Since the large drum assembly with the encoder was removed to

allow mounting of the alignment target, the line sync signal generation was provided by an external pulse generator.

The required test equipment for recording the output waveforms is as follows:

Oscilloscope – Tektronix 7844 dual beam or 7904

Vertical plug-in amplifiers – 7A24 dual trace high speed, 7A13 differential offset, 7A19 single channel

Time base – 7B92A

Pulse generator – Tektronix PG502 in a TM 506 power module

Following is a description of the scope photographs taken, including the waveform being monitored and sufficient information on the test setup to allow duplication at a future time.

NOTE: It was noticed by Fairchild that the signal level from the arrays with the new lamps installed was considerably higher than previously recorded at Fairchild. It is therefore suggested that on a roughly weekly basis during our testing we reverify the signal level of the raw video outputs in order to monitor changes due to aging of the light source.

BASELINE TEST – PHOTOGRAPHS AND DESCRIPTIONS

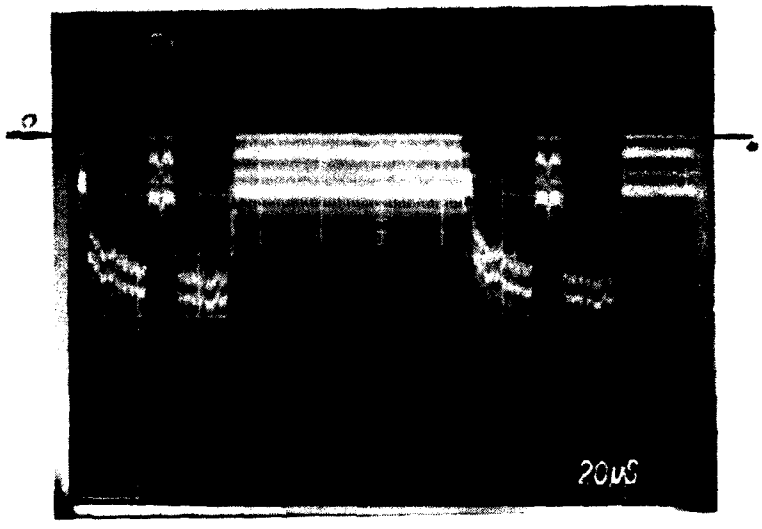

1. Channel 1A raw video showing line integration time

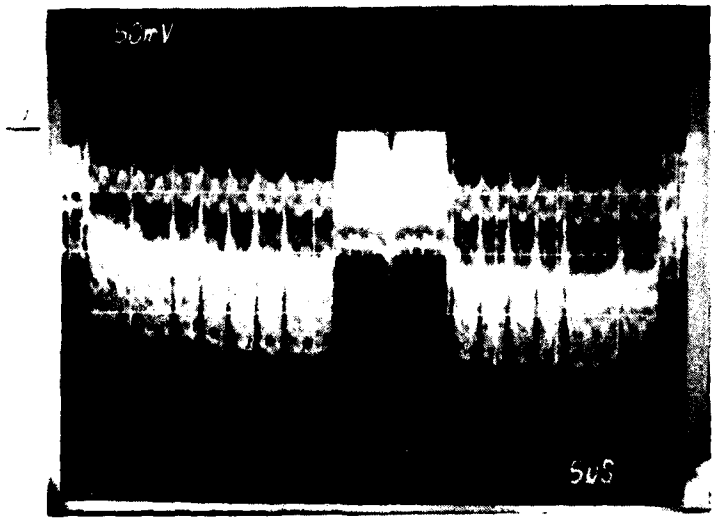

2. Channel 1A raw video

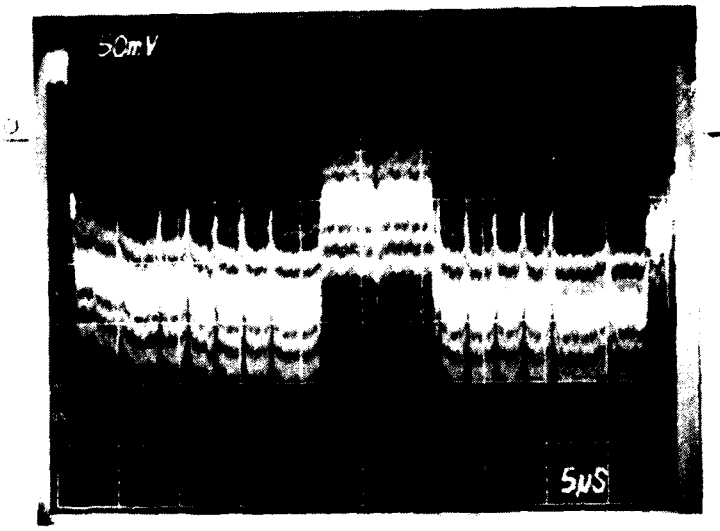

3. Channel 1B raw video

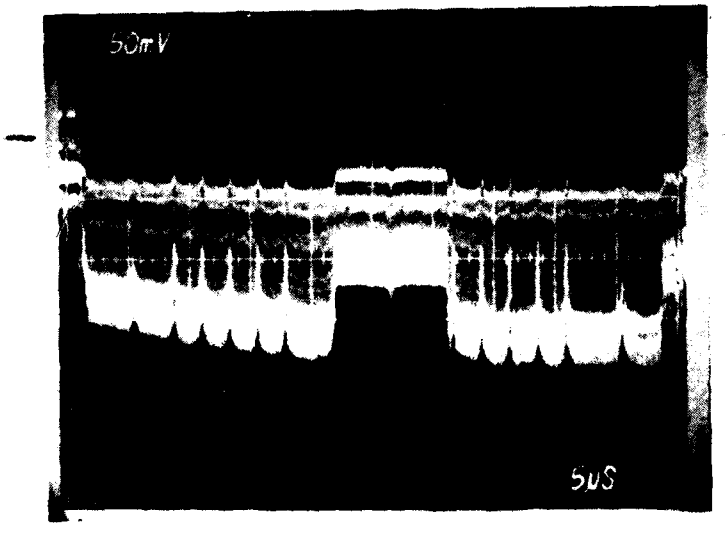

4. Channel 2A raw video

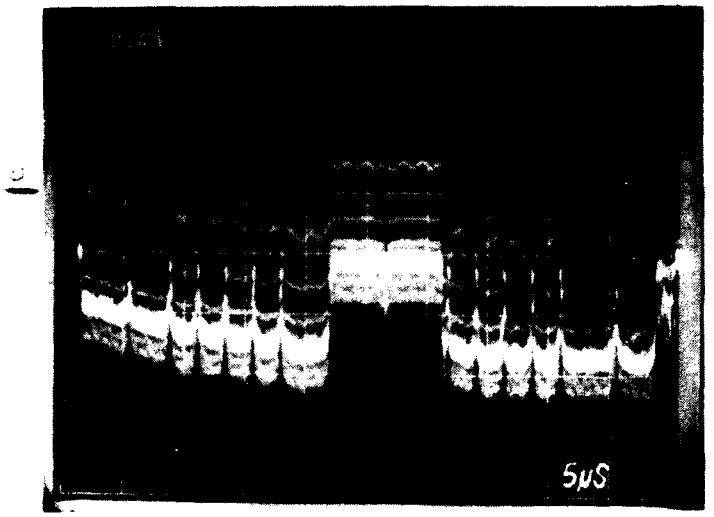

5. Channel 2B raw video

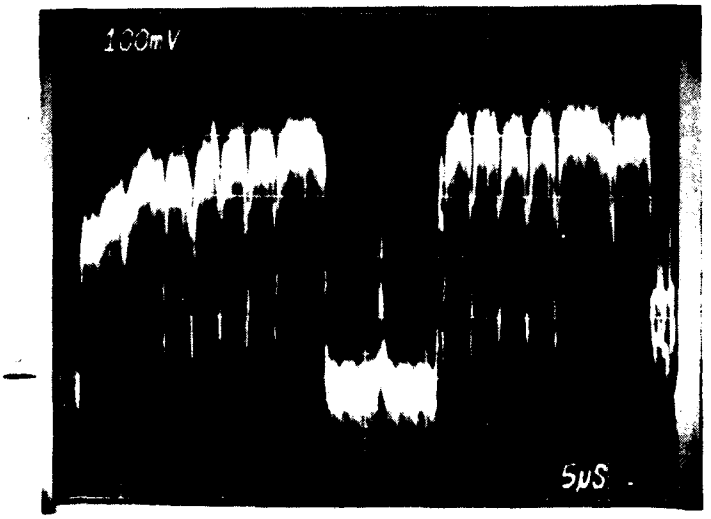

6. Channel 1A matched filter output

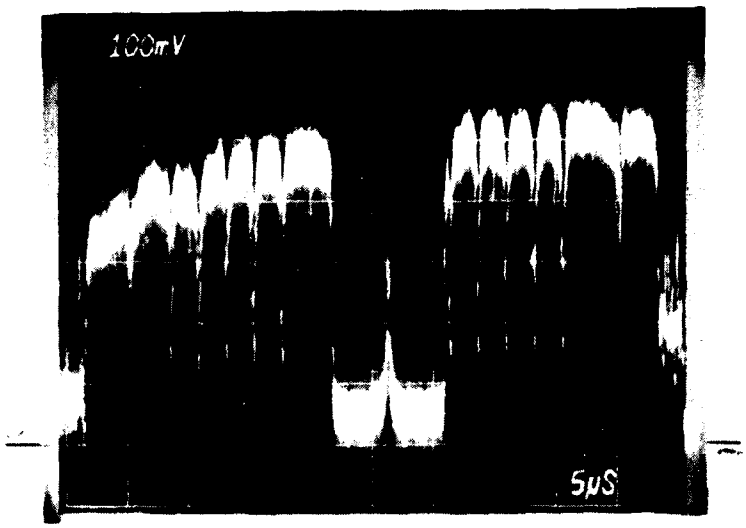

7. Channel 1B matched filter output

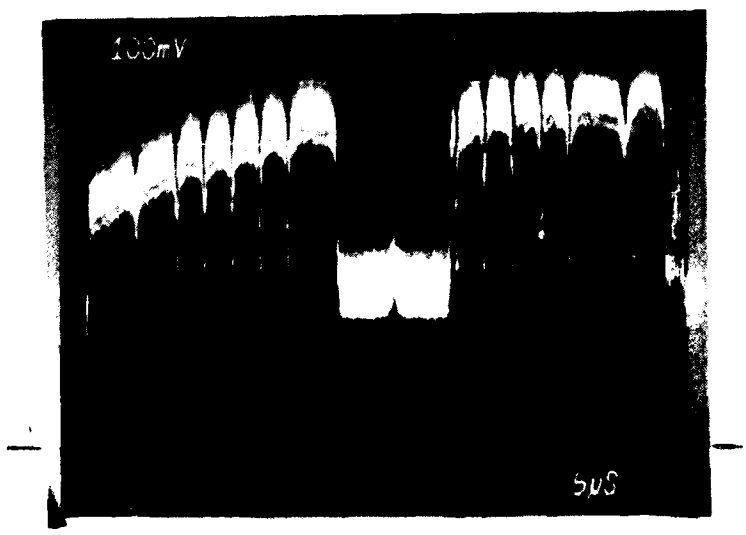

8. Channel 2A matched filter output

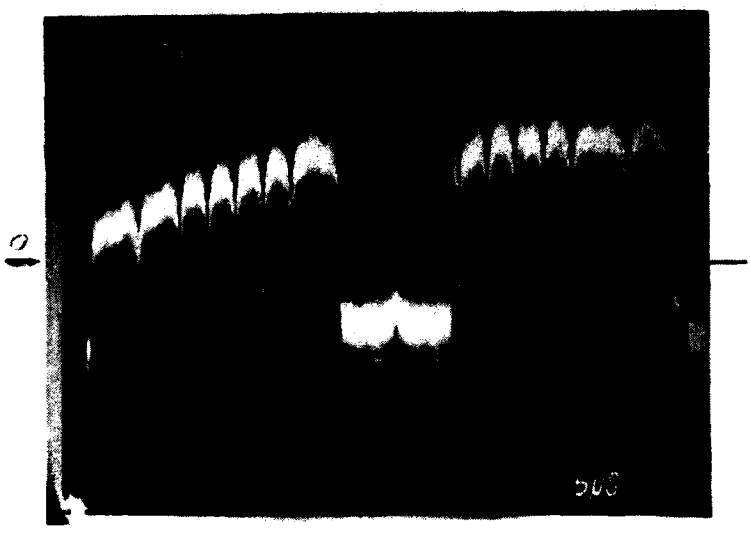

9. Channel 2B matched filter output

10. Combined video channel 1

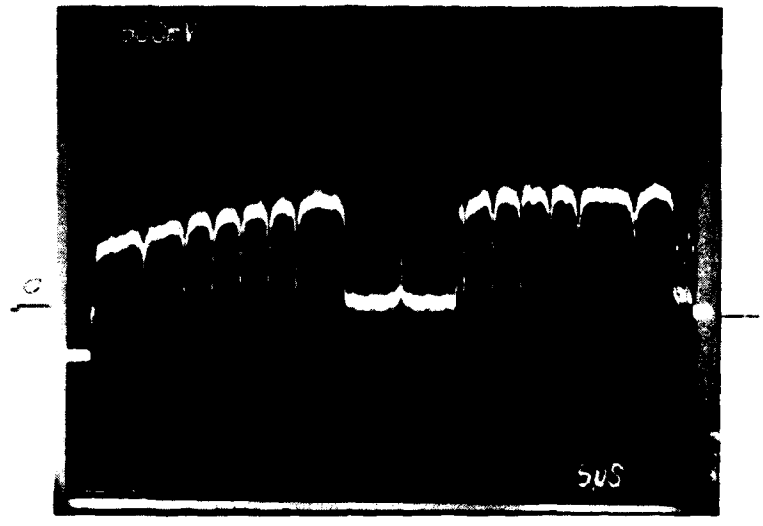

11. Combined video channel 2

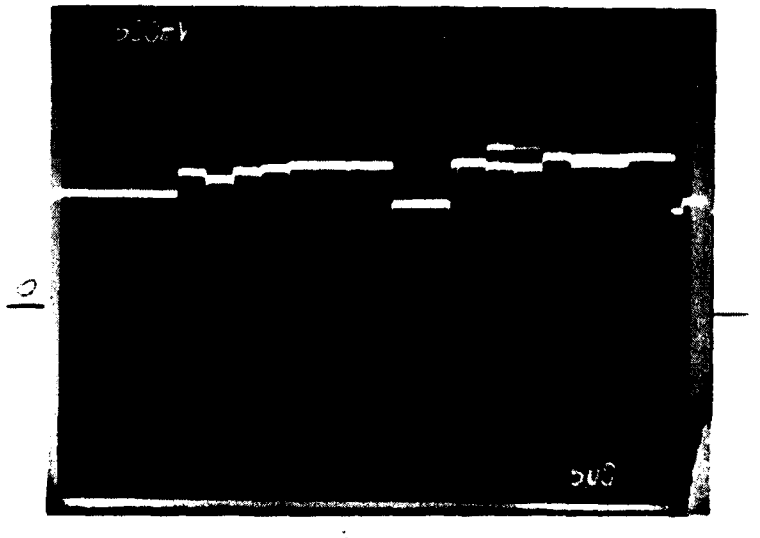

12. Channel 1 reference level

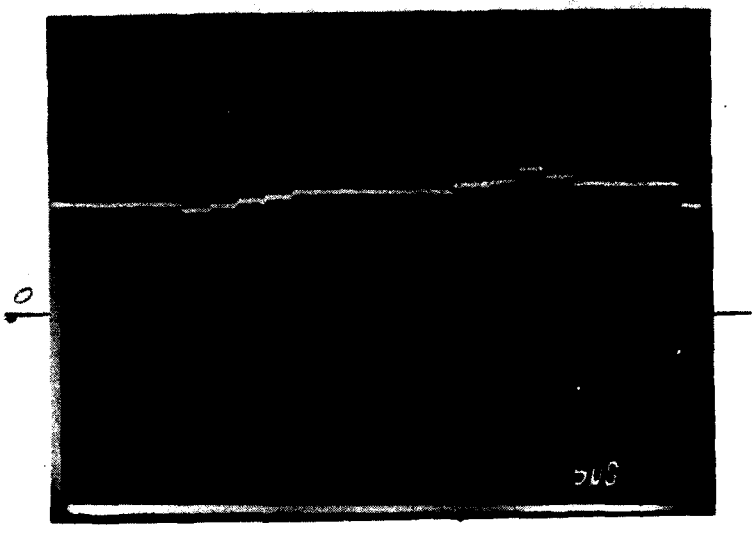

13. Channel 2 reference level

14. Top trace – Video Valid, second trace – channel 1 combined video, third trace – channel 2 combined video. This is intended to show the overlap or left right alignment of an expanded scale. Video Valid signal is active high true.

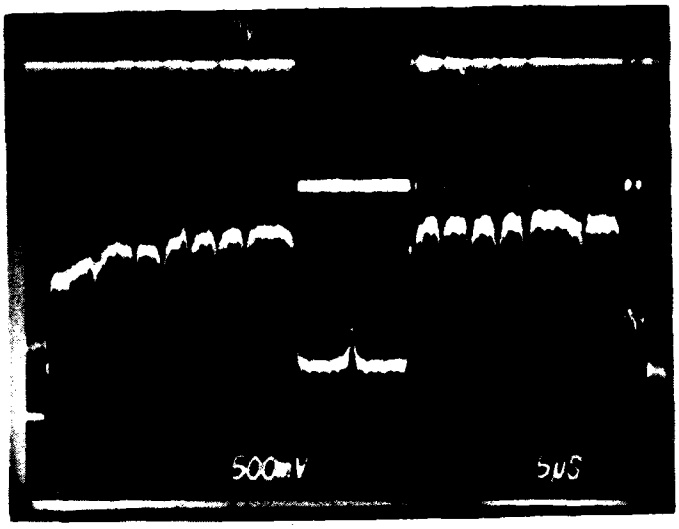

15. Threshold digital video output channel 1

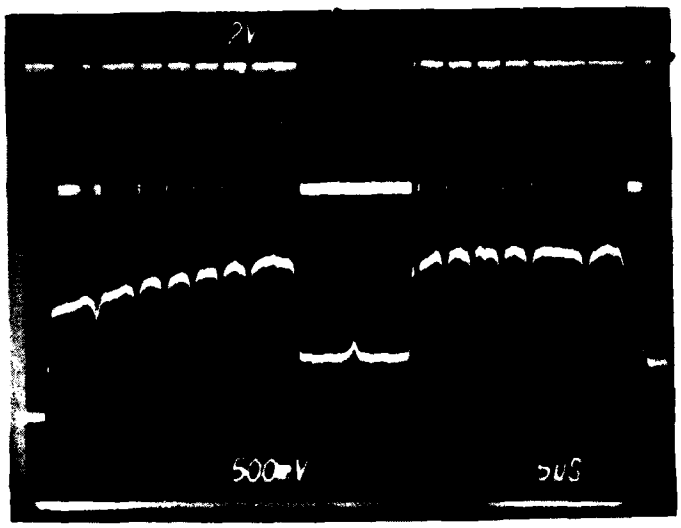

16. Threshold digital video output channel 2. For the above two photographs top trace is digital video (TTL levels) at the outputs of the ECL receivers. The bottom trace is combined video output after thresholding.